

Implementation of a Landslide Early Warning System considering informal settlements in Medellín (Colombia)

Moritz Stanislaus Gamperl

Complete reprint of the dissertation approved by the TUM School of Engineering and Design
of the Technical University of Munich for the award of the

Doktor der Ingenieurwissenschaften (Dr.-Ing.)

Chair: Prof. Dr. Michael Krautblatter

Examiners:

1. Prof. Dr. Kurosch Thuro
2. Prof. Dr. Christian Zangerl

The dissertation was submitted to the Technical University of Munich on 2 October 2023 and
accepted by the TUM School of Engineering and Design on 29 January 2024.

Acknowledgments

First of all, I would like to thank my supervisor, Kurosch Thuro, who introduced me to this topic after supervising my master's thesis on a completely different topic and gave me the opportunity to work on this fantastic project. Kurosch, thank you for your constant support! Thank you for the freedom you gave me to work on the project and for knowing that you always had my back even in difficult situations (of which there were quite a few).

My mentor John Singer was the person I worked with closest in course of writing this dissertation. I learned a tremendous amount from him and could always rely on his support, no matter the topic. Thank you, John, for your supervision and support through the last four years.

Thank you to my colleague and friend Tamara Breuninger, who I know since the beginning of my bachelor's studies and with whom it was a pleasure to work on the Inform@Risk project. Thank you for the partnership and the great times we had together!

To fellow Inform@Risk teammates Lisa Seiler, Carolina Garcia-Londono, David Ceron, Julian Castaneda and Isabel Basombrio: Thank you all so much for the unique partnership in our project and the great times in Medellín! It was a pleasure!

I thank the community in Bello Oriente, to whom I owe a lot and who I share very special memories with (including a jam session above Medellín). A big thanks especially to our many helpers during mapping and the ERT campaigns and to Jeisson, our reliable driver.

The rest of the Inform@Risk team: Heike Schäfer, Christian Werthmann, Marta Sapena-Moll, Marlene Kühnl, Hannes Taubenböck, Sebastian Schröck, Wolfgang Dorner, Klaus Martin. Thank you all!

I would also like to thank Michael Krautblatter for his support and knowledge to better understand and interpret the geophysical investigations in Bello Oriente. Bettina Menschik, who helped me and Tamara a lot with the hazard analysis and always had an open ear. I thank Christian Zangerl for Co-supervising this thesis and the fruitful discussions about the ambitious goals we follow with our project.

I am grateful to all of the students who helped us during this project, be it in the field, in the lab, or by helping us by interpreting some of the data we could gather in Colombia. I thank especially Severin Hueber, Svenja Rothe, Isabelle Leisgang, Agnes Demharter, Christian Kerczek and Andreas Grabmeier.

Last but not least I want to thank my family and friends, firstly my partner Lina Seybold for always supporting me and sometimes guiding me back to a proper 'geologic' interpretation of things. I am especially grateful to my father for his support in my decision to become a geologist and somewhat tread in his footsteps.

Abstract

Landslides are one of the most dangerous natural hazards worldwide. As climate change increases and populations around the world urbanize endangered slopes more and more, often as informal settlements, fatalities in urban landslide-prone environments increase. An effective way of strengthening the resilience of endangered communities, next to resettlement, are early warning systems (EWS). On local and regional scales, they have both been applied and tested in many areas around the world. However, these systems are not always efficient in informal settlements, as for a functioning EWS in these cases there are several challenges beyond technical aspects, as cost efficiency, acceptance of the local community and reproducibility. Therefore, the goal of the Inform@Risk project was to test and install a cost efficient, easily reproducible local EWS in an endangered informal settlement with detailed monitoring together with social work. In a pilot project in Medellín, Colombia, in the informal settlement of Bello Oriente, located on the steep slopes of the Aburra valley hosting the city of Medellín, the project investigated how such a system could be implemented. This thesis is part of the Inform@Risk project and deals with (1) the landslide and geological assessment on site, (2) the conception of a fitting sensor network, and (3) the manufacturing, installation and evaluation of this sensor network. The first part of the thesis focuses on the geological assessment, done via a combination of direct observations such as mapping and drilling, and indirect observations using electrical resistivity tomography (ERT). These were employed successively in order to gain detailed knowledge from the combination. On the steep slopes of our investigation site, the dunite rock in the subsurface is deeply weathered to a depth of over 50 m. This fact, which was not apparent in the primary ERT campaign, only was obvious once the drillings were completed. The drilling results in turn allowed us to re-interpret the ERT results and obtain 2.5D information about the subsurface. The final geological model based on the combined methods was used to plan the sensor system of part 2 and 3 in detail. According to the geological data and social structure of the project area, the sensor system had to fulfill certain specific requirements. The second part of this thesis describes the conceptualization of a system meeting these requirements with a low-cost geosensor network in combination with other point- and line measurement systems. The geosensor network is based on internet-of-things (IoT) devices which communicate via the LoRa (Long Range) communication protocol. The devices are connected to multiple gateways which collect the data and transfer them to an online server via mobile network. To evaluate the sensor design, a first test of the geosensor network was done in southern Germany. Subsequently, the optimized system was installed on the study site Bello Oriente in 2022 and is running well since then. The experiences of the first installation and its integration into public space are described in part 3 of this thesis together with a description on our efforts to share the knowledge on the developed system with a larger community: All information on the newly developed sensor designs and the overall system were published on a new wiki page, and are now freely available for contributors and interested parties. Finally, recommendations are given on how similar systems could be replicated and what has to be paid special attention to for doing so. The thesis ends with a conclusion and overall discussion of key points: Geological-geotechnical assessment should be performed in detail so that the placement of a sensor system can be done efficiently. IoT systems will become increasingly important for monitoring and early warning of landslides and other natural hazards, but what is done with the data afterwards is just as important.

The implementation of integrated EWS is important and should be aimed at when working in urbanized areas at risk. An outlook is additionally given on how the measurement system and especially the data analysis could be improved in the future. The former is possible by several changes to the sensor design, which can be achieved by collective work on the wiki page, the latter by incorporating such a measurement system with physically-based, regional models to increase the affected area.

Zusammenfassung

Hangbewegungen sind eine der gefährlichsten Naturgefahren weltweit. Mit dem fortschreitenden Klimawandel und der zunehmenden Besiedelung gefährdeter Hänge, oft in Form informeller Siedlungen, steigt die Zahl der Todesopfer in hangbewegungsgefährdeten, städtischen Gebieten. Ein wirksames Mittel zur Stärkung der Widerstandsfähigkeit gefährdeter Areale sind – neben Umsiedlung – Frühwarnsysteme (Early Warning System - EWS). Auf lokaler und regionaler Ebene wurden sie in vielen Gebieten der Welt angewandt und getestet. Allerdings sind diese Systeme in informellen Siedlungen nicht immer effizient, da es für ein funktionierendes EWS in diesen Fällen neben technischen Aspekten auch eine Reihe von Herausforderungen gibt, wie Kosteneffizienz, Akzeptanz der lokalen Gemeinschaft und Reproduzierbarkeit. Ziel des Inform@Risk-Projekts war es daher, ein kosteneffizientes, leicht reproduzierbares lokales EWS in einer gefährdeten informellen Siedlung zu testen und zu installieren, das zusammen mit Sozialarbeit ein detailliertes Monitoring ermöglicht. In dem Projekt wurde untersucht, wie ein solches System in einem Pilotprojekt in Medellín, Kolumbien, in der informellen Siedlung Bello Oriente an den steilen Hängen des Aburra-Tals, in dem die Stadt Medellín liegt, umgesetzt werden kann. Diese Arbeit ist Teil des Inform@Risk-Projekts und befasst sich mit (1) der geologischen- und Gefahrenbewertung vor Ort, (2) der Konzeption eines passenden Sensornetzwerks und (3) der Herstellung, Installation und Auswertung dieses Sensornetzwerks. Der erste Teil der Arbeit befasst sich mit der geologischen Bewertung, die durch eine Kombination aus direkten Beobachtungen wie Kartierungen und Bohrungen und indirekten Beobachtungen mit Hilfe der elektrischen Widerstandstomographie (ERT) erfolgt. Diese wurden nacheinander eingesetzt, um aus der Kombination detaillierte Erkenntnisse zu gewinnen. An den steilen Hängen unseres Untersuchungsgebietes ist das vorliegende Gestein (Dunit/Serpentinit) im Untergrund bis in eine Tiefe von über 50 m verwittert. Diese ungewöhnlich große Verwitterungstiefe, die in der ersten ERT-Kampagne nicht erkennbar war, wurde erst nach Abschluss der Bohrungen deutlich. Diese wiederum ermöglichten es uns, die ERT-Ergebnisse neu zu interpretieren und 2,5D-Informationen über den Untergrund zu erhalten. Das endgültige geologische Modell, das auf den kombinierten Methoden basiert, wurde verwendet, um das Sensorsystem von Teil 2 und 3 im Detail zu planen. Entsprechend der geologischen Daten und der sozialen Struktur des Projektgebietes musste das Sensorsystem bestimmte Anforderungen erfüllen. Der zweite Teil dieser Arbeit beschreibt die Konzeption eines Systems, das diese Anforderungen mit einem kostengünstigen Geosensornetz in Kombination mit anderen Punkt- und Linienmesssystemen erfüllt. Das Geosensornetzwerk basiert auf Internet-of-Things (IoT) Geräten, die über das LoRa (Long Range) Kommunikationsprotokoll kommunizieren. Die Geräte sind mit mehreren Gateways verbunden, die die Daten sammeln und sie über ein Mobilfunknetz an einen Online-Server übertragen. Um das Sensordesign zu bewerten, wurde ein erster Test des Geosensornetzwerks in Süddeutschland durchgeführt. Anschließend wurde das optimierte System im Jahr 2022 am Pilotprojekt Bello Oriente installiert und funktioniert seitdem. Die Erfahrungen mit der ersten Installation und ihrer Integration in den öffentlichen Raum werden in Teil 3 dieser Arbeit beschrieben, zusammen mit einer Beschreibung unserer Bemühungen, das Wissen über das entwickelte System mit einer größeren Fachgemeinschaft zu teilen: Alle Informationen über die neu entwickelten Sensordesigns und das Gesamtsystem wurden auf einer neuen Wiki-Seite veröffentlicht und sind nun für Mitwirkende und Interessierte frei zugänglich.

Abschließend werden Empfehlungen gegeben, wie ähnliche Systeme nachgebaut werden könnten und worauf dabei besonders zu achten ist. Die Arbeit endet mit einer Schlussfolgerung und einer allgemeinen Diskussion der wichtigsten Punkte: Die geologisch-geotechnische Bewertung sollte detailliert durchgeführt werden, damit die Planung und Implementierung eines Sensorsystems effizient erfolgen kann. IoT-Systeme werden für die Überwachung und Frühwarnung vor Hangbewegungen und anderen Naturgefahren immer wichtiger, wie jedoch die Daten anschließend ausgewertet werden, ist ebenso elementar. Die Implementierung von integrierten EWS ist wichtig und sollte bei der Arbeit in gefährdeten urbanen Gebieten angestrebt werden. Darüber hinaus wird ein Ausblick gegeben, wie das Messsystem und insbesondere die Datenanalyse in Zukunft verbessert werden könnten. Ersteres ist durch verschiedene Änderungen am Sensordesign möglich, die durch kollektive Arbeit auf der Wiki-Seite erreicht werden können, letzteres durch die Einbindung eines solchen Messsystems mit physikalisch basierten, regionalen Modellen zur Vergrößerung des überwachten Gebietes.

Resumen

Los deslizamientos son uno de los riesgos naturales más peligrosos en todo el mundo. A medida que incrementa el cambio climático y las poblaciones de todo el mundo urbanizan cada vez más las laderas en peligro, a menudo como asentamientos informales, aumentando las víctimas mortales en entornos urbanos propensos a deslizamientos. Una forma eficaz de reforzar la resiliencia de las comunidades en peligro, junto al reasentamiento, son los Sistemas de Alerta Temprana (SAT). A escala local y regional, se han aplicado y probado en muchas zonas del mundo. Sin embargo, los sistemas de prueba no siempre son eficientes en los asentamientos informales, ya que para que un SAT funcione en estos casos existen varios retos más allá de los aspectos técnicos, como la rentabilidad, la aceptación de la comunidad local y la reproducibilidad. Por ello, el objetivo del proyecto Inform@Risk era probar e instalar un sistema local de alerta temprana rentable y fácilmente reproducible en un asentamiento informal en peligro, con un seguimiento detallado y trabajo social. El proyecto investigó cómo podría implementarse un sistema de este tipo en un proyecto piloto en Medellín, Colombia, en el asentamiento informal de Bello Oriente, situado en las empinadas laderas del Valle de Aburrá que alberga la ciudad de Medellín. Esta tesis forma parte del proyecto Inform@Risk y aborda (1) la evaluación geológica y de deslizamientos in situ, (2) la concepción de una red de sensores de adaptación, y (3) la fabricación, instalación y evaluación de esta red de sensores. La primera parte de la tesis se centra en la evaluación geológica, realizada mediante una combinación de observaciones directas, como la cartografía, perforaciones y observaciones indirectas, con el uso de Tomografías de Resistividad Eléctrica (ERT). Estas se emplearon sucesivamente para obtener un conocimiento detallado de la combinación. En las empinadas laderas de nuestra zona de investigación, la roca dunita subsuperficial está profundamente meteorizada hasta una profundidad de más de 50 m. Este hecho, que no era evidente en la campaña primaria de ERT, sólo se hizo evidente una vez finalizadas las perforaciones. Éstos, a su vez, nos permitieron reinterpretar los resultados de la ERT y obtener información 2.5D del subsuelo. El modelo geológico final basado en los métodos combinados se utilizó para planificar detalladamente el sistema de sensores de las partes 2 y 3. De acuerdo con los datos geológicos y la estructura social de la zona del proyecto, el sistema de sensores debía cumplir ciertos requisitos específicos. La segunda parte de esta tesis describe la conceptualización de un sistema que cumpla estos requisitos con una red de geosensores de bajo costo en combinación con otros sistemas de medición puntual y lineal. La red de geosensores se basa en dispositivos Internet-of-Things (IoT) que se comunican a través del protocolo de comunicación LoRa (Long Range). Los dispositivos están conectados a múltiples Gateways que recogen los datos y los transfieren a un servidor en línea a través de redes móviles. Para evaluar el diseño de los sensores, se realizó una primera prueba del sistema de geosensores en el sur de Alemania. Posteriormente, el sistema optimizado se instaló en el sitio de estudio Bello Oriente en el 2022 y funciona bien desde entonces. Las experiencias de la primera instalación y su integración en el espacio público se describen en la parte 3 de esta tesis, junto con una descripción de nuestros esfuerzos por compartir los conocimientos sobre el sistema desarrollado con una comunidad más amplia: Toda la información sobre los nuevos diseños de los sensores y el sistema en general se publicaron en una nueva página wiki, y ahora están disponibles de forma gratuita para los colaboradores y las partes interesadas. Por último, se dan recomendaciones sobre cómo podrían reproducirse sistemas similares

y a qué hay que prestar especial atención para hacerlo. La tesis termina con una conclusión y una discusión general de los puntos clave: La evaluación geológico-geotécnica debe realizarse en detalle para que la disposición del sistema de sensores pueda hacerse de forma eficiente. Los sistemas IoT serán cada vez más importantes para la monitorización y alerta temprana de deslizamientos y otros riesgos naturales, pero lo que se haga después con los datos es igual de importante. La implementación de sistemas de alerta temprana integrados es importante y debería ser el objetivo cuando se trabaja en zonas urbanizadas de riesgo. Además, se ofrece una perspectiva sobre cómo podría mejorarse en el futuro el sistema de medición y, especialmente, el análisis de datos. Lo primero es posible mediante varios cambios en el diseño de los sensores, que pueden lograrse mediante el trabajo colectivo en la página wiki, lo segundo incorporando dicho sistema de medición con modelos regionales de base física para aumentar el área afectada.

Contents

Acknowledgments.....	i
Abstract.....	iii
Zusammenfassung	v
Resumen.....	vii
Contents.....	viii
1 Introduction	1
1.1 Motivation.....	1
1.2 The Inform@Risk Project.....	2
1.3 Research Questions	3
1.4 Thesis Outline	3
2 Background.....	7
2.1 Landslide Early Warning Systems.....	7
2.1.1 Local versus Regional Landslide Early Warning Systems	7
2.1.2 Integrated (Landslide) Early Warning Systems	9
2.2 Monitoring Systems	9
2.2.1 GNSS/GPS	10
2.2.2 Tacheometry	11
2.2.3 Photogrammetry.....	11
2.2.4 Radar interferometry (GB-InSAR/SB-InSAR)	11
2.2.5 Fiber Optics & TDR	11
2.2.6 Geo-Sensor- Networks and Low-Cost Sensors	12
3 Scientific Articles	15
3.1 Paper 1: Improvement of landslide investigation in deeply weathered Ultramafites by parallelizing ERT with direct field observations	15
3.2 Paper 2: Internet of Things Geosensor Network for Cost-Effective Landslide Early Warn- ing Systems	16
3.3 Paper 3: Recommendations for Landslide Early Warning Systems in Informal Settle- ments Based on a Case Study in Medellín, Colombia.....	18
4 Synopsis and Discussion	21
4.1 Geological-Geotechnical Investigation for Local Integrated Early Warning Systems.....	21
4.2 Geosensor Networks and Landslide Early Warning	22
4.3 Replication of the Proposed Sensor Network in Other Areas	23
4.4 Integrated Landslide Early Warning Systems: Challenges and Next Steps.....	24
4.4.1 Selected Lessons Learned from Inform@Risk.....	24

4.4.2	Challenges of Integrated Early Warning Systems	25
4.4.3	Next Steps: Standardization	26
5	Outlook.....	27
5.1	Further improvement of the Inform@Risk Measurement System.....	27
5.1.1	Sensor improvements	27
5.1.2	A Spark for a Do-It-Yourself Landslide Early Warning Community: Further im- provements of the Inform@Risk Wiki	28
5.2	Data Analysis.....	28
5.2.1	Numerical Analysis using a GIS-code in combination with measurement data.....	28
5.2.2	Data Analysis using Machine Learning and Neural Networks	30
5.2.3	Further data analysis of the Bello Oriente pilot project.....	30
	Bibliography	31
	Appendix A - Full Journal Articles	49
	Gamperl et al. (2023) Improvement of landslide investigation in deeply weathered ultramafites by parallelizing ERT with direct field observations	51
	Gamperl et al. (2021) Internet of Things Geosensor Network for Cost-Effective Landslide Early Warning.....	69
	Gamperl et al. (2023) Recommendations for Landslide Early Warning Systems in Informal Settlements Based on a Case Study in Medellín, Colombia	93
	Appendix B - Full Journal Articles as Coauthor	117
	Thuro et al. (2020) Development of an early warning system for landslides in the tropical Andes (Medellín; Colombia).....	118
	Breuninger et al. (2021) Investigation of Critical Geotechnical, Petrological and Mineralogical Parameters for Landslides in Deeply Weathered Dunite Rock (Medellín, Colombia)	132
	Sapena et al. (2023) Cost estimation for the instrumentalization of Early Warning Systems in landslide prone areas	159

1. Introduction

1.1. Motivation

The UN secretary-general António Guterres stated the goal to protect everyone on earth against extreme weather and climate change on march 23, 2022. To do this, it was proclaimed that one target is to implement Early Warning Systems (EWS) against these threats (United Nations Climate Change, 2022). This is important because only two-thirds of the worlds population currently is protected by them, and the areas not covered are mostly developing countries of the global south.

The need for EWSs is apparent in various areas, from primary natural hazards such as extreme weather events, earthquakes, as well as from secondary events, such as floods, tsunamis or landslides. In all of these areas, EWSs can be employed in local, regional or even larger scale (Copernicus, 2023). They can be a tool to immediately increase the resilience of local communities against natural hazards (Werthmann et al., 2023).

Landslides are one of the most dangerous natural hazards, with 55.997 fatalities from 2004 to 2016 alone (Froude & Petley, 2018). Since most landslides are triggered by rainfall, heavier precipitation, which is to be expected due to climate change, will lead to more frequent landslide events in the coming decades (Crozier, 2010; Haque et al., 2019; IPCC, 2022). These events will impact the global south, namely Asia, South America and Africa overproportionally (Froude & Petley, 2018), but at the same time the global south is under-investigated with regard to climate impact on landslide occurrence (Gariano & Guzzetti, 2016).

One example is Colombia, one of the most landslide prone countries in the world (Sapena et al., 2023). Most of it's population is living in high and very high landslide hazard in the Andean mountains (Ruiz Peña et al., 2017). There are many examples for deadly landslides in the last decades (Aristizábal & Sánchez, 2020). Two of the most prominent ones are the Villa Tina disaster in Medellín in 1987 (Coupé et al., 2007; Garcia-Londoño, 2005), with more than 500 casualties and about 100 houses destroyed, and the Mocoa landslide of 2017, which was a large debris flow caused by many shallow landslides after heavy rainfall. The latter event caused the deaths of 333 people and injured 398 people (García-Delgado et al., 2019). A second factor which is likely to increase deadly landslides is the unplanned urbanization in informal settlements, neighborhoods constructed outside of governmental planning regulations (Werthmann et al., 2023), which is increasing constantly (Taubenböck et al., 2012).

Thus, more detailed landslide investigation and EWSs for landslides (also subsequently called landslide early warning systems, LEWSs), are needed especially for areas where high relief and rapid urbanization come together. There is especially a gap in affordable local LEWSs which use deformation measurements to make accurate predictions (Gamperl et al., 2023b). While local LEWS are used commonly on sites where the landslide location is more or less known, they are rarely applied on slope-

scale with deformation measurements, where the exact failure location is not known, mostly because doing so would be very expensive (Gamperl et al., 2021, 2023b). Regional systems, which for example use satellite data to calculate likely future failure locations, can on the other hand not predict precise locations or failure times.

1.2. The Inform@Risk Project

Inform@Risk is an interdisciplinary research project led by Christian Werthmann and his team of landscape architects at the Leibniz-University of Hannover (Werthmann, 2018, 2023; Werthmann et al., 2023; Thuro et al., 2020). On the German side, the project team consists of geologists (Technical University of Munich, TUM), geoinformation experts (Deggendorf Institute of Technology, THD) and remote sensing experts (Deutsches Luft- und Raumfahrtzentrum, DLR). On the Colombian side, the EAFIT University (URBAM), the Alcaldía de Medellín, the disaster response agency of the city (DAGR), the metropolitan region (AMVA), the early warning system of the Valle de Aburrá, SIATA, the geological society of Colombia (SCG) and the NGOs Tejearañas, Corporación Convivamos and Fundación Palomá were involved. The project was funded from 2019-2023 by the German ministry of education and research (BMBF), Client II program, funding number 03G0883C.

The project aims at improving the resilience of informal settlements at the outskirts of Medellín against shallow landslides. This includes (1) creating a technical solution for improved early warning from landslides and (2) improving the risk knowledge and the social structures in the neighborhood. Such an approach was created using certain guidelines. The resulting LEWS needs to be:

1. Socially integrated
2. Spatially integrated
3. Multiscalar
4. Multisectoral
5. Precise
6. Inexpensive
7. Easily replicable

The project originally ran from 2019 to 2022 and was prolonged for one year until June 2023 because of the travel restrictions caused by the Covid-19 crisis. In this four-year span, the necessary tasks to fulfill the needs specified above were performed by the team, both in Germany and Colombia on-site. For a more detailed overview of the whole project, please refer to Werthmann et al. (2023).

1.3. Research Questions

As part of the project described above, this thesis deals with the geological-geotechnical challenges specifically, as well as the monitoring system for the project. The following research questions are addressed:

- How can the landslide hazard in informal settlements be evaluated with a focus on geophysical and geological methods?
- How should a measurement system for low-cost landslide early warning systems in high-hazard, densely populated informal settlements be designed?
- How can such a system be replicated best for as many people as possible?

1.4. Thesis Outline

To answer these research questions, the main focus of this thesis is the development of a new measurement system and interlinking it with the social structure of the neighborhood and the community. The investigation of landslide hazard and risk onsite is addressed also in the first part of the thesis by evaluation of a combination of geological and geophysical methods. The detailed landslide hazard evaluation is however the focus of another thesis by Tamara Breuninger. This dissertation is publication-based and contains two accepted first-author peer reviewed journal articles (Gamperl et al., 2021, 2023b) and one submitted first-author paper (Gamperl et al., 2023a) which are included in appendix A.

Before the publication sections, an overall introduction into EWSs and landslide monitoring systems is given. A general introduction into landslide mechanics is omitted, as it is expected to be basic knowledge for readers. For general information regarding this topic, please refer to Cruden & Varnes (1996); Hungr et al. (2014) and Thiebes (2012).

The first paper is presented in section 3.1. It discusses the threat of landslides in Medellín, Colombia and how the landslide-prone dunite unit in the east of the city can be investigated. A multi-step approach, including mapping, core drilling and electrical resistivity tomography is applied to identify the most landslide-susceptible areas in an especially endangered neighborhood. The resulting differing geological models during this multi-step investigation are presented and compared. The article ends with recommendations for combining different methods for efficient landslide investigation on other sites.

In section 3.2, the second article deals with the conceptualization and test of a monitoring system which is optimized for informal settlements and complies with the goals stated in section 1.1. The resulting system is based on an Internet of Things (IoT)-based geosensor network which is combined with line CSM (Continuous Shear Monitor) measurements and sensors in vertical drillings. The data collected is processed and analyzed to assess short- to medium-term hazard levels, and early warnings and alarms can be issued if deformation is detected.

Based on the tested concept for the sensor network, the system was installed on-site in Medellín in 2022. The resulting insights from this installation and the subsequent open-source publication of all the newly developed parts, together with in-depth guides and lists of the monitoring system, were then published in the third paper shown in section 3.3. Particular emphasis is placed on the social integration of the system into the social structure of the neighborhood. For all parts of the system, from risk analysis to reaction capacity, methods are described which help with regard to their socio-spatial integration into the neighborhood. Recommendations are given on basis of this data on the deployment of future integrated LEWSs in similar areas.

The findings of the papers are summarized in a comprehensive discussion in section 4. In section 5, a forward-looking perspective is presented, offering an outlook with potential directions for further research and investigations.

Appendix A contains the full papers of sections 3.1, 3.2 and 3.3. Additionally, appendix B contains three accepted journal articles with the thesis author as co-author (Sapena et al., 2023; Thuro et al., 2020; Breuninger et al., 2021b).

Following, the major articles that comprise this thesis, as well as additional journal articles and conference proceedings by the author that are indirectly a part of this thesis are listed:

- **Gamperl, M.**, Breuninger, T., Singer, J., García-Londoño, C., Menschik, B., & Thuro, K. (2021a). Development of a Landslide Early Warning System in informal settlements in Medellín, Colombia. In Proceedings of the 13th International Symposium on Landslides (pp.8). Cartagena, Colombia: International Society for Soil Mechanics and Geotechnical Engineering.
- **Gamperl, M.**, Singer, J., Garcia-Londoño, C., Seiler, L., Castañeda, J., Cerón-Hernandez, D., & Thuro, K. (2023c). Recommendations for Landslide Early Warning Systems in Informal Settlements Based on a Case Study in Medellín, Colombia. *Land*, 12(7), 1451, doi:10.3390/land12071451.
- **Gamperl, M.**, Singer, J., & Thuro, K. (2021b). Internet of Things Geosensor Network for Cost-Effective Landslide Early Warning Systems. *Sensors*, 21(8), 2609, doi:10.3390/s21082609.
- **Breuninger, T.**, Gamperl, M., Menschik, B., & Thuro, K. (2021a). First Field Findings and their Geological Interpretations at the Study Site Bello Oriente, Medellín, Colombia (Project Inform@Risk). In Proceedings of the 13th International Symposium on Landslides (pp.7). Cartagena, Colombia: International Society for Soil Mechanics and Geotechnical Engineering.
- **Breuninger, T.**, Garcia-Londoño, C., Gamperl, M., & Thuro, K. (2021b). Initial Experiences of Community Involvement in an Early Warning System in Informal Settlements in Medellín, Colombia. In K. Sassa, M. Miko, S. Sassa, P. T. Bobrowsky, K. Takara, & K. Dang (Eds.), *Understanding and Reducing Landslide Disaster Risk* (pp. 597602). Cham: Springer International Publishing. Series Title: ICL Contribution to Landslide Disaster Risk Reduction. http://link.springer.com/10.1007/978-3-030-60196-6_53.
- **Breuninger, T.**, Menschik, B., Demharter, A., Gamperl, M., & Thuro, K. (2021c). Investigation

of Critical Geotechnical, Petrological and Mineralogical Parameters for Landslides in Deeply Weathered Dunite Rock (Medellín, Colombia). *International Journal of Environmental Research and Public Health*, 18(21), doi:10.3390/ijerph182111141.

- Thuro, K., Singer, J., Menschik, B., Breuninger, T., & **Gamperl, M.** (2020). Development of a Landslide Early Warning System in informal settlements in Medellín, Colombia. *Geomechanics and Tunneling*, 13(1), 103115, doi:10.1002/geot.201900071.
- Singer, J., Thuro, K., **Gamperl, M.**, Breuninger, T., & Menschik, B. (2021). Technical Concepts for an Early Warning System for Rainfall Induced Landslides in Informal Settlements. In N. Casagli, V. Tofani, K. Sassa, P. T. Bobrowsky, & K. Takara (Eds.), *Understanding and Reducing Landslide Disaster Risk: Volume 3 Monitoring and Early Warning* (pp. 209215). Cham: Springer International Publishing. https://doi.org/10.1007/978-3-030-60311-3_24.
- Sapena, M., **Gamperl, M.**, Kühnl, M., Singer, J., Garcia-Londoño, C., & Taubenbock, H. (2023). Cost estimation for the instrumentalization of Early Warning Systems in landslide prone areas. *Natural Hazards and Earth System Sciences*, preprint, <https://doi.org/10.5194/nhess-2023-41>.
- Werthmann, C., Sapena, M., Kühnl, M., Singer, J., Garcia, C., Breuninger, T., **Gamperl, M.**, Menschik, B., Schäfer, H., Schröck, S., Seiler, L., Thuro, K. & Taubenböck, H. (2023). Insights into the Development of a Landslide Early Warning System Prototype in an Informal Settlement: the Case of Bello Oriente in Medellín, Colombia. *Natural Hazards and Earth System Sciences*, preprint, 2023.

2. Background

2.1. Landslide Early Warning Systems

By the United Nations General Assembly, a framework for disaster reduction was written in March 2015 (Sendai framework). It aims at reducing global disaster mortality, number of affected people, economic loss and damage to critical infrastructure in the timespan from 2015 to 2030 (UNDRR, 2015). One of seven targets to achieve this is by increasing people's access to multi-hazard early warning systems, including disaster risk information and risk assessment. Therefore, EWSs are pivotal mechanisms in disaster risk reduction strategies. If successful, they can provide timely and accurate information to mitigate the impact of hazardous events (Calvello, 2017; Thiebes & Glade, 2016). As societies become increasingly vulnerable to a spectrum of natural and anthropogenic threats, the development and implementation of sophisticated EWSs is becoming more and more important (Basher, 2006).

EWSs for landslides exist since around the 1980s. They usually consist of four main components: (1) disaster risk knowledge (2) hazard monitoring, analysis and forecasting (3) warning dissemination and communication, and (4) response capability (Basher, 2006). The effective functioning of such a system relies on the coordination of these four interconnected elements both within sectors and across multiple levels. Additionally, a feedback mechanism must be integrated to ensure continuous improvement. A breakdown in any of these components or a failure to synchronize them could result in the overall system's collapse. The term 'early warning' refers to the point in time at which a warning can be issued relative to the actual event. The warning should therefore happen with sufficient time prior to the event, so that warnings can be issued and, if necessary, evacuation measures can be taken.

Modern EWSs are also evolving towards an integrated and multi-hazard approach, recognizing the interconnectedness of hazards and their cascading impacts. By incorporating data from different sources and considering multiple hazards, EWSs can provide comprehensive risk assessments and more accurate early alerts. This approach facilitates a holistic understanding of complex risk scenarios, aiding decision-makers in devising effective response strategies (UNDRR, 2015).

2.1.1. Local versus Regional Landslide Early Warning Systems

Recent advancements in sensor technology, data analytics, and communication systems have significantly bolstered the effectiveness of EWSs. Real-time data collection through various sensors, including seismic, meteorological, hydrological, and remote sensing devices, enables constantly improving event detection and accurate forecasting (Kühnl et al., 2021; Deng et al., 2021; Pradhan et al., 2019; Wu et al., 2020; Fiolleau & Uhlemann, 2022). These technologies can be integrated with robust data processing techniques, such as machine learning algorithms and artificial intelligence, to enhance prediction accuracy and reduce false alarms (Linardos et al., 2022; Dong et al., 2020).

The difference between regional (also referred to as territorial) and local LEWSs can be drawn by the size of the area of interest (Guzzetti et al., 2008). Usually, if a larger region is investigated - which can

range from a municipality to a whole nation (even a global scale has been suggested (Guzzetti et al., 2008)) - no measurements on-site are being made and the parameters are obtained by remote sensing methods (Cepeda et al., 2020; Guzzetti et al., 2020; Piciullo et al., 2018). Sometimes, some precipitation measurements in the area of interest are taken into consideration, but usually no deformation measurements are taken and the emphasis is put on rainfall measurements (Harilal et al., 2019; Lee et al., 2001). Thus, while a general assessment of endangered slopes can be made, identification of single slopes that are likely to fail is not possible at this point (Thiebes & Glade, 2016).

Such regional systems are widespread globally by now. The first LEWS "Landslip" is active since 1977 in Hongkong and proved to be effective in reducing fatal landslides by introducing slope management and educational campaigns (Malon, 1997; Wong et al., 2014). In Italy, regional LEWSs are also commonly used (Piciullo et al., 2017; Tiranti & Rabuffetti, 2010; Tiranti et al., 2019; Segoni et al., 2015) as well as in other parts of Asia (Liao et al., 2010; Harilal et al., 2019; Osanai et al., 2010; Chen et al., 2019; Hidayat et al., 2019). There also are examples for regional systems in Colombia and Antioquia, which provide early warnings based on susceptibility maps and rainfall thresholds (Aristizábal et al., 2010; Gutiérrez Alvis et al., 2018; Huggel et al., 2010, 2008). The model TRIGRS developed by Baum et al. (2008) is used by some researchers in the Aburrá Valley to predict shallow landslides, which could be the basis of a future regional system (Marín et al., 2019; Marin, 2020; García-Aristizábal et al., 2019). The national-scale LEWS IDEAM combines daily precipitation forecasts and a susceptibility map to indicate the daily threat of landslides, which are not further distinguished in the system (IDEAM - Instituto de Hidrología, Meteorología y Estudios Ambientales, 2020).

Local systems on the other hand are usually slope-scale in dimension, or only cover one more or less active landslide (Pecoraro et al., 2019; Thiebes & Glade, 2016). In both cases, the area of interest is usually densely monitored with deformation- and/or hydrological measurements of varying degrees of technical complexity and, accordingly, cost. The most important factors found by Pecoraro et al. (2019) were displacement measurements, and groundwater- as well as precipitation measurements, as the latter is the most important trigger for landslides (Chae et al., 2017). Alarms or warnings can therefore be given with much greater confidence on basis of thresholds, which have to be determined in a preliminary training phase (Thuro et al., 2013). Examples for such systems differ mostly in the type of measurement system applied (see section 2.2), and the efforts put into community integration (see section 2.1.2). A review of local systems is given by Pecoraro et al. (2019). Abraham et al. (2020) used field monitoring in a large area in combination with rainfall thresholds to get the advantages of both ground sensor data and large-scale regional analysis, improving the efficiency of the model by 8%.

The four components of a LEWS (section 2.1) are more important in local LEWSs: Especially warning dissemination and response capability have to be coordinated and communicated with the inhabitants (if applicable) much more in detail than for a regional system. This requires training and communication efforts by the team implementing the LEWS (more on this in section 2.1.2). Depending on the type of system, this effort can be equal to the effort for the measurement system (Breuninger et al., 2021a; Werthmann et al., 2023). One step further in the direction of community integration are integrated LEWS, which will be the topic of the following section.

2.1.2. Integrated (Landslide) Early Warning Systems

The idea with integrated LEWSs is that, as the name suggests, they are integrated into the social structure of the area they are located in (Fathani et al., 2017; UN-ISDR, 2006). An other name for such systems would be community-based EWSs. In such systems, the overall design is user-centered and built on engagement by the community, an emphasis is thus put on the "last mile" (Karnawati et al., 2011). By involving local communities in system development, tailoring alerts to specific user needs, and utilizing various communication channels (e.g., mobile apps, social media, sirens), such LEWSs enhance their reach and impact (Marchezini et al., 2018). Since the effectiveness of early warning systems hinges on their ability to deliver timely alerts and information to end-users, integrated LEWS emphasize user-centered design principles and community engagement and can also be called a "hybrid socio-technical approach" (Karnawati et al., 2011). As the technological part of a LEWS is often more advanced and relatively easy to implement, the weak link often is the communication between the actors (Baudoin et al., 2016; Garcia & Fearnley, 2012). It is important that many different actors are included in such systems, including policy-makers, first responders and especially NGOs (Lassa, 2018). Interdisciplinary teams have proven to be most effective in bringing together these different actors (Baudoin et al., 2016; Alexander, 1989).

To meet the goals of the Sendai Framework mentioned previously, a new standard for integrated or community based EWS has been developed by the Indonesian disaster management authority (BNPB, Fathani et al. (2023, 2016)): ISO 22327:2018 (ISO International Organization for Standardization, 2018). The goal of this standard is to have a baseline for a simple and low-cost EWS. Details on how to accomplish such a system are not given in the ISO, since the measures have to be adopted to the conditions on-site. Nevertheless, examples are given how an integrated system should be structured in its organizational framework and how for example the flow of warning information should be between sensors, experts (here called "Disaster Preparedness team"), authorities and vulnerable people. Also, optional and necessary monitoring devices are listed. The former are rain gauges and surface deformation meters (extensometers and tiltmeters), for the latter, under ground deformation meters, groundwater level meters, pore water pressure sensors, soil moisture sensors and survey stakes (manual sort of crack-meters) are given as examples. Such survey stakes or manual sensors have been employed in several studies, for example by Breuninger et al. (2021a) or Bandara et al. (2013).

2.2. Monitoring Systems

No LEWS can be successful without an effective monitoring system which produces reliable and continuous data on the site. Depending on the scope (regional/local) of the LEWS, varying levels of detail are necessary with regard to the monitoring system. Some regional systems, for example, measure only one parameter, precipitation, on a large scale using radar systems or rain gauges. On basis of this single parameter, hazard levels are calculated with static ground factors such as geology or ground inclination (Piciullo et al., 2017; Aristizábal et al., 2010; Pecoraro et al., 2017). Local- or slope-scale systems, on the other hand, due to more information available on the ground conditions, can often be monitored in a much more detailed manner including both deformation- and trigger measurements. This includes very sophisticated, high-tech monitoring systems such as Radar-interferometry and low-tech

systems such as manual crackmeters.

Following is an overview of current monitoring systems, with an emphasis on local LEWSs. Examples for different monitoring systems, with or without an attached EWS are given also. An effort will be made in comparing these systems with regard to their spatial and temporal measurement density, availability and reliability, capability to measure deformation- and/or trigger signals and, of course, their economic costs. The systems are compared in summary in table 1. Note that in table 1, costs are defined by the authors after discussion with various experts and are not based on literature references. One reason for this is that studies on monitoring systems for LEWS often omit the question of cost, even though it is one of the most important parameters (Gamperl et al., 2021; Pecoraro et al., 2019; Baro & Supper, 2013). Other systems like geophysical methods or elastic wave velocity, which have been used only punctually, are not included (Whiteley et al., 2020; Uhlemann et al., 2017; Chen et al., 2018). Traditional monitoring methods such as piezometers, inclinometers and others are not included as they are often used in combination with one other main measurement system or component.

Table 1 Qualitative comparison of measurement systems for landslide monitoring- and early warning systems.

Measurement System	Deformation	Trigger	Spatial Density	Temporal Density	Availability/Reliability	Cost
GNSS	✓	x	-	+	+	- / 0
Tacheometry	✓	x	-	+	-	-
Photogrammetry	✓	x	+	0	-	+
GB-InSAR	(✓)	x	+	+	0	-
SB-InSAR	(✓)	x	0	-	-	-
Fibre Optics	(✓)	x	0	+	+	-
TDR/CSM	(✓)	x	0	+	+	0
Geo-Sensor Network	(✓)	✓	-	+	+	+ / 0

2.2.1. GNSS/GPS

Monitoring of landslides using Global Navigation Satellite System (GNSS) is one of the most prominent methods currently used. With Real-time Kinematic Positioning (RTK), very precise measurements can be made which provide detailed insights into deformations on the surface of a landslide (Huang et al., 2023). Thus, this method is easy to implement and its application is comparatively straightforward. The temporal density is very good if automatic measurements are being made. Disadvantages are that deformations can commonly only be measured on the surface - subsurface tilting for example is not covered. Also, only point measurements are possible, and therefore not the whole slope can be monitored at once. The costs are comparably high, depending on the size of the landslide and the type of GNSS positioning being used (RTK vs PPP - Precise Point Positioning). Low-Cost GNSS tools are becoming more and more precise and will likely become important tools for low-cost EWS in the future (Tu et al., 2013; Thuro et al., 2014; Notti et al., 2020; Benoit et al., 2015).

2.2.2. Tacheometry

With tacheometry, highly accurate measurements can be made from a tacheometer, which is located on stable ground and can automatically measure multiple target points. This method is advantageous if extreme demands are put onto the precision and costs are not as much of a factor. In combination with for example TDR and GNSS systems, it can be of great help (Thuro et al., 2009). Similar to GNSS, only point measurements are made, so the spatial density is not optimal.

2.2.3. Photogrammetry

Photogrammetry can be used on image information, derived from aerial photographs of unmanned aerial vehicles (UAVs), plane flights or satellites (Hermle et al., 2021). The advantage is the achievable spatial density. Area-wide, direct information on deformation on the surface can be obtained and surface displacements can be measured and the size of landslides can be determined easily (Walstra et al., 2007). The precision of this information is dependent on the resolution of the images. The temporal density also depends on the type of input data - if satellite images are used, the time spans can range from days to years. If an UAV is used, custom intervals can be defined, depending on the obtained deformation rates. Also, usually much higher resolution can be obtained this way. The availability of this method also depends: while satellite data generally has become much easier available in the last decades, very precise data is still usually not open data and thus costly, if obtainable at all by observers. The disadvantages of using an UAV are that, firstly, intensive field surveys are necessary and secondly, in inhabited areas it is usually not well perceived to have drones flying above the houses in regular intervals. An additional option is the use of close range photogrammetry (CRP), a very cost-effective, yet high-effort solution (Mohd Mokhtar et al., 2021).

2.2.4. Radar interferometry (GB-InSAR/SB-InSAR)

Both ground-based and satellite-based interferometric synthetic aperture radar (GB-InSAR/SB-InSAR) are methods which can measure deformation with excellent precision (up to sub-mm, Monserrat et al. (2014)). Microwave signals are sent and received by a radar sensor while the latter moves on a rail which can be of varying sizes. Additionally, soil-moisture measurements for the top soil layer can be obtained (Thiebes & Glade, 2016). An advantage is that large areas can be monitored with little effort, that is, if sufficient funds are available as a GB-InSAR device is rather expensive. A drawback is that measurements perpendicular to the line of sight cannot be measured using this method (Monserrat et al., 2014) and it is dependent on a clear line of sight, albeit this is not as important as with photogrammetry. GB-InSAR is often used on sites where an initial movement has occurred and the subsequent deformations on the slope are to be observed continually, as for example was the case at the Preonzo rockslope failure in Switzerland (Loew et al., 2017) or the 2023 Brienz rockslide where a GB-InSAR system was combined with a Doppler radar rockfall system (Schneider et al., 2023).

2.2.5. Fiber Optics & TDR

For this method, a fiber optic cable is installed in the subsurface, most commonly in boreholes, which can provide multiple parameters such as soil temperature, strain and indirectly moisture content, along the cable (Moore et al., 2010; Ye et al., 2022). The cable is installed in a loose tube and can be installed vertically (or horizontally). A signal is sent through the cable and partly reflected on areas of strain,

allowing the measurement of this reflection and thus identifying the strain location very precisely. The system therefore offers a very high temporal density (measurements can be made almost continually) and can be installed relatively easily. The spatial density along the line is also very good, but between such measurement lines, no measurements are available, naturally, which limits this method to a certain degree. Costs are relatively high, unfortunately.

TDR (Time Domain Reflectometry) is a similar system where a coaxial cable is used instead, which can be installed vertically in boreholes or horizontally in trenches. Here, an electric pulse is sent through the cable and reflected on parts where the cable is deformed due to the change in distance between the two conductors (Singer et al., 2010). The cable is embedded in grout, and when a shear deformation occurs, the grout breaks and thus creates a distinct shear zone where the signal can be reflected clearly. By the grout's composition the sensitivity and amount of shear deformation the cable can withstand before breaking is controlled. If the system is calibrated well, not only the exact location of the deformation, but even the amount of shear deformation can be obtained, as shown by Thuro et al. (2010). The latter is possible with the so called "Continuous Shear Monitor (CSM)" which was developed by Singer (2019).

Fiber optics and especially TDR have the advantage of a high temporal density and higher reliability than commonly used inclinometer systems. Also, the cost is significantly lower than a comparable, yet higher precision, chain inclinometer system. The high effort for digging trenches can be lowered by combining the installation works with for example road works or additional installation of drainages or extensometer systems (Singer, 2019).

2.2.6. Geo-Sensor- Networks and Low-Cost Sensors

Geo-sensor networks (GSN) are a relatively new method compared to some of the systems above. First systems have been in use since the early 2000s (Nittel et al., 2004; Thuro et al., 2011; Fernandez-Steeger et al., 2009). A GSN is a wireless network of nodes that monitor parameters in geographic space. They usually have at least (1) a microcontroller for computing tasks; (2) a wireless transceiver for communication and (3) one or multiple sensors for measuring tasks (Duckham, 2013). The sensors can for example be of acoustic, chemical, electromagnetic, optical, thermal or mechanical type. It is important to make a distinction between a sensor node from the sensor s.s.: the latter is only one part of the former, and usually only able to monitor one parameter, such as temperature. A sensor node on the other hand can include multiple sensors of different types (Duckham, 2013). The crux of modern GSN are their data transmission systems: they determine datarate, transmission intervals and power usage, and thus which sensors can be used in the system.

Following, the topics of sensors and data transmission are described in more detail.

Low-Cost Sensors

While the type of data transmission determines which sensors are used, the sensors in use determine the type of system and the type of landslides that can be measured. Sensors that have been in use in

GSNs for landslide monitoring range from low-cost GPS receivers (Benoit et al., 2015), smart boulders (Dini et al., 2021), to rain gauges (Ramesh, 2009) and tiltmeters (Uchimura et al., 2010, 2015; Dikshit et al., 2018) or a combination of these (Yang et al., 2017, 2020). Recently, also low-cost acoustic emission monitoring has also been applied for early warning (Dixon et al., 2018). This method is based on detecting transient elastic waves travelling through the underground materials (Jurich & Miller, 1987). Another example would be the alpEWAS system installed in the Bavarian Alps (Aggenalm) in 2007-2010 (Thuro et al., 2011). This system combined multiple measurement methods already explained above such as TDR in boreholes, reflectorless video tacheometry and a GNSS point sensor network.

Recent low-cost monitoring systems have increasingly been based on MEMS (micro-electro-mechanical system) sensors. They are small sensors with usually low cost because of their high production numbers. They can be used for different measurement tasks such as acceleration, humidity and temperature and are easy to attach to dataloggers and implement in a larger sensor and monitoring setup. The most common use of MEMS sensors are as tilt sensors. Accelerometers can be used for this purpose, given the sensor is precise enough (Cmielewski et al., 2013). Dikshit et al. (2018) use tilting sensors at shallow depths to measure small changes in inclination in combination with long-term GPS and radar monitoring to measure long-term displacements of the overall slopes. This development was based on the works of Uchimura et al. (2010) who reported in detail how tilt sensors can be applied monitoring of shallow landslides and tested this in the laboratory. The setup was subsequently tested in the field (Uchimura et al., 2015) and developed further into a multi-segment inclinometer which works similarly to a conventional in-place inclinometer. The tilting sensors were amended by water content sensors also on MEMS basis. A methodically similar study has been performed by Lin et al. (2017), with test sites in Taiwan and Japan. Both studies defined precaution levels at tilting rates of $0.01^\circ/\text{h}$ and warning levels at $0.1^\circ/\text{h}$ and Lin et al. (2017) concluded that the system costs one-third of comparable monitoring methods, allowing more monitoring points on slopes.

Data transmission and distribution - the Internet of Things

Systems in which sensors are linked within a network, are described by the term Internet of Things (IoT). Such systems exist much longer than this term though, which is only around since 1999 (Lueth, 2014). First IoT systems for LEWSs, as described above, used mainly multi-hop networks which used short range communication between sensors (Centenaro et al., 2016; Fernandez-Steeger et al., 2009), or cellular technologies which have longer range but use a lot of power (2G/GSM or GPRS). In the last decade, systems using low-power and low bandwidth in long range sub-gigahertz frequency bands have become the most commonly used data transmission tools for GSNs and a common tool used in IoT generally. For LEWSs, these so called low-power wide area networks (LPWANs) have advantages over usually more widespread wireless networks such as Wi-Fi or bluetooth: they have a very low power consumption and can send and receive data over distances of 2-15 km depending on the line of sight and other factors (LoRa Alliance, 2019; Mekki et al., 2019; Centenaro et al., 2016). The most popular LPWANs are currently LoRa/LoRaWAN and Sigfox. These two advantages come at cost of the possible datarate: 243 bytes is the maximum amount that LoRa technology can send in one package, the comparable Sigfox specification only sends 12 byte long payloads. Thus, many newly developed

systems rely on LoRa (Cecílio et al., 2020; Dini et al., 2021; Moulat et al., 2018) or comparable LPWANs (Duc-Tan et al., 2015; Giorgetti et al., 2016; Ramesh, 2009).

Generally, LPWANs consist of four layers: the Perception Layer, the Network Layer, the Middle-ware Layer and the Application Layer (Oguz et al., 2019). IoT devices (nodes) form the Perception Layer and send the data they collect, using the Network Layer, to the Middle-ware Layer (gateway), where the data is stored and processed for user display in the Application Layer (Web-interface, app, or similar). In such a construct, nodes almost exclusively send data to the Middle-ware Layer (uplink), but some LPWANs allow for downlink data transfer. This is useful if commands are to be sent to nodes, for example to change measurement types or intervals.

3. Scientific Articles

The following subsections briefly summarize the full paper journals which are enclosed in the appendix. In addition, the contributions of the authors to the paper are reported using the CRediT (Contributor Roles Taxonomy) author statement.

3.1. Paper 1: Improvement of landslide investigation in deeply weathered Ultramafites by parallelizing ERT with direct field observations

The threat of landslides to lives of inhabitants in mountainous areas, especially in the global south, is rising due to global warming and increasing population. In Medellín, the second largest city of Colombia, the heavily weathered dunite unit in the east of the city is the most landslide-susceptible unit, where most of the landslides of the last 100 years have taken place (Werthmann et al., 2012). This, together with the rapid population increase in this area increases the danger of more fatalities in the future (Sapena et al., 2022). Thus, the project Inform@Risk aims towards strengthening the resilience of the residents of the area by developing a landslide early warning system for shallow landslides, triggered by rainfall and anthropogenic activities (Garcia-Delgado et al., 2022). For such a system, it is necessary to have a detailed geological-geotechnical assessment as a basis for hazard-and risk evaluation.

The dunite is composed of several minerals prone to weathering and serpentinization processes (Garcia-Casco et al., 2020; Breuninger et al., 2021b). The latter can occur primarily during the formation and exhumation of these rock units, or secondarily with meteoric water (Tobón-Hincapié, 2011). Weathering and serpentinization are also the cause for solution processes resulting in karst-like structures, often called "pseudokarst" structures (Tobón-Hincapié, 2011; Breuninger et al., 2021b; Jairo, 2003).

To investigate the subsurface of the study site Bello Oriente, we employed a multi-step approach, combining electrical resistivity tomography (ERT) perpendicular and parallel along the slope with detailed mapping, deep core drillings, and structural analysis of discontinuities with scanlines (Perrone et al., 2014; PRIEST, 1993). The indirect ERT was performed first to determine the drilling locations and re-evaluated once the cores of the drillings were available, together with the mapping results. This approach allowed us to place the drillings in the areas where they were most efficient and most questions needed to be answered. The drilling results in turn could be used for a more detailed evaluation and calibration of the ERT data.

The first ERT investigation showed a bedrock of heavily weathered ultramafites (dunites & serpentinites) with pseudokarst structures and overlying colluvium material which has been deposited by former landslides. It became apparent that the geological model, based merely on mapping and ERT, was not sufficient to describe the site as the layering of weathered dunite and saprolite on top of non-fractured dunite was not existing. Rather, the drill cores showed that the fractured dunite reaches down more than 50 m in some parts, and there is only little saprolite cover above the fractured bedrock or previously

moved block-in-matrix structure. Additionally, the weathered dunite shows pseudokarst phenomena like karren, dolines and cavities. The results from the structural analysis underline the occurrence of several fracture systems perpendicular and parallel to the slope, both in large and small scale. Based on the results from mapping, drilling and structural analysis, the ERT data were re-evaluated and that way, detailed 2.5D information could be achieved, allowing for a more detailed interpretation and more confident results, showing the deep fracturing and shallow soil cover.

The strong fracturing and alteration of the Medellín Dunite, which was described by Botero Arango (1963) and Breuninger et al. (2021b), could be confirmed and delineated as good as possible with the given investigation density. The ERT transects showed the weathering but could not distinguish block-in matrix material from saprolite in necessary detail (Ündül et al., 2015). For landslide occurrence, both these units are highly susceptible. The cavities in the serpentinites described by Tobón-Hincapié (2011) could be observed in smaller scale, although not in the ERT transects as described by Yassin et al. (2014). Based on these results, a hazard map and subsequently the sensor system for the landslide early warning as well as other mitigative measures could be planned, demonstrating how accurately calibrated electrical resistivity tomography measures combined with direct field and subsurface observations can achieve considerable knowledge increase for landslide hazard assessment in deeply weathered ultramafites.

The corresponding paper (Gamperl et al., 2023a) is fully enclosed in Appendix A-1.

CRedit authorship contribution statement

Conceptualization, M.G., K.T., T.B., B.M.; methodology, M.G. and T.B.; software, M.G.; validation, M.G. and T.B.; investigation, M.G. and T.B.; writing—original draft preparation, M.G.; writing—review and editing, M.G., K.T., B.M. and T.B.; visualization, M.G. and T.B.; project administration, B.M. and K.T.; funding acquisition, B.M. and K.T.

3.2. Paper 2: Internet of Things Geosensor Network for Cost-Effective Landslide Early Warning Systems

Worldwide, cities with mountainous areas struggle with an increasing landslide risk as a consequence of global warming and population growth, especially in low-income informal settlements (Smith et al., 2018). Landslide Early Warning Systems (LEWS) are an effective measure to quickly reduce these risks until long-term risk mitigation measures can be realized (Werthmann et al., 2012). To date however, local LEWS with detailed social work and measurement systems have rarely been implemented in informal settlements due to their high costs and complex operation (Uchimura et al., 2015). To strengthen the resilience of informal settlements, such a system is installed in an informal settlement on the steep slopes of Medellín, Colombia. The project Inform@Risk aims at an integrated LEWS with deep social integration and a low-cost monitoring system (Thuro et al., 2020). To achieve this, the sys-

tem is conceptualized and manufactured by an interdisciplinary group of scientists from Germany and Colombia.

The neighborhood "Bello Oriente" was selected as a pilot site based on numerous criteria such as hazard level, social structure and building density. The measurement system for the LEWS is based on modern Internet of Things (IoT) technologies such as micro-electro-mechanical systems (MEMS) sensors and the LoRa (Long Range) communication protocol, to create a cost-effective geosensor network specifically designed for use in a LEWS for informal settlements (Oguz et al., 2019; Mekki et al., 2019; Duc-Tan et al., 2015).

The system consists of a geosensor network (GSN) of versatile LoRa sensor nodes which have a set of MEMS sensors such as tilt and temperature sensors on board. These MEMS sensors can be connected to various different external sensors including a newly developed low cost subsurface sensor probe (SSP) for the detection of ground movements and groundwater level measurements. This sensor probe allows the installation of a chain of tilt sensors, creating a "Low Cost Chain Inclinator". The sensors are based on a single-design circuit board centered around an Arduino microprocessor with a LoRa module and analog-digital converters as well as digital connections on board. This point-based geosensor network is amended by other measurement systems such as the Continuous Shear Monitor (CSM) and extensometers in horizontal and vertical lines (Singer, 2019; Singer et al., 2021, 2010) and piezometers and inclinometers in drillings. These sensors are designed to monitor movement and deformation of the subsurface or existing infrastructure, as well as changes in groundwater levels. The sensor locations are statistically distributed based on landslide risk and detailed mapping of possible sensor locations on-site. The system was tested on a site in southern Germany, where some LoRa nodes were installed on a small landslide site and evaluated regarding durability, installation and power consumption.

All data of the system is being collected by multiple gateways using LoRa communication (GSN) or cable connections (measurement lines) and sent to a central server, where it is stored and analyzed by a flexible data management and analysis system (Singer et al., 2021). The data collected by the sensors is processed and analyzed to assess short- to medium-term hazard levels, and early warnings and alarms are issued if deformation is detected. Sensitivity analyses are planned using geological/geomechanical models created during the hazard analysis, as well as timeseries-analyses performed on the collected data. The thresholds used for the different sensor types at the different locations are first determined based on these analyses and include absolute values as well as rates where applicable (e.g., deformation rate). Later with increasing length of observation, the thresholds are adapted using the results from timeseries-analyses performed on the collected data. This also includes trigger information, especially for rainfall, one of the most important trigger factors.

To incorporate the local community into the development of the EWS, concepts are presented on the participation of local residents in the development and implementation of the LEWS. This is essential for the success, as it helps build trust and ensures that the system is designed to meet the specific needs of the community. Therefore a mobile app is planned as access medium for the local people,

which is developed currently by THD. The app should allow community members to access real-time data on landslide risks and receive early warnings and alarms.

There are many challenges still in the field of monitoring systems and LEWS for informal settlements. LEWS can help reduce the loss of life and property damage caused by landslides, and can also help improve the resilience of communities to future landslide events. It is necessary to have a comprehensive approach to risk reduction that includes both structural and non-structural measures, and to have community participation in the whole process of development and implementation of LEWS. This is why all the newly developed hardware and firmware is open source and can be replicated freely. Some of the newly developed sensor systems are not as precise as high-quality geotechnical sensors, but they are very cost-effective and offer a new tool for landslide monitoring and LEWSs in informal settlements.

The corresponding paper (Gamperl et al., 2021) is fully enclosed in Appendix A-2.

CRedit authorship contribution statement

Conceptualization, J.S. and M.G.; methodology, J.S. and M.G.; software, M.G.; validation, M.G. and J.S.; investigation, J.S. and M.G.; resources, J.S. and M.G.; writing—original draft preparation, M.G.; writing—review and editing, J.S., K.T. and M.G.; visualization, M.G.; supervision, J.S. and K.T.; project administration, J.S. and K.T.; funding acquisition, J.S. and K.T.

3.3. Paper 3: Recommendations for Landslide Early Warning Systems in Informal Settlements Based on a Case Study in Medellín, Colombia

Fatalities from landslides are rising worldwide, especially in cities in mountainous regions which are often expanding into the steep slopes surrounding them (Haque et al., 2019). For residents, often living in poor neighborhoods and informal settlements in such steep areas, this means that their lives and homes are at risk (Pollock & Wartman, 2020). As resettlement is often not possible, integrated landslide early warning systems (LEWS) can be a viable solution if they are affordable and easily replicable (Smith et al., 2020; Eberhardt et al., 2008). Such a LEWS should be adapted to the local situation and be integrated into the social structure of the neighborhood. All parts of the LEWS, risk management, monitoring and forecasting, risk analysis, alert dissemination, and reaction capacity, should be integrated into and developed with the local community. Thus, interdisciplinary teams are needed consisting of geengineers, social workers, administrative personnel and much more (Sharma, 2021).

We developed a LEWS in Medellín, Colombia with the abovementioned goals in mind, which can be applied in such semi-urban situations. All the components of the LEWS, from hazard and risk assessment to the monitoring system and the reaction capacity have been developed with and are supported by all local stakeholders including local authorities, agencies, NGO's and especially the local commu-

nity to build up trust (Breuninger et al., 2021a). It is well integrated into the social structure of the neighborhood, while still delivering precise and dense deformation and trigger measurements (Singer et al., 2021).

The prototype system has been built and installed in 2022 comprising a dense network of line- and point measurements and gateways (Gamperl et al., 2021). A total 111 measurement nodes, over 1 km of horizontal measurement lines, and three gateways were installed on site. All four components of the LEWS have a community component to them, which is described in detail. First thresholds of the monitoring system could be defined and are updated as more and more data is available from the system. Additionally, all newly developed knowledge, from sensor hardware and software to installation manuals have been compiled on a new wiki-page to facilitate distribution of the individual parts and, hopefully, replication of the (adapted) system in other parts of the world.

Due to the experiences made during the conceptualization and installation of the LEWS, we are able to also give recommendations for the implementation of LEWSs in similar, inhabited and landslide-prone areas, based on the ISO 22327 (ISO International Organization for Standardization, 2018; Fathani et al., 2023). We based the recommendations again on the four components of an EWS and also give an example how an organizational framework for such systems could look. These recommendations, together with the ISO norm, can possibly be a tool for people who want to implement similar systems. We also intend the wiki-page to be an exchange platform, where interested parties can share their designs and ideas, which in turn can be used, modified and replicated by others.

Our installation of the system at the test site proved, on one hand, that such systems are technically feasible and, on the other hand, showed that substantial efforts need to be made, especially in the field of social integration. The information flow between stakeholders with regular meetings and communication channels is also essential for an effective system. The designs of the sensors, with informative elements and interactive parts such as the smartphone app were essential. At the time of writing, no equipment has been stolen or tampered with, which shows the success of the social work.

An outlook on future data evaluation possibilities is given, for example data fusion methods which can help combine data from different sources to a comprehensive information about early movements with increased warning times. The replication of such systems in other areas is shortly addressed, while an economic estimation is given in (Sapena et al., 2023). The limitations of the system are important to be kept in mind, especially regarding the technical and economic feasibility, which has to be fulfilled for such a system to make sense. Also, if the social structure is too precarious or there are no prevailing organizations doing social work, it might be more effective installing such a system elsewhere, where more results can be expected.

The corresponding paper (Gamperl et al., 2023b) is fully enclosed in Appendix A-3.

CRedit authorship contribution statement

Conceptualization, J.S. and M.G.; methodology, J.S., L.S. and M.G.; software, M.G. and J.S.; validation, M.G., L.S. and J.S.; investigation, J.S., L.S., J.C., D.C., C.G and M.G.; resources, J.S., L.S. and M.G.; writing original draft preparation, M.G., C.G., L.S.; writing review and editing, J.S., K.T., J.C., L.S., C.G and M.G.; visualization, M.G., L.S. and C.G; supervision, J.S. and K.T.; project administration, J.S., C.G. and K.T.; funding acquisition, J.S. and K.T. All authors have read and agreed to the published version of the manuscript.

4. Synopsis and Discussion

The two vectors of increased urbanization and ever stronger weather events due to climate change pose an enormous threat to endangered communities worldwide. This necessitates new and more accessible early warning systems. This thesis, as part of the Inform@Risk project, contributes to finding such new systems. The three parts of this thesis aim at covering the gap between geologic-geotechnical investigation, sensor design and their installation and integration into public space. Ultimately, recommendations are given on how such a system might be replicated in the future, embedded in larger frameworks such as the ISO 22327. In the following, three topics will be discussed in more detail. Several other aspects have been individually discussed in the papers already, which are discussed in summary and the larger perspective of the whole thesis here.

4.1. Geological-Geotechnical Investigation for Local Integrated Early Warning Systems

Detailed geological-geotechnical investigation is essential for hazard and risk assessment, which again is indispensable for local EWSs. Breuninger et al. (2021b) show how the investigation of geotechnical parameters is important for this, and Gamperl et al. (2023a) show how the investigation of the geologic and hydrogeologic situation at an endangered slope can be put through in a multi-step approach. This includes conventional approaches such as mapping, drilling and electrical resistivity tomography, which are applied interconnectedly as to gain the best insight and to use each method to its fullest advantage. The combination of indirect and direct investigation methods proved to be very effective.

While geologic-geotechnical investigation is invaluable for local EWSs, the methodology chosen for the following hazard- and risk assessment is just as important. National or sub-national approaches for hazard- and risk assessment can vary tremendously, which we also experienced with the Inform@Risk project, where the difference between the "Swiss approach" common to the German researchers (Heinimann et al., 1998) was contrasted against the Colombian approach as stated in the POT (Alcaldía de Medellín, 2014): The former proposes a semi-quantitative approach which puts an emphasis on the experience of investigators/geologists to determine event frequencies and magnitudes, while the latter followed a more rigid, yet quantitative approach with a defined workflow including limit-equilibrium models. No matter in which direction the assessment is leaning, it is important that the assessment is made on-site and with the EWS in mind. Overall, weak structures, possible failure locations and possible safe spaces should be checked first and most importantly. As the on-site assessment progresses, the sensor placement can ideally already be kept in mind and should also be based on data obtained on-site. As detailed in Gamperl et al. (2021), only with a sound hazard and risk assessment, when processes are understood by experts and risk managers, can the data of the subsequently installed measurement system be interpreted properly and with confidence.

At the same time, if sensors can be placed confidently on basis of an in-depth hazard and risk assess-

ment, costs can be saved with sensor placement, making the whole system more efficient. Another effect is a better or shorter training phase if causes and effects of landslides in a specific region are well known. Warning thresholds can be primarily set better and deformation rates and tilt directions can be interpreted, again, with more confidence. A future tool for this could be augmented or virtual reality (AR/VR). We used this technology for sensor placement briefly in 2020 when travel was not possible. The 3D model of Bello Oriente was investigated with a VR headset to get a better feeling for building density, structures and materials in order to get a first version of our sensor placement. This proved to be a great time saver, as we obviously could do this in Munich and could jump back and forth freely in the terrain. While this of course this can only be a first, preliminary step towards real, on-site sensor planning, it is definitely helpful and speeds up the time spent in the field tremendously.

4.2. Geosensor Networks and Landslide Early Warning

In order to provide access to LEWSs to the most vulnerable groups, cost effective monitoring solutions are necessary, as shown in section 2.2. We deemed the use of geosensor networks in combination with other low-cost methods such as extensometers and CSM-lines the most effective solution, as summarized in section 3.1. Particularly new developments in the area of the internet of things have led to promising opportunities: Open-source sensor designs are distributed freely, as for example the Arduino MKR WAN 1310 used in the Inform@Risk project, which is sold by Arduino, but can alternatively be reproduced much cheaper and is thus available by other manufacturers for a lower price. But also individual sensor designs of e.g. accelerometers are constantly updated and become more economically feasible. Hopefully, this should allow decisionmakers and communities in areas at risk to reproduce and develop systems more easily.

We found the low-cost sensors to be precise enough for the measurements applied in our system (Gamperl et al., 2023b). While they do not yet reach the precision of high quality geotechnical sensors, the cost is much lower and the advantages outweigh the problems. One has to keep in mind, though, that such sensors usually, because of their low cost, have a higher tendency to failure as conventional sensors (Duckham, 2013). However, it can be expected, as was the experience of the last decade, that the quality and reliability of low-cost IoT sensors will continue to increase. Generally, GSNs can be of advantage also if they do not replace but complement high-tech warning systems (Duckham, 2013; Ciampalini et al., 2021). This is also the case with our system to some extent, as we use inclinometers and piezometers - which are not low-cost - in the vertical drillings in tandem with low-cost extensometer and CSM systems. It can be expected that in future IoT sensors will supplement even more traditional measurement methods, for example for inclinometer measurements in deep drillings or automatic laser distance sensors. Such was the case on the Hochvogel EWS, where a cable-based system was amended and ultimately exchanged for a LoRa system (Leinauer et al., 2021). In summary, future generations of IoT sensors will very likely come in better quality, have lower battery consumption and provide better precision, as for example for low-cost GNSS sensors (more on this in section 5).

There are other measurement systems which will probably become more important in the next decades: More detailed and frequent remote sensing data can lead to improvements especially in the field of

regional EWSs, bridging the gap towards local systems. Increasing processing speeds can lead to more efficient inclusion of photogrammetry data in EWSs. Such larger amounts of sensor data will also be evaluated more quickly by new developments as neural networks. Whether this can provide real prediction possibilities is still doubtful, though.

While data transfer through the network layer in IoT systems is one of its strong points, what is done with this data afterward is just as important. The huge amount of data produced by GSNs can become hard to handle and most of the data collected is not relevant for forecasts or warning. The data collected by one sensor always has to be seen in context with the rest of the system. Duckham (2013) compares data from a single node to a single pixel in a picture or movie. Only when all sensors are viewed together, can the whole frame be understood completely and the datapoints together over time then combine into the movie. This means that, as the amount of data collected increases, the effort for implementing automatic data analysis and interpretation methods has to increase (over-) proportionally - maybe even exponentially. We started thinking about possible options for this (see section 5).

Contemplating the importance of data analysis raises the question: What do the inclination changes tell us about the whole slope, and is the data representative of the changes in the subsurface? Petley et al. (2005) show that depending on the pore pressure conditions locally in the slope, different movement patterns can be observed in a large landslide, differing mostly in strain velocity. It can be expected that in smaller landslides, this effect will be less pronounced, but the change of tilt will still be observable. Such effects and movements need to be observed in further investigations as this is an area where not much experience is available currently. For other types of movement, of course the measurement system has to be adapted. As our developed system is modular, this should be easy to achieve while staying in our overall framework.

4.3. Replication of the Proposed Sensor Network in Other Areas

The replication of such a GSN and how its cost would scale when applied to different areas of Medellín as an example has been studied by Sapena et al. (2023) and is attached in Appendix B-3. The study is in essence a more sophisticated version of the table we used at the beginning of the project in order to find our study site Bello Oriente. In this study, we estimated landslide susceptibility on city scale using existing landslide database entries and topographic and geological factors combined in a random forest model. This gave us exposed, landslide-prone sites. These sites were amongst others filtered for their general suitability for such a GSN. Afterwards, the costs were estimated using a cost function based on the experiences of the pilot project in Bello Oriente. Exact numbers for sensor and installation costs could be used as a basis, although the almost impossible to easily scale CSM-EXT systems were omitted for this study, only using the GSN. Social work was also excluded as it is very hard to calculate and depends highly on local factors such as already existing NGO work in an area. The cost function includes the GSN nodes and gateways.

The results allow authorities to make decisions about where a system would be most cost-effective and where it would affect most people. We ended up with 32 sites with an average population density of

224 people per hectare and a cost ranging from 26000€ to 157000€ or 5€ to 41€ per inhabitant. As an example, it can be shown that with these results, the city could decide how e.g. a fixed amount of money could be used most efficiently for most people, by looking at the estimated cost per person. Also, prioritisation based on e.g. cost per person, susceptibility or vulnerable population is easily possible with such a function.

Such an investigation, while of course only being an estimation, is highly unique as costs for monitoring systems are usually not shared openly and made transparent. This study was possible because the newly developed sensor systems were designed in a modular way which allows easy scalability, according to the project goals (section 1.2). Of course, the calculation is very coarse as the basis of the data is only the one installation in Bello Oriente and changing conditions on-site may still influence the sensor layout, density and functionality on that site. The lack of social work costs in the function of course is a large gap, which can currently not be filled in a meaningful way.

4.4. Integrated Landslide Early Warning Systems: Challenges and Next Steps

Early warning systems can help decrease the landslide risk for vulnerable settlements in hazardous areas. Because those settlements are, more often than not, poor and informal settlements, access to functioning and effective LEWSs can be key for decreasing the growing inequalities around the world (Sorensen, 2000). In such inhabited areas at risk, integrated LEWSs need to be employed in order to include the inhabitants, distribute knowledge and create acceptance for the technical system. Most important for such systems is sustainability - trust needs to and can only be gained over long periods of time, in which community work has to be performed constantly. Next to such social and technical problems, an important, often overlooked topic is financial sustainability: Integrated LEWS projects need constant funds to keep up the social and technical work. If the funding situation is unstable, it becomes difficult to provide the above described sustainability. An example of this is discussed in the next section.

4.4.1. Selected Lessons Learned from Inform@Risk

The Inform@Risk project was successful in building up trust in the local community, even though difficulties through the covid-19 times restricted this to some extent (Werthmann et al., 2023). Yet, after the system was handed over to the authorities in Colombia (DAGR), the technical and especially the community work suffered as social staff could not be appointed in time and other administrative hurdles appeared. In the technical regard, our pilot project has shown that the local knowledge on electronics and programming, as well as geological topics such as landslide- and weathering processes need to be strengthened. This is not to say that the geological and technical training in Colombia generally is not sufficient - quite the opposite is the case. Yet, more efforts need to be put into training local knowledge instead of bringing in knowledge from extraneous countries and regions, developing a project, and then draining that knowledge away again when such a project ends. We tried to prevent this by working closely with the local authorities on risk management (DAGR) and trying to get them to be

as active as possible already in the development of the project. Unfortunately, the covid-crisis hindered us in building trust on-site early in the project, and we could not completely bridge this gap in the year of installation we had left after travel was possible again. At the same time it became evident that the political situation in Medellín was also not helping this approach: Short-term contracts with technicians were a problem in training staff for long-term monitoring and maintenance tasks, but also the local risk management project SIATA was only working and planning from year to year and thus could not be an efficient partner in long term planning of the system and its development. Another administrative hurdle were the often changing heads of departments in Medellín: Before the start of the project, the then leader of SIATA was extremely cooperative and interested and plans were made for close collaboration. Once the project started, a new leader was appointed, who, partly understandable, did not like carrying over that "old" baggage and rather follow their own agenda. Thus, a partner we relied on heavily to be active in development and installation of the system required some encouragement to participate. This was also, to a lesser extent, the case with the DAGRD leadership which also changed during the project. Future similar projects should take care to keep such possibilities in mind and plan everything so that they don't rely too heavily on a single partner - there is not much else one can do, unfortunately. Overall, as could probably be expected, it proved extremely difficult to get all stakeholders together on one table as displayed in figure 1 in Gamperl et al. (2023b). Also, being on the city border meant that things were more complicated as we had to deal with city authorities and - outside of the city - with the authorities of the Aburrá Valley (AMVA) and sometimes unclear jurisdictions. Another organizational issue we ran into too late in the project is customs: We underestimated the amount of time and money needed to send equipment to Colombia and overcome customs and import issues there. Having legal counsel in Colombia from the start of the project would have made sense in hindsight. In summary, from the experiences of more than four years of Inform@Risk, we can confirm that such an integrated EWS relies at least as much on social bonds and time invested as it relies on technical equipment and infrastructure. Ensuring this requires a continuous focus on social involvement, which presents perhaps the most substantial challenge. It should not be exclusively reliant on governmental authorities. To cultivate resilience, it must be firmly rooted within the community, encompassing both social and physical dimensions.

4.4.2. Challenges of Integrated Early Warning Systems

Despite significant progress, challenges persist in the field of early warning systems. These include issues related to data quality, interoperability of systems, institutional coordination, and financial sustainability. Community-centered approaches can also have their disadvantages, as illustrated by Preuner et al. (2017), who describes a system in Austria where the inhabitants did not perceive their integration in the decision-making as positive, and did not want to interfere with the "experts". Generally, the implications of false alarms and the probability of false negative alarms have to be communicated to the inhabitants in a way that they can relate to what is happening in such a case (Thiebes & Glade, 2016). In any case, the limitations of a system should be communicated clearly from the beginning, so there are no false expectations about the safety gained from the system.

4.4.3. Next Steps: Standardization

The small amount of integrated EWS projects implemented worldwide this far shows that these systems are still young and in development. By the ISO 22327 (ISO International Organization for Standardization, 2018) and Fathani et al. (2023), efforts in creating a reproducible standard for integrated EWS was successful. However, this standard is very general and offers little specific guidelines. This shows how difficult it is to establish one standard procedure for EWS, which can be reproduced. The projects of integrated EWS available now rather show new developments every time. This was also the case of our system, which is based on some previous sensor systems (Uchimura et al., 2010; Lin et al., 2017; Dikshit et al., 2018) and ideas for integrated EWS (Garcia & Fearnley, 2012; Smith et al., 2021) but does not follow one previous approach directly. Obviously, it would generally be more efficient to reproduce a system already described before, as shown in section 4.3 and Sapena et al. (2023). Yet, new systems are developed constantly, which is also a good thing, as this field is relatively new and needs as many new impulses as possible. A reason for this is also that conditions in informal settlements can vary tremendously, thus such adaptations are necessary and thus, to a certain extent, such systems will probably always have a "unique" and a "living lab" character (Perlman, 2010; Werthmann, 2023; Hossain et al., 2019). A very promising way to accommodate this while increasing social integration could be to combine such EWSs with citizen science projects, as proposed by Paul et al. (2020) and Pudifoot et al. (2021). Going in this direction requires initially more emphasis on social work, but most likely can result in much better community integration.

Following is an outlook which dives in more detail into what can be done in the future.

5. Outlook

The ideas and solutions proposed in this thesis add a meaningful contribution to the improvement of LEWSs, especially for the use case of informal settlements. Nevertheless, many things can be improved, as with any such new systems. Of course, not only the possible technical improvements mentioned below are needed, but especially with regard to the social integration into the neighborhood, improvements are needed and possible.

5.1. Further improvement of the Inform@Risk Measurement System

5.1.1. Sensor improvements

Despite general improvements possible due to advances in IoT sensors in the last years, several specific improvements on the sensors used in the pilot study in Medellín are thinkable and are described subsequently.

An area in which the design could be improved significantly is the microprocessor unit and the printed circuit board (PCB) itself. Based on the recommendations already given in Gamperl et al. (2021) and Gamperl et al. (2023b), there is room for improvement regarding the hardware, especially considering that it has only gone through two manufactured and on-site tested iterations. Such improvements could produce a (1) more efficient, (2) more reliable and (3) cheaper node. Following are some concrete examples of possible changes to the nodes and subsurface sensors:

- Including the arduino microprocessor and LoRaWAN unit directly on the PCB could significantly reduce manufacturing costs and increase reliability. The node could also be fitted much more efficiently and in a way so that the ports are more accessible in the enclosure.
- The quality of cables and connectors connecting the nodes with power supply and external sensors should be as high as possible as these proved to be weak points of the nodes after some months of use.
- Node installation is somewhat complicated by the Arduino IDE: Since setting up the node during installation cannot be avoided (often the type and amount of attached sensors can only be determined on-site, even if the circumstances seem to be obvious beforehand), it is important to make this as easy as possible in the field. This was not yet the case with the IDE during our pilot study. We tried to mediate the somewhat complicated installation process by only having one document where all the changes can be made quickly, but for technicians with little experience this still complicates the installation task. Therefore, a different solution should be implemented for future systems where changes can be done in a simple selection form.
- The reliability of subsurface sensors could be improved: we experienced some corrosion on the cables and the contacts, while overall the water resistance proved to be sufficient after approximately one year of running.

- The installation of the subsurface sensors has potential for improvement in terms of its ease and practicality.

5.1.2. A Spark for a Do-It-Yourself Landslide Early Warning Community: Further improvements of the Inform@Risk Wiki

As mentioned in section 4.4, the development of integrated EWSs is still in its starting phase. We tried to create a incentive for a community of likeminded experts and stakeholders with the Inform@Risk Wiki page. For us, the wiki page was first and foremost a place to upload all our collected information and to have it available in one location. Yet, our motivation always also was to also use it as a distribution tool for all information that was from the start planned to be freely available under open-source licences. An essential part of this is that anybody can log into our wiki page and add and modify the information there (after registration, of course).

We hope that this site can thus become not only a place to share information, but that a genuine community can form there and in the future similar efforts - which will be needed more year by year - can work together on this platform. This is why we created the wiki in three languages (english, spanish, german) with the possibility to add more. The layout of the wiki reflects the four components of a LEWS (see section 2.1) and therefore is very general in structure. Currently, the wiki is strongly defined by the installation of the LEWS in the pilot project in Medellín, but the descriptions are kept in general terms so that the described methodologies and designs are applicable elsewhere, with the examples coming from the installation in Medellín.

5.2. Data Analysis

The more sensors a monitoring system has, the more important automated mechanisms for data analysis and interpretation become, as mentioned earlier (section 4.2). During our project, we developed the concepts for sensor fusion that could be applied to monitoring systems with multiple sensor and sensor node types in combination. On basis of these concepts, further development is possible and needed. Outside of the aforementioned sensor fusion methods, we consider how a connection between local and regional LEWSs can be made - by expanding sensor systems outside of the local scale and using the data often used in regional scale systems for forecasts in both scales. This is mostly a question of data analysis and explored in the following section on the example of a GIS system combined with a 3D limit equilibrium code. Subsequently, opportunities for data analysis using machine learning and neural networks as well as further data analysis methods which can be used on the data from the Inform@Risk pilot project, are laid out.

5.2.1. Numerical Analysis using a GIS-code in combination with measurement data

Combining the measurement data of a sensor system with deterministic, physically based models could be a promising way towards new LEWSs outside of the categories of local and regional systems. Such, mostly GIS based models, are currently being used for landslide susceptibility mapping mostly. If sensor data could be incorporated in a meaningful way, these models could be used not only for such approaches, but could be implemented in local LEWSs and be key in expanding them to more

widespread, (semi-)regional systems. Such an approach is laid out in this section.

The software `r.slope.stability`, which was created by Martin Mergili in 2014, is a model based on C (model code), Python (parallel implementation) and GRASS GIS (visualization) which uses a 3D sliding surface model by Hovland (1977). The documentation, as of 2023, is very extensive and accessible also for non-programmers (Mergili et al., 2014). The model uses raster files (.tiff or ascii) of various parameters such as elevation, soil classes and depths, groundwater depth and so on. The model then creates output raster maps containing the results such as the factor of safety, failure probability, standard deviation and much more. Additionally, text files documenting the results and surrounding information are printed.

There are a few possible ways to incorporate this – or similar – models with the proposed sensor system and LEWS of this work in the future. Examples are given in the following, sorted in rising complexity:

- Interpolating the live groundwater data from deep drillings and, if applicable, the shallow sensors (SMN and LCI) into a groundwater table raster map in a fixed time scale (for example every 30 minutes) and computing the otherwise static `r.slope.stability` model could be an easy first step of generating 'live' data from the model.
- It should be possible to incorporate a hydrogeologic model and using data from for example a rainfall radar in order to predict the groundwater level in the future, such as in the next 6 hours or next day(s). This groundwater raster could then again be used in the deterministic model to assess the current hazard level.
- Deformation and inclination data is more difficult to include in such a system as the granularity of the sensor system does not fit the granularity of the regional deterministic model. Rather, it could be of use to have a feedback loop from the deterministic model back to the sensor analysis (sensor fusion + thresholds) algorithm as an incentive for a more detailed deformation assessment than what the model would usually have produced. The deterministic model would therefore act as a sort of "top layer" over the sensor fusion decision-making, similar to what Abraham et al. (2020) propose, where tilting angles are used to reduce false alarms.

In conclusion, adding a deterministic model to a local monitoring system adds an easily automatable component. This effort is reasonable only if the input data of the slope at local scale is detailed enough and if the information about factors such as the connection between rainfall and groundwater levels are precise. Generally it would be advisable to only test this in an area where the sensor system has been running for some time ('training phase' was completed) and sufficient geological and hydrogeological data is available to get meaningful results from the model. In such a case, combining the two approaches can lead to (1) larger observed areas with (2) more detail knowledge available. As processor capabilities have improved significantly in the last years, computation times are also not as much a factor any more, allowing larger and more fine grained models.

5.2.2. Data Analysis using Machine Learning and Neural Networks

As stated previously, analyzing the large amounts of data an EWS and especially a GSN produces can become a problem. Machine learning (ML) and neural networks (NN) are being used increasingly in disaster management and for all kinds of disaster types (Linardos et al., 2022). If sufficient training data is available, both can be used to understand complex connections in sensor data, which are not perceivable by humans. ML is currently, amongst others, used in remote sensing (Kühnl et al., 2021), for susceptibility analysis (Pradhan et al., 2019; Zhang et al., 2022b) and for assessment of landslide kinematics with acoustic emissions (Deng et al., 2021). A combination of ML and various sensors in the slope (moisture, displacement, stress) has been proposed by Zhang et al. (2022a), although the setup was only tested in the laboratory. A similar system, but on a field site was installed by Dong et al. (2020) with GPS, inclinometers, tilt meters, crack meters and groundwater level measurements. Displacements were subsequently predicted using ML.

While this field is promising, massive amounts of data are needed, which can be achieved with a GSN. Yet, an equal distribution of sensors on a slope or in an area is advantageous. As before, such a system should be tested on a slope where the mechanisms are understood well and monitoring data of some time is available.

5.2.3. Further data analysis of the Bello Oriente pilot project

The monitoring data of our test site in Bello Oriente can be used for future theses with a focus on the topic of data analysis. While the above described methods for data analysis are promising, such a thesis should start with a simpler approach and consider in the aforementioned pathways at a later stage. We have started setting thresholds for the individual sensor readings such as tilting and groundwater levels (Gamperl et al., 2023b). These thresholds can be fine-tuned about 1-2 years after the installation, when yearly variations can be seen in the data, and maybe even some deformations have occurred, indicating which inclination rates potentially belong to a real event. From individual thresholds one has to look at multiple sensors at the same time and this is where sensor fusion comes into the picture: The distance between sensors should be added as another factor, and the amount of sensors which exceed thresholds should determine the warning level, based on if they are close together (causal relationship likely) or if they are far apart and separated by other sensors with no exceeding (no causal relationship, tampering or other factors likely). In a next step, trigger data, of which there are also good quality measurements available in Bello Oriente (both piezometers and a weather station), should be added into the picture and analyzed in conjunction with deformation data. Thus, the relationships between rainfall and deformations can be analyzed in more detail and the warning times can be assessed better than they are currently.

The installed measurement system, due to the large amount of data collected, is a great "playing field" to try different approaches in order to get the most reliable prediction from data analysis. From the relatively simple sensor fusion methods to more sophisticated (but harder to predict and understand) ML models, several options have been laid out. I think it is important to stress that when working with the data from Bello Oriente, in the (hopefully) air-conditioned office in Colombia or even in Germany, the whole system on-site, not only the technical part but also the people, should always be kept in

mind. Any scientist working on the data should, if possible, make regular field visits, even in a solely data-analysis part of the study.

Bibliography

- Abraham, M. T., Satyam, N., Bulzinetti, M. A., Pradhan, B., Pham, B. T., & Segoni, S. (2020). Using Field-Based Monitoring to Enhance the Performance of Rainfall Thresholds for Landslide Warning. *Water*, 12(12), 3453, doi:10.3390/w12123453. <https://www.mdpi.com/2073-4441/12/12/3453>.
- Alcaldía de Medellín (2014). Acuerdo 48 de 2014, Plan de Ordenamiento Territorial de Medellín. <https://www.medellin.gov.co/es/wp-content/uploads/2022/10/POT-Medellin.pdf>.
- Alexander, D. (1989). Urban landslides. *Progress in Physical Geography: Earth and Environment*, 13(2), 157–189, doi:10.1177/030913338901300201. <http://journals.sagepub.com/doi/10.1177/030913338901300201>.
- Aristizábal, E., Gamboa, M. F., & Leoz, F. J. (2010). Sistema de Alerta Temprana por Movimientos en Masa Inducidos por Lluvia para el Valle de Aburrá, Colombia. *Revista EIA*, 13, 155–169.
- Aristizábal, E. & Sánchez, O. (2020). Spatial and temporal patterns and the socioeconomic impacts of landslides in the tropical and mountainous Colombian Andes. *Disasters*, 44(3), 596–618, doi:10.1111/disa.12391. <https://onlinelibrary.wiley.com/doi/abs/10.1111/disa.12391>.
- Bandara, R. M. S., Bhasin, R. K., Kjekstad, O., & Arambepola, N. M. S. I. (2013). Examples of Cost Effective Practices for Landslide Monitoring for Early Warning in Developing Countries of Asia. In C. Margottini, P. Canuti, & K. Sassa (Eds.), *Landslide Science and Practice* (pp. 581–588). Berlin, Heidelberg: Springer Berlin Heidelberg. http://link.springer.com/10.1007/978-3-642-31445-2_76.
- Baro, I. & Supper, R. (2013). Application and reliability of techniques for landslide site investigation, monitoring and early warning outcomes from a questionnaire study. *Natural Hazards and Earth System Sciences*, 13(12), 3157–3168, doi:10.5194/nhess-13-3157-2013. <https://nhess.copernicus.org/articles/13/3157/2013/>.
- Basher, R. (2006). Global early warning systems for natural hazards: systematic and people-centred. *Philosophical Transactions of the Royal Society A: Mathematical, Physical and Engineering Sciences*, 364(1845), 2167–2182, doi:10.1098/rsta.2006.1819. <https://royalsocietypublishing.org/doi/10.1098/rsta.2006.1819>.
- Baudoin, M.-A., Henly-Shepard, S., Fernando, N., Sitati, A., & Zommers, Z. (2016). From Top-Down to Community-Centric Approaches to Early Warning Systems: Exploring Pathways to Improve Disaster Risk Reduction Through Community Participation. *International Journal of Disaster Risk Science*, 7(2), 163–174, doi:10.1007/s13753-016-0085-6. <http://link.springer.com/10.1007/s13753-016-0085-6>.
- Baum, R. L., Savage, W. Z., & Godt, J. W. (2008). *TRIGRSA Fortran Program for Transient Rainfall Infiltration and Grid-Based Regional Slope-Stability Analysis, Version 2.0*. Open-File Report 2008-1159, U.S. Geological Survey, USA. Series: Open-File Report.

- Benoit, L., Briole, P., Martin, O., Thom, C., Malet, J.-P., & Ulrich, P. (2015). Monitoring landslide displacements with the Geocube wireless network of low-cost GPS. *Engineering Geology*, 195, 111–121, doi:10.1016/j.enggeo.2015.05.020. <https://linkinghub.elsevier.com/retrieve/pii/S001379521500174X>.
- Botero Arango, G. (1963). *Contribución al Conocimiento de la Geología de la Zona Central de Antioquia*. Technical Report 57, Universidad Nacional de Colombia, Medellín.
- Breuninger, T., Garcia-Londoño, C., Gamperl, M., & Thuro, K. (2021a). Initial Experiences of Community Involvement in an Early Warning System in Informal Settlements in Medellín, Colombia. In K. Sassa, M. Miko, S. Sassa, P. T. Bobrowsky, K. Takara, & K. Dang (Eds.), *Understanding and Reducing Landslide Disaster Risk* (pp. 597–602). Cham: Springer International Publishing. Series Title: ICL Contribution to Landslide Disaster Risk Reduction. http://link.springer.com/10.1007/978-3-030-60196-6_53.
- Breuninger, T., Menschik, B., Demharter, A., Gamperl, M., & Thuro, K. (2021b). Investigation of Critical Geotechnical, Petrological and Mineralogical Parameters for Landslides in Deeply Weathered Dunite Rock (Medellín, Colombia). *International Journal of Environmental Research and Public Health*, 18(21), doi:10.3390/ijerph182111141. <https://www.mdpi.com/1660-4601/18/21/11141>.
- Calvello, M. (2017). Early warning strategies to cope with landslide risk. *Rivista Italiana di Geotecnica*, (pp.30), doi:10.19199/2017.2.0557-1405.063.
- Cecílio, J., Ferreira, P. M., & Casimiro, A. (2020). Evaluation of LoRa Technology in Flooding Prevention Scenarios. *Sensors*, 20(14), 4034, doi:10.3390/s20144034. <https://www.mdpi.com/1424-8220/20/14/4034>.
- Centenaro, M., Vangelista, L., Zanella, A., & Zorzi, M. (2016). Long-range communications in unlicensed bands: the rising stars in the IoT and smart city scenarios. *IEEE Wireless Communications*, 23(5), 60–67, doi:10.1109/MWC.2016.7721743. <http://ieeexplore.ieee.org/document/7721743/>.
- Cepeda, J., Luca, P., Davide, T., Gaetano, P., & Michele, C. (2020). *Comparison of the performance of different Territorial Landslide Early Warning Systems*. other, display. <https://meetingorganizer.copernicus.org/EGU2020/EGU2020-21648.html>.
- Chae, B.-G., Park, H.-J., Catani, F., Simoni, A., & Berti, M. (2017). Landslide prediction, monitoring and early warning: a concise review of state-of-the-art. *Geosciences Journal*, 21(6), 1033–1070, doi:10.1007/s12303-017-0034-4. <http://link.springer.com/10.1007/s12303-017-0034-4>.
- Chen, Y., Irfan, M., Uchimura, T., Cheng, G., & Nie, W. (2018). Elastic wave velocity monitoring as an emerging technique for rainfall-induced landslide prediction. *Landslides*, 15(6), 1155–1172, doi:10.1007/s10346-017-0943-3. <http://link.springer.com/10.1007/s10346-017-0943-3>.
- Chen, Y., Irfan, M., Uchimura, T., Wu, Y., & Yu, F. (2019). Development of elastic wave velocity threshold for rainfall-induced landslide prediction and early warning. *Landslides*, 16(5), 955–968, doi:10.1007/s10346-019-01138-2. <http://link.springer.com/10.1007/s10346-019-01138-2>.
- Ciampalini, A., et al. (2021). Integration of Satellite InSAR with a Wireless Network of Geotechnical Sensors for Slope Monitoring in Urban Areas: The Pariana Landslide Case (Massa, Italy). *Remote Sensing*, 13(13), 2534, doi:10.3390/rs13132534. <https://www.mdpi.com/2072-4292/13/13/2534>.

- Cmielewski, B., Kontny, B., & mielewski, Kazimierz (2013). Use of low-cost MEMS technology in early warning system against landslide threats. *Acta Geodynamica et Geomaterialia*, 10(4), 485–490, doi:10.13168/AGG.2013.0049. http://www.irms.cas.cz/index_en.php?page=acta_detail_doi&id=59.
- Copernicus (2023). Global Flood Awareness System (GloFAS). <https://www.globalfloods.eu/general-information/about-glofas/>.
- Coupé, F., Arboleda G., E., & Garcia L., C. (2007). Villa tina: Algunas reflexiones 20 años después de la tragedia. *Gestión y Ambiente*, 10(2), 31–52.
- Crozier, M. (2010). Deciphering the effect of climate change on landslide activity: A review. *Geomorphology*, 124(3-4), 260–267, doi:10.1016/j.geomorph.2010.04.009. <https://linkinghub.elsevier.com/retrieve/pii/S0169555X10001881>.
- Cruden, D. & Varnes, D. (1996). Landslide Types and Processes. In A. K. Turner & R. L. Schuster (Eds.), *Landslides: investigation and mitigation*, number 247 in Special report (pp. 685). Washington, D.C: Transport Research Board, National Research Council.
- Deng, L., Smith, A., Dixon, N., & Yuan, H. (2021). Automatic classification of landslide kinematics using acoustic emission measurements and machine learning. *Landslides*, 18(8), 2959–2974, doi:10.1007/s10346-021-01676-8. <https://link.springer.com/10.1007/s10346-021-01676-8>.
- Dikshit, A., Satyam, D. N., & Towhata, I. (2018). Early warning system using tilt sensors in Chibo, Kalimpong, Darjeeling Himalayas, India. *Natural Hazards*, 94(2), 727–741, doi:10.1007/s11069-018-3417-6. <http://link.springer.com/10.1007/s11069-018-3417-6>.
- Dini, B., Bennett, G. L., Franco, A. M. A., Whitworth, M. R. Z., Cook, K. L., Senn, A., & Reynolds, J. M. (2021). Development of smart boulders to monitor mass movements via the Internet of Things: a pilot study in Nepal. *Earth Surface Dynamics*, 9(2), 295–315, doi:10.5194/esurf-9-295-2021. <https://esurf.copernicus.org/articles/9/295/2021/>.
- Dixon, N., Smith, A., Flint, J. A., Khanna, R., Clark, B., & Andjelkovic, M. (2018). An acoustic emission landslide early warning system for communities in low-income and middle-income countries. *Landslides*, 15(8), 1631–1644, doi:10.1007/s10346-018-0977-1. <http://link.springer.com/10.1007/s10346-018-0977-1>.
- Dong, M., Wu, H., Hu, H., Azzam, R., Zhang, L., Zheng, Z., & Gong, X. (2020). Deformation Prediction of Unstable Slopes Based on Real-Time Monitoring and DeepAR Model. *Sensors*, 21(1), 14, doi:10.3390/s21010014. <https://www.mdpi.com/1424-8220/21/1/14>.
- Duc-Tan, T., Dinh-Chinh, N., Duc-Nghia, T., & Duc-Tuyen, T. (2015). Development of a Rainfall-Triggered Landslide System using Wireless Accelerometer Network. *International Journal of Advancements in Computing Technology*, 7(5), 14–24.
- Duckham, M. (2013). *Decentralized spatial computing: foundations of geosensor networks*. Heidelberg ; New York: Springer. OCLC: ocn815832963.

- Eberhardt, E., Watson, A. D., & Löw, S. (2008). Improving the interpretation of slope monitoring and early warning data through better understanding of complex deep-seated landslide failure mechanisms. In Z. Chen, J. Zhang, Z. Li, F. Wu, & K. Ho (Eds.), *Landslides and Engineered Slopes: From the Past to the Future* (pp.51): Taylor & Francis. Section: 39. <http://hdl.handle.net/20.500.11850/13068>.
- Fathani, T. F., Karnawati, D., & Wilopo, W. (2016). An integrated methodology to develop a standard for landslide early warning systems. *Natural Hazards and Earth System Sciences*, 16(9), 2123–2135, doi:10.5194/nhess-16-2123-2016. <https://nhess.copernicus.org/articles/16/2123/2016/>.
- Fathani, T. F., Karnawati, D., & Wilopo, W. (2017). Promoting a Global Standard for Community-Based Landslide Early Warning Systems (WCoE 20142017, IPL-158, IPL-165). In K. Sassa, M. Miko, & Y. Yin (Eds.), *Advancing Culture of Living with Landslides* (pp. 355–361). Cham: Springer International Publishing. http://link.springer.com/10.1007/978-3-319-59469-9_30.
- Fathani, T. F., Karnawati, D., Wilopo, W., & Setiawan, H. (2023). Strengthening the Resilience by Implementing a Standard for Landslide Early Warning System. In K. Sassa, K. Konagai, B. Tiwari, . Arbanas, & S. Sassa (Eds.), *Progress in Landslide Research and Technology, Volume 1 Issue 1, 2022* (pp. 277–284). Cham: Springer International Publishing. https://doi.org/10.1007/978-3-031-16898-7_20.
- Fernandez-Steeger, T., et al. (2009). SLEWS-a prototype system for flexible real time monitoring of landslides: Using an open spatial data infrastructure and wireless sensor networks. *Geotechnol. Sci. Rep.*, 13, 3–15.
- Folleau, S. & Uhlemann, S. (2022). Combined passive seismic and low-cost tiltmeters measurement to monitor an urban slow-moving landslide. In *Proceedings of the 8 Canadian Conference on Geotechnique and Natural Hazards: Innovative geoscience for tomorrow*. (pp. 477–483). Quebec, Canada: Canadian Geotechnical Society.
- Froude, M. J. & Petley, D. N. (2018). Global fatal landslide occurrence from 2004 to 2016. *Natural Hazards and Earth System Sciences*, 18(8), 2161–2181, doi:10.5194/nhess-18-2161-2018. <https://nhess.copernicus.org/articles/18/2161/2018/>.
- Gamperl, M., Breuninger, T., Cerón-Hernandez, D., Menschik, B., & Thuro, K. (2023a). Improvement of landslide investigation in deeply weathered ultramafites by parallelizing ERT with direct field observations. *Frontiers in Earth Science*, (pp.20).
- Gamperl, M., Singer, J., Garcia-Londoño, C., Seiler, L., Castañeda, J., Cerón-Hernandez, D., & Thuro, K. (2023b). Recommendations for Landslide Early Warning Systems in Informal Settlements Based on a Case Study in Medellín, Colombia. *Land*, 12(7), 1451, doi:10.3390/land12071451. <https://www.mdpi.com/2073-445X/12/7/1451>.
- Gamperl, M., Singer, J., & Thuro, K. (2021). Internet of Things Geosensor Network for Cost-Effective Landslide Early Warning Systems. *Sensors*, 21(8), 2609, doi:10.3390/s21082609. <https://www.mdpi.com/1424-8220/21/8/2609>.

- Garcia, C. & Fearnley, C. J. (2012). Evaluating critical links in early warning systems for natural hazards. *Environmental Hazards*, 11(2), 123–137, doi:10.1080/17477891.2011.609877. <http://www.tandfonline.com/doi/abs/10.1080/17477891.2011.609877>.
- Garcia-Casco, A., Restrepo, J. J., Correa-Martínez, A. M., Blanco-Quintero, I. F., Proenza, J. A., Weber, M., & Butjosa, L. (2020). The Petrologic Nature of the Medellín Dunite Revisited: An Algebraic Approach and Proposal of a New Definition of the Geological Body. In J. Gomez & A. Pinilla-Pachon (Eds.), *The Geology of Colombia, Volume 2 Mesozoic*, number 36 in Publicaciones Geológicas Especiales (pp. 31). Bogotá: Servicio Geológico Colombiano. <https://www2.sgc.gov.co/LibroGeologiaColombia/Paginas/v2ch2.aspx>.
- Garcia-Delgado, H., Petley, D. N., Bermúdez, M. A., & Sepúlveda, S. A. (2022). Fatal landslides in Colombia (from historical times to 2020) and their socio-economic impacts. *Landslides*, 19(7), 1689–1716, doi:10.1007/s10346-022-01870-2. <https://link.springer.com/10.1007/s10346-022-01870-2>.
- Garcia-Londoño, C. (2005). El Deslizamiento de Villatina. In M. Hermelin (Ed.), *Desastres de Origen Natural en Colombia 1979-2004*. (pp. 55–64). Medellín: Universidad EAFIT.
- García-Aristizábal, E. F., Aristizabal Giraldo, E. V., Marín Sánchez, R. J., & Guzman Martinez, J. C. (2019). Implementación del modelo TRIGRS con análisis de confiabilidad para la evaluación de la amenaza a movimientos en masa superficiales detonados por lluvia. *TecnoLógicas*, 22(44), 111–129, doi:10.22430/22565337.1037. <https://revistas.itm.edu.co/index.php/tecnologicas/article/view/1037>.
- García-Delgado, H., Machuca, S., & Medina, E. (2019). Dynamic and geomorphic characterizations of the Mocoa debris flow (March 31, 2017, Putumayo Department, southern Colombia). *Landslides*, 16(3), 597–609, doi:10.1007/s10346-018-01121-3. <http://link.springer.com/10.1007/s10346-018-01121-3>.
- Gariano, S. L. & Guzzetti, F. (2016). Landslides in a changing climate. *Earth-Science Reviews*, 162, 227–252, doi:10.1016/j.earscirev.2016.08.011. <https://linkinghub.elsevier.com/retrieve/pii/S0012825216302458>.
- Giorgetti, A., et al. (2016). A Robust Wireless Sensor Network for Landslide Risk Analysis: System Design, Deployment, and Field Testing. *IEEE Sensors Journal*, 16(16), 6374–6386, doi:10.1109/JSEN.2016.2579263. <http://ieeexplore.ieee.org/document/7488208/>.
- Gutiérrez Alvis, D. E., Bornachera Zarate, L. S., & Mosquera Palacios, D. J. (2018). Sistema de alerta temprana por movimiento en masa inducido por lluvia para Ciudad Bolívar (Colombia). *Revista Ingeniería Solidaria*, 14(26), doi:10.16925/in.v14i26.2453. <https://revistas.ucc.edu.co/index.php/in/article/view/2547>.
- Guzzetti, F., Gariano, S. L., Peruccacci, S., Brunetti, M. T., Marchesini, I., Rossi, M., & Melillo, M. (2020). Geographical landslide early warning systems. *Earth-Science Reviews*, 200, 102973, doi:10.1016/j.earscirev.2019.102973. <https://linkinghub.elsevier.com/retrieve/pii/S0012825219304635>.

- Guzzetti, F., Peruccacci, S., Rossi, M., & Stark, C. P. (2008). The rainfall intensity-duration control of shallow landslides and debris flows: an update. *Landslides*, 5(1), 3–17, doi:10.1007/s10346-007-0112-1. <http://link.springer.com/10.1007/s10346-007-0112-1>.
- Haque, U., et al. (2019). The human cost of global warming: Deadly landslides and their triggers (1995-2014). *Science of The Total Environment*, 682, 673–684, doi:10.1016/j.scitotenv.2019.03.415. <https://linkinghub.elsevier.com/retrieve/pii/S0048969719314214>.
- Harilal, G. T., Madhu, D., Ramesh, M. V., & Pullarkatt, D. (2019). Towards establishing rainfall thresholds for a real-time landslide early warning system in Sikkim, India. *Landslides*, 16(12), 2395–2408, doi:10.1007/s10346-019-01244-1. <http://link.springer.com/10.1007/s10346-019-01244-1>.
- Heinimann, H. R., Hollenstein, K., Kienholz, H., Krummenacher, B., & Mani, P. (1998). *Umwelt-Materialien Nr. 85 - Methoden zur Analyse und Bewertung von Naturgefahren*. Technical report.
- Hermle, D., Keuschnig, M., Hartmeyer, I., Delleske, R., & Krautblatter, M. (2021). Timely prediction potential of landslide early warning systems with multispectral remote sensing: a conceptual approach tested in the Sattelkar, Austria. *Natural Hazards and Earth System Sciences*, 21(9), 2753–2772, doi:10.5194/nhess-21-2753-2021. <https://nhess.copernicus.org/articles/21/2753/2021/>.
- Hidayat, R., Sutanto, S. J., Hidayah, A., Ridwan, B., & Mulyana, A. (2019). Development of a Landslide Early Warning System in Indonesia. *Geosciences*, 9(10), 451, doi:10.3390/geosciences9100451. <https://www.mdpi.com/2076-3263/9/10/451>.
- Hossain, M., Leminen, S., & Westerlund, M. (2019). A systematic review of living lab literature. *Journal of Cleaner Production*, 213, 976–988, doi:10.1016/j.jclepro.2018.12.257. <https://linkinghub.elsevier.com/retrieve/pii/S0959652618339830>.
- Hovland, H. (1977). Three-dimensional slope stability analysis method. *Journal of Geotechnical Engineering*, 103(GT9), 971–986.
- Huang, G., Du, S., & Wang, D. (2023). GNSS techniques for real-time monitoring of landslides: a review. *Satellite Navigation*, 4(1), 5, doi:10.1186/s43020-023-00095-5. <https://satellite-navigation.springeropen.com/articles/10.1186/s43020-023-00095-5>.
- Huggel, C., Khabarov, N., Obersteiner, M., & Ramírez, J. M. (2010). Implementation and integrated numerical modeling of a landslide early warning system: a pilot study in Colombia. *Natural Hazards*, 52(2), 501–518, doi:10.1007/s11069-009-9393-0. <http://link.springer.com/10.1007/s11069-009-9393-0>.
- Huggel, C., Ramirez, J. M., Calvache, M., González, H., Gutierrez, C., & Krebs, R. (2008). A landslide early warning system within an integral risk management strategy for the Combeima-Tolima Region, Colombia. In *Proceedings of the International Disaster and Risk Conference (IDRC)* (pp. 273–276). Davos, Switzerland: Global Risk Forum. <https://www.zora.uzh.ch/id/eprint/5448>.
- Hungr, O., Leroueil, S., & Picarelli, L. (2014). The Varnes classification of landslide types, an update. *Landslides*, 11(2), 167–194, doi:10.1007/s10346-013-0436-y. <http://link.springer.com/10.1007/s10346-013-0436-y>.

- IDEAM - Instituto de Hidrología, Meteorología y Estudios Ambientales (2020). Pronóstico de la amenaza diaria por deslizamientos. <http://www.pronosticosyalertas.gov.co/web/pronosticos-y-alertas/pronostico-de-la-amenaza-diaria-por-deslizamientos>.
- IPCC (2022). *Sixth Assessment Report. Working Group II - Impacts, Adaptation and Vulnerability*. Technical Report 6th, Intergovernmental Panel on Climate Change. https://www.ipcc.ch/report/ar6/wg2/downloads/report/IPCC_AR6_WGII_HeadlineStatements.pdf.
- ISO International Organization for Standardization (2018). ISO 22327: Security and resilience - Emergency management - Guidelines for implementation of a community-based landslide early warning system.
- Jairo, H. A. (2003). *CARSO DE ALTA MONTAÑA EN SANTA ELENA*. Technical report, Universidad Nacional de Colombia, Medellín.
- Jurich, D. M. & Miller, R. J. (1987). Acoustic Monitoring of Landslides. *Transportation Research Record*, 1119, 9.
- Karnawati, D., Fathani, T. F., Wilopo, W., Setianto, A., & Andayani, B. (2011). Promoting the hybrid socio-technical approach for effective disaster risk reduction in developing countries. In *WIT Transactions on The Built Environment* (pp. 175–182). Orlando, USA. <http://library.witpress.com/viewpaper.asp?pcode=DMAN11-016-1>.
- Kühnl, M., Sapena, M., & Taubenböck, H. (2021). Categorizing Urban Structural Types using an Object-Based Local Climate Zone classification Scheme in Medellín, Colombia. In *Proceedings of REAL CORP 2021, 26th International Conference on Urban Development, Regional Planning and Information Society* (pp. pp. 173–182). Wien, Austria. <http://repository.corp.at/id/eprint/745>.
- Lassa, J. A. (2018). Roles of Non-Government Organizations in Disaster Risk Reduction. *Oxford Research Encyclopedia of Natural Hazard Science*, doi:10.1093/acrefore/9780199389407.013.45. <https://oxfordre.com/naturalhazardscience/view/10.1093/acrefore/9780199389407.001.0001/acrefore-9780199389407-e-45>.
- Lee, C. F., Li, J., Xu, Z. W., & Dai, F. C. (2001). Assessment of landslide susceptibility on the natural terrain of Lantau Island, Hong Kong. *Environmental Geology*, 40(3), 381–391, doi:10.1007/s002540000163. <http://link.springer.com/10.1007/s002540000163>.
- Leinauer, J., Jacobs, B., & Krautblatter, M. (2021). High alpine geotechnical real time monitoring and early warning at a large imminent rock slope failure (Hochvogel, GER/AUT). *IOP Conference Series: Earth and Environmental Science*, 833(1), 012146, doi:10.1088/1755-1315/833/1/012146. <https://iopscience.iop.org/article/10.1088/1755-1315/833/1/012146>.
- Liao, Z., Hong, Y., Wang, J., Fukuoka, H., Sassa, K., Karnawati, D., & Fathani, F. (2010). Prototyping an experimental early warning system for rainfall-induced landslides in Indonesia using satellite remote sensing and geospatial datasets. *Landslides*, 7(3), 317–324, doi:10.1007/s10346-010-0219-7. <http://link.springer.com/10.1007/s10346-010-0219-7>.

- Lin, W., Shunsaku, N., Taro, U., Ikuo, T., Ling, S., & Shangning, T. (2017). An Early Warning System of Unstable Slopes by Multi-point MEMS Tilting Sensors and Water Contents. In M. Miko, . Arbanas, Y. Yin, & K. Sassa (Eds.), *Advancing Culture of Living with Landslides* (pp. 147–154). Cham: Springer International Publishing.
- Linardos, V., Drakaki, M., Tzionas, P., & Karnavas, Y. (2022). Machine Learning in Disaster Management: Recent Developments in Methods and Applications. *Machine Learning and Knowledge Extraction*, 4(2), 446–473, doi:10.3390/make4020020. <https://www.mdpi.com/2504-4990/4/2/20>.
- Loew, S., Gschwind, S., Gischig, V., Keller-Signer, A., & Valenti, G. (2017). Monitoring and early warning of the 2012 Preonzo catastrophic rockslope failure. *Landslides*, 14(1), 141–154, doi:10.1007/s10346-016-0701-y. <http://link.springer.com/10.1007/s10346-016-0701-y>.
- LoRa Alliance (2019). LoRaWAN 1.0.3 Specification. <https://lora-alliance.org/lorawan-for-developers>.
- Lueth, K. L. (2014). Why the Internet of Things is called Internet of Things: Definition, history, disambiguation. <https://iot-analytics.com/internet-of-things-definition/>.
- Malon, D. A. W. (1997). Risk Management and Slope Safety in Hong Kong. *HKIE Transactions*, 4(2-3), 12–21, doi:10.1080/1023697X.1997.10667719. <https://www.tandfonline.com/doi/full/10.1080/1023697X.1997.10667719>.
- Marchezini, V., Horita, F. E. A., Matsuo, P. M., Trajber, R., Trejo-Rangel, M. A., & Olivato, D. (2018). A Review of Studies on Participatory Early Warning Systems (P-EWS): Pathways to Support Citizen Science Initiatives. *Frontiers in Earth Science*, 6, 184, doi:10.3389/feart.2018.00184. <https://www.frontiersin.org/article/10.3389/feart.2018.00184/full>.
- Marin, R. J. (2020). Physically based and distributed rainfall intensity and duration thresholds for shallow landslides. *Landslides*, 17(12), 2907–2917, doi:10.1007/s10346-020-01481-9. <http://link.springer.com/10.1007/s10346-020-01481-9>.
- Marín, R. J., García-Aristizábal, E., & Aristizábal, E. (2019). Rainfall thresholds for shallow landslides based on physical models: application in a sub-basin of the Valle de Aburrá (Colombia). *DYNA*, 86(210), 312–322, doi:10.15446/dyna.v86n210.77166. <https://revistas.unal.edu.co/index.php/dyna/article/view/77166>.
- Mekki, K., Bajic, E., Chaxel, F., & Meyer, F. (2019). A comparative study of LPWAN technologies for large-scale IoT deployment. *ICT Express*, 5(1), 1–7, doi:10.1016/j.icte.2017.12.005. <https://linkinghub.elsevier.com/retrieve/pii/S2405959517302953>.
- Mergili, M., Marchesini, I., Alvioli, M., Metz, M., Schneider-Muntau, B., Rossi, M., & Guzzetti, F. (2014). A strategy for GIS-based 3-D slope stability modelling over large areas. *Geoscientific Model Development*, 7(6), 2969–2982, doi:10.5194/gmd-7-2969-2014. <https://gmd.copernicus.org/articles/7/2969/2014/>.
- Mohd Mokhtar, M. R., Abdul Wahab, S. N., Husain, M. N., Hashim, H., & Che Kasim, A. (2021). Landslide Monitoring Using Close Range Photogrammetry. *PLANNING MALAYSIA*, 19, doi:10.21837/pm.v19i19.1068. <https://www.planningmalaysia.org/index.php/pmj/article/view/1068>.

- Montserrat, O., Crosetto, M., & Luzi, G. (2014). A review of ground-based SAR interferometry for deformation measurement. *ISPRS Journal of Photogrammetry and Remote Sensing*, 93, 40–48, doi:10.1016/j.isprsjprs.2014.04.001. <https://linkinghub.elsevier.com/retrieve/pii/S0924271614000884>.
- Moore, J. R., Gischig, V., Button, E., & Loew, S. (2010). Rockslide deformation monitoring with fiber optic strain sensors. *Natural Hazards and Earth System Sciences*, 10(2), 191–201, doi:10.5194/nhess-10-191-2010. <https://nhess.copernicus.org/articles/10/191/2010/>.
- Moulat, M. E., Debauche, O., Mahmoudi, S., Brahim, L. A., Manneback, P., & Lebeau, F. (2018). Monitoring System Using Internet of Things For Potential Landslides. *Procedia Computer Science*, 134, 26–34, doi:10.1016/j.procs.2018.07.140. <https://linkinghub.elsevier.com/retrieve/pii/S1877050918311037>.
- Nittel, S., et al. (2004). Report from the first workshop on geo sensor networks. *ACM SIGMOD Record*, 33(1), 141–144, doi:10.1145/974121.974146. <https://dl.acm.org/doi/10.1145/974121.974146>.
- Notti, D., Cina, A., Manzino, A., Colombo, A., Bendea, I. H., Mollo, P., & Giordan, D. (2020). Low-Cost GNSS Solution for Continuous Monitoring of Slope Instabilities Applied to Madonna Del Sasso Sanctuary (NW Italy). *Sensors*, 20(1), 289, doi:10.3390/s20010289. <https://www.mdpi.com/1424-8220/20/1/289>.
- Oguz, E. A., Robinson, K., Depina, I., & Thakur, V. (2019). IoT-Based Strategies for Risk Management of Rainfall-Induced Landslides: A Review. In *Proceedings of the 7th International Symposium on Geotechnical Safety and Risk (ISGSR 2019)*: Research Publishing Services. <http://rpsonline.com.sg/proceedings/9789811127250/html/IS13-2.xml>.
- Osanaï, N., Shimizu, T., Kuramoto, K., Kojima, S., & Noro, T. (2010). Japanese early-warning for debris flows and slope failures using rainfall indices with Radial Basis Function Network. *Landslides*, 7(3), 325–338, doi:10.1007/s10346-010-0229-5. <http://link.springer.com/10.1007/s10346-010-0229-5>.
- Paul, J. D., et al. (2020). Applying Citizen Science for Sustainable Development: Rainfall Monitoring in Western Nepal. *Frontiers in Water*, 2, 581375, doi:10.3389/frwa.2020.581375. <https://www.frontiersin.org/articles/10.3389/frwa.2020.581375/full>.
- Pecoraro, G., Calvello, M., & Piciullo, L. (2019). Monitoring strategies for local landslide early warning systems. *Landslides*, 16(2), 213–231, doi:10.1007/s10346-018-1068-z. <http://link.springer.com/10.1007/s10346-018-1068-z>.
- Pecoraro, G., Piciullo, L., & Calvello, M. (2017). Regional Landslide Early Warning Systems: Comparison of Warning Strategies by Means of a Case Study. In M. Miko, . Arbanas, Y. Yin, & K. Sassa (Eds.), *Advancing Culture of Living with Landslides* (pp. 183–191). Cham: Springer International Publishing. http://link.springer.com/10.1007/978-3-319-53487-9_21.
- Perlman, J. E. (2010). *Favela four decades of living on the edge in Rio de Janeiro*. New York: Oxford University Press. OCLC: 1303480415.

- Perrone, A., Lapenna, V., & Piscitelli, S. (2014). Electrical resistivity tomography technique for landslide investigation: A review. *Earth-Science Reviews*, 135, 65–82, doi:10.1016/j.earscirev.2014.04.002. <https://linkinghub.elsevier.com/retrieve/pii/S0012825214000701>.
- Petley, D., Mantovani, F., Bulmer, M., & Zannoni, A. (2005). The use of surface monitoring data for the interpretation of landslide movement patterns. *Geomorphology*, 66(1-4), 133–147, doi:10.1016/j.geomorph.2004.09.011. <https://linkinghub.elsevier.com/retrieve/pii/S0169555X0400217X>.
- Piciullo, L., Calvello, M., & Cepeda, J. (2018). Territorial early warning systems for rainfall-induced landslides. *Earth-Science Reviews*, 179, 228–247, doi:10.1016/j.earscirev.2018.02.013. <https://linkinghub.elsevier.com/retrieve/pii/S0012825217302209>.
- Piciullo, L., Gariano, S. L., Melillo, M., Brunetti, M. T., Peruccacci, S., Guzzetti, F., & Calvello, M. (2017). Definition and performance of a threshold-based regional early warning model for rainfall-induced landslides. *Landslides*, 14(3), 995–1008, doi:10.1007/s10346-016-0750-2. <http://link.springer.com/10.1007/s10346-016-0750-2>.
- Pollock, W. & Wartman, J. (2020). Human Vulnerability to Landslides. *GeoHealth*, 4(10), doi:10.1029/2020GH000287. <https://onlinelibrary.wiley.com/doi/10.1029/2020GH000287>.
- Pradhan, A. M. S., Lee, S.-R., & Kim, Y.-T. (2019). A shallow slide prediction model combining rainfall threshold warnings and shallow slide susceptibility in Busan, Korea. *Landslides*, 16(3), 647–659, doi:10.1007/s10346-018-1112-z. <http://link.springer.com/10.1007/s10346-018-1112-z>.
- Preuner, P., Scolobig, A., Linnerooth Bayer, J., Ottowitz, D., Hoyer, S., & Jochum, B. (2017). A Participatory Process to Develop a Landslide Warning System: Paradoxes of Responsibility Sharing in a Case Study in Upper Austria. *Resources*, 6(4), 54, doi:10.3390/resources6040054. <http://www.mdpi.com/2079-9276/6/4/54>.
- PRIEST, S. D. (1993). The Collection and Analysis of Discontinuity Orientation Data for Engineering Design, with Examples. In J. A. HUDSON (Ed.), *Rock Testing and Site Characterization* (pp. 167–192). Oxford: Pergamon. <https://www.sciencedirect.com/science/article/pii/B978008042066050015X>.
- Pudifoot, B., Cárdenas, M. L., Buytaert, W., Paul, J. D., Narraway, C. L., & Loiselle, S. (2021). When It Rains, It Pours: Integrating Citizen Science Methods to Understand Resilience of Urban Green Spaces. *Frontiers in Water*, 3, 654493, doi:10.3389/frwa.2021.654493. <https://www.frontiersin.org/articles/10.3389/frwa.2021.654493/full>.
- Ramesh, M. V. (2009). Real-Time Wireless Sensor Network for Landslide Detection. In *2009 Third International Conference on Sensor Technologies and Applications* (pp. 405–409). Athens, Greece: IEEE. <http://ieeexplore.ieee.org/document/5210898/>.
- Ruiz Peña, G. L., Barrera Pinales, L. A., Gamboa Rodríguez, C. A., & Sandoval Ramírez, J. H. (2017). *Las amenazas por movimientos en masa de Colombia: una visión a escala 1:100.000*. Bogotá, Colombia: Servicio Geológico Colombiano, 1 edition.

- Sapena, M., Gamperl, M., Kühnl, M., Singer, J., Garcia-Londoño, C., & Taubenbock, H. (2023). Cost estimation for the instrumentalization of Early Warning Systems in landslide prone areas. *Natural Hazards and Earth System Sciences*, in prep., doi:<https://doi.org/10.5194/nhess-2023-41>.
- Sapena, M., Kühnl, M., Wurm, M., Patino, J. E., Duque, J. C., & Taubenböck, H. (2022). Empiric recommendations for population disaggregation under different data scenarios. *PLOS ONE*, 17(9), e0274504, doi:10.1371/journal.pone.0274504. <https://dx.plos.org/10.1371/journal.pone.0274504>.
- Schneider, M., Oestreicher, N., & Loew, S. (2023). *Rockfall monitoring with a Doppler radar on an active rock slide complex in Brienz/Brinzauls (Switzerland)*. preprint, Landslides and Debris Flows Hazards. <https://egusphere.copernicus.org/preprints/2023/egusphere-2023-555/>.
- Segoni, S., Lagomarsino, D., Fanti, R., Moretti, S., & Casagli, N. (2015). Integration of rainfall thresholds and susceptibility maps in the Emilia Romagna (Italy) regional-scale landslide warning system. *Landslides*, 12(4), 773–785, doi:10.1007/s10346-014-0502-0. <http://link.springer.com/10.1007/s10346-014-0502-0>.
- Sharma, R. (2021). Community Based Flood Risk Management: Local Knowledge and Actors Involvement Approach from Lower Karnali River Basin of Nepal. *Journal of Geoscience and Environment Protection*, 09(06), 35–65, doi:10.4236/gep.2021.96003. <https://www.scirp.org/journal/doi.aspx?doi=10.4236/gep.2021.96003>.
- Singer, J. (2019). Monitoring von Hangbewegungen mit dem Continuous Shear Monitor (CSM) - Anwendungsbeispiele. In Deutsche Gesellschaft für Geotechnik e.V. (Ed.), *Tagungsband zu den Fachsektionstagen Geotechnik* (pp. 42–46). Würzburg: Deutsche Gesellschaft für Geotechnik e.V.
- Singer, J., Thuro, K., & Festl, J. (2010). Development and testing of a time domain reflectometry (TDR) monitoring system for subsurface deformations. In *Proceedings of the European Rock Mechanics Symposium (EUROCK 2010)* (pp. 4). Lausanne, Switzerland: CPC/Balkema (Taylor & Francis).
- Singer, J., Thuro, K., Gamperl, M., Breuninger, T., & Menschik, B. (2021). Technical Concepts for an Early Warning System for Rainfall Induced Landslides in Informal Settlements. In N. Casagli, V. Tofani, K. Sassa, P. T. Bobrowsky, & K. Takara (Eds.), *Understanding and Reducing Landslide Disaster Risk: Volume 3 Monitoring and Early Warning* (pp. 209–215). Cham: Springer International Publishing. https://doi.org/10.1007/978-3-030-60311-3_24.
- Smith, H., Coupé, F., Garcia-Ferrari, S., Rivera, H., & Castro Mera, W. E. (2020). Toward negotiated mitigation of landslide risks in informal settlements: reflections from a pilot experience in Medellín, Colombia. *Ecology and Society*, 25(1), art19, doi:10.5751/ES-11337-250119. <https://www.ecologyandsociety.org/vol25/iss1/art19/>.
- Smith, H., et al. (2018). Learning from Co-Produced Landslide Risk Mitigation Strategies in Low-Income Settlements in Medellín (Colombia) and São Paulo (Brazil). In *N-AERUS XIX* Stuttgart, Germany: Department of International Urbanism, University of Stuttgart.
- Smith, H., et al. (2021). Exploring appropriate socio-technical arrangements for the co-production of landslide risk management strategies in informal neighbourhoods in Colom-

- bia and Brazil. *International Journal of Urban Sustainable Development*, 14(1), 242–263, doi:10.1080/19463138.2021.1872082. <https://www.tandfonline.com/doi/full/10.1080/19463138.2021.1872082>.
- Sorensen, J. H. (2000). Hazard Warning Systems: Review of 20 Years of Progress. *Natural Hazards Review*, 1(2), 119–125, doi:10.1061/(ASCE)1527-6988(2000)1:2(119). <http://ascelibrary.org/doi/10.1061/%28ASCE%291527-6988%282000%291%3A2%28119%29>.
- Taubenböck, H., Esch, T., Felbier, A., Wiesner, M., Roth, A., & Dech, S. (2012). Monitoring urbanization in mega cities from space. *Remote Sensing of Environment*, 117, 162–176, doi:10.1016/j.rse.2011.09.015. <https://linkinghub.elsevier.com/retrieve/pii/S0034425711003427>.
- Thiebes, B. (2012). *Landslide Analysis and Early Warning Systems: Local and Regional Case Study in the Swabian Alb, Germany*. Springer Theses. Berlin, Heidelberg: Springer Berlin Heidelberg. <http://link.springer.com/10.1007/978-3-642-27526-5>.
- Thiebes, B. & Glade, T. (2016). Landslide Early Warning Systems fundamental concepts and innovative applications. In S. Aversa, L. Cascini, L. Picarelli, & C. Scavia (Eds.), *Landslides and Engineered Slopes. Experience, Theory and Practice*. (pp.9). Napoli, Italy: Associazione Geotecnica Italiana.
- Thuro, K., Singer, J., & Festl, J. (2011). Towards a low cost 3D early warning system for unstable Alpine slopes the Aggenalm Landslide monitoring system. (pp.12).
- Thuro, K., Singer, J., & Festl, J. (2013). A Geosensor Network Based Monitoring and Early Warning System for Landslides. In C. Margottini, P. Canuti, & K. Sassa (Eds.), *Landslide Science and Practice* (pp. 79–86). Berlin, Heidelberg: Springer Berlin Heidelberg. http://link.springer.com/10.1007/978-3-642-31445-2_10.
- Thuro, K., et al. (2010). New landslide monitoring techniques developments and experiences of the alpEWAS project. *Journal of Applied Geodesy*, 4(2), 69–90, doi:10.1515/jag.2010.008. <https://www.degruyter.com/doi/10.1515/jag.2010.008>.
- Thuro, K., Singer, J., Menschik, B., Breuninger, T., & Gamperl, M. (2020). Development of a Landslide Early Warning System in informal settlements in Medellín, Colombia. *Geomechanics and Tunneling*, 13(1), 103–115, doi:10.1002/geot.201900071. <https://onlinelibrary.wiley.com/doi/abs/10.1002/geot.201900071>.
- Thuro, K., et al. (2009). Low cost 3D early warning system for instable alpine slopes - the Aggenalm Landslide monitoring system. *Geomechanik und Tunnelbau*, 2(3), 221–237, doi:10.1002/geot.200900024. <http://doi.wiley.com/10.1002/geot.200900024>.
- Thuro, K., et al. (2014). Low Cost 3D Early Warning System for Alpine Instable Slopes: The Aggenalm Landslide Monitoring System. In F. Wenzel & J. Zschau (Eds.), *Early Warning for Geological Disasters* (pp. 289–306). Berlin, Heidelberg: Springer Berlin Heidelberg. Series Title: Advanced Technologies in Earth Sciences. http://link.springer.com/10.1007/978-3-642-12233-0_15.
- Tiranti, D., Nicolò, G., & Gaeta, A. R. (2019). Shallow landslides predisposing and triggering factors in developing a regional early warning system. *Landslides*, 16(2), 235–251, doi:10.1007/s10346-018-1096-8. <http://link.springer.com/10.1007/s10346-018-1096-8>.

- Tiranti, D. & Rabuffetti, D. (2010). Estimation of rainfall thresholds triggering shallow landslides for an operational warning system implementation. *Landslides*, 7(4), 471–481, doi:10.1007/s10346-010-0198-8. <http://link.springer.com/10.1007/s10346-010-0198-8>.
- Tobón-Hincapié, M. P. (2011). *MEDIDAS DE MITIGACIÓN DE LA LADERA ORIENTAL DEL VALLE DE ABURRÁ ENTRE LAS QUEBRADAS LA POBLADA Y LA SANÍN*. Technical report, Alcaldia de Medellín.
- Tu, R., et al. (2013). Cost-effective monitoring of ground motion related to earthquakes, landslides, or volcanic activity by joint use of a single-frequency GPS and a MEMS accelerometer. *Geophysical Research Letters*, 40(15), 3825–3829, doi:10.1002/grl.50653. <http://doi.wiley.com/10.1002/grl.50653>.
- Uchimura, T., et al. (2010). Simple monitoring method for precaution of landslides watching tilting and water contents on slopes surface. *Landslides*, 7(3), 351–357, doi:10.1007/s10346-009-0178-z. <http://link.springer.com/10.1007/s10346-009-0178-z>.
- Uchimura, T., Towhata, I., Wang, L., Nishie, S., Yamaguchi, H., Seko, I., & Qiao, J. (2015). Precaution and early warning of surface failure of slopes using tilt sensors. *Soils and Foundations*, 55(5), 1086–1099, doi:10.1016/j.sandf.2015.09.010. <https://linkinghub.elsevier.com/retrieve/pii/S0038080615001122>.
- Uhlemann, S., et al. (2017). Four-dimensional imaging of moisture dynamics during landslide reactivation: Imaging of Landslide Moisture Dynamics. *Journal of Geophysical Research: Earth Surface*, 122(1), 398–418, doi:10.1002/2016JF003983. <http://doi.wiley.com/10.1002/2016JF003983>.
- UN-ISDR (2006). Developing an early warning system: a checklist. In *Early Warning From concept to action The Conclusions of the Third International Conference on Early Warning* (pp.10). Bonn, Germany.
- UNDRR (2015). *Sendai Framework for Disaster Risk Reduction 2015 - 2030*. Technical report, United Nations Office for Disaster Risk Reduction. <https://www.undrr.org/quick/11409>.
- United Nations Climate Change (2022). UN: Early Warning Systems Must Protect Everyone Within Five Years. <https://unfccc.int/news/un-early-warning-systems-must-protect-everyone-within-five-years>.
- Walstra, J., Chandler, J. H., Dixon, N., & Dijkstra, T. A. (2007). Aerial photography and digital photogrammetry for landslide monitoring. *Geological Society, London, Special Publications*, 283(1), 53–63, doi:10.1144/SP283.5. <https://www.lyellcollection.org/doi/10.1144/SP283.5>.
- Werthmann, C. (2018). *Stärkung der Resilienz informeller Siedlungen gegen Hangbewegungen durch die Vernetzung von Frühwarnsystemen, Web-Technologien und Landschaftsplanung in partizipativen Prozessen - Fallstudie Medellín, Kolumbien*. Funding proposal, Leibniz Universität Hannover, Hannover.
- Werthmann, C. (2023). Reporting from the front. *Natural Hazards*, doi:10.1007/s11069-023-05815-3. <https://link.springer.com/10.1007/s11069-023-05815-3>.
- Werthmann, C., Echeverri, A., & Elvira Vélez, A. (2012). *Rehabitar La Ladera: Shifting Ground*. Research Report, Universidad EAFIT, Medellín.

- Werthmann, C., et al. (2023). Inform@Risk. The Development of a Prototype for an Integrated Landslide Early Warning System in an Informal Settlement: the Case of Bello Oriente in Medellín, Colombia. *Natural Hazards and Earth System Science*, (pp.42)., doi:10.5194/nhess-2023-53. <https://nhess.copernicus.org/preprints/nhess-2023-53/>.
- Whiteley, J., et al. (2020). Landslide monitoring using seismic refraction tomography The importance of incorporating topographic variations. *Engineering Geology*, 268, 105525, doi:10.1016/j.enggeo.2020.105525. <https://linkinghub.elsevier.com/retrieve/pii/S0013795219309792>.
- Wong, A. C. W., Ting, S. M., Shiu, Y. K., & Ho, K. K. S. (2014). Latest Developments of Hong Kong's Landslip Warning System. In K. Sassa, P. Canuti, & Y. Yin (Eds.), *Landslide Science for a Safer Geoenvironment* (pp. 613–618). Cham: Springer International Publishing.
- Wu, Y., Niu, R., Wang, Y., & Chen, T. (2020). A Fast Deploying Monitoring and Real-Time Early Warning System for the Baige Landslide in Tibet, China. *Sensors*, 20(22), 6619, doi:10.3390/s20226619. <https://www.mdpi.com/1424-8220/20/22/6619>.
- Yang, Z., Shao, W., Qiao, J., Huang, D., Tian, H., Lei, X., & Uchimura, T. (2017). A Multi-Source Early Warning System of MEMS Based Wireless Monitoring for Rainfall-Induced Landslides. *Applied Sciences*, 7(12), 1234, doi:10.3390/app7121234. <http://www.mdpi.com/2076-3417/7/12/1234>.
- Yang, Z., Wang, L., Qiao, J., Uchimura, T., & Wang, L. (2020). Application and verification of a multivariate real-time early warning method for rainfall-induced landslides: implication for evolution of landslide-generated debris flows. *Landslides*, 17(10), 2409–2419, doi:10.1007/s10346-020-01402-w. <http://link.springer.com/10.1007/s10346-020-01402-w>.
- Yassin, R. R., Muhammad, R. F., Taib, S. H., & Al-Kouri, O. (2014). Application of ERT and Aerial Photographs Techniques to Identify the Consequences of Sinkholes Hazards in Constructing Housing Complexes Sites over Karstic Carbonate Bedrock in Perak, Peninsular Malaysia. *Journal of Geography and Geology*, 6(3), p55, doi:10.5539/jgg.v6n3p55. <http://www.ccsenet.org/journal/index.php/jgg/article/view/38162>.
- Ye, X., Zhu, H., Wang, J., Zhang, Q., Shi, B., Schenato, L., & Pasuto, A. (2022). Subsurface MultiPhysical Monitoring of a Reservoir Landslide With the FiberOptic Nerve System. *Geophysical Research Letters*, 49(11), doi:10.1029/2022GL098211. <https://onlinelibrary.wiley.com/doi/10.1029/2022GL098211>.
- Zhang, D., Wei, K., Yao, Y., Yang, J., Zheng, G., & Li, Q. (2022a). Capture and Prediction of Rainfall-Induced Landslide Warning Signals Using an Attention-Based Temporal Convolutional Neural Network and Entropy Weight Methods. *Sensors*, 22(16), 6240, doi:10.3390/s22166240. <https://www.mdpi.com/1424-8220/22/16/6240>.
- Zhang, H., Yin, C., Wang, S., & Guo, B. (2022b). Landslide susceptibility mapping based on landslide classification and improved convolutional neural networks. *Natural Hazards*, 116(2), 41, doi:10.1007/s11069-022-05748-3. <https://link.springer.com/10.1007/s11069-022-05748-3>.

Ündül, ., Turul, A., Özyalın, ., & Zarif, . H. (2015). Identifying the changes of geo-engineering properties of dunites due to weathering utilizing electrical resistivity tomography (ERT). *Journal of Geophysics and Engineering*, 12(2), 273–281, doi:10.1088/1742-2132/12/2/273. <https://academic.oup.com/jge/article/12/2/273/5110319>.

Appendix

Appendix A - Full Journal Articles

Appendix A-1

Title	Improvement of landslide investigation in deeply weathered ultramafites by parallelizing ERT with direct field observations				
Journal	Frontiers in Earth Science				
DOI	-				
Year	2023	Volume	-	Impact Factor (2023)	2.9
Accepted	No, under review	Position of the candidate in the authors list			1
Authors	Moritz Gamperl, Tamara Breuninger, Kurosch Thuro, David Cerón-Hernandez, Bettina Menschik				

This article was submitted to Frontiers in Earth Science on 26.09.2023. This article is an open access article distributed under the terms and conditions of the Creative Commons Attribution (CC BY) license, thus permission to reprint the article is not necessary.

Improvement of landslide investigation in deeply weathered ultramafites by parallelizing ERT with direct field observations

1 Moritz Gamperl^{1*}, Tamara Breuninger¹, Kurosch Thuro¹, David Cerón-Hernandez², Bettina
2 Menschik¹

3 ¹Chair of Engineering Geology, School of Engineering and Design, Technical University of Munich,
4 Munich, Germany

5 ²Geological Society of Colombia, Antioquia Chapter, 50016 Medellín, Colombia

6 * **Correspondence:**

7 Moritz Gamperl

8 moritz.gamperl@tum.de

9 **Keywords: landslides, electrical resistivity tomography, dunite, Medellín, block-in-matrix**
10 **structure, ultramafites, weathering.**

11 Nr. of words: 4909 Nr. of figures: 7

12 Abstract

13 The threat of landslides to lives of inhabitants in mountainous areas, especially in the global south, is
14 rising due to global warming and increasing population. In Medellín, the second largest city of
15 Colombia, the heavily weathered dunite unit in the east of the city is the most landslide-susceptible
16 unit, where most of the landslides of the last 100 years have taken place. Thus, the project
17 Inform@Risk aims towards strengthening the resilience of the residents of the area by developing a
18 landslide early warning system. Detailed on-site investigation of landslide-prone slopes is essential
19 for the planning of this system. To accomplish this for the study area Bello Oriente, we developed a
20 multi-step approach, combining electrical resistivity tomography with mapping, core drilling, and
21 structural analysis of discontinuities. While electrical resistivity tomography was performed first to
22 determine the drilling locations, it was re-evaluated once the cores of the drillings were available.
23 This efficient approach allowed us to place the drillings in areas where the most questions needed to
24 be answered. The drilling results in turn could be used for a more detailed evaluation of the electrical
25 resistivity tomography data. The investigation showed a bedrock of heavily weathered ultramafites
26 (dunites & serpentinites) with pseudokarst structures and overlying colluvium material which has
27 been deposited by former landslides. It became apparent that the first geological model was not
28 sufficient to describe the site as the layering of weathered dunite and saprolite on top of non-fractured
29 dunite was not existing. Rather, the fractured dunite reaches down to more than 50 m in some parts,
30 and there is only little saprolite cover above the fractured bedrock or the landslide deposits.
31 Additionally, the weathered dunite shows pseudokarst phenomena like karren, dolines and cavities.
32 Based on these results, a hazard map and subsequently the sensor system for the landslide early
33 warning as well as other mitigative measures can be planned, demonstrating how accurately
34 calibrated electrical resistivity tomography measures combined with direct field and subsurface
35 observations can achieve considerable knowledge increase for landslide hazard assessment in deeply
36 weathered ultramafites.

37 **1 Introduction**

38 **1.1 Motivation**

39 In the city of Medellín, an estimated 70.000 persons live in a high hazard area, which amounts to
40 about 3°% of the total population (Kühnl et al., 2021). Additionally, 131.000 persons live in medium
41 hazard areas, so in total more than 200.000 persons live in a hazard prone area. These numbers
42 increase over-proportionally each year as the population increase is higher in these landslide prone
43 areas than in the city on average (Sapena et al., 2022). In the last 80 years, at least 854 people have
44 died from mass movements in the Aburrà Valley (Servicio Geológico Colombiano, n.d.; Werthmann
45 et al., 2012). The main trigger factors have been heavy rainfalls and anthropogenic activity.

46 To reduce these risks, there are two options: Either (1) a relocation of the inhabitants to safer areas or
47 (2) mitigation of the high hazard slopes. (1) Relocation is often not possible due to missing living
48 space or the high economic cost, and also the people at risk often do not want to leave their self-built
49 homes. (2) Mitigation measures are economically not feasible for the many high hazard zones that a
50 city like Medellín covers. Therefore, a third option is necessary, which can at least provide a
51 medium-term solution. Early Warning Systems (EWS) can, if certain prerequisites are met, provide
52 this solution (UNDRR, 2015). While in the long term (> 25 years), local EWS are not the best
53 solution, they can provide immediate, relatively cost-efficient risk reduction for the inhabitants.
54 Especially in informal settlements, where there is only inexpensive infrastructure available, the
55 systems can be aimed only at saving lives and thus can be more efficient.

56 The Project Inform@Risk aims to strengthen the resilience of informal settlements in Colombia and
57 other developing countries. The goal is to develop an integrated, low-cost Early Warning System
58 (EWS) that can easily be replicated at other sites and countries (Singer et al., 2021; Thuro et al., 2020;
59 Werthmann, 2023; Werthmann et al., 2023). Thus, a study site in the east of the city was selected
60 based on criteria such as hazard level, endangered population, as well as social structure of the
61 neighborhood. The site Bello Oriente is subject of a pilot project in which the implementation of such
62 an EWS is tested. The first step in this process is the hazard assessment by thorough geological and
63 geotechnical investigation.

64 **1.2 Geological site conditions**

65 The geology of the city of Medellín consists of Mesozoic igneous and metamorphic rocks, highly
66 influenced by the Andean orogenesis. Due to this tectonic history several major fault systems occur
67 around the city, the most dominant one striking NNW-SSE (Rodas fault). The Aburrà Valley floor
68 comprises deposits of the Medellín river (Breuninger et al., 2021b).

69 The project area Bello Oriente lies entirely in the geological unit of the Medellín Dunite, an
70 ultramafic, highly and deeply fractured rock composed of mainly olivine, pyroxene, amphibolite,
71 chlorite, talc, and serpentine (Breuninger et al., 2021b; Garcia-Casco et al., 2020). The presence of
72 serpentine in the rock suggests that the unit has been altered by metamorphic processes. Therefore,
73 the name ‘dunite’ is mineralogically not accurate. ‘Serpentinite’, ‘harzburgite’, and ‘ultramafite’ have
74 been suggested as names for the unit in the past (Botero Arango, 1963; Breuninger et al., 2021b;
75 Garcia-Casco et al., 2020). Nevertheless, ‘Medellín Dunite’ is still the expression for this unit
76 commonly used.

77 Ultramafic rocks like the Medellín Dunite are highly susceptible to chemical weathering due to their
78 high content of ferrous minerals like pyroxene, amphibole and olivine. Alteration processes start

79 right after the formation of the rock, namely sea floor serpentization (Mével, 2003). This
80 serpentization process has most likely already started during the formation of the rock as part of a
81 Triassic ophiolitic complex (Garcia-Casco et al., 2020). The heat source of this metamorphosis was
82 the proximate basaltic magma at the mid-ocean ridge. The serpentization starts at the fracture
83 surfaces and works its way into the rock from there. Serpentization of ultramafic rocks can also be
84 induced by meteoric water (Ündül and Tuğrul, 2012). During this secondary serpentization process,
85 forsterite, in combination with meteoric water, is transformed into serpentine minerals and the
86 magnesium hydroxide brucite, precipitating at open fractures and karst holes (Breuninger et al.,
87 2021b; Tobón-Hincapié, 2011). This process is especially strong in tropical regions, since rainfall is
88 very frequent and temperatures very high, increasing the speed of the serpentization and its depth in
89 the rock.

90 Due to the high content of olivine and other ferrous minerals and the tropical climate, the Medellín
91 Dunite is extremely weathered and fragmented, up to a depth of at least 50 m (Breuninger et al.,
92 2021b). One phenomenon that contributes to this is so called ‘Pseudokarst’. In distinction to normal
93 karst formation in carbonate and gypsum rock, it is a phenomenon present in the Medellín Dunite and
94 clearly visible in typical karst structures such as karst holes, dolines, spurrillen, and karren
95 (Breuninger et al., 2021b; Jairo, 2003; Tobón-Hincapié, 2011). It is a solution process, closely linked
96 to the secondary serpentization by meteoric water. This solution of forsterite and precipitation of
97 brucite at other places creates a mass deficit resulting in karst structures in the Medellín Dunite, most
98 visible in the southernmost part, but present throughout the whole unit (Breuninger et al., 2021b;
99 Tobón-Hincapié, 2011). The process, like the initial serpentization, takes its strongest hold along
100 the fractures which were formed during the tectonic history of the area. The cavities formed by the
101 pseudokarst are up to 1 meters in diameter and mostly filled with silty and clayey weathering
102 material, washed in by meteoric and ground water (Tobón-Hincapié, 2011).

103 **1.3 Goals & Scope of this Paper**

104 Because of the complex nature of the Medellín Dunite, an in-depth morphological, geological, and
105 geotechnical investigation of the study area is necessary in order to perform the hazard and risk
106 assessment needed to plan the EWS. This is realized in this project via mapping, core drillings,
107 laboratory analysis and electrical resistivity tomography (ERT). All of the activities are by design
108 integrated and performed together with the community (Breuninger et al., 2021a; Gamperl et al.,
109 2023; Werthmann et al., 2023).

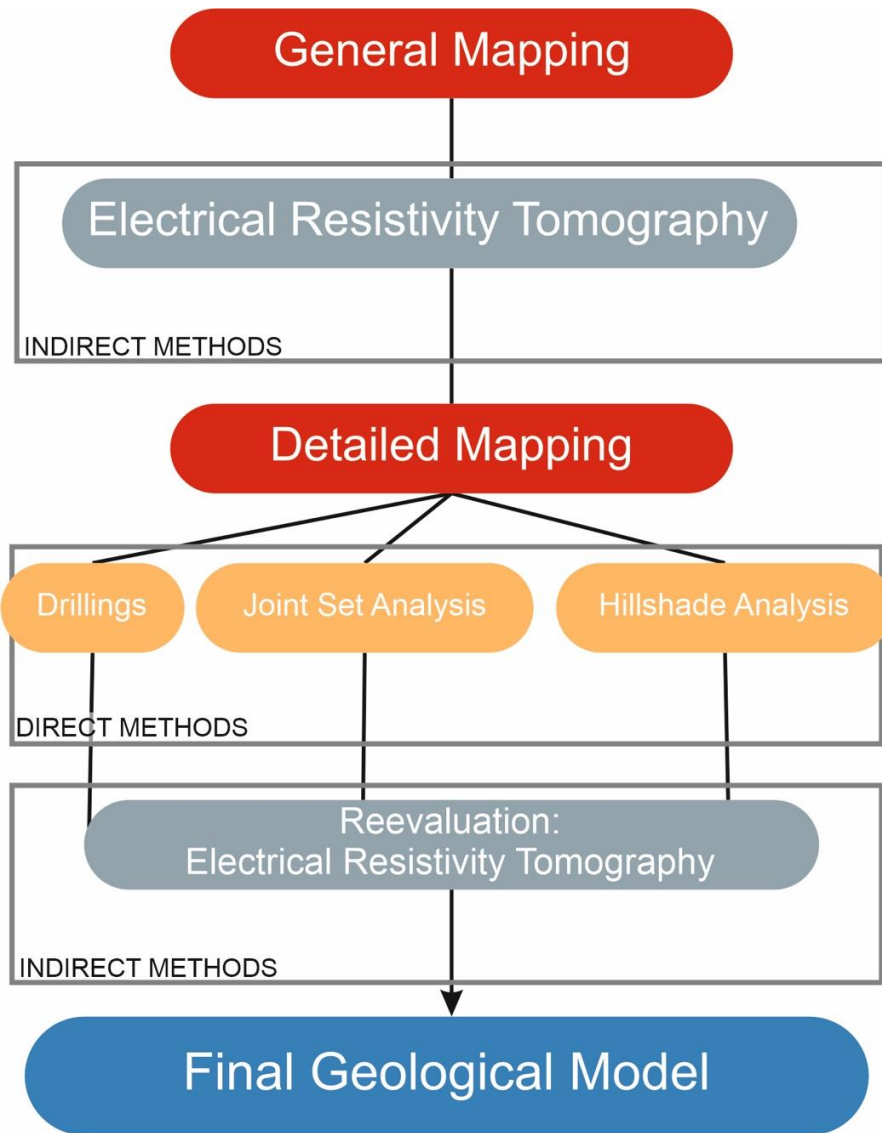
110 Preliminary information about the geology and the geologic investigations in the study site have been
111 published by Breuninger et al., 2021 and Breuninger et al., 2021b. Yet, the information was
112 complemented by core drillings since, and the geological model could be updated. Especially the
113 ERT analyses could be re-interpreted on basis of the drilling results. The scope of this study is to
114 present the new model in context with the preexisting information and compare the two versions of
115 the interpretation, illustrating the advantages of combining direct and indirect investigation methods.

116 **2 Methods**

117 To investigate the morphology, geology and hydrogeology of the landslide-prone slope, a workflow
118 consisting of several steps was devised (figure 1). The steps are divided into direct and indirect
119 investigation methods, which are employed and re-interpreted in turn.

120 Primarily, general morphological, geological and process mappings were used to get an overview of
121 the area and define the further steps. Subsequently, we decided to use ERT (electrical resistivity

122 tomography) both perpendicular and parallel to the slope in order to find a rough outline of the
 123 geological structures. Following, we employed a more detailed geological mapping. These results
 124 were the basis for deciding the locations of four core drillings. The purpose of the drillings was both
 125 for geotechnical and hydrogeological assessment as well as for slope monitoring, as groundwater and
 126 deformation sensors were also installed (see also Gamperl et al., 2023, 2021; Singer et al., 2021). The
 127 observations of the drill cores were combined with an analysis of the large-scale geologic structures
 128 using digital elevation models (in form of hillshades) on the basis of UAV flights and on-site joint set
 129 analysis using the scanline method.



130
 131 **Figure 1: Workflow of step-by-step approach depicting the re-evaluation of indirect results**
 132 **after direct results are available.**

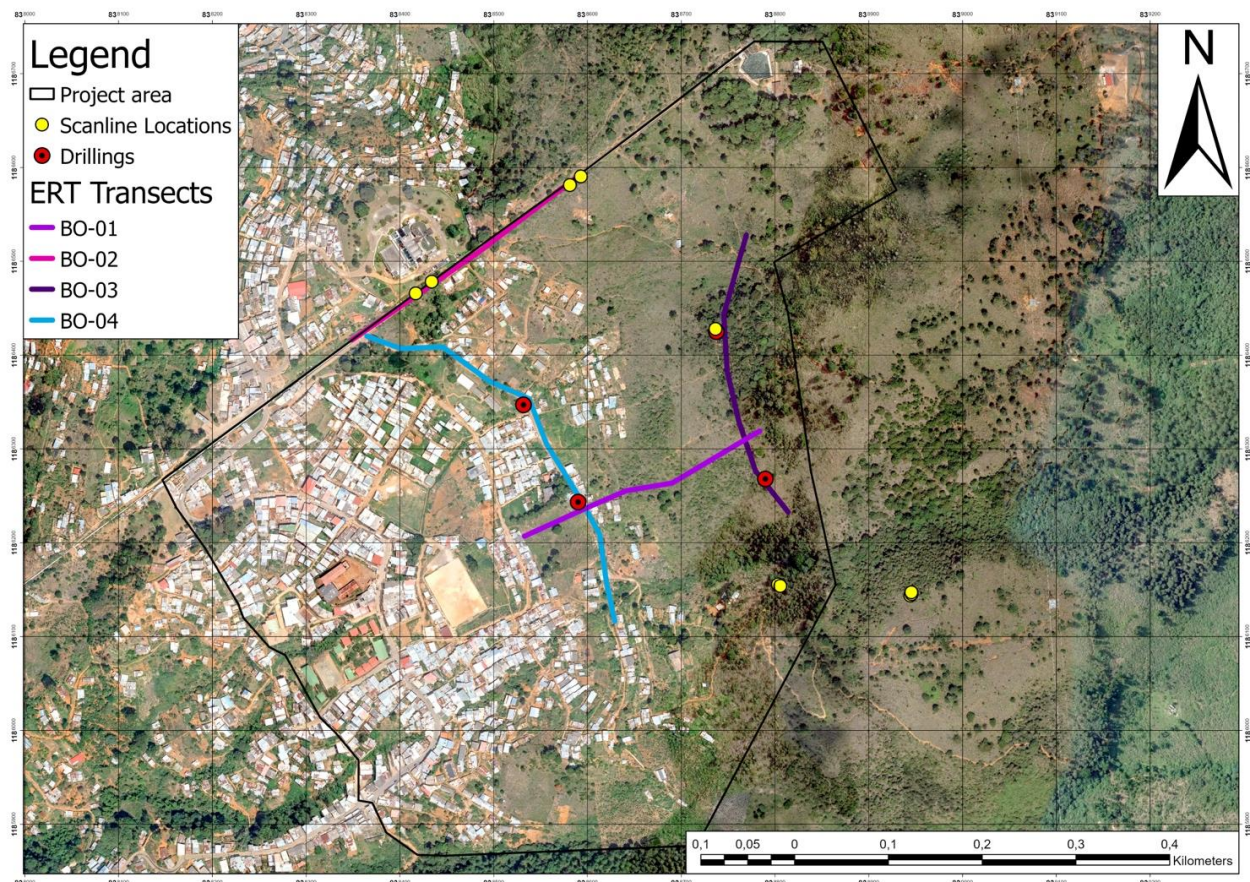
133 This direct information was used to re-evaluate the ERT results and to calibrate them accordingly.
 134 The final geological and geotechnical sections and maps were derived from the combination of all
 135 these methods, and, together with the geotechnical parameters from laboratory tests on drilling and
 136 surface samples, were used to finalize the geological model. All investigation locations (ERT
 137 sections, core drillings, scanlines) are visualized in figure 2.

138

139 2.1 Mapping and core drilling

140 During two field trips in August 2019 and February 2020, a process map, depicting former
141 landslides, and a geological map, depicting the weathering-related ratio of blocks and matrix of the
142 dunite rock in the barrio, were created. The process map was produced with help of the community
143 members, since most old landslides structures are not visible anymore due to intense building
144 activities, especially in the lower part of the barrio. The geological map depicts areas of fractured but
145 stable rock, saprolite, and block-in-matrix structures of differing ratios of blocks and matrix
146 (Breuninger et al., 2021b).

147 The drilling locations were chosen to intersect with the ERT-profiles in order to correlate as much
148 information as possible. Additionally, the drillings were used to install first sensors for the early
149 warning system. Therefore, the locations were also chosen due to an expected depth of block-in-
150 matrix structure of at least 10 m to monitor the structure's behavior. Drillings A1 and A2 reached a
151 depth of approximately 30 m, while the two deeper drillings B1 and B2 both reached a depth of
152 50.0 m. All drillings were performed by double core wireline drilling method without oriented core
153 and an inner diameter of 101.6 mm (drillings B1 and B2) and 63.5 mm (drillings A1 and A2). All
154 drillings were evaluated regarding core loss, weathering, RQD, fracture ratio and orientation, and
155 alteration type (Breuninger et al., 2021b).



156

157 **Figure 2: Location of study area Bello Oriente with drillings, scanlines and ERT profiles.**

158 **2.2 Structural analysis**

159 The core drilling and detailed mapping results required a further investigation of the structural
160 geology of the area as the joint network proved to be essential in understanding the geology
161 (Breuninger et al., 2021b). Therefore, investigations in two scales were put through: (1) a hillshade
162 (DEM) analysis which provides the general distribution of fractures in the study area, and (2)
163 scanlines on some outcrops in the study area which provide a very detailed account of the local
164 fracture network. The combination of the two together with preexisting information about fractures in
165 the Medellín Dunite aims at a complete picture of the fracture network in the area.

166 The hillshade analysis was performed on a digital elevation model which was generated using UAV
167 elevation data of the study site. The data was received and analyzed by the Deggendorf Institute of
168 Technology as part of the Inform@Risk research project (Werthmann et al., 2023). The structures
169 visible in the hillshade were combined with the preexisting structural geology of the Aburrá Valley
170 (Garcia-Casco et al., 2020).

171 The scanline analysis was performed on eleven areas of the study site, on outcrops of 2.5 to 7 m
172 width after Priest, 1993 (figure 2). The results of the scanline were compared with fracture
173 distribution in the drilling and the fracture dip angle and dip direction of the city model and checked
174 for plausibility. The resulting fracture system for the study area was combined to a map and
175 structural model.

176 **2.3 Electrical Resistivity Tomography**

177 Electrical Resistivity Tomography (ERT) is a geophysical method, which measures the apparent
178 resistivity of the subsurface between two points by inducing current on two other points. By
179 performing numerous measurements along a transect while changing the distance, the apparent
180 resistivity along a 2D-profile can be obtained. Inversion of these apparent resistivities over depth
181 yields the specific resistance of the subsurface. This method is advantageous because a large area can
182 be covered with reasonable efforts and the subsurface is undisturbed, in contrast to e.g., drillings. For
183 landslide investigation, ERT is used in various ways for reconnaissance, characterization and early
184 warning (Drahor et al., 2006; Pánek et al., 2008; Perrone et al., 2014; Revil et al., 2020). In the
185 context of landslide investigation, ERT can be especially helpful in identifying horizontal
186 discontinuities and shallow landslides using Wenner or Wenner-Schlumberger arrays (Perrone et al.,
187 2014). Another advantage is that time series can be measured on transects with fixed electrode
188 locations, thus enabling researchers to observe changes in e.g. groundwater or permafrost (Holmes et
189 al., 2020; Scandroglio et al., 2021; Uhlemann et al., 2017), or due to weathering (Ündül and Tuğrul,
190 2012). This method is especially useful in scenarios where cavities in the subsurface need to be
191 identified or the location of lateral or vertical changes in geology are asked for (Prins et al., 2019;
192 Youssef et al., 2012).

193 The ERT investigations were put through in August 2019, after the first mapping campaign. The
194 transects BO-01 to BO-04 were chosen in a way so they are located perpendicular along and across
195 the slope (figure 2). The measurements were made using an ABEM LS2 with an electrode spacing of
196 5 m and cable lengths of 315 m for transects BO 01-03 and 465 m for transect BO-04. After a first
197 test of Wenner, Schlumberger and Dipole-Dipole- arrays on a small section of BO-01, Wenner was
198 used for all measurements for better sensibility for lateral changes in the subsurface. During the main
199 surveys, a preliminary contact test showed that sufficient contact between electrodes and ground was
200 available, although due to the (relatively) dry season prior to the investigation, the soil was
201 significantly dried up and some of the electrodes had to be treated with saltwater first.

202 For inversion and display of the results, the software RES2DINV by Geotomo was used, with
203 smoothness-constrained least-squares/robust inversion. Model refinement was selected to display the
204 large variations of resistivities on the surface. For calibration of the results, first, for a rough
205 identification, a dunite block of about 20x15x10 cm with visually little weathering was used and
206 tested in the laboratory. The result was a mean apparent resistivity of 22 kΩm. Further calibration
207 was possible in a subsequent step after the drillings were performed: The direct information retrieved
208 by the drillings was used to validate and calibrate the interpretation of the ERT results.

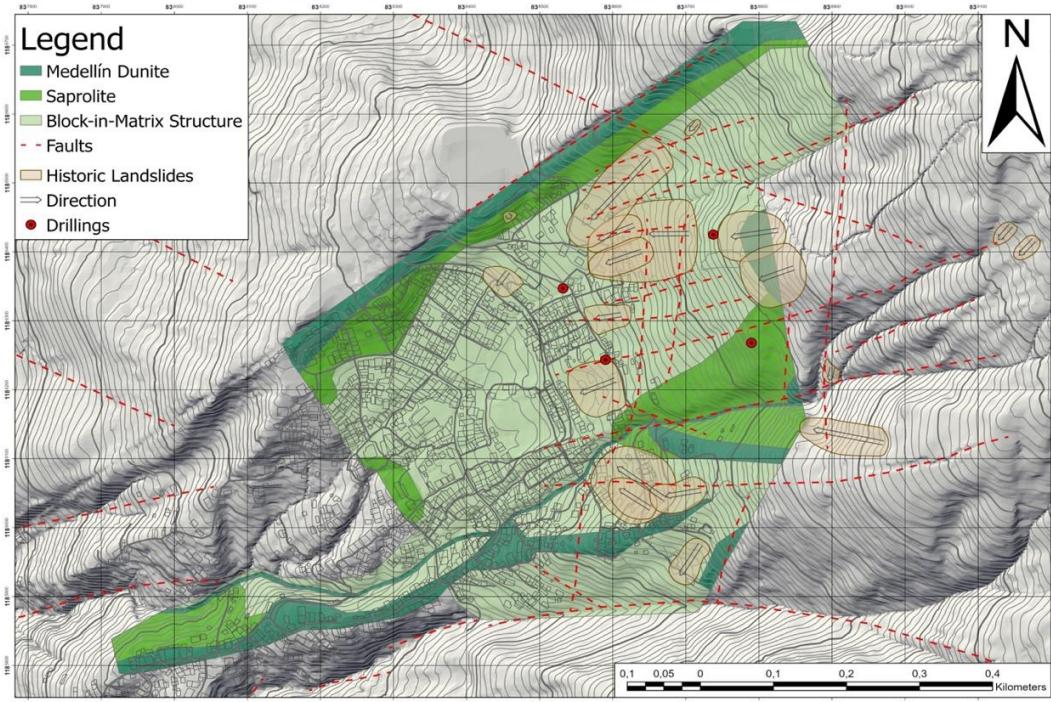
209 3 Results

210 3.1 Mapping

211 Multiple small to medium size historic landslides were detected (figure 3). All landslides are of
212 shallow to medium depth and cover up to 10.000 m² (one landslide 15.000 m²). They are mostly
213 located in the uppermost part of the inhabited area in Bello Oriente and the uninhabited slope above.
214 None of the landslides have been fatal so far, which is most likely due to their small size. Possibly
215 there are older landslides in Bello Oriente that have happened before the area was inhabited but are
216 not visible anymore due to construction works and weathering processes.

217 The area contains several approx. SW-NE striking ridges of heavily weathered but still intact rock
218 (dark green in figure 3), that are stable and not prone to landslides. The saprolite (medium green)
219 is mostly adjacent to the ridges. This material is deeply in-situ weathered rock, that shows a low friction
220 angle and cohesion and is therefore prone to landslides. The rest of the study site is composed of
221 material in block-in-matrix structure with varying ratios of blocks and matrix, mainly with blocks
222 dominating the ratio (light green). These areas with block-in-matrix structure are most prone to
223 landslides and contain the majority of mapped historic landslides in the barrio.

224



225 **Figure 3: Synthesis map depicting the general geology, fault structures, historic landslides of**
226 **the study site in Bello Oriente.**

227 **3.2 First ERT results**

228 First results of the ERT campaign, with a superficial interpretation of one profile show a high
229 variation of resistivities (10 to 10000 Ωm) near the surface, while further below the resistivities are
230 lower, around 200-700 Ωm . The soil-rock boundary was expected to be found below, at a depth of
231 about 30-50 m with resistivities of the rock above 1000 Ωm . The difference in resistivities indicated
232 the soil above the rock to be clearly delineated from the rock below, which was in line with the first
233 overall geological model.

234 RMS (root-mean-square) deviation was limited to 5.7 to 7.1%, except for BO-02 which showed a
235 deviation of 48.6% and therefore was subsequently not used for interpretation. The high RMS error
236 can be attributed to a water pipe located close to the transect which caused extremely low resistivities
237 in the profile.

238 **3.3 Core drillings**

239 Four double tube core barrel drillings (A1, A2, B1, B2) were sunk as part of the project in fall 2020
240 and 2021. The depth of all four drillings was defined to reach the expected boundary between loose
241 and undisturbed rock at 30-50 m. None of the drillings reached this boundary and all drilling cores
242 showed heavy weathering and fragmentation down to their base.

243 The recovered material is generally heterogeneous. Fragmented and fine-grained sections alternate
244 with sections of solid rock of up to 6.5 m. Some fractures are filled up to 50 cm thick with silt and
245 clay. This material is either brown (oxidized) or grey/green (chlorite, talc, and serpentine minerals).
246 The oxidized material is most likely washed in weathering residue, the grey/green material is most
247 likely residue from the pseudokarst process (second serpentinization). No correlation can be made
248 between depth and occurrence of either oxidized or serpentinization-material.

249 The segments of solid rock show oxidation and serpentinization, most strongly along fractures (figure
250 4). Both processes occur together as well as separately. There are no parts in any drilling with more
251 than a few centimetres of unaltered rock. Some sections are solely fragmented with no fine material
252 or oxidation apparent (figure 4). This material was altered by the second serpentinization process
253 (pseudokarst), which has weakened the rock but not disintegrated it completely.



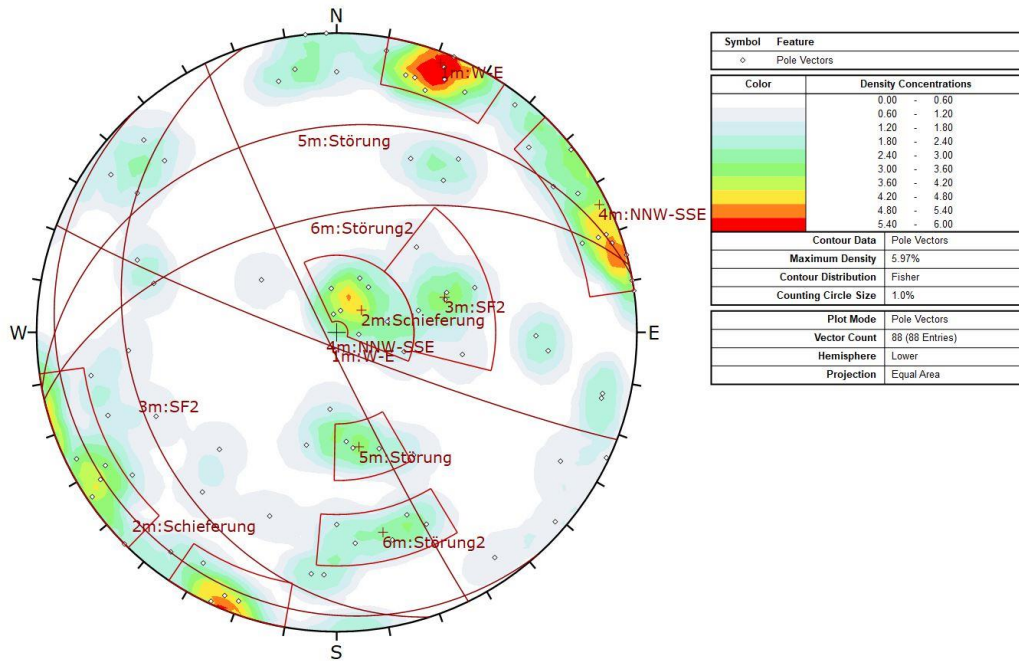
254

255 **Figure 4: (a) Blocky material on the surface; (b) karstic holes under the excavated trench on**
256 **the upper part of the area; (c) trench in relatively undisturbed saprolite material with a lack of**
257 **large blocks. Pictures by (a) Josefina Ziegler, (b) Carolina Garcia-Londoño, (c) David Ceron.**

258 **3.3.1 Structural Analysis**

259 The structural analysis of both hillshade and the on-site scanlines indicate a strong E-W directed fault
260 system, as well as systems perpendicular to it (NNE-SSW) and parallel to the slope. Some subsets of
261 fractur systems also show NNW orientation. The structural model resulting from the scanlines is
262 shown in figure 5.

263



264

265 **Figure 5: Structural Analysis of 11 Scanlines.**

266 **3.4 Re-interpretation of ERT data**

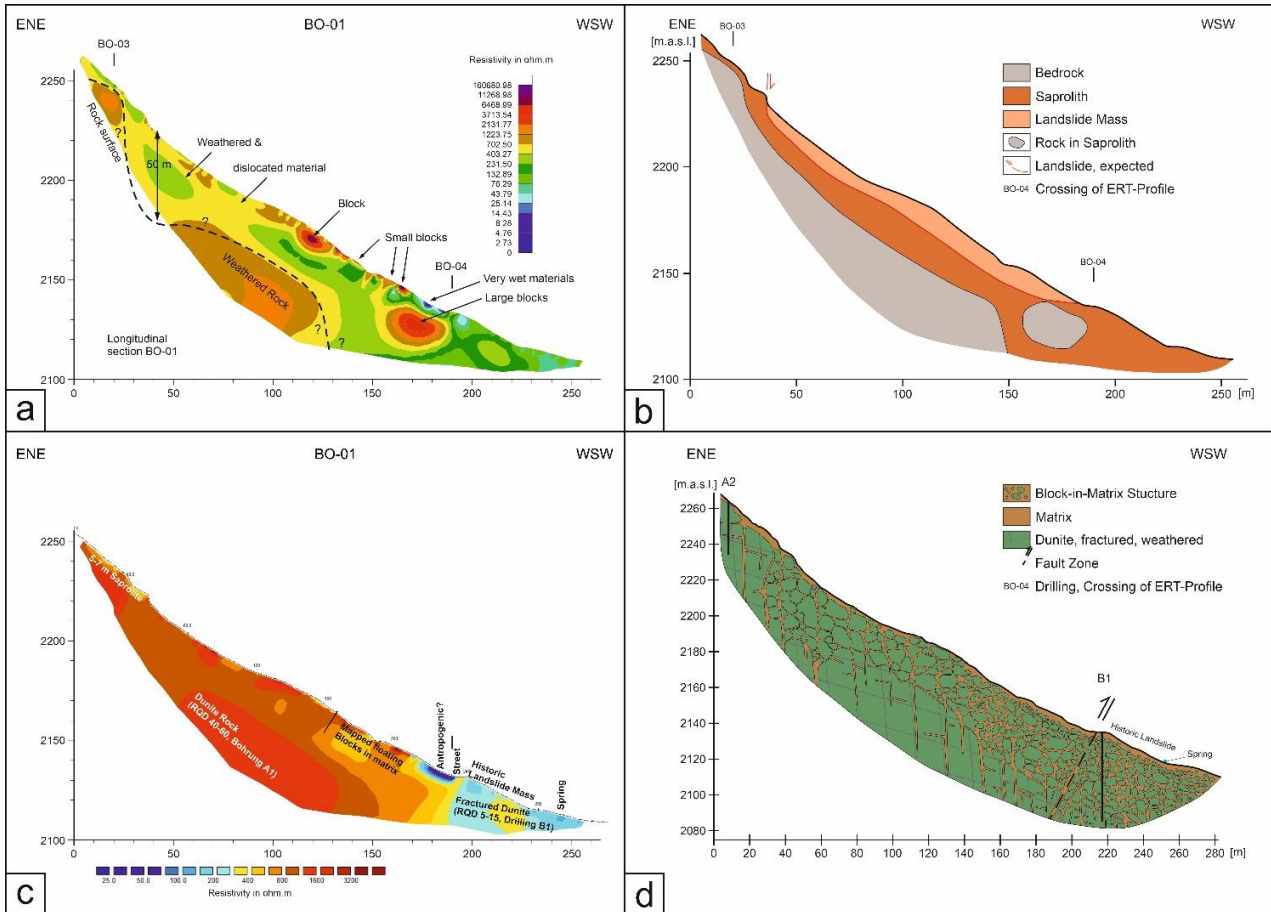
267 The preliminary geological model based on the first mapping comprised a relatively simple
268 geological section with sharp contrasts between the dunite rock in the subsurface and loose material
269 consisting of saprolite (fine material) and colluvium (previously moved landslide material, chaotic
270 distribution, BIM structure). This is shown as an example on one profile across the slope in figure 6.

271 This model was also based on the to-be-expected weathering profile in the dunite, which goes
272 through all weathering steps, ranging from fresh rock to highly weathered rock and, at the end,
273 residual soil on top. Bringing this weathering profile in line with the first ERT results was possible
274 and resulted in the - at the time - plausible section b (figure 6).

275 When incorporating the results from the previous sections into the interpretation, the geological
276 model becomes more complex. The gradual weathering profile mentioned before could not be
277 observed, instead we found a complex sequence comprising colluvium in varying proportions of
278 blocks and surrounding matrix. There is a gradual transition between this material and the underlying
279 fractured Medellín Dunite, and a distinction cannot be made when only looking at the drill cores. The

280 ERT sections on the other hand show an increase of resistivities below 20-30 m. Additionally, the
 281 previously mentioned ‘pseudokarst’ structures could be observed in drillings and trenches, although
 282 on a smaller scale than expected (figure 6).

283 This was confirmed by the joint set and hillshade analysis which both showed a dense network of
 284 fractures in large and small scale.



285
 286 **Figure 6: Results of ERT transects and their interpretation – before and after drilling results**
 287 **were available. (a) Preliminary ERT result and first interpretation as published in Thuro et al.**
 288 **2020. (b) Geological section on basis of (a) and mapping (Breuninger et al 2021 ISL). (c)**
 289 **Updated interpretation of ERT results on basis of the drilling results. (d) geological section BO-**
 290 **01 on basis of updated interpretation.**

291 4 Discussion

292 4.1 Implications for the subsurface of the study site

293 The Medellín Dunite is highly altered, which is apparent due to the presence of serpentine minerals in
 294 the rock. Depending on the sampling location, the serpentine minerals have replaced the olivines and
 295 pyroxenes completely (Botero Arango, 1963; Breuninger et al., 2021b). These weathering processes
 296 are so advanced, that the Medellín Dunite is dismantled into a block-in-matrix (BIM) structure of at
 297 least 50 m depth (Breuninger et al., 2021b). There is no distinct boundary to the ‘non-weathered’
 298 dunite below – ‘non-weathered’ here meaning no secondary serpentinization and pseudokarst

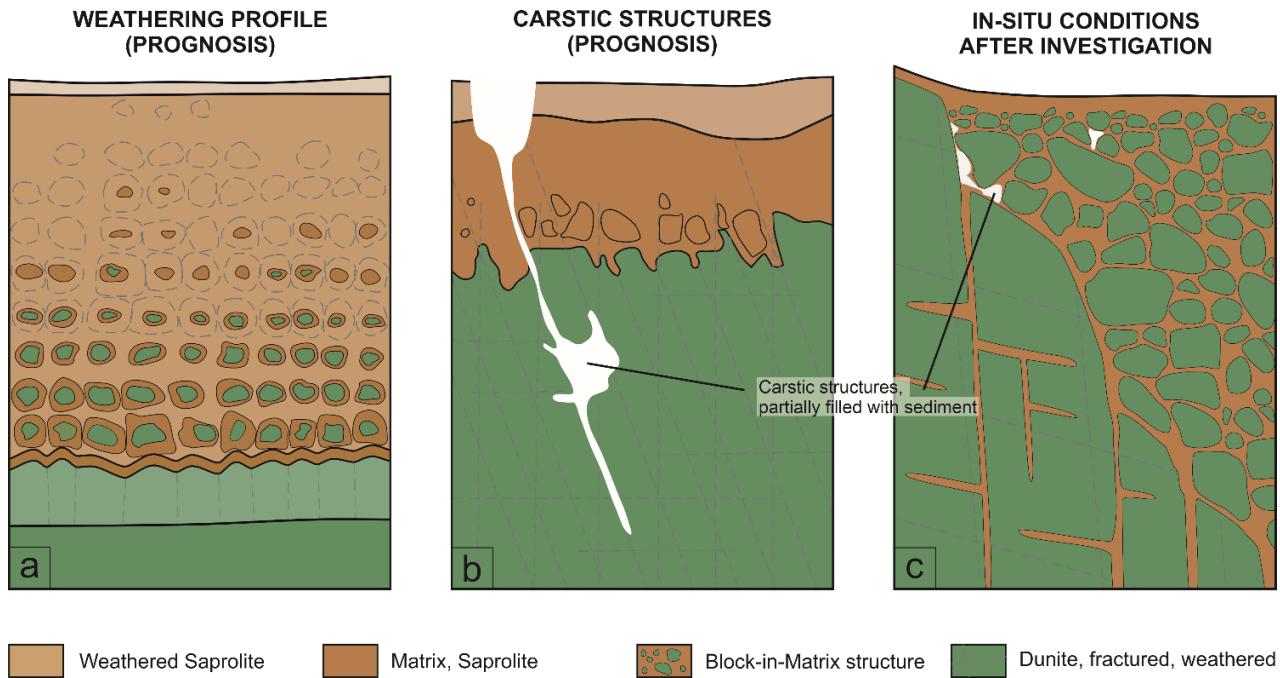
299 processes. This is also indicated by laboratory tests which show a chaotic distribution of tensile and
300 compressive strengths, independent of the depth of sample locations (Breuninger et al., 2021b).

301 Generally, the resistivities in the subsurface up to 60 m are much lower than the 22 kΩm measured
302 on the calibration block and more in line with the numbers described in the literature (Savin et al.,
303 2003; Ündül et al., 2015; Yassin et al., 2014), granted they are measured in slightly differing
304 geological conditions. The calibration block can thus be estimated as the resistivity of the intact rock,
305 which is plausible due to its low porosity, compactness, and lack of conducting minerals (mean
306 density 2.75 g/cm³). The lower resistivities measured in all transects can be attributed to the intensive
307 fracturing of the rock mass observed in the drillings. The soil material comprising the saprolite and
308 the oxidized matrix in the BIM structure is expected to have a very low resistivity as it is soft, water
309 saturated and high in clay minerals.

310 As ultramafites are relatively rare rocks, there exist only few studies about geophysical methods in
311 ultramafic rocks. Ündül et al., 2015 investigated the correlation of geotechnical parameters and
312 weathering with ERT results in a short ERT transect in dunite. The study shows the weathering by
313 both serpentinization and oxidation, which can occur together or separate. With this weathering
314 comes a decrease of geotechnical strength properties and an increase in fractures and porosity.

315 From these results, we compiled a conceptual weathering profile for the study site. The resulting
316 weathering profiles for the first and the updated geological model are displayed in figure 7. Figure 7a
317 shows the model as described in Werthmann et al., 2012, with the regular weathering model ranging,
318 in a fairly structured manner, from unweathered rock to soil material. Figure 7b shows the weathering
319 model including the pseudokarst phenomena as shown by Tobón-Hincapié, 2011. Although it
320 includes the mentioned secondary weathering phenomena, this model still is not sufficient to explain
321 the situation in our study site. Additionally to pseudokarst and deep weathering, the weathered
322 surface also shows many irregularities, as detailed above. While in some areas, the unweathered
323 dunite rock reaches up to the surface, in other areas the block-in matrix cover can reach depths of up
324 to 50 m. This is illustrated in figure 7c. The pseudokarst phenomena we found in the field (figure 4),
325 which ranged up to 1 m of open cavities, were not as large as the ones described in the literature
326 (Tobón-Hincapié, 2011),.

327



328

329

330

331

Figure 7: Weathering profiles before and after the new interpretation. (a) is the weathering model after Werthmann et al., (2012). (b) model after (Tobón-Hincapié, 2011). (c) in-situ conditions found in our investigations.

332

333

334

335

336

Regarding the implications for the landslide hazard, the ubiquitous distribution of colluvium shows that there is a high landslide hazard throughout the slope. If there was less vegetation and a different climate zone, many more historic landslides would be visible. On the other hand, the large blocks in the subsurface can be expected to effectively act against larger landslides as new landslides will likely form around the blocks and stay shallow in depths of several meters only.

337

4.2 Advantages of combining indirect and direct investigation methods

338

339

340

341

342

343

344

345

346

347

The results of our study show that combining indirect and direct methods to investigate the subsurface of landslide sites is viable and can lead to better results, as the methods complement each other. The comparison of the preliminary model (before direct observations) to the more developed model, which includes direct observations from drillings showed that only the indirect observations were not sufficient in this complex geological setting to fully investigate the geological conditions. While some questions are still not answered, a much deeper and denser insight into the subsurface is available now. The 2D ERT transects provided a spatially comprehensive, albeit sometimes fuzzy picture of the subsurface, and the high-effort, expensive, drillings ‘sharpen’ the picture, showing exact borders where available. Also, with the help of the ERT transects, the number of core drillings could be kept to a minimum.

348

349

350

351

The results also show the extraordinary heterogeneity of the Medellín Dunite, which is due to its long geologic history of multiple serpentinization, and further fractioning caused by tectonic activities. The current situation only adds to this heterogeneity because of the steep topography, which prevents the formation of a deep saprolite and soil cover in favor of the chaotic block-in-matrix structure.

352 The karstic sinkholes, which were observed at the surface (figure 4) and likely encountered in some
353 of the drillings, could not as easily be seen in the ERT surveys. This might be due to their mostly
354 small size, or because the sinkholes themselves – mostly filled with matrix – have relatively similar
355 resistivities to the fractured dunite surrounding them. Literature values for sinkholes range from
356 about 2000 Ωm (Youssef et al., 2012) to between 3000 and 6000 Ωm (Yassin et al., 2014). This is
357 similar to what we found in the deeper subsurface and attribute to the fractured dunite with less
358 matrix (figure 6), so that potential sinkholes, if large enough to be picked up by ERT, are likely
359 masked by this effect.

360 Generally, we can recommend multi-step approaches combining direct and indirect observations for
361 future investigation efforts. Especially the combination of ERT and drillings is helpful in difficult
362 geologic circumstances, although which specific methods are applied surely can vary tremendously
363 depending on the topography, geology, vegetation and many more factors. Care has to be taken to
364 always start with at least some direct observations (e.g. mapping) as a basis for the subsequent
365 indirect investigations, so they are based on reliable data.

366 **5 Conflict of Interest**

367 *The authors declare that the research was conducted in the absence of any commercial or financial*
368 *relationships that could be construed as a potential conflict of interest.*

369 **6 Author Contributions**

370 MG, KT, TB and BM contributed to conception and design of the study. MG, DC and TB performed
371 the measurements, analysis and validation. MG wrote the first draft of the manuscript. TB wrote
372 sections of the manuscript. Visualization by MG and TB. KT and BM supervised the project. All
373 authors contributed to manuscript revision, read, and approved the submitted version.

374 **7 Funding**

375 This research was funded by the German Federal Ministry of Education and Research, grant number
376 03G0883A-F.

377 **8 Acknowledgments**

378 We would like to thank the local community of Bello Oriente for their help in mapping and the ERT
379 investigations, as well as volunteers from Servicio Geológico Colombiano. We thank DAGRD in
380 Medellín for transportation and further support. We especially thank Ms. Fretzdorff and Ms. Putbrese
381 from Project Management Jülich for their continuous support. We thank Prof. M. Krautblatter for
382 guidance in the interpretation of ERT data.

383 **9 References**

384 Botero Arango, G., 1963. Contribución al Conocimiento de la Geología de la Zona Central de
385 Antioquia (No. 57), Anales de la Facultad de Minas. Universidad Nacional de Colombia, Medellín.

386 Breuninger, T, Gamperl, M., Menschik, B., Thuro, K., 2021. First Field Findings and their
387 Geological Interpretations at the Study Site Bello Oriente, Medellín, Colombia (Project
388 Inform@Risk), in: Proceedings of the 13th International Symposium on Landslides. Presented at the

- 389 XIII International Symposium on Landslides, International Society for Soil Mechanics and
390 Geotechnical Engineering, Cartagena, Colombia, p. 7.
- 391 Breuninger, Tamara, Garcia-Londoño, C., Gamperl, M., Thuro, K., 2021a. Initial Experiences of
392 Community Involvement in an Early Warning System in Informal Settlements in Medellín,
393 Colombia, in: Sassa, K., Mikoš, M., Sassa, S., Bobrowsky, P.T., Takara, K., Dang, K. (Eds.),
394 Understanding and Reducing Landslide Disaster Risk, ICL Contribution to Landslide Disaster Risk
395 Reduction. Springer International Publishing, Cham, pp. 597–602. https://doi.org/10.1007/978-3-030-60196-6_53
- 397 Breuninger, Tamara, Menschik, B., Demharter, A., Gamperl, M., Thuro, K., 2021b. Investigation of
398 Critical Geotechnical, Petrological and Mineralogical Parameters for Landslides in Deeply
399 Weathered Dunite Rock (Medellín, Colombia). *International Journal of Environmental Research and
400 Public Health* 18. <https://doi.org/10.3390/ijerph18211141>
- 401 Drahor, M.G., Göktürkler, G., Berge, M.A., Kurtulmuş, T.Ö., 2006. Application of electrical
402 resistivity tomography technique for investigation of landslides: a case from Turkey. *Environ Geol*
403 50, 147–155. <https://doi.org/10.1007/s00254-006-0194-4>
- 404 Gamperl, M., Breuninger, T., Singer, J., García-Londoño, C., Menschik, B., Thuro, K., 2021.
405 Development of a Landslide Early Warning System in informal settlements in Medellín, Colombia,
406 in: *Proceedings of the 13th International Symposium on Landslides*. Presented at the XIII
407 International Symposium on Landslides, International Society for Soil Mechanics and Geotechnical
408 Engineering, Cartagena, Colombia, p. 8.
- 409 Gamperl, M., Singer, J., Garcia-Londoño, C., Seiler, L., Castañeda, J., Cerón-Hernandez, D., Thuro,
410 K., 2023. An integrated, replicable Landslide Early Warning System for informal settlements – case
411 study in Medellín, Colombia (preprint). *Databases, GIS, Remote Sensing, Early Warning Systems
412 and Monitoring Technologies*. <https://doi.org/10.5194/nhess-2023-20>
- 413 Garcia-Casco, A., Restrepo, J.J., Correa-Martínez, A.M., Blanco-Quintero, I.F., Proenza, J.A.,
414 Weber, M., Butjosa, L., 2020. The Petrologic Nature of the “Medellín Dunite” Revisited: An
415 Algebraic Approach and Proposal of a New Definition of the Geological Body, in: Gomez, J.,
416 Pinilla-Pachon, A.O. (Eds.), *The Geology of Colombia, Volume 2 Mesozoic*, Publicaciones
417 Geológicas Especiales. Servicio Geológico Colombiano, Bogotá, p. 31.
- 418 Holmes, J., Chambers, J., Meldrum, P., Wilkinson, P., Boyd, J., Williamson, P., Huntley, D., Sattler,
419 K., Elwood, D., Sivakumar, V., Reeves, H., Donohue, S., 2020. Four-dimensional electrical
420 resistivity tomography for continuous, near-real-time monitoring of a landslide affecting transport
421 infrastructure in British Columbia, Canada. *Near Surface Geophysics* 18, 337–351.
422 <https://doi.org/10.1002/nsg.12102>
- 423 Jairo, H.A., 2003. *CARSO DE ALTA MONTAÑA EN SANTA ELENA*. Universidad Nacional de
424 Colombia, Medellín.
- 425 Kühnl, M., Sapena, M., Taubenböck, H., 2021. Categorizing Urban Structural Types using an
426 Object-Based Local Climate Zone classification Scheme in Medellín, Colombia, in: *Proceedings of
427 REAL CORP 2021, 26th International Conference on Urban Development, Regional Planning and
428 Information Society*. Presented at the *CITIES 20.50 – Creating Habitats for the 3rd Millennium:
429 Smart – Sustainable – Climate Neutral*, Wien, Austria, pp. 173–182.

- 430 Mével, C., 2003. Serpentinization of abyssal peridotites at mid-ocean ridges. *Comptes Rendus*
431 *Geoscience* 335, 825–852. <https://doi.org/10.1016/j.crte.2003.08.006>
- 432 Pánek, T., Hradecký, J., Šilhán, K., 2008. Application of electrical resistivity tomography (ERT) in
433 the study of various types of slope deformations in anisotropic bedrock: Case studies from the flysh
434 carpathians. *Stud. Geomorphol. Carpatho Balc.* 42, 57–73.
- 435 Perrone, A., Lapenna, V., Piscitelli, S., 2014. Electrical resistivity tomography technique for
436 landslide investigation: A review. *Earth-Science Reviews* 135, 65–82.
437 <https://doi.org/10.1016/j.earscirev.2014.04.002>
- 438 PRIEST, S.D., 1993. The Collection and Analysis of Discontinuity Orientation Data for Engineering
439 Design, with Examples, in: HUDSON, J.A. (Ed.), *Rock Testing and Site Characterization*. Pergamon,
440 Oxford, pp. 167–192. <https://doi.org/10.1016/B978-0-08-042066-0.50015-X>
- 441 Prins, C., Thuro, K., Krautblatter, M., Schulz, R., 2019. Testing the effectiveness of an inverse
442 Wenner-Schlumberger array for geoelectrical karst void reconnaissance, on the Swabian Alb high
443 plain, new line Wendlingen–Ulm, southwestern Germany. *Engineering Geology* 249, 71–76.
444 <https://doi.org/10.1016/j.enggeo.2018.12.014>
- 445 Revil, A., Soueid Ahmed, A., Coperey, A., Ravanel, L., Sharma, R., Panwar, N., 2020. Induced
446 polarization as a tool to characterize shallow landslides. *Journal of Hydrology* 589, 125369.
447 <https://doi.org/10.1016/j.jhydrol.2020.125369>
- 448 Sapena, M., Kühnl, M., Wurm, M., Patino, J.E., Duque, J.C., Taubenböck, H., 2022. Empiric
449 recommendations for population disaggregation under different data scenarios. *PLoS ONE* 17,
450 e0274504. <https://doi.org/10.1371/journal.pone.0274504>
- 451 Savin, C., Robineau, B., Monteil, G., Beauvais, A., Parisot, J.C., Ritz, M., 2003. Electrical imaging
452 of peridotite weathering mantles as a complementary tool for nickel ore exploration in New
453 Caledonia. *ASEG Extended Abstracts 2003*, 1–5. <https://doi.org/10.1071/ASEG2003ab148>
- 454 Scandroglio, R., Draebing, D., Offer, M., Krautblatter, M., 2021. 4D quantification of alpine
455 permafrost degradation in steep rock walls using a laboratory-calibrated electrical resistivity
456 tomography approach. *Near Surface Geophysics* 19, 241–260. <https://doi.org/10.1002/nsg.12149>
- 457 Servicio Geológico Colombiano, n.d. SIMMA Sistema de Información de Movimientos en Masa.
458 Accessed: 30.03.2023.
- 459 Singer, J., Thuro, K., Gamperl, M., Breuninger, T., Menschik, B., 2021. Technical Concepts for an
460 Early Warning System for Rainfall Induced Landslides in Informal Settlements, in: Casagli, N.,
461 Tofani, V., Sassa, K., Bobrowsky, P.T., Takara, K. (Eds.), *Understanding and Reducing Landslide*
462 *Disaster Risk: Volume 3 Monitoring and Early Warning*. Springer International Publishing, Cham,
463 pp. 209–215. https://doi.org/10.1007/978-3-030-60311-3_24
- 464 Thuro, K., Singer, J., Menschik, B., Breuninger, T., Gamperl, M., 2020. Development of a Landslide
465 Early Warning System in informal settlements in Medellín, Colombia. *Geomechanics and Tunnelling*
466 13, 103–115. <https://doi.org/10.1002/geot.201900071>

- 467 Tobón-Hincapié, M.P., 2011. MEDIDAS DE MITIGACIÓN DE LA LADERA ORIENTAL DEL
468 VALLE DE ABURRÁ ENTRE LAS QUEBRADAS LA POBLADA Y LA SANÍN.
- 469 Uhlemann, S., Chambers, J., Wilkinson, P., Maurer, H., Merritt, A., Meldrum, P., Kuras, O., Gunn,
470 D., Smith, A., Dijkstra, T., 2017. Four-dimensional imaging of moisture dynamics during landslide
471 reactivation: Imaging of Landslide Moisture Dynamics. *J. Geophys. Res. Earth Surf.* 122, 398–418.
472 <https://doi.org/10.1002/2016JF003983>
- 473 UNDRR, 2015. Sendai Framework for Disaster Risk Reduction 2015 - 2030. United Nations Office
474 for Disaster Risk Reduction. <https://www.undrr.org/quick/11409>
- 475 Ündül, Ö., Tuğrul, A., 2012. The Influence of Weathering on the Engineering Properties of Dunites.
476 *Rock Mech Rock Eng* 45, 225–239. <https://doi.org/10.1007/s00603-011-0174-1>
- 477 Ündül, Ö., Tuğrul, A., Özyalın, Ş., Zarif, İ.H., 2015. Identifying the changes of geo-engineering
478 properties of dunites due to weathering utilizing electrical resistivity tomography (ERT). *Journal of*
479 *Geophysics and Engineering* 12, 273–281. <https://doi.org/10.1088/1742-2132/12/2/273>
- 480 Werthmann, C., 2023. Reporting from the front. *Nat Hazards*. [https://doi.org/10.1007/s11069-023-](https://doi.org/10.1007/s11069-023-05815-3)
481 [05815-3](https://doi.org/10.1007/s11069-023-05815-3)
- 482 Werthmann, C., Echeverri, A., Elvira Vélez, A., 2012. Rehabitar La Ladera: Shifting Ground
483 (Research Report). Universidad EAFIT, Medellín.
- 484 Werthmann, C., Sapena, M., Kühnl, M., Singer, J., Garcia, C., Menschik, B., Schäfer, H., Schröck,
485 S., Seiler, L., Thuro, K., Taubenböck, H., 2023. Inform@Risk. The Development of a Prototype for
486 an Integrated Landslide Early Warning System in an Informal Settlement: the Case of Bello Oriente
487 in Medellín, Colombia. *Natural Hazards and Earth System Science* 42. [https://doi.org/10.5194/nhess-](https://doi.org/10.5194/nhess-2023-53)
488 [2023-53](https://doi.org/10.5194/nhess-2023-53)
- 489 Yassin, R.R., Muhammad, R.F., Taib, S.H., Al-Kouri, O., 2014. Application of ERT and Aerial
490 Photographs Techniques to Identify the Consequences of Sinkholes Hazards in Constructing Housing
491 Complexes Sites over Karstic Carbonate Bedrock in Perak, Peninsular Malaysia. *JGG* 6, p55.
492 <https://doi.org/10.5539/jgg.v6n3p55>
- 493 Youssef, A.M., El-Kaliouby, H., Zabramawi, Y.A., 2012. Sinkhole detection using electrical
494 resistivity tomography in Saudi Arabia. *J. Geophys. Eng.* 9, 655–663. [https://doi.org/10.1088/1742-](https://doi.org/10.1088/1742-2132/9/6/655)
495 [2132/9/6/655](https://doi.org/10.1088/1742-2132/9/6/655)
- 496

Appendix A-2

Title	Internet of Things Geosensor Network for Cost-Effective Landslide Early Warning Systems				
Journal	Sensors				
DOI	https://doi.org/10.3390/s21082609				
Year	2021	Volume	21(8)	Impact Factor (2022)	3.9
Accepted	Yes	Position of the candidate in the authors list			1
Authors	Moritz Gamperl, John Singer, Kurosch Thuro				

This article was published in Sensors; 21(8); Moritz Gamperl, John Singer, Kurosch Thuro; Internet of Things Geosensor Network for Cost-Effective Landslide Early Warning Systems; Copyright 2021 by the authors. License MDPI, Basel, Switzerland. This article is an open access article distributed under the terms and conditions of the Creative Commons Attribution (CC BY) license, thus permission to reprint the article is not necessary.

Article

Internet of Things Geosensor Network for Cost-Effective Landslide Early Warning Systems

Moritz Gamperl ^{1,*} , John Singer ²  and Kurosch Thuro ¹¹ Chair of Engineering Geology, Technical University of Munich, 82024 Munich, Germany; thuro@tum.de² AlpGeorisk, 85716 Unterschleißheim, Germany; singer@alpgeorisk.de

* Correspondence: moritz.gamperl@tum.de

Abstract: Worldwide, cities with mountainous areas struggle with an increasing landslide risk as a consequence of global warming and population growth, especially in low-income informal settlements. Landslide Early Warning Systems (LEWS) are an effective measure to quickly reduce these risks until long-term risk mitigation measures can be realized. To date however, LEWS have only rarely been implemented in informal settlements due to their high costs and complex operation. Based on modern Internet of Things (IoT) technologies such as micro-electro-mechanical systems (MEMS) sensors and the LoRa (Long Range) communication protocol, the Inform@Risk research project is developing a cost-effective geosensor network specifically designed for use in a LEWS for informal settlements. It is currently being implemented in an informal settlement in the outskirts of Medellin, Colombia for the first time. The system, whose hardware and firmware is open source and can be replicated freely, consists of versatile LoRa sensor nodes which have a set of MEMS sensors (e.g., tilt sensor) on board and can be connected to various different sensors including a newly developed low cost subsurface sensor probe for the detection of ground movements and groundwater level measurements. Complemented with further innovative measurement systems such as the Continuous Shear Monitor (CSM) and a flexible data management and analysis system, the newly developed LEWS offers a good benefit-cost ratio and in the future can hopefully find application in other parts of the world.

Keywords: early warning system; landslides; geosensors; monitoring; Colombian Andes; low income settlements; informal settlements; IoT



Citation: Gamperl, M.; Singer, J.; Thuro, K. Internet of Things Geosensor Network for Cost-Effective Landslide Early Warning Systems. *Sensors* **2021**, *21*, 2609. <https://doi.org/10.3390/s21082609>

Academic Editor: Rafiq Azzam

Received: 5 March 2021

Accepted: 6 April 2021

Published: 8 April 2021

Publisher's Note: MDPI stays neutral with regard to jurisdictional claims in published maps and institutional affiliations.



Copyright: © 2021 by the authors. Licensee MDPI, Basel, Switzerland. This article is an open access article distributed under the terms and conditions of the Creative Commons Attribution (CC BY) license (<https://creativecommons.org/licenses/by/4.0/>).

1. Project Overview Inform@Risk

1.1. Project Background and Goals

Landslide hazard is increasing year by year due to more intense and frequent rainfall as a consequence of climate change [1]. Additionally, secondary causes such as wildfires play an important role in promoting landslides [2]. The poorest residents are often the most vulnerable to landslides because in many cases they live in the most dangerous areas [3–6]. This is especially true in the Andes, where more than 10 million people are exposed to natural hazards and a high degree of inequality is prevalent [7,8]. In Colombia, recent developments have led to an increased rural depopulation and migration into cities, leading to an exponential increase in landslide casualties in the last 50 years [9], with more than half a million families affected by landslides in the past 100 years [9,10]. Rainfall is the most important triggering mechanism for these landslides, although human interference also is an important trigger [11,12].

The research project Inform@Risk aims to strengthen the resilience of informal settlements against rainfall-induced landslides. Since long term risk reduction solutions, as, e.g., the relocation of the endangered inhabitants or the implementation of physical mitigation measures, are currently not feasible due to the high social, political and monetary efforts required and their potential to harm the landscape and ecosystem [13], the Inform@Risk

project is designing and implementing a Landslide Early Warning System (LEWS) as a short- to medium-term risk reduction solution. In order to ensure the successful implementation of such a system, many different technical and social challenges have to be overcome. The main challenges are the design of a cost-effective, reliable and spatially and temporally highly resolved monitoring system and its social integration into the informal settlement where it is implemented. The system can not succeed if it is not supported and trusted by the local residents it is designed for. Adequate risk perception and knowledge of the population is another important factor that determines whether the system can make a lasting impact [14]. Overall, the system needs to address the following points to be successful. It needs to be:

1. Socially integrated;
2. Spatially integrated;
3. Multiscalar;
4. Multisectoral;
5. Precise;
6. Inexpensive;
7. Easily replicable.

This requires intensive interdisciplinary cooperation between scientists, governmental and social institutions as well as the local communities. Therefore, a “living lab” approach is pursued, in which all measures, from geological investigations and the layout of the early warning system to the testing and training phase, are intensively discussed and consulted with the local residents.

To address this, the German team of the Inform@Risk project includes landscape architects (Leibniz University Hannover, LUH), geologists (Technical University of Munich, TUM), geotechnical instrumentation experts (AlpGeorisk, AGR), remote sensing experts (German Aerospace Center Oberpfaffenhofen, DLR and Expert Office for Aerial Image Evaluation and Environmental Issues, SLU), and software developers (Technical University Deggendorf, THD). The Colombian team is comprised of representatives from the center of urban studies (EAFIT university, Medellín) and several municipal agencies responsible for risk management in the city of Medellín (e.g., SIATA, DAGRD) as well as two local NGOs and the Colombian Geological Society.

In the following, after shortly introducing the study area, the technical design of the proposed LEWS is presented, focusing on the newly developed wireless geosensor network. Other essential elements of the research project, for example the landslide hazard and risk assessment and the social work are only covered superficially and will be published in detail elsewhere. A list of publications related to the Inform@Risk research project can be found at <https://www.bmbf-client.de/projekte/informrisk> (accessed on 1 March 2021).

At the time of writing, the Inform@Risk project has reached about two thirds of its 3-year duration (2019–2022) with the finalization of the design of the LEWS. The implementation of the system has been delayed due to the COVID-19 crisis and is currently scheduled for summer/fall 2021.

1.2. Project Area

In Medellín, the second largest Colombian city, landslides are the most common and deadly natural hazard [15]. Compared to the rest of the larger region (Valle de Aburrá), Medellín has by far the highest number of landslide reports [16]. Especially the steep slopes in the east of the city are prone to landslides [17,18]. The four deadliest landslides in Medellín in the last 100 years took place in this area, where at the same time informal settlements have shown some of the highest growth rates in the city. This led to a continuously increasing landslide risk and heavy losses of life in the past 100 years. Based on a 2012 study, more than 200,000 inhabitants in the Aburrá Valley are subject to medium or high landslide risk and live in precarious settlements [17].

This is also where the barrio “Bello Oriente” (Communa 3) is located, which was selected as a test site for the early warning system of the Inform@Risk project. The informal

settlement lies on the urban-rural border of the city and was chosen based on a preliminary qualitative risk assessment at city scale as well as additional social factors (security, community management etc.).

1.3. Geology and Landslide Processes

The geology of Medellín is dominated by magmatic and metamorphic rocks, as well as landslide debris and alluvial deposits. In the east of the city, amphibolites and dunites are the predominant rocks. The Medellín Dunite is primarily serpentinized and highly fractured due to tectonic processes. This leads to complex weathering profiles, which makes the dunite particularly prone to landslides [19]. Geophysical investigations have shown that the weathering depth can reach up to 50 m in some areas [20]. On top of the bedrock, residual soil (saprolite) alternates with slope deposits (colluvium) of varying depth. While the saprolite is usually clay dominated and free of stones and blocks near the surface, the composition of the slope deposits can vary greatly. It can best be described as “block in matrix” material, where many stones and blocks are embedded in a clay dominated matrix. Overall, the soil profile on top of the weathered dunite is very complex and heterogeneous.

As geological and morphological mapping of the project area has shown, the prevalent landslide process is rotational sliding, followed by a comparably small number of translational slides, debris flows in the creeks and minor rockfall at the few rock outcrops within the project area [18]. The slides usually are of small to medium size and depth (up to about 50 m in length and width, and up to 10 m deep). Due to the geological heterogeneity of the subsurface, it is impossible to predict exactly where future slides within the soil cover might occur. However, mainly based on the depth of soil cover (colluvium and saprolite) and the slope inclination it is possible to spatially differentiate the level of landslide hazard throughout the project area. Regarding the velocities of the landslides, we expect initial slow to moderate movements, which can accelerate to rapid and very rapid movements, depending on the water saturation [21].

2. Landslide Early Warning Systems

Since their origin in the 1980s, numerous Landslide Early Warning Systems (LEWS) have been designed and implemented. Some of them focus on a regional, national or global scale (so called “territorial systems”), while other systems focus only on a single slope or landslide (local LEWS). Guzzetti et al. (2020) and Piciullo et al. (2018) highlight a number of territorial systems and present the challenges and possibilities that are inherent to LEWS of this scale [22,23]. Because of the scale, for these types of LEWS only a generalized warning for a region is possible, while localized early warning of a specific area or slope is not possible.

Local LEWS usually include multiple sensors on site, cover a much smaller area (<0.1 km² to 1 km²) [24] and, most importantly, usually are installed in areas where slow movements have already been detected and thus the exact location of a potential landslide is already known. Pecoraro et al. (2019) reviewed several local LEWS around the world and found that the primary parameter used for warning is displacement, followed by the trigger—mostly rainfall—and groundwater parameters. This makes sense since rainfall is the most important triggering factor for landslide early warning [25]. By Pecoraro et al. (2019), also a comparison of the sensor systems in use is made, with the most important monitoring systems being classical geotechnical methods such as inclinometers and piezometers, as well as geophysical (geophones), geodetic (GPS) and remote sensing methods. Yet, such studies rarely take costs into account, which is one of the most important parameters when working in low-income countries [24,26]. Low-Cost monitoring systems until now are mostly limited to GPS networks, acoustic emissions or radio communication [27–31].

2.1. LEWS in Medellín and Colombia

In Colombia, a LEWS on national scale already exists by “IDEAM”—Instituto de Hidrología, Meteorología y Estudios Ambientales [32]. Another system focussing on debris flows exists in Combeima-Tolima, which combines rainfall and geophone data on a regional scale to react once the dynamic thresholds are reached [14,33,34]. On the municipal level, LEWS exist in Bogotá and Medellín (www.idiger.gov.co) (accessed on 1 March 2021), although most of them are regional systems. There are local LEWS in Colombia that focus on landslides, for example a system in the city of Bolivar, based on an open-source system which measures humidity and temperature to determine the risk of landslides [35]. Yet, site-specific warning systems, especially with community involvement and evacuation alarms, are still rare in urban regions [36].

2.2. The Internet of Things and Landslide Monitoring

In the last decade, the Internet of Things (IoT) has become an important concept for landslide monitoring. Its definition, “Sensors and actuators embedded in physical objects are linked through wired and wireless networks” [37], describes why the concept is well applicable to landslide monitoring and early warning. The IoT can help circumvent the problem of often very expensive monitoring systems and other possible problems such as difficult maintenance and rigidity of cable-based (non wireless) systems [38].

IoT systems consist of the Perception layer, the Network layer, the Middle-ware layer and the Application layer [38]. The Perception layer consists of multiple IoT devices that collect data, which is then sent via the Network layer to the Middle-ware layer. Here, the data can be stored and analyzed before it is processed for the user in the Application layer.

One of the most important technologies which is the basis of the IoT is wireless communication technology. Several wireless communication standards for different application profiles have been developed. While some, as, e.g., Wi-Fi offer very high data rates, they are less suitable for battery powered setups where low current consumption and at the same time large communication range is required (other systems such as GSM or satellite communications are less likely to be employed due to their comparably high costs [39]). Systems like Bluetooth offer low energy consumption (Bluetooth Low Energy), but are restricted in terms of their range. The LoRa technology is one of numerous low power wide area networks (LPWANs) which offer very low power consumption, while at the same time providing a wide coverage of 2–5 km in urban and 10–15 km in rural areas refs. [40–42]. For landslide monitoring, LoRa has several advantages over similar LPWANs, for example a payload size which is sufficient for data from multiple sensors on one sensor node (max. 243 bytes) [41]. Furthermore, it is bidirectional, which allows a degree of control over the sensors from the application layer (e.g., changing the time between measurements or updating firmware). Alternatives to LoRa are, e.g., Sigfox and NB-IoT, but LoRa offers the best parameters for this application: it is unlicensed (which NB-IoT is not) and bidirectional (which Sigfox is not), both important factors for a flexible, open-source system [41]. LoRa is being used worldwide in various natural hazard scenarios [39,43,44]. Other landslide early warning systems use or have used similar LPWAN technologies [45,46].

A LoRa data transmission is divided into uplink (device to gateway) and downlink (gateway to device). The uplink usually is significantly bigger than the optional downlink. The uplink packet size has a theoretical maximum of 255 bytes, depending, among others, on the distance from the device to the gateway [39]. In practice, the packet size should not exceed 51 bytes [40]. The LoRaWAN protocol restricts the maximum airtime of devices to 30 s per day, resulting in 20–500 messages per day, depending again on the distance/data rate and the payload size. This ensures that many devices can be in the same network without problems.

Another important technology, which has made the IoT possible, is the development of MEMS (micro-electro-mechanical system) sensors. These combine micro-mechanical elements and electronics in a single chip, allowing to develop small, highly available and low cost sensors for different measurement tasks. MEMS-based sensor systems al-

ready are being widely used for geotechnical instrumentation and landslide monitoring, especially since open-source microprocessors have become readily available in the last years [31,43–57]. They can be a good addition to classic monitoring methods, as discussed by Cmielewski et al. (2013) who investigated the accuracy and precision of a low-cost MEMS accelerometer [53]. They have been in use for rockfall monitoring [43,58,59], but also for shallow rotational landslides. Dikshit et al. (2018) developed a MEMS-based subsurface sensor with a volumetric water content sensor and a tiltmeter [60]. This concept, which is based on that proposed by Uchimura et al. (2010) [61] has also been applied for other LEWS/sites [52,54,62].

3. Inform@Risk Monitoring System

As stated before (Section 1.3), the geology of the project area is quite heterogeneous and complex, while at the same time a high landslide risk is present. With traditional measurement systems, monitoring this area is not possible, especially since it is an informal settlement where cost is one of the most important factors.

Therefore, we developed a LEWS which bridges the gap between local and territorial systems. It offers comparably high spatial and temporal resolution while at the same time being able to monitor a whole neighbourhood where the exact failure location is unknown. On the other hand, it is capable of issuing reliable site specific early warnings without previously knowing where a landslide will develop. Additionally, the system should be low in cost and should be designed specifically for the use in urbanized low-income areas. Existing monitoring technology—including promising remote sensing techniques as, e.g., SB/GB D-InSAR, laser scanning and drone based photogrammetry—cannot achieve this, because they do not have the required temporal or spatial resolution, are not reliable enough during bad weather conditions, are too complex in operation or are too expensive.

To meet these goals, the EWS requires a network of geosensors throughout the area, which in general are statistically distributed. The sensor density thereby is varied based on the landslide risk. This approach improves the benefit-cost ratio of the system, since in areas with low landslide risk, less sensors are distributed and therefore the density in high-risk areas can be increased. Hence, prior to planning the system, at least a qualitative risk assessment should be performed for a successful and effective system.

In this chapter, the newly developed sensor systems are presented. First, we give an overview of the general layout of the EWS which comprises a combination of traditional landslide monitoring systems as well as new geosensors which use IoT technology. The overall system has been presented before in preliminary studies [20,63,64] but here we give a more detailed and in-depth description of the newly developed IoT devices (LoRa nodes).

3.1. Monitoring System Layout

The LEWS mainly consists of deformation measurement-systems installed on the surface (e.g., attached to existing infrastructure), shallow subsurface up to about 1 m depth (e.g., inclination sensor probes and linear extension and shear measurement systems placed in trenches) and at some points deep subsurface in drillings. The system is based on the following sensors/measurement devices:

1. Horizontal Continuous Shear Monitor (CSM) measurement lines and extensometer (EXT);
2. Wireless LoRa sensor nodes;
3. Piezometers, extensometers and vertical CSM in drillings.

These devices as well as the gateways and data management system are shown in a schematic layout of the whole EWS in Figure 1.

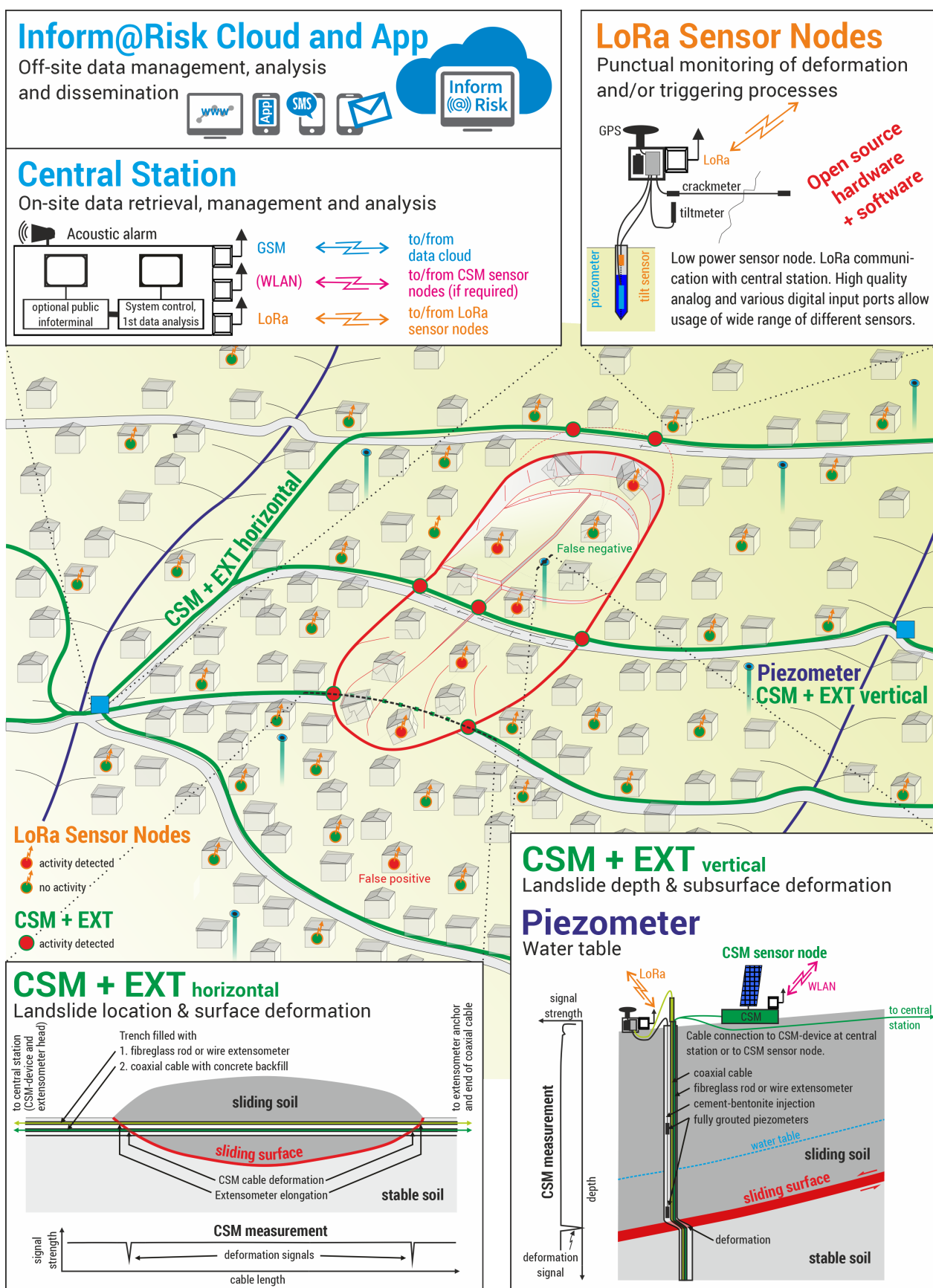


Figure 1. Schematic layout of the Inform@Risk monitoring system [64]. Data from CSM (Continuous Shear Monitor) and extensometer (bottom), as well as LoRa (Long Range) Nodes (top right) are combined in the Inform@Risk network and cloud system (top left).

The horizontal and vertical CSM lines provide spatially and temporally highly resolved measurements of shear deformation along coaxial measurement cables. The cables are installed horizontally across the slope in trenches (ideally on multiple levels throughout the slope) and vertically in boreholes, so that possible landslide movement will be oriented orthogonally to the cable axis, thus shearing the cable [27,65]. If shear deformation occurs, the CSM measurements allow to detect the exact location of deformation and to estimate the amount of deformation [27,65]. The wire-extensometers which are installed parallel to CSM provide additional extension measurements, which allow to observe large deformation amounts in the dm to m range. While the CSM and EXT provide seamless observations along the measurement lines, their application is limited by the required free space and the laborious installation procedure. To fill the gaps between the CSM and EXT lines and to make the implementation of a wide range of sensors possible, the system is complemented by LoRa sensor nodes in different setups. They all share the same basic design but differ by their placement and the number and types of sensors attached to them. As shown in Figure 1, there should be at least two LoRa gateways in the system because of redundancy. Ideally, these gateways are positioned at points where the horizontal CSM lines intersect and/or where drillings are located. This makes it possible for the different measurements systems to share the required infrastructure (e.g., enclosure, power, data connection) with the LoRa gateways. The connection from the gateways to the internet (“Network-” to “Middle-ware” -layer) is achieved using GSM modems and/or DSL via landline.

In the following, as one of the most important new developments of the Inform@Risk project, the LoRa nodes are described in detail [20,66].

3.2. Measurement Concept for the LoRa Sensor Nodes

A modular design has been chosen for the Inform@Risk LoRa sensor nodes. While all nodes share the same central hardware, as, e.g., the microprocessor, some basic sensors and the LoRa communication hardware (Inform@Risk LoRa base module), additional components can be added depending on the requirements of the specific monitoring task and installation location. This especially applies for the power supply (solar, battery and external power source) and optional sensor attachments. While the LoRa base module in general offers the flexibility to attach a wide range of different sensors, two specific sensor attachments have been designed for the use in the Inform@Risk LEWS. As a consequence, three types of sensor nodes can be distinguished which mainly build up the LoRa geosensor network of the LEWS: the Infrastructure Node (IN), the Subsurface Node (SN) and the Low-Cost Chain Inclinator (LCI). While the IN only consists of the base module (with the option to attach further sensors based on need), the SN and the LCI have specifically designed sensor attachments. Each type of node serves a different measurement purpose: The IN is designed to be attached directly to existing infrastructure on site (e.g., buildings, posts, retention walls) and to monitor their movement/deformation. This is mainly done based on high accuracy inclination measurements utilizing an integrated MEMS sensor. When needed, additional sensors such as crackmeters or extensometers can be added to improve the quality of observation.

The LCI and SN both are designed to monitor subsurface deformation and ground- or seepage-water levels. While the LCI is based on the principle of inclinometer measurements and allows to quantify horizontal displacement, the SN only delivers a qualitative indication and possibly a semi-quantitative assessment of deformation through time. On the other hand the SN allows to perform highly resolved open pipe groundwater-level measurements based on a buoyancy rod, while the LCI utilizes a series of float switches usually with 0.5 or 1 m distance, thus delivering a much lower resolved information on groundwater levels.

As the requirement for the successful implementation of a LCI sensor probe is to penetrate the basal shear surface of a landslide, these probes have to be installed into greater depths than the SN. The LCI consists of a series of inclination sensors (0.5 or 1 m interval) installed into an easily deformable PVC pipe, while the SN only has one

inclination sensor and is installed into a stiff steel pipe. As the LCI penetrates through the sliding mass and the bottom lies in the stable subsurface, the tilt observed by the chain of inclination sensors can be used to calculate a profile of horizontal displacement throughout the subsurface, allowing to determine the depth and amount of deformation in the landslide. Provided the movement is a rotational slide, the SN will tilt upwards if it “floats” in the sliding mass, and tilt downwards if the SN reaches stable ground (Figure 2). As the exact geometry of the landslide is unknown, SN measurements can only semi-quantitatively monitor landslide movement. These mechanics are also described by Qiao et al. (2020) who explored the direction and pre-failure tilting behavior of slopes and how this affects measured tilting angles of steel rods of different sizes [60,67].

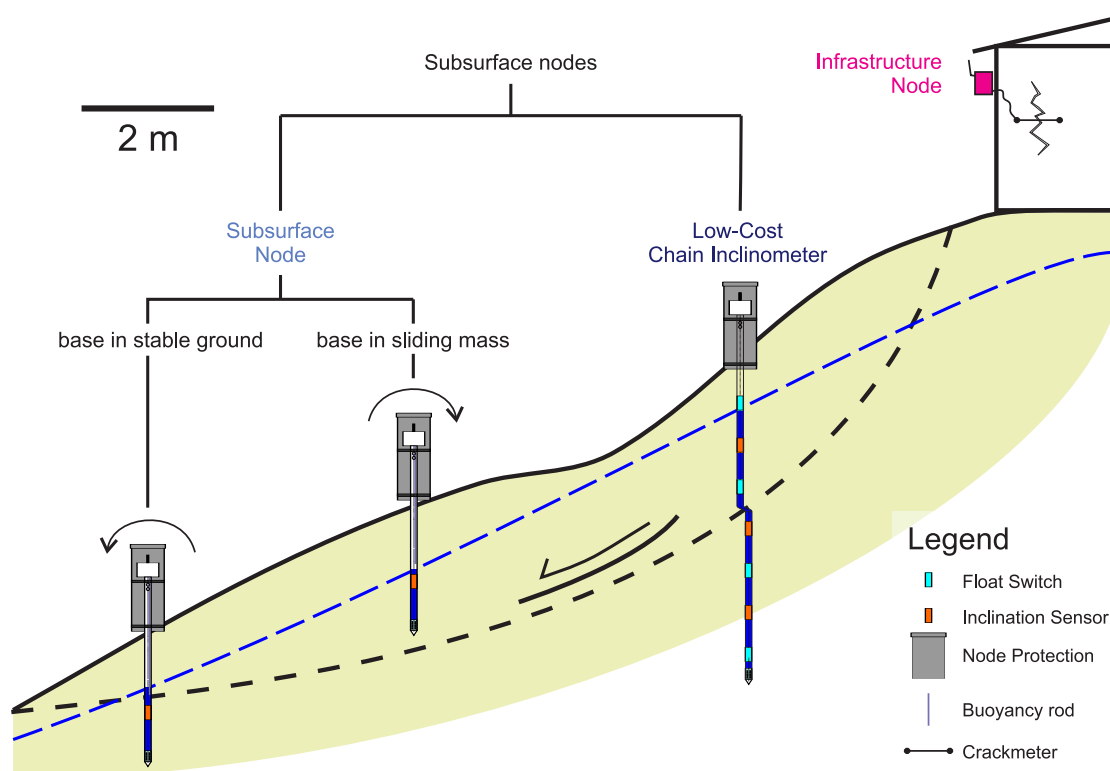


Figure 2. Measurement concept for the Infrastructure node (IN), Subsurface Node (SN) and Low-Cost Chain Incliner (LCI).

As stated earlier, the sensor placement should generally be adapted according to the previously performed risk analysis. Additionally, it is important that each individual sensor location is checked before the installation to ensure that the sensor will be able to detect and measure a possible landslide. Therefore, it is also compulsory that each node location and installation is documented in detail, so it is possible to interpret the data in a meaningful way. In order to facilitate this process, we plan to add an interactive sensor installation guide and documentation feature into the Inform@Risk app.

3.3. Inform@Risk LoRa Base Module

The Inform@Risk LoRa base module is designed around a SAMD21 32-bit micro-processor board (Arduino MKR WAN 1310) with an integrated LoRa module (Murata CMWX1ZZABZ). This processor board has the benefit of combining very low power consumption with good flexibility in terms of analog and digital in- and outputs. Furthermore, its design is open-source and it is easily available all over the world. Figure 3 shows the basic design with the attached sensors (and the optional power- and sensor attachments). The detailed circuit board design, schematics and hardware specifications are referenced in Section 6. For easy reproducibility and further development a breadboard-based design

is available. For actual applications it is recommended to use printed circuit boards (PCB) which make node construction much easier. The PCB and the breadboard-based designs are available for download on our website (Section 6).

Three different power supplies can be used: battery power (4–8 AA batteries), solar power (6V solar panel, 1–2 W, LiPo battery and battery charging regulator) or an outside power connection (DC 4–18 V input, optional with LiPo battery). All these options are connected to a voltage regulator, which supplies the required DC 3.3V internal system voltage. Additionally a step-up/down converter offers switchable DC 12 V for, e.g., external 4–20 mA devices. If batteries are used, an input voltage of about 6 to 12 V, corresponding to 4 to 8 AA batteries in series, is recommended.

The base module includes a low-cost IMU (Inertial Measurement Unit), which measures the acceleration (0.04° precision) and orientation of the node, as well as temperature and barometric pressure. Additionally, all Infrastructure Nodes include a high-precision inclination sensor. Because of its price, this unit is optional for all subsurface sensor nodes, where the inclination of the basic module itself is not as important. The sensor can simply be plugged into the circuit board when needed. We also developed a 3D-printed mount which allows the sensor to be placed horizontally, independent of the placement of the node enclosure (e.g., on a skew retaining wall).

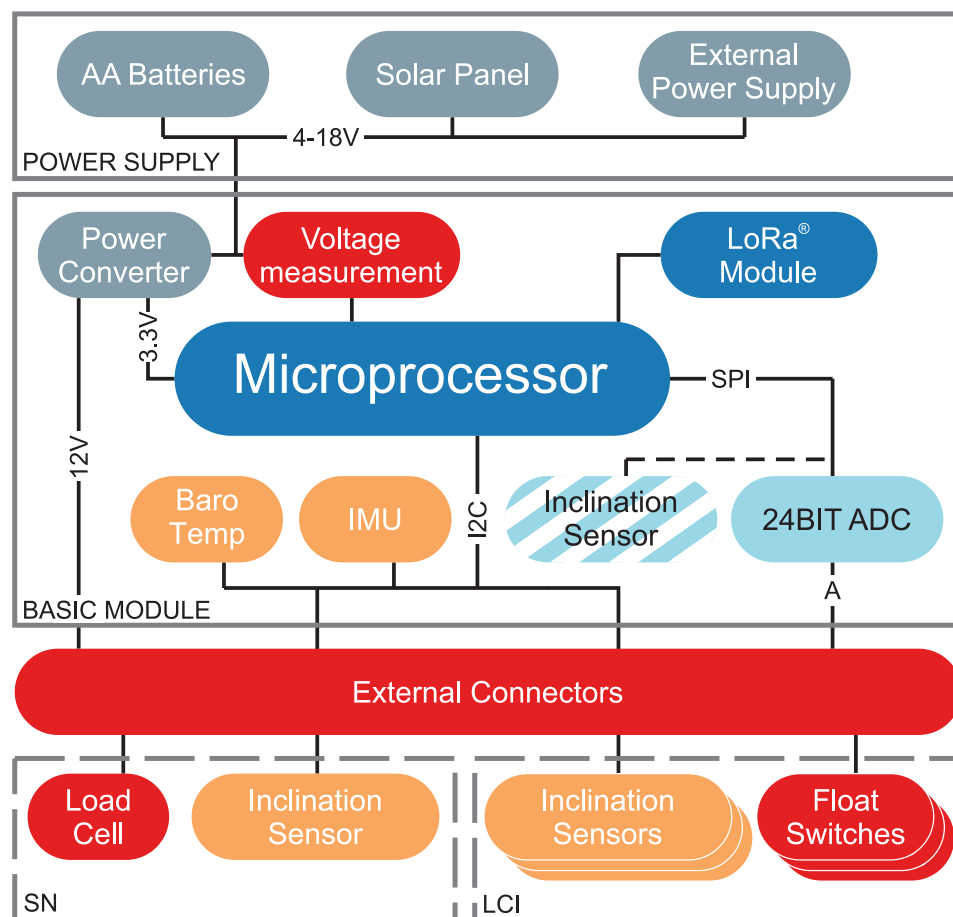


Figure 3. Schematic depiction of the Inform@Risk basic module and the additional sensors for subsurface measurements (SN, LCI). The colors show the data transmission: red: analog signal; orange: I2C (Inter-Integrated Circuit) bus; violet: SPI (Serial Peripheral Interface) bus.

Furthermore, included on all nodes is a 24-bit analog-digital converter (Texas Instruments ADS1220), to which external geotechnical or other sensors can be attached. It has four channels, which can be combined to max. two differential voltage measurements (e.g.,

for potentiometers) or can individually measure voltage referenced to ground (used, e.g., in combination with a measurement resistors for 4–20 mA measurements).

The firmware for the nodes is written in the Arduino programming environment (Integrated Development Environment, IDE) and can easily be accessed and changed with the IDE. The code is distributed via Github (see Section 6).

The software comprises five stages: initialization of the sensors, measurements, computation, and LoRa up- and downlink. Although these stages are fixed, multiple parameters can be changed to accommodate for varying on-site requirements. For example, the overall measurement duration as well as the measurement frequency for each sensor can be changed. These parameters can not only be changed when installing the node but also remotely with commands transmitted via LoRa communication. Furthermore, for each sensor it is possible to decide whether median or mean values should be sent to the gateway. For example for the accelerometer, it is best to calculate the median of the measured values since it is less sensitive to outliers from external influences (e.g., vibrations, impacts). For all other values, usually mean values can be chosen. The calculation is done by the microprocessor to save power and on-air time during LoRa communication, which uses the most power. With an average sleep interval of 15 min, the measured lifetime should be at least two years for the basic infrastructure node with six AA batteries (daily power consumption at 3.3 V is ca. 5–6 mAh).

After the measurement, calculations and LoRa-uplink, the device receives an optional downlink from the gateway. This can be one of several predefined commands such as setting the looptime (time taken for measurements and time the device is asleep), changing measurement duration or activating/deactivating individual sensors on the device. After receiving commands, the device makes the changes and goes into a sleep mode, in which current consumption is minimized. More information on the firmware can be found in the documentation provided on the Github page (Section 6).

3.4. LoRa Sensor Nodes

3.4.1. Infrastructure Node (IN)

The IN is the base module usually with the optional internal high quality inclination sensor installed. This sensor (Murata SCL3300) has a precision of 0.003° , and thereby, even very slight changes in inclination can be measured (e.g., if a 1 m high retaining wall tilts by more than 0.1 mm, this movement should be detected). The PCB is placed in a waterproof housing, still allowing optional sensors to be attached, as stated earlier.

3.4.2. Subsurface Node (SN)

The SN and LCI are both subsurface attachments to the base module. After they are installed in the subsurface on site, the base module can simply be installed on top of the housing with a simple 3D-printed adapter (see Section 6). Inside the rod of the SN, one inclination sensor is included to be able to detect tilting of the rod. The casing of the rod can be made of PVC or stainless steel, but steel casings are preferable since they can be installed without pre-drilling. The detailed sensor- and connection-layout is shown in Figure 4.

The inclination measurement is performed by a triaxial accelerometer (BMA456, 0.02° precision). It is connected to the basic node via the I2C bus. To house this sensor, a 3D-printed housing has been developed. It provides safety for the sensor, as well as a steady fixture for accurate readings. The sensor unit itself and the cable connections are waterproofed with a 2-component sealing gel. The SN is usually installed into depths of up to about 2 m.

The groundwater measurement is performed using a load cell together with a buoyancy rod made of PVC, which allows for continuous measurement, but only in the top part above the inclination sensor, depending on the length of the rod.

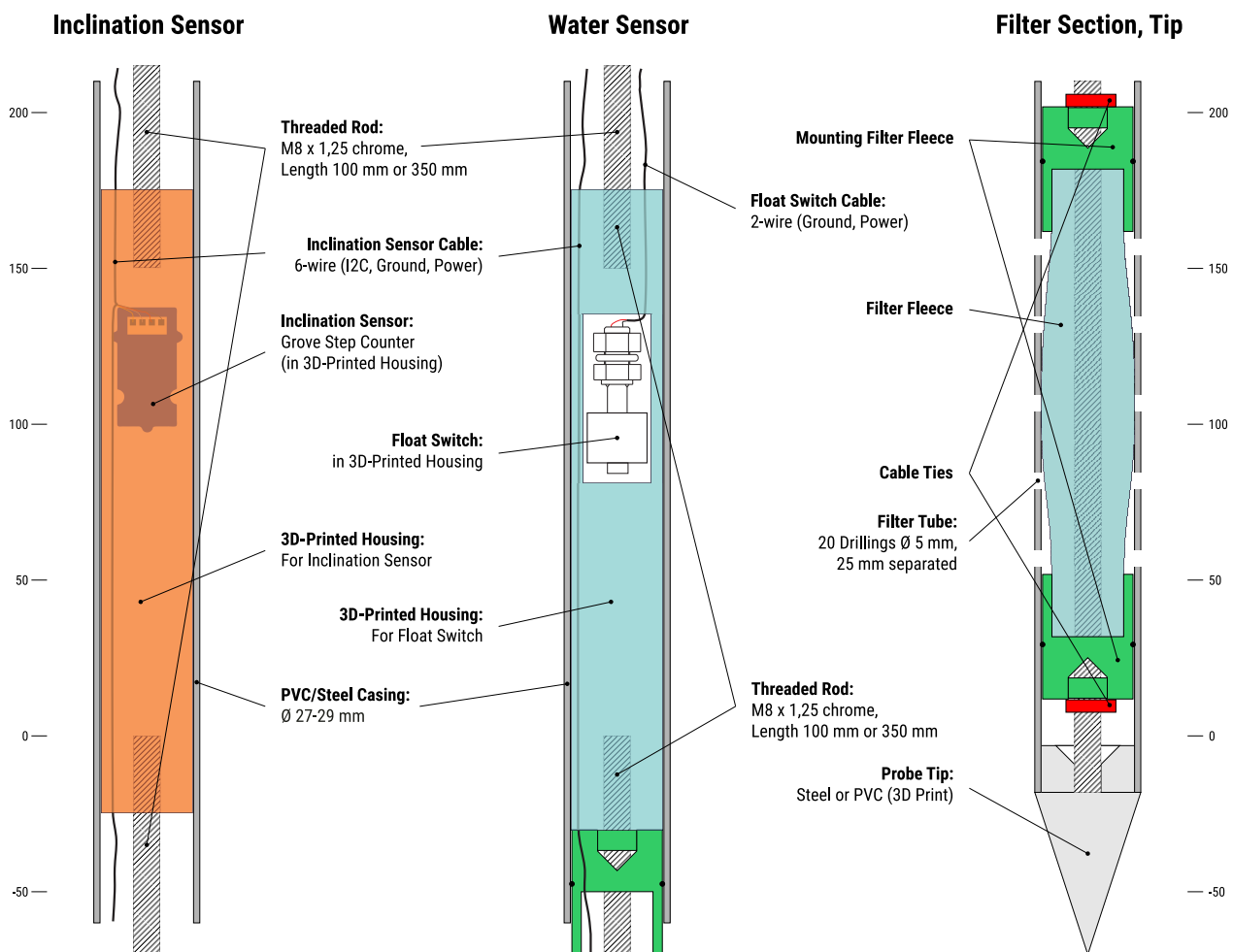


Figure 4. Hardware design of the inclination sensor, the groundwater sensor and the tip and filter section for both the SN and LCI.

3.4.3. Low-Cost Chain Incliner (LCI)

The LCI is similar to the SN but includes inclination sensors every m, resulting in up to 6 inclination measurements in the subsurface. They are all connected in serial to the I2C bus. Each of them is wired to a different digital port or addressed differently on the I2C bus, respectively. In contrast to the SN, the casing should be made of PVC in order to allow for deformation of the rod to determine the shear depth. The inclination sensor is the same as for the SN. Currently due to limitations of the used digital bus (I2C) the max. achievable depth for the LCI is about 6 m. The groundwater measurement is achieved with a float switch each m, alternating with the inclination sensor. They act as a series of resistors in parallel, which increase the resistance with increasing groundwater level. They are connected to the analog input of the microprocessor or the ADC. Therefore, the groundwater measurement of the LCI is not as good as the one the SN provides, since it is not continuous. Still, the most important information—whether there is water in the top meters—can be gained this way.

3.5. Installation

In general, the installation of the subsurface probes (SN and LCI) can be done with three different techniques, as shown in Figure 5. The first option is direct insertion of the steel casing, using a hydraulic, pneumatic or petrol jackhammer or heavy dynamic probing equipment (DPH). The second option is to pre-drill a borehole of 45–50 mm using a drilling method fitting to the geological conditions and afterwards insert the casing (steel or PVC pipe). The third option allows to directly insert a PVC pipe into the ground using a

jackhammer or DPH equipment. This is achieved by placing the steel drilling rod inside the pvc pipe and using a “lost” metal tip, which is only loosely attached to the drilling rod and stays in the ground when the drilling is completed and the drilling rod is retracted. To ensure the PVC pipe is pushed into the ground simultaneously with the drilling rod, a small metal plate with a diameter larger than the pipe is attached to the top of the drilling rod.

Which installation technique can be used mainly depends on the subsurface material, the depth and the probe type to be installed. For the SN usually drilling method 1 and for the LCI drilling method 3 will be the best option, as long as no hard rock (stones/blocks or bedrock) is encountered. If this is the case, drilling method 2 will have to be used, which—depending on the required drilling method—makes the installation more complex and costly. This limitation is more significant for the LCI, as it requires higher drilling depths.

After the insertion of the casing, the sensors, which are prefabricated on the threaded rods (see Figure 4) to lengths of 1 m are installed in the casing and connections are made between each m-segment during the installation. Once all sensors are inserted in the borehole, the LoRa node itself is attached to the top of the casing and the subsurface sensors are connected to the node. Depending on the situation, a protective pipe or some other kind of protection should be added over the node.

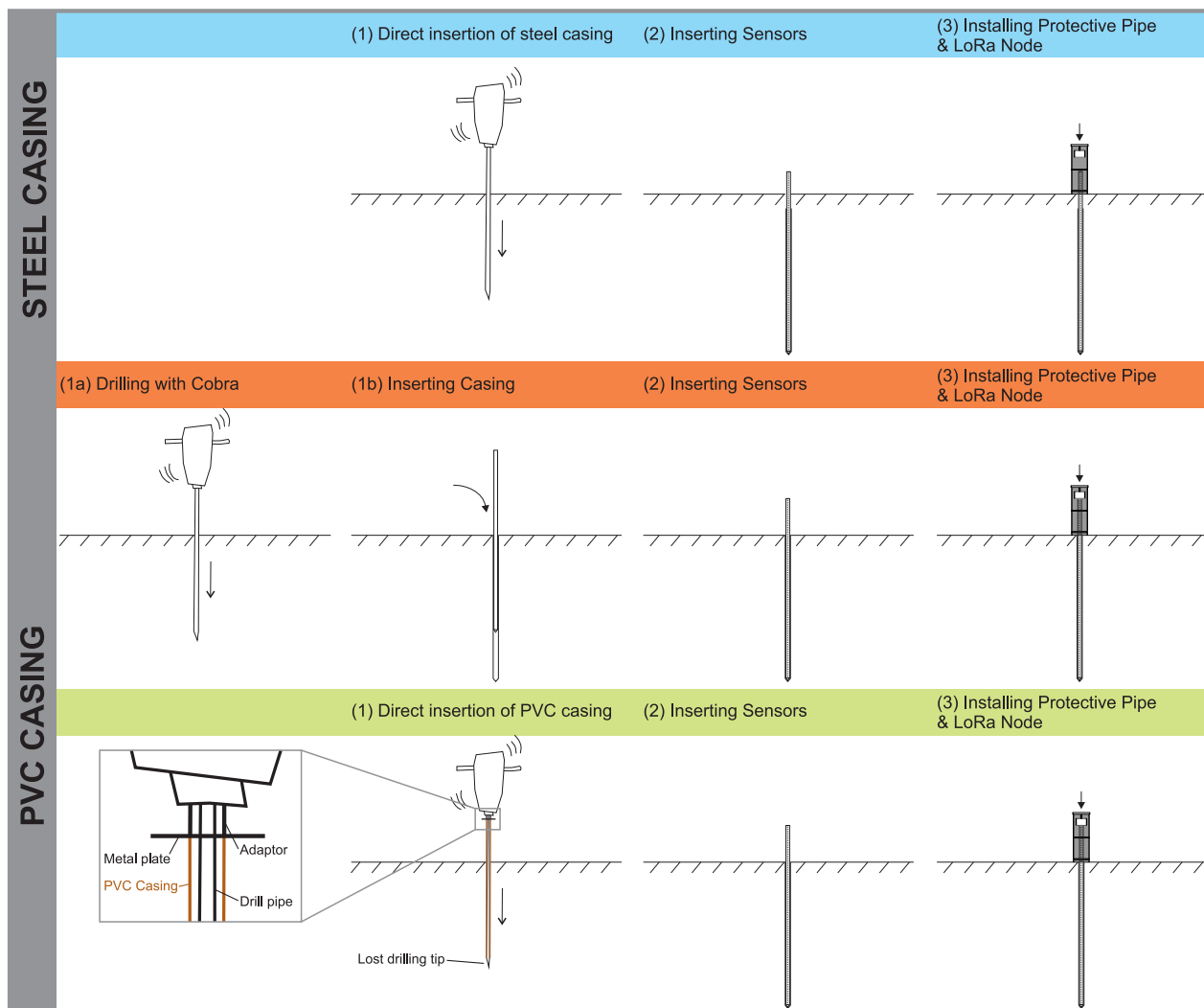


Figure 5. Installation suggestions for steel casing (blue) and PVC casing (red, green).

The installation of these sensors has been tested on a field site in southern Germany (see Section 3.6). Here, also different sensors and attachments were tested in order to find the now final sensor layout. Pictures of this test installation are shown in Figure 6.

As stated before, the main goal of the system is to increase availability by keeping the costs to a minimum, where possible. The LoRa base module costs about 100 €, including all electronics and power supply. Depending on the attachments, the IN then costs on average 50 € more and the SN and LCI are approximately 100–150 € more expensive because of the casings and the subsurface sensors. The work hours are not taken into account and we are aware that this is also an important cost factor. Yet, it is hard to determine these costs and also, it has been our experience that the local residents are often very willing to help, and they gain more trust to the system if they are engaged in the installation process. If the Inform@Risk PCB is used, the assembly should take about 15–30 min per node, with an additional 30 min for the SN and LCI. The installation on site varies from about 30 min (IN) to 2–4 h for the SN and 4–6 h for the LCI (including drilling), of course depending on the geology and other conditions on site.



Figure 6. Pictures from a field installation where the presented sensors were tested and evaluated and the installation procedures were developed. (a) Steel and PVC housings with drilled holes for the filter section. (b) Left: installation of sensors into the housing, right: preliminary sensor encasing. (c) Installation of the housing with a jackhammer. (d) Preliminary circuit board for the IN on a wall with attached potentiometer.

Comparing these costs with a regular chain inclinometer (starting from approx. 5000 € excl. drilling), our system is more cost effective, although it is clear that the same data quality cannot be achieved. While a chain inclinometer produces absolute deformation measurements with very high accuracy and precision, the SN only provides semi-quantitative data, as we only measure the tilting of the top layer. The LCI on the

other hand should provide absolute inclination data, but is limited in its depth and its setup is less robust than a regular chain inclinometer due to the 3D-printed housings and threaded rod system. The most important factors about the developed LoRa sensor nodes are summarized in Table 1.

Table 1. Overview of the LoRa sensor nodes, in comparison with a regular drilling and installation of a chain inclinometer. Installation: (++): easy, (+): intermediate, (-): difficult, (--) : very difficult. RD: relative deformation measurements, AD: absolute deformation measurements, SQ: semi-quantitative measurements, GW: groundwater measurements.

Type	Depth [m]	Pipe	Installation	Data Quality	Cost
IN	-	-	++	RD; Wide range of sensors;	~150 €
SN	<2.5	Steel	+	SQ (Tilt sensor); GW	~200 €
LCI	3–6	PVC	-	AD (Tilt sensor); GW	~250 €
Chain Inclinometer	>5	PVC/Alu	-	AD	>>5000 €

3.6. Test Site Near Regensburg, Germany

To test these LoRa nodes, we created a number of prototypes in order to test the functionality and longevity in a field installation. Because of the pandemic, it was not possible to do this in Colombia, so we chose a site in southern Germany near Regensburg, which has similar properties. A rotational landslide in fine-grained material (sand, silt and clay in varying proportions) started to develop some years ago and is slowly moving towards railroad tracks. This slope is already being monitored by two inclinometers. In parallel to these, we have installed six of the Inform@Risk LoRa nodes: Two IN on a wall (Figure 6d) and four variations of the SN and LCI in different depths and sensor constellations. The data are being collected by a LoRa gateway which is about 100 m from the sensors. The sensors, which were installed in July 2020, show a robust and continuous data transmission. However, no inclination measurements could be detected right now which could be confirmed by the inclinometer measurements. This installation helped us in improving the hardware, software and installation procedure to be more reliable. In Figure 7, the inclination data of the IMU in one node is shown as an example. Although only temperature cycles are visible, they show that even the low-cost sensor is capable of replicating these slight changes in inclination.

While the presented subsurface sensors offer an effective method of directly measuring subsurface deformations, it must be emphasized that they are mainly applicable to shallow rotational landslides. Especially the SN might not detect the movement if other landslide mechanisms (e.g., purely translational sliding) are present. In general the application of the proposed sensors has to be critically checked based on the geological process and hazard analysis. While the presented systems have been tested for about half a year now, still further testing is required to prove the full functionality of the system. This includes tests to determine the sensitivity of the SN for different geometrical setups and direct comparisons of LCI measurements with classic inclinometer measurements.

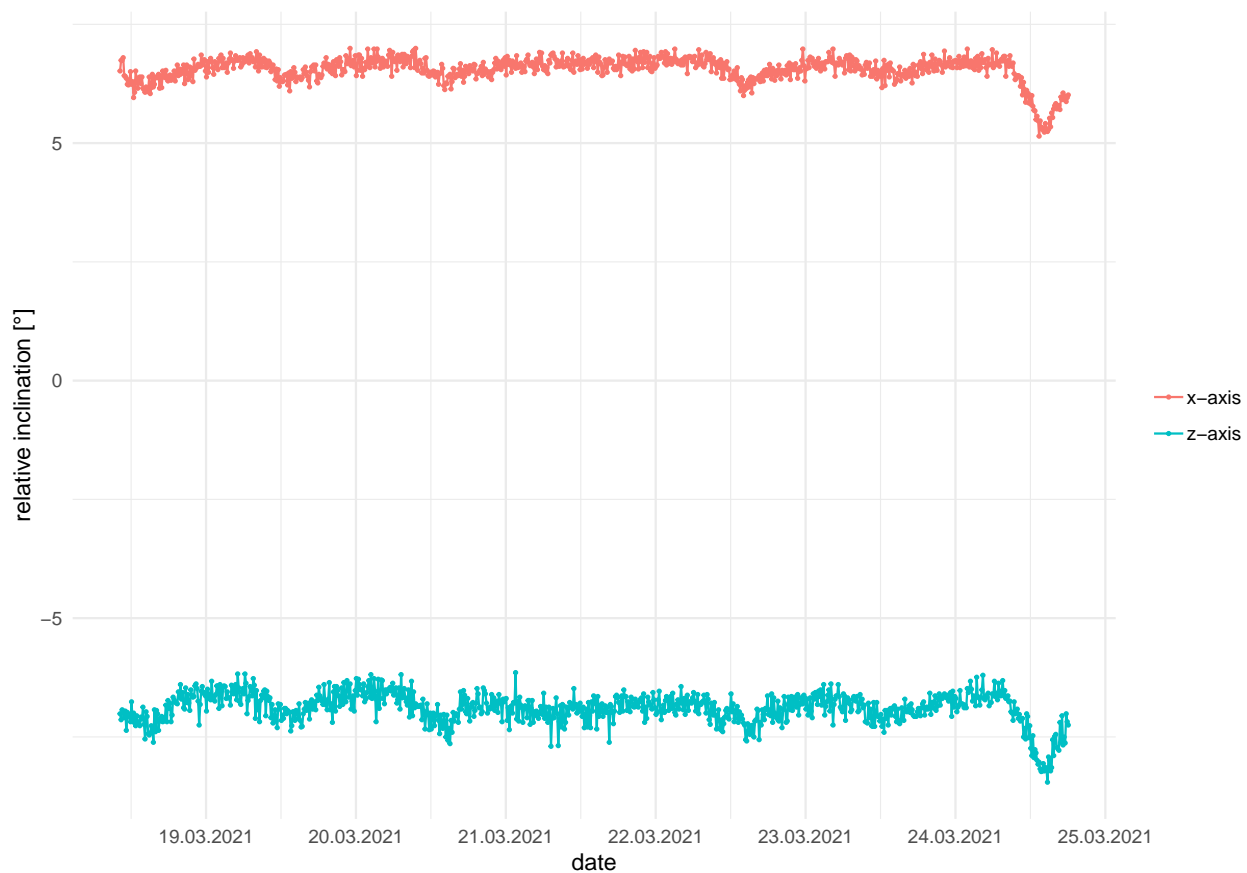


Figure 7. Exemplary inclination data taken from an accelerometer on top of a subsurface node. While the measurements do not yet show deformations, daily cycles as well as sensor noise are visible. The sensor noise in this real-world application is higher than that measured in the laboratory.

4. Data Processing

All data acquired in the geosensor network is immediately transferred to an off-site central server (Inform@Risk cloud), where it is processed and analyzed in near real time.

4.1. Data Transmission and Storage

In case of the LoRa geosensor network the encrypted data packets sent from the nodes are relayed through the LoRa gateways on site to an off-site LoRa Network Server server using a redundant internet connection via DSL, Cellular network and/or microwave radio (Figure 8). The LoRa server manages the LoRa communication and relays the data to the LoRa application server, which then analyses and decodes the encrypted data packets and writes the data into the Inform@Risk cloud database. The LoRa server is also responsible for sending control commands to the LoRa nodes via the most appropriate gateway. For the inform@risk project the open-source LoRa network server “Chirpstack” (www.chirpstack.io) (accessed on 1 March 2021) is used.

As the CSM measurements produce a large amount of data (up to about 350 kB uncompressed data per measurement), LoRa can not be used to transmit the CSM data. Therefore, the system is designed so that, whenever possible, the CSM measurement devices are located at the LoRa-gateways. This allows the CSM devices to directly utilize the internet connection of the gateways to transfer the data to the Inform@Risk cloud. Whenever this is not possible, local wireless LAN connections with directional antennas are used to relay the data to the gateways. All gateways are equipped with backup batteries (200 Ah) which allow them to operate for two weeks without external power in case of an emergency. An open source MariaDB database is used as central data storage. In

general, the raw data received from the sensors is stored and kept unchanged in the database. Any further processing (see below) of the data is stored at different locations in the database, making it possible to change calibration and analysis parameters afterwards if deemed necessary.

4.2. Data Management

In the Inform@Risk project the AlpGeorisk ONLINE (www.alpgeorisk.com) (accessed on 1 March 2021) data management platform is used to manage the large amounts of data (several GB per month) which are generated by the geosensor network. This platform is responsible for data quality management (identification of data errors), calibration (conversion of raw data to measurement data), storage (structured storage in a relational database), analysis (see below) and visualization via web-portal as well as system management (sensor status checks) and control (e.g., change acquisition interval) and notifications (alarms and early warnings via email, SMS and/or sirens etc.). As part of the Inform@Risk project, a mobile app is being developed to complement the AlpGeorisk ONLINE data management system and make the data more accessible and understandable for the residents in informal settlements. The presented monitoring system can of course also be used in combination with a different data management platform (e.g., if one is already available), but the combination with the AlpGeorisk system is very convenient since it is already adapted to the specific requirements.

4.3. Data Analysis

The data analysis methodology being developed for the Inform@Risk LEWS is based on a combination of dynamic thresholds for trigger- and deformation observations, sensor fusion methods and pattern recognition methods. As the geosensor network is designed for densely populated areas, accidental or intentional tampering with the sensors has to be taken into account. Otherwise, a large number of false alarms would be the consequence—which, even if reviewed by an expert before issuance of a notification, would most likely make an effective operation of the system impossible. For this reason we plan to apply sensor fusion and pattern recognition techniques to filter the incoming data and separate the significant from the insignificant data. For example, when a threshold is surpassed on a single inclination sensor, the system checks if any of the surrounding sensor nodes have also registered a deformation increase. It also checks if any of the sensors monitoring the triggering factors (rainfall, groundwater, seismic events etc.) show an increased level. Depending on the severity and degree of confidence of the observation, either the event is temporarily ignored or appropriate action is taken, which ranges from marking the event for review through the system manager to issuing an alarm. In any case, the system will instruct the relevant sensors to increase the measurement interval and as further data of the event is collected throughout time, the system will reevaluate the event utilizing pattern recognition methods on the time series of the relevant deformation and triggering datasets. This cycle is continued until the event is identified as an outside influence, or—if the situation remains uncertain—is reviewed and classified by the system manager. With time, the system will collect a database of classified events, which can be reviewed periodically and serve as training data for the pattern recognition algorithms. The thresholds used for the different sensor types at the different locations are first determined based on sensitivity analyses performed using the geological/geomechanical models created during the hazard analysis and include absolute values as well as rates where applicable (e.g., deformation rate). Later with increasing length of observation the thresholds are adapted using the results from timeseries-analyses performed on the collected data. This also includes trigger informations, especially for rainfall, one of the most important trigger factors. The data analysis methodology for the Inform@Risk LEWS outlined above is currently still in development. Its functionality will be evaluated and improved during a planned “learning-phase” of the LEWS of at least one year.

4.4. Data Dissemination

Based on the analysis results, the short- to medium-term hazard level is assessed, and— if deformation is detected—early warnings and alarms are issued. The main information dissemination tool will be a newly developed mobile app.

4.4.1. Short- to Medium Term Hazard Level

In order to assess the short- to medium-term hazard level, mainly the triggering factors rainfall and groundwater height are considered. On the one hand, time series analyses will be performed to identify causal and temporal relationships between short-, medium- and long-term rainfall and groundwater levels [68]. On the other hand, the hazard level is determined using groundwater level thresholds at, e.g., 50, 75 and 90 percent of the critical water table derived from the geological/geomechanical models created during the hazard analysis. The threshold values thereby are determined individually for different geological homogeneous zones throughout the project area and are applied to the according sensors in this area.

4.4.2. Early Warning and Alarms

Early warnings are issued only if significant deformation has been detected. Depending on the amount of deformation observed, different early warning levels are issued. The number and value of thresholds used to define these levels are currently being determined, but early warning will most probably cover the range from mm per year up to cm or dm per hour. Based on how many and which neighbouring sensor nodes show deformation, the affected area and landslide mass are estimated and reported. If a further or sudden strong acceleration is detected, the system can issue an immediate (evacuation)-alarm using acoustic and/or light signals. Another factor that is important for the early warning are measurements of the trigger parameters, most importantly rainfall. It is measured on site by a weather station and a rainfall radar of the city of Medellín is used for forecasts. To make the connection between rainfall and groundwater levels, a hydrogeological model is used and combined with the data gathered during the test phase of the system. This test phase serves to make the system more accurate for predicting the influence of rainfall on groundwater levels, and therefore, hazard levels. Depending on the hazard state, deformation rate and the affected area different actors (experts, trained community members, first responders, whole population) are informed. Usually warnings will be checked by an expert before they are sent to the inhabitants. Only when at least two neighboring sensor nodes show very strong acceleration at the same time and the data has successfully been crosschecked according to the above data analysis procedure, the warnings are issued without review. Right now, we plan on warning the inhabitants using the Inform@Risk App, as well as multiple sirens which will be installed in the area. The exact definition of the warning levels, warning contents and the information dissemination paths are being developed in a participatory process, ensuring that, if possible, each actor gets the required information at the right point in time.

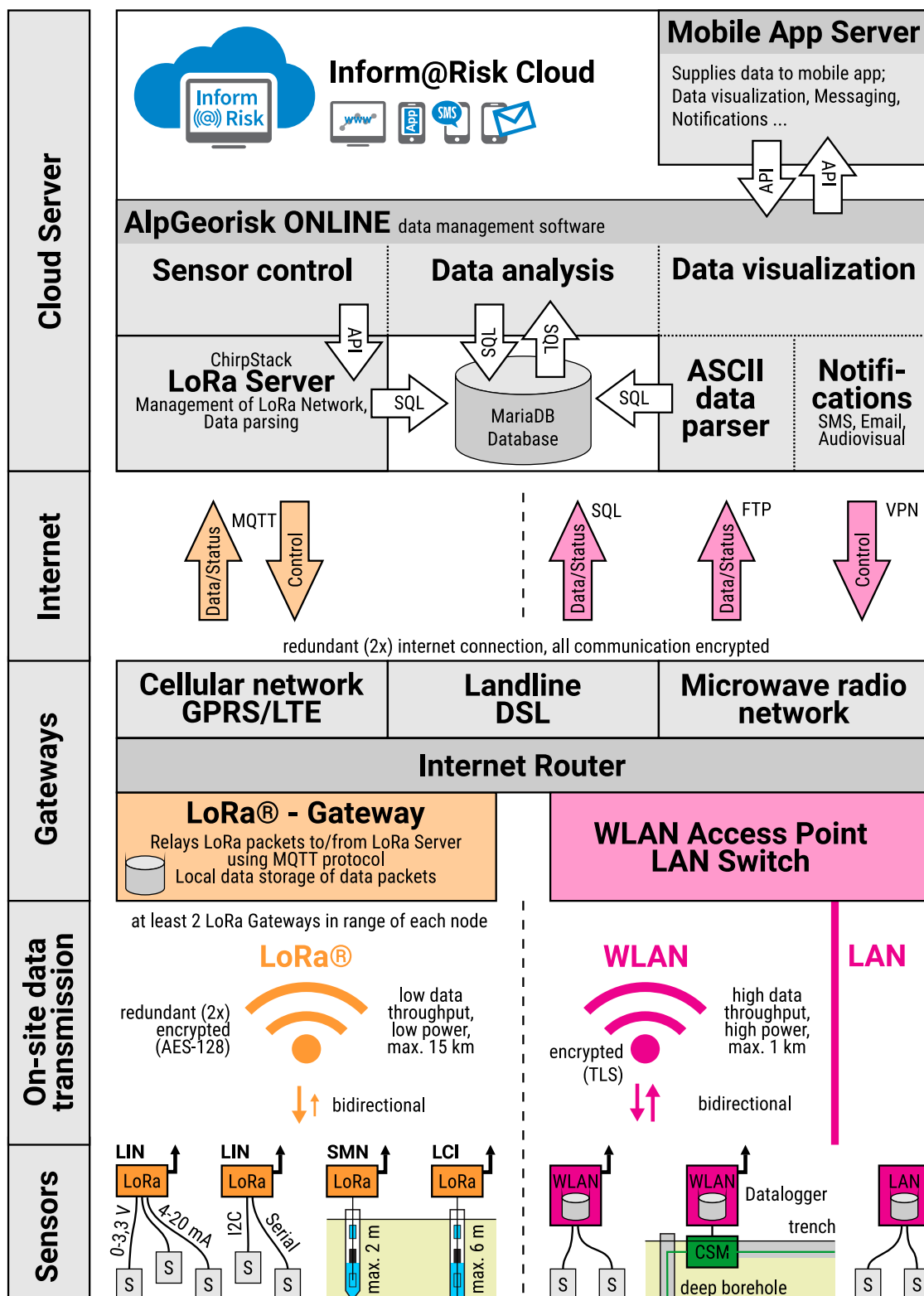


Figure 8. Data processing concept of the Inform@Risk project.

5. Summary and Outlook

A new IoT based geosensor network for communities in informal settlements has been developed, mainly based on open-source hardware and software. The sensor network consists of three different sensor nodes, which allow to monitor movement/deformation of the subsurface (SN, LCI) or existing infrastructure (IN) as well as the groundwater

conditions in near surface soil layers. The subsurface sensors operate most efficiently for shallow rotational landslides. If translational or deep seated landslides are expected, the effectiveness of the system is reduced. In general, the applicability and placement of each sensor node has to be evaluated based on the expected landslide processes and vulnerability to outside influences.

While the newly developed sensor nodes are not as precise as existing high quality geotechnical sensors for landslide monitoring, they offer reasonable measurement quality at much lower cost. Thus, they can be distributed in comparably high numbers over an area, whereby sensor density is varied depending on the hazard level and the expected landslide mechanism. This leads to the necessary spatial density of observations, which is required to reliably detect the onset of landslide movements anywhere in the monitored area. When additionally complemented with other monitoring techniques as, e.g., the Continuous Shear Monitor (CSM) and sensors observing the triggering factors, a versatile, robust and flexible LEWS can be created.

A limitation of the system can be expected when very small landslides occur. Since the scenario this system aims at is quite difficult (shallow landslide at unknown location), it is possible that a small landslide occurs in between the sensors. This risk depends on the quality of the hazard and risk assessment and the density of CSM lines and LoRa sensor nodes. Bigger landslides should easily be detected by this system, except for very large and slow creeping which does not cause noticeable shearing and tilting on the surface. These slow movements, on the other hand, are not as relevant to this system because they pose less risk to the residents' lives. Another possible drawback of this system might insufficient pre-failure deformation before the event. If there are no significant shear- or tilt-deformations on the surface before an event, it is not possible to issue a warning based on deformation data. This is especially the case with the shallow measurements this system is based on. Therefore, the system needs to incorporate trigger data and it is incessant to have a learning phase where the thresholds for both trigger and deformation data can be defined and evaluated.

The large amount of data produced by the system and the high number of outside influences make new data processing procedures necessary, in order to ensure an effective operation and prevent false alarms. These procedures have been outlined here and will be presented in more detail in a future contribution after the system has been implemented and tested. Especially the relation between weather forecasts, groundwater levels and deformation measurements will be addressed in more detail.

As already stated, currently further tests of the sensor system are carried out in Germany. As soon as the COVID-19 related restrictions allow for it, the first installation of the proposed LEWS will be performed in Colombia. This system will comprise about 130 Sensor nodes, five drillings with instrumentation and about 1.5 km of horizontal CSM/EXT lines. The installation will also be used to gain further experiences in terms of the social integration of the system. Concepts as, e.g., 'sensor god-fatherhood', meaning that if, e.g., a sensor node is installed on a house wall, the house will take care of the sensor node, will be tested. After an operation of about one year the complete system will be evaluated and recommendations for future developments stated.

All new findings of the Inform@Risk project are being developed as open source and will be distributed freely. Hopefully this work can encourage researchers and risk managers throughout the world to implement and further develop comparable LEWS, especially in such areas of the world, which were often overlooked in the past. Please feel free to comment and actively contribute to the development on the provided project websites (see Section 6). Any criticism, suggestions or advice is welcome.

6. Resources

All hardware and software being developed in this project is open source and can be accessed and freely replicated (GPL-3.0).

The firmware for the sensor nodes can be accessed via our Github page:

<https://github.com/moritzgamperl/informrisk-lora-node> (accessed on 1 March 2021). Here, the firmware for the sensor nodes, the documentation, as well as the required libraries can be found.

The hardware specifications (schematics, circuit board files and documentation) and documentation for the individual sensors can be found on the following webpage, which will be updated regularly: www.informrisk.alpgeorisk.com (accessed on 1 March 2021). Here, also the files for 3D-printing can be accessed.

Author Contributions: Conceptualization, J.S. and M.G.; methodology, J.S. and M.G.; software, M.G.; validation, M.G. and J.S.; investigation, J.S. and M.G.; resources, J.S. and M.G.; writing—original draft preparation, M.G.; writing—review and editing, J.S., K.T. and M.G.; visualization, M.G.; supervision, J.S. and K.T.; project administration, J.S. and K.T.; funding acquisition, J.S. and K.T. All authors have read and agreed to the published version of the manuscript.

Funding: This research was funded by the German Federal Ministry of Education and Research, grant number 03G0883A-F.

Data Availability Statement: As stated above, the sensor hardware and software developed in this study can be downloaded freely. Measurement data is available on request from the authors.

Acknowledgments: We thank Isabelle Leisgang and Andreas Grabmaier for help in test installations and the development of the sensor nodes.

Conflicts of Interest: The authors declare no conflict of interest. The funders had no role in the design of the study, in the collection, analyses, or interpretation of data, in the writing of the manuscript, or in the decision to publish the results.

References

1. Smith, H.; Garcia-Ferrari, S.; Medero, G.; Rivera, H.; Caballero, H.; Castro, W.; Abiko, A.; Marinho, F.; Ferreira, K. *Learning from Co-Produced Landslide Risk Mitigation Strategies in Low-Income Settlements in Medellín (Colombia) and São Paulo (Brazil)*; N-AERUS XIX; Department of International Urbanism, University of Stuttgart: Stuttgart, Germany, 2018.
2. Rengers, F.K.; McGuire, L.A.; Oakley, N.S.; Kean, J.W.; Staley, D.M.; Tang, H. Landslides after wildfire: Initiation, magnitude, and mobility. *Landslides* **2020**, *17*, 2631–2641. [[CrossRef](#)]
3. Petley, D.N. On the impact of urban landslides. *Geol. Soc. Lond. Eng. Geol. Spec. Publ.* **2009**, *22*, 83–99. [[CrossRef](#)]
4. Samaddar, S.; Tatano, H. Where do Individuals Seek Opinions for Evacuation? A Case Study from Landslide-prone Slum Communities in Mumbai. *J. Nat. Disaster Sci.* **2015**, *36*, 13–24. [[CrossRef](#)]
5. Alexander, D. Urban landslides. *Prog. Phys. Geogr. Earth Environ.* **1989**, *13*, 157–189. [[CrossRef](#)]
6. Anderson, M.B. Metropolitan Areas and Disaster Vulnerability: A Consideration for Developing Countries. In *Environmental Management and Urban Vulnerability*; Kreimer, A., Munasinghe, M., Eds.; Number 168 in World Bank Discussion Papers; The World Bank: Washington, DC, USA, 1992; pp. 77–92.
7. Peduzzi, P.; Deichmann, U.; Dao, Q.H.; Herold, C.; Chatenoux, B.; De Bono, A. 2009 Global Assessment Report on Disaster Risk Reduction: Patterns, Trends and Drivers. Available online: <https://archive-ouverte.unige.ch/unige:32362> (accessed on 1 March 2021).
8. Franco, E.G. *The Global Risks Report 2020*; Technical Report 15; World Economic Forum: Geneva, Switzerland, 2020.
9. Aristizábal, E.; Sánchez, O. Spatial and temporal patterns and the socioeconomic impacts of landslides in the tropical and mountainous Colombian Andes. *Disasters* **2020**, *44*, 596–618. [[CrossRef](#)]
10. Ruiz Peña, G.L.; Barrera Pinales, L.A.; Gamboa Rodríguez, C.A.; Sandoval Ramírez, J.H. *Las Amenazas por Movimientos en Masa de Colombia: Una Visión a Escala 1:100.000*, 1st ed.; Servicio Geológico Colombiano: Bogotá, Colombia, 2017.
11. Sepúlveda, S.A.; Petley, D.N. Regional trends and controlling factors of fatal landslides in Latin America and the Caribbean. *Nat. Hazards Earth Syst. Sci.* **2015**, *15*, 1821–1833. [[CrossRef](#)]
12. Froude, M.J.; Petley, D.N. Global fatal landslide occurrence from 2004 to 2016. *Nat. Hazards Earth Syst. Sci.* **2018**, *18*, 2161–2181. [[CrossRef](#)]
13. Uchimura, T.; Towhata, I.; Wang, L.; Nishie, S.; Yamaguchi, H.; Seko, I.; Qiao, J. Precaution and early warning of surface failure of slopes using tilt sensors. *Soils Found.* **2015**, *55*, 1086–1099. [[CrossRef](#)]
14. Huggel, C.; Ramirez, J.M.; Calvache, M.; González, H.; Gutierrez, C.; Krebs, R. A landslide early warning system within an integral risk management strategy for the Combeima-Tolima Region, Colombia. In Proceedings of the International Disaster and Risk Conference (IDRC), Global Risk Forum, Davos, Switzerland, 25–29 August 2008. [[CrossRef](#)]

15. Polanco, C.; Bedoya Sanmiguel, G. Compilación y análisis de los desastres naturales reportados en el departamento de Antioquia, exceptuando los municipios del Valle de Aburrá-Colombia, entre 1920–1999. *Ing. Cienc.* **2005**, *1*, 45–65.
16. Aristizábal, E.; Gómez, J. Inventario de emergencias y desastres en el Valle de Aburrá originados por fenómenos naturales y antrópicos en el periodo 1880–2007. *Gestión y Ambiente* **2007**, *10*, 17–30.
17. Werthmann, C.; Echeverri, A.; Elvira Vélez, A. *Rehabitar La Ladera: Shifting Ground*; Research Report; Universidad EAFIT: Medellín, Colombia, 2012.
18. Breuninger, T.; Gamperl, M.; Menschik, B.; Thuro, K. First Field Findings and their Geological Interpretations at the Study Site Bello Oriente, Medellín, Colombia (Project Inform@Risk). In Proceedings of the 13th International Symposium on Landslides, International Society for Soil Mechanics and Geotechnical Engineering, Cartagena, Colombia, 22–26 February 2021.
19. Ündül, Ö.; Tuğrul, A. On the variations of geo-engineering properties of dunites and diorites related to weathering. *Environ. Earth Sci.* **2016**, *75*, 1326. [[CrossRef](#)]
20. Gamperl, M.; Breuninger, T.; Singer, J.; García-Londoño, C.; Menschik, B.; Thuro, K. Development of a Landslide Early Warning System in informal settlements in Medellín, Colombia. In Proceedings of the 13th International Symposium on Landslides, International Society for Soil Mechanics and Geotechnical Engineering, Cartagena, Colombia, 22–26 February 2021.
21. Cruden, D.; Varnes, D. Landslide Types and Processes. In *Landslides: Investigation and Mitigation*; Turner, A.K., Schuster, R.L., Eds.; Number 247 in Special Report; Transport Research Board, National Research Council: Washington, DC, USA, 1996.
22. Guzzetti, F.; Gariano, S.L.; Peruccacci, S.; Brunetti, M.T.; Marchesini, I.; Rossi, M.; Melillo, M. Geographical landslide early warning systems. *Earth Sci. Rev.* **2020**, *200*, 102973. [[CrossRef](#)]
23. Piciullo, L.; Calvello, M.; Cepeda, J.M. Territorial early warning systems for rainfall-induced landslides. *Earth Sci. Rev.* **2018**, *179*, 228–247. [[CrossRef](#)]
24. Pecoraro, G.; Calvello, M.; Piciullo, L. Monitoring strategies for local landslide early warning systems. *Landslides* **2019**, *16*, 213–231. [[CrossRef](#)]
25. Chae, B.G.; Park, H.J.; Catani, F.; Simoni, A.; Berti, M. Landslide prediction, monitoring and early warning: A concise review of state-of-the-art. *Geosci. J.* **2017**, *21*, 1033–1070. [[CrossRef](#)]
26. Baroñ, I.; Supper, R. Application and reliability of techniques for landslide site investigation, monitoring and early warning—Outcomes from a questionnaire study. *Nat. Hazards Earth Syst. Sci.* **2013**, *13*, 3157–3168. [[CrossRef](#)]
27. Thuro, K.; Singer, J.; Festl, J.; Wunderlich, T.; Wasmeier, P.; Reith, C.; Heunecke, O.; Glabsch, J.; Schuhbäck, S. New landslide monitoring techniques—Developments and experiences of the alpEWAS project. *J. Appl. Geod.* **2010**, *4*, 69–90. [[CrossRef](#)]
28. Notti, D.; Cina, A.; Manzano, A.; Colombo, A.; Bendea, I.H.; Mollo, P.; Giordan, D. Low-Cost GNSS Solution for Continuous Monitoring of Slope Instabilities Applied to Madonna Del Sasso Sanctuary (NW Italy). *Sensors* **2020**, *20*, 289. [[CrossRef](#)]
29. Benoit, L.; Briole, P.; Martin, O.; Thom, C.; Malet, J.P.; Ulrich, P. Monitoring landslide displacements with the Geocube wireless network of low-cost GPS. *Eng. Geol.* **2015**, *195*, 111–121. [[CrossRef](#)]
30. Dixon, N.; Smith, A.; Flint, J.A.; Khanna, R.; Clark, B.; Andjelkovic, M. An acoustic emission landslide early warning system for communities in low-income and middle-income countries. *Landslides* **2018**, *15*, 1631–1644. [[CrossRef](#)]
31. Fernandez-Steeger, T.; Arnhardt, C.; Walter, K.; Haß, S.E.; Niemeyer, F.; Nakaten, B.; Homfeld, S.D.; Asch, K.; Azzam, R.; Bill, R.; et al. SLEWS—a prototype system for flexible real time monitoring of landslides: Using an open spatial data infrastructure and wireless sensor networks. *Geotechnol. Sci. Rep.* **2009**, *13*, 3–15.
32. IDEAM—Instituto de Hidrología, Meteorología y Estudios Ambientales. *Pronóstico de la Amenaza Diaria por Deslizamientos*. Available online: www.pronosticosyalertas.gov.co/web/pronosticos-y-alertas/pronostico-de-la-amenaza-diarria-por-deslizamientos (accessed on 1 March 2021).
33. Thiebes, B. *Landslide Analysis and Early Warning Systems: Local and Regional Case Study in the Swabian Alb, Germany*; Springer Theses; Springer: Berlin/Heidelberg, Germany, 2012. [[CrossRef](#)]
34. Huggel, C.; Khabarov, N.; Obersteiner, M.; Ramírez, J.M. Implementation and integrated numerical modeling of a landslide early warning system: A pilot study in Colombia. *Nat. Hazards* **2010**, *52*, 501–518. [[CrossRef](#)]
35. Gutiérrez Alvis, D.E.; Bornachera Zarate, L.S.; Mosquera Palacios, D.J. Sistema de alerta temprana por movimiento en masa inducido por lluvia para Ciudad Bolívar (Colombia). *Rev. Ing. Solidar.* **2018**, *14*. [[CrossRef](#)]
36. Aristizábal, E.; Gamboa, M.F.; Leoz, F.J. Sistema de Alerta Temprana por Movimientos en Masa Inducidos por Lluvia para el Valle de Aburrá, Colombia. *Rev. EIA* **2010**, *13*, 155–169.
37. Lueth, K.L. *Why the Internet of Things is called Internet of Things: Definition, History, Disambiguation*. Available online: <https://iot-analytics.com/internet-of-things-definition/> (accessed on 1 March 2021).
38. Oguz, E.A.; Robinson, K.; Depina, I.; Thakur, V. IoT-Based Strategies for Risk Management of Rainfall-Induced Landslides: A Review. In Proceedings of the 7th International Symposium on Geotechnical Safety and Risk (ISGSR 2019), Taipei, Taiwan, 11–13 December 2019. [[CrossRef](#)]
39. Cecílio, J.; Ferreira, P.M.; Casimiro, A. Evaluation of LoRa Technology in Flooding Prevention Scenarios. *Sensors* **2020**, *20*, 4034. [[CrossRef](#)]
40. LoRa Alliance. LoRaWAN™ 1.0.3 Specification. Available online: <https://lora-alliance.org/lorawan-for-developers> (accessed on 1 March 2021).
41. Mekki, K.; Bajic, E.; Chaxel, F.; Meyer, F. A comparative study of LPWAN technologies for large-scale IoT deployment. *ICT Express* **2019**, *5*, 1–7. [[CrossRef](#)]

42. Centenaro, M.; Vangelista, L.; Zanella, A.; Zorzi, M. Long-range communications in unlicensed bands: The rising stars in the IoT and smart city scenarios. *IEEE Wirel. Commun.* **2016**, *23*, 60–67. [[CrossRef](#)]
43. Dini, B.; Bennett, G.; Franco, A.; Whitworth, M.R.Z.; Senn, A.; Cook, K. Monitoring boulder movement using the Internet of Things: Towards a landslide early warning system. In Proceedings of the EGU General Assembly Conference Abstracts, Vienna, Austria, 4–8 May 2020; p. EGU2020-17392. [[CrossRef](#)]
44. Moulat, M.E.; Debauche, O.; Mahmoudi, S.; Brahim, L.A.; Manneback, P.; Lebeau, F. Monitoring System Using Internet of Things For Potential Landslides. *Procedia Comput. Sci.* **2018**, *134*, 26–34. [[CrossRef](#)]
45. Azzam, R.; Fernandez-Steeger, T.M.; Arnhardt, C.; Shou, K.J. Monitoring of landslides and infrastructures with wireless sensor networks in an earthquake environment. In Proceedings of the 5th International Conference on Earthquake Geotechnical Engineering, Santiago, Chile, 1–13 January 2011.
46. Duc-Tan, T.; Dinh-Chinh, N.; Duc-Nghia, T.; Duc-Tuyen, T. Development of a Rainfall-Triggered Landslide System using Wireless Accelerometer Network. *Int. J. Adv. Comput. Technol.* **2015**, *7*, 14–24.
47. De Capua, C.; Lugarà, M.; Morello, R. A Smart-Sensor Based on MEMS Technology for Monitoring Landslides. In Proceedings of the First National Conference 265 on Sensors, Rome, Italy, 15–17 August 2012.
48. Tu, R.; Wang, R.; Ge, M.; Walter, T.R.; Ramatschi, M.; Milkereit, C.; Bindi, D.; Dahm, T. Cost-effective monitoring of ground motion related to earthquakes, landslides, or volcanic activity by joint use of a single-frequency GPS and a MEMS accelerometer. *Geophys. Res. Lett.* **2013**, *40*, 3825–3829. [[CrossRef](#)]
49. Smethurst, J.A.; Smith, A.; Uhlemann, S.; Wooff, C.; Chambers, J.; Hughes, P.; Lenart, S.; Saroglou, H.; Springman, S.M.; Löfroth, H.; et al. Current and future role of instrumentation and monitoring in the performance of transport infrastructure slopes. *Q. J. Eng. Geol. Hydrogeol.* **2017**, *50*, 271–286. [[CrossRef](#)]
50. Ramesh, M.V. Real-Time Wireless Sensor Network for Landslide Detection. In Proceedings of the 2009 Third International Conference on Sensor Technologies and Applications, Athens, Greece, 9–10 February 2009; pp. 405–409. [[CrossRef](#)]
51. Hons, M.; Stewart, R.; Lawton, D.; Bertram, M. Ground motion through geophones and MEMS accelerometers: Sensor comparison in theory, modeling, and field data. In *SEG Technical Program Expanded Abstracts*; Society of Exploration Geophysicists: Tulsa, OK, USA, 2007. [[CrossRef](#)]
52. Abraham, M.T.; Satyam, N.; Pradhan, B.; Alamri, A.M. IoT-Based Geotechnical Monitoring of Unstable Slopes for Landslide Early Warning in the Darjeeling Himalayas. *Sensors* **2020**, *20*, 2611. [[CrossRef](#)] [[PubMed](#)]
53. Cmielewski, B.; Kontny, B.; Ćmielewski, Kazimierz. Use of low-cost MEMS technology in early warning system against landslide threats. *Acta Geodyn. Geomater.* **2013**, *10*, 485–490. [[CrossRef](#)]
54. Yang, Z.; Shao, W.; Qiao, J.; Huang, D.; Tian, H.; Lei, X.; Uchimura, T. A Multi-Source Early Warning System of MEMS Based Wireless Monitoring for Rainfall-Induced Landslides. *Appl. Sci.* **2017**, *7*, 1234. [[CrossRef](#)]
55. Chaturvedi, P.; Srivastava, S.; Kaur, P.B. Landslide Early Warning System Development Using Statistical Analysis of Sensors' Data at Tangni Landslide, Uttarakhand, India. In *Proceedings of Sixth International Conference on Soft Computing for Problem Solving*; Deep, K., Bansal, J.C., Das, K.N., Lal, A.K., Garg, H., Nagar, A.K., Pant, M., Eds.; Springer: Singapore, 2017; pp. 259–270.
56. Giorgetti, A.; Lucchi, M.; Tavelli, E.; Barla, M.; Gigli, G.; Casagli, N.; Chiani, M.; Dardari, D. A Robust Wireless Sensor Network for Landslide Risk Analysis: System Design, Deployment, and Field Testing. *IEEE Sensors J.* **2016**, *16*, 6374–6386. [[CrossRef](#)]
57. Gian, Q.A.; Tran, D.T.; Nguyen, D.C.; Nhu, V.H.; Tien Bui, D. Design and implementation of site-specific rainfall-induced landslide early warning and monitoring system: A case study at Nam Dan landslide (Vietnam). *Geomat. Nat. Hazards Risk* **2017**, *8*, 1978–1996. [[CrossRef](#)]
58. Gronz, O.; Hiller, P.H.; Wirtz, S.; Becker, K.; Iserloh, T.; Seeger, M.; Brings, C.; Aberle, J.; Casper, M.C.; Ries, J.B. Smartstones: A small 9-axis sensor implanted in stones to track their movements. *CATENA* **2016**, *142*, 245–251. [[CrossRef](#)]
59. Caviezel, A.; Schaffner, M.; Cavigelli, L.; Niklaus, P.; Buhler, Y.; Bartelt, P.; Magno, M.; Benini, L. Design and Evaluation of a Low-Power Sensor Device for Induced Rockfall Experiments. *IEEE Trans. Instrum. Meas.* **2018**, *67*, 767–779. [[CrossRef](#)]
60. Dikshit, A.; Satyam, D.N.; Towhata, I. Early warning system using tilt sensors in Chibo, Kalimpong, Darjeeling Himalayas, India. *Nat. Hazards* **2018**, *94*, 727–741. [[CrossRef](#)]
61. Uchimura, T.; Towhata, I.; Lan Anh, T.T.; Fukuda, J.; Bautista, C.J.B.; Wang, L.; Seko, I.; Uchida, T.; Matsuoka, A.; Ito, Y.; et al. Simple monitoring method for precaution of landslides watching tilting and water contents on slopes surface. *Landslides* **2010**, *7*, 351–357. [[CrossRef](#)]
62. Xie, J.; Uchimura, T.; Chen, P.; Liu, J.; Xie, C.; Shen, Q. A relationship between displacement and tilting angle of the slope surface in shallow landslides. *Landslides* **2019**, *16*, 1243–1251. [[CrossRef](#)]
63. Singer, J.; Thuro, K.; Gamperl, M.; Breuninger, T.; Menschik, B. Technical Concepts for an Early Warning System for Rainfall Induced Landslides in Informal Settlements. In *Understanding and Reducing Landslide Disaster Risk: Volume 3 Monitoring and Early Warning*; Casagli, N., Tofani, V., Sassa, K., Bobrowsky, P.T., Takara, K., Eds.; Springer International Publishing: Cham, Switzerland, 2021; pp. 209–215. [[CrossRef](#)]
64. Thuro, K.; Singer, J.; Menschik, B.; Breuninger, T.; Gamperl, M. Development of a Landslide Early Warning System in informal settlements in Medellín, Colombia. *Geomech. Tunn.* **2020**, *13*, 103–115. [[CrossRef](#)]
65. Singer, J. Monitoring von Hangbewegungen mit dem Continuous Shear Monitor (CSM)—Anwendungsbeispiele. In *Tagungsband zu den Fachsektionstagen Geotechnik*; Deutsche Gesellschaft für Geotechnik e.V., Ed.; Deutsche Gesellschaft für Geotechnik e.V.: Würzburg, Germany, 2019; pp. 42–46.

66. Singer, J.; Thuro, K.; Festl, J. Development and testing of a time domain reflectometry (TDR) monitoring system for subsurface deformations. In Proceedings of the SRM International Symposium-EUROCK 2010, Lausanne, Switzerland, 15–18 June 2010.
67. Qiao, S.; Feng, C.; Yu, P.; Tan, J.; Uchimura, T.; Wang, L.; Tang, J.; Shen, Q.; Xie, J. Investigation on Surface Tilting in the Failure Process of Shallow Landslides. *Sensors* **2020**, *20*, 2662. [[CrossRef](#)] [[PubMed](#)]
68. Festl, J.; Thuro, K. Determination of thresholds at the Aggenalm landslide (Bayrischzell, Germany) by time series analysis and numerical modeling. In *Landslides and Engineered Slopes. Experience, Theory and Practice*; Aversa, S., Cascini, L., Picarelli, L., Scavia, C., Eds.; CRC Press: London, Germany, 2016; pp. 909–916.

Appendix A-3

Title	Recommendations for Landslide Early Warning Systems in Informal Settlements Based on a Case Study in Medellín, Colombia				
Journal	Land				
DOI	https://doi.org/10.3390/land12071451				
Year	2023	Volume	12(7)	Impact Factor (2022)	3.9
Accepted	Yes	Position of the candidate in the authors list			1
Authors	Moritz Gamperl, John Singer, Carolina Garcia-Londoño, Lisa Seiler, Julián Castañeda, David Cerón-Hernandez, Kurosch Thuro				

This article was published in Land; 12(7); Moritz Gamperl, John Singer, Carolina Garcia-Londoño, Lisa Seiler, Julián Castañeda, David Cerón-Hernandez, Kurosch Thuro; Recommendations for Landslide Early Warning Systems in Informal Settlements Based on a Case Study in Medellín, Colombia; Copyright 2023 by the authors. Licensee MDPI, Basel, Switzerland. This article is an open access article distributed under the terms and conditions of the Creative Commons Attribution (CC BY) license, thus permission to reprint the article is not necessary.

Article

Recommendations for Landslide Early Warning Systems in Informal Settlements Based on a Case Study in Medellín, Colombia

Moritz Gamperl, John Singer, Carolina Garcia-Londoño, Lisa Seiler, Julián Castañeda, David Cerón-Hernandez and Kuroschi Thuro

Special Issue

New Perspectives for the Monitoring and Early Detection of Geohazards

Edited by

Dr. Nikolaos Depountis, Dr. Maria Ferentinou, Dr. Vassilis Marinou and Prof. Dr. Constantinos Loupasakis



Article

Recommendations for Landslide Early Warning Systems in Informal Settlements Based on a Case Study in Medellín, Colombia

Moritz Gamperl ^{1,*} , John Singer ², Carolina Garcia-Londoño ³, Lisa Seiler ⁴, Julián Castañeda ³, David Cerón-Hernandez ³ and Kurosch Thuro ¹

¹ Chair of Engineering Geology, Technical University of Munich, 80333 Munich, Germany; thuro@tum.de

² AlpGeorisk, 86609 Donauwörth, Germany; singer@alpgeorisk.de

³ Geological Society of Colombia, Antioquia Chapter, 50016 Medellín, Colombia; cargalon@gmail.com (C.G.-L.); juliancastval@gmail.com (J.C.); davidceron02@gmail.com (D.C.-H.)

⁴ Chair of Landscape Architecture and Design, Institute of Landscape Architecture, Leibniz University Hannover, 30167 Hannover, Germany; seiler@ila.uni-hannover.de

* Correspondence: moritz.gamperl@tum.de

Abstract: Fatalities from landslides are rising worldwide, especially in cities in mountainous regions, which often expand into the steep slopes surrounding them. For residents, often those living in poor neighborhoods and informal settlements, integrated landslide early warning systems (LEWS) can be a viable solution, if they are affordable and easily replicable. We developed a LEWS in Medellín, Colombia, which can be applied in such semi-urban situations. All the components of the LEWS, from hazard and risk assessment, to the monitoring system and the reaction capacity, were developed with and supported by all local stakeholders, including local authorities, agencies, NGO's, and especially the local community, in order to build trust. It was well integrated into the social structure of the neighborhood, while still delivering precise and dense deformation and trigger measurements. A prototype was built and installed in a neighborhood in Medellín in 2022, comprising a dense network of line and point measurements and gateways. The first data from the measurement system are now available and allow us to define initial thresholds, while more data are being collected to allow for automatic early warning in the future. All the newly developed knowledge, from sensor hardware and software to installation manuals, has been compiled on a wiki-page, to facilitate replication by people in other parts of the world. According to our experience of the installation, we give recommendations for the implementation of LEWSs in similar areas, which can hopefully stimulate a lively exchange between researchers and other stakeholders who want to use, modify, and replicate our system.

Keywords: landslide early warning system; informal settlement; low-cost monitoring; socially integrated; Medellín; Colombia



Citation: Gamperl, M.; Singer, J.; Garcia-Londoño, C.; Seiler, L.; Castañeda, J.; Cerón-Hernandez, D.; Thuro, K.; Recommendations for Landslide Early Warning Systems in Informal Settlements Based on a Case Study in Medellín, Colombia. *Land* **2023**, *12*, 1451. <https://doi.org/10.3390/land12071451>

Academic Editors: Nikolaos Depountis, Maria Ferentinou, Vassilis Marinou and Constantinou Loupasakis

Received: 20 June 2023

Revised: 13 July 2023

Accepted: 14 July 2023

Published: 20 July 2023



Copyright: © 2023 by the authors. Licensee MDPI, Basel, Switzerland. This article is an open access article distributed under the terms and conditions of the Creative Commons Attribution (CC BY) license (<https://creativecommons.org/licenses/by/4.0/>).

1. Introduction

1.1. Landslide Impact and Losses in Colombia and the Aburrá Valley

Worldwide, a rise in the amount of deadly landslides has been observed in the last 50 years, especially in the period between 1995 and 2014 [1,2]. Rainfall therein was a major factor, especially in combination with densely populated areas. Such endangered populated areas are often located on very steep slopes of informal settlements [3–6]. In these informal settlements, the vulnerability to landslides is naturally higher than in other urban areas, both physically (low construction standard of houses) and socially (response capability, hazard education and awareness) [7,8]. Thus, in areas with low income and high inequality, landslides are a greater impeding factor [9]. This divide in landslide risk between rich and poor is expected to increase in the subsequent decades, due to climate change and other

factors, such as increased urbanization in mountainous environments, population growth, and deforestation [2,10]. With changing precipitation characteristics, inhabited areas will be more at risk than in the past [11], while other hazards such as wildfires can act as a promoting factor for future landslides [12].

In South America (e.g., Colombia), high relief, dense population, and high seasonal precipitation are major factors promoting fatal landslides [5]. Thus, fatalities mostly occur in populated mountainous regions, where mortality rates are significantly higher in less developed countries. Cases of deadly landslides have been rising in the last 20 years in Colombia and were triggered mostly by rainfall and anthropogenic factors [13]. The most fatal landslides, on the other hand, were triggered by volcanic activity and earthquakes [9]. The department of Antioquia, which is located in the northwest of Colombia, has the highest total number of landslide events and the second highest total fatalities in Colombia [13,14]. The area of Medellín and the Aburrá Valley are landslide hot spots, especially when looking only at anthropogenic triggers—one half of the landslides that were triggered by human activity in Colombia took place in the Medellín area [9]. Additionally, the third biggest landslide in Colombia, called Villatina landslide, occurred in Medellín in 1987 and caused 500 fatalities [15,16]. It was caused by human activity (water mismanagement) and located in an area that is very similar and close to the area that is taken as a case study here (see Section 1.3).

1.2. Local and Multisectoral Landslide Early Warning Systems

In areas with a high landslide hazard and dense urbanization, where structural mitigation methods are not feasible, the only remaining option—resettlement—is usually not possible, because of the significant economic costs and other complex reasons [17,18]. In addition, the community members usually have no interest in relocating, even if they are aware of the landslide risk they are exposed to [19]. Low-cost mitigation measures can and should be applied, but they can only reduce the risk to a limited extent, without being too costly. For these reasons, landslide early warning systems (LEWS) can be an effective measure to close this gap for some years, until other measures can be applied [20]. It is important to note that, in areas such as the case study of this project, LEWS should be seen as a mid-term, not a long-term, solution.

Examples of such systems have been proposed before, but they have tended to be limited to remote sensing or environmental monitoring [21–24]. Other studies have shown that combining community measurement and warning systems with low-cost technical measurement systems can be effective [25–30], especially when communities are involved in all parts of the risk management cycle [31]. Owing to its complex nature, urban landslide risk can only be reduced by interdisciplinary approaches, including, e.g., geologists, engineers, social scientists, and landscape architects [32,33]. A LEWS resulting from this approach can be called an integrated LEWS (Figure 1).

Notwithstanding the monitoring and forecasting effort, which has to be adapted to the local circumstances, the other components of risk management, risk analysis, alert dissemination, and reaction capacity also have to be addressed. For all of the parts of the system to work together effectively, it is especially important to increase the communication between the actors, to improve the risk education of the local population and to incorporate them into the process of developing and sustaining the warning system [31,34,35]. Considering this, the social aspect of the LEWS is as important as the technical system, especially since local communities are the most involved party and often the first responders after an event [36,37]. Nevertheless, their involvement in early warning systems is often overlooked [38].

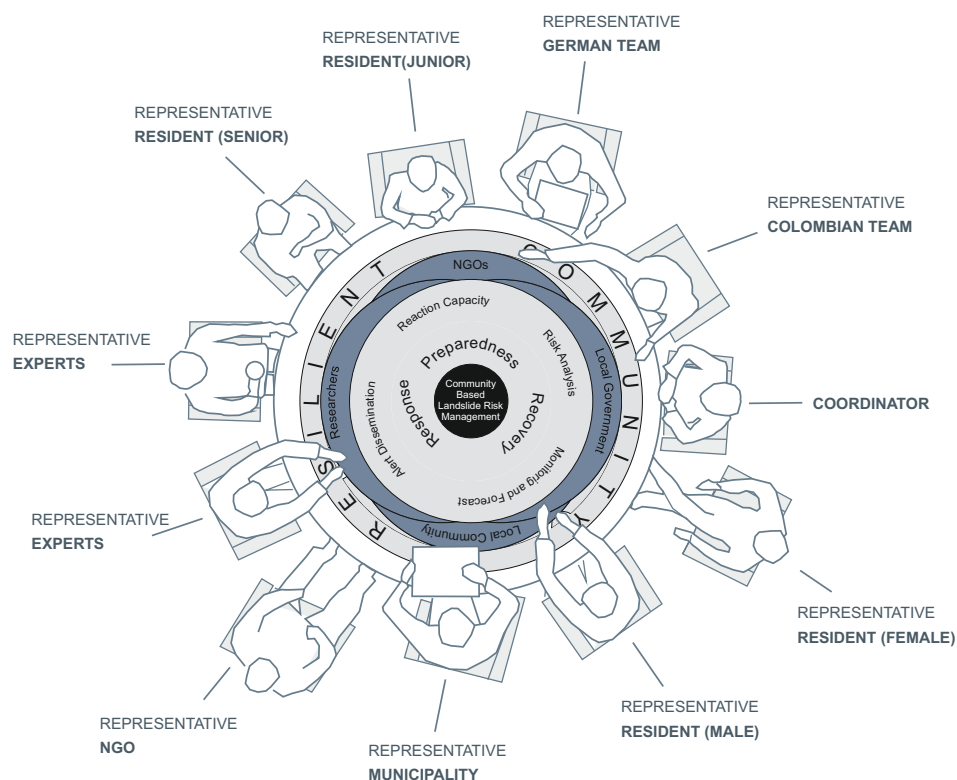


Figure 1. Example of a typical monthly stakeholder meeting for an integrated LEWS. The involvement of all stakeholders is deeply interlinked with the risk cycle and the four elements of the LEWS (risk analysis, monitoring and forecast, alert dissemination, and reaction capacity). Adapted from Sharma [38] and Werthmann [39].

1.3. Project Overview and Goals of the Inform@Risk Project

To tackle the challenges posed by landslide risk in informal settlements, the Inform@Risk project was established. It is a consortium of German universities, research institutes, and small companies, together with Colombian universities, agencies, NGOs, and local communities. The project aims at: (1) socially and (2) spatially integrated, (3) multi-scalar and (4) multi-sectoral LEWS, which at the same time provides (5) accurate measurements using (6) low-cost equipment, and whose technology and guidelines are (7) replicable and transferable to other similar areas [40–42]. To achieve this, the LEWS has been developed as a living lab, in which the stakeholders collaborate by sharing ideas and knowledge, thus contributing to and improving the system [43].

An informal settlement with a high landslide hazard was selected in Medellín, Colombia, to design and test such a system. The study area is located in the upper part of the neighborhood of Bello Oriente in the north-east of the city in Comuna 3. It has an area of about 36.78 ha with approx. 4600 inhabitants living in 1285 buildings, 49% of which, around 2270 inhabitants, are located in a high hazard area [40]. The site is located at the city border and is currently expanding into the as yet uninhabited rural parts upslope to the east.

In Medellín, landslides are a prominent hazard, since the city is surrounded by mountains and therefore has a very steep topography east and west of its center (up to 30° in the east [41,44]). The elevation difference between the valley floor and the surrounding highland is about 1000 m [45]. The steep hills in the east of Medellín mostly comprise dunite rock, an ultramafic rock mainly composed olivine and pyroxene, which weathers easily and deeply due to primary and secondary serpentinization and subsequent chemical weathering into clay minerals and iron oxides and hydroxides [46,47]. Therefore, these slopes are generally more susceptible to landslides [45,47]. This is especially striking when looking at the most devastating landslides in Aburrá Valley of the last 100 years that caused

around 800 deaths: most of them were located on the eastern slopes, where dunite rock outcrops are present [44]. The area is mostly threatened by small- to medium-size shallow landslides, which occur in the weathered layers above the dunite rock. The second most likely hazard is mudflows.

Based on the goals of the Inform@Risk project mentioned above, we designed a monitoring system that can be applied to slopes in inhabited areas with high landslide hazard, where however the exact location of a future landslide cannot be determined [42,48]. To be able to reliably detect critical landslides, the system needs to cover the complete high-hazard area with sufficient spatial and temporal resolution. This is dependent on the expected size landslide and, of course, is an aspect which also affects the economic cost. In order to achieve an efficient system, hazard- and risk-based variation of the density and type of sensors is essential.

The technical concepts and details of the monitoring system have previously published [42,48]. In this contribution, we report the installation and integration of this technical system into the public space and into the dynamics of the local community of the study site in Bello Oriente, Medellín. This pilot study, in which a large monitoring system was put in place in collaboration with the local authorities, based on the previously mentioned technical and social concepts, then allowed us to propose recommendations for future LEWSs in informal settlements. These recommendations are displayed as a framework with a modular design, which allows for future additions and improvements. To facilitate this, a freely available wiki website with details about the implemented technical and social parts was created.

2. Methodology of the Inform@Risk LEWS

In the following section, we give a short outline of the methodology of our LEWS, regarding hazard and risk assessment, monitoring, community integration, and socio-spatial integration.

2.1. Hazard- and Risk Assessment

Before installing any measurement system, a detailed hazard and risk analysis has to be carried out [35]. The goal of a risk assessment is a risk map, which combines the landslide hazard, including events with different processes and sizes, with the local vulnerability and elements at risk. To assess the hazard, a detailed investigation, including on-site geological, geomorphological and process mapping, as well as direct and indirect geological studies, such as drillings, geophysical methods, and numerical modeling, should be performed. Which of these methods are applied in a specific scenario needs to be decided after a preliminary (preferably on-site) analysis [41].

For assessing the hazard from geological findings, we decided to use an approach that combines the locally used hazard analysis defined in the POT 2014 (Plan de Ordenamiento Territorial de Medellín [49]) with Swiss methods for analyzing and assessing natural hazards. The latter are based on detailed geological investigation and delineation of hazard scenarios for different processes and return periods [50]. This was subsequently blended with maps of the elements at risk; especially a detailed map of population density and a building usage classification (e.g., residential, commercial, and public buildings, such as as schools, meeting places, etc.) to arrive at a semi-quantitative risk map [51]. Due to the low quality of most buildings, their vulnerability was not differentiated throughout the area [40].

2.2. Combination of Measurement Systems for a Low-Cost System: CSM and Inform@Risk Geosensor Network

A measurement system was designed based on the requirements of the project (Section 1.3). The system has been described in detail before [42,48].

The monitoring system is based on deformation measurement lines and a newly developed low-cost wireless geosensor network. While the former allows detecting and

locating shear and extensional deformation along measurement lines up to about 300 m in length, the latter provides punctual deformation (e.g., based on an inclination sensor or jointmeter) and other measurements relevant to landslide monitoring; e.g., the triggering factors of ground water level and rainfall. A schematic layout of such a system can be seen in Figure 1 in Gamperl et al. [48].

The deformation measurement lines consist of a combination of CSM (continuous shear monitor, Thuro et al. [52]) and a series of wire extensometers. These were installed horizontally into trenches, which followed streets and pathways across the slope or vertically into geological exploration drillings. If an event occurs and the lateral or basal rupture surface of the landslide passes through one of the measurement lines, the failure location and amount of shear and extensional deformation can be assessed. Ideally, if the sensor lines run across and through (in depth, in boreholes) the landslide, an accurate depiction of the size, depth, and activity of the landslide can be derived.

The newly developed open source geosensor network utilizes IoT (Internet of Things) technologies, e.g., LoRa[®] (Long Range) data communication and micro-electromechanical-system (MEMS) sensors to provide a flexible versatile platform for additional relevant measurements of the surface and shallow subsurface. The wireless measurement nodes act as dataloggers with an integrated inclination, barometric pressure, and temperature sensor, and have been designed so that they can be attached directly to walls or other infrastructure and monitor their tilting [48]. The measurement node can also be installed on top of a shallow subsurface probe, in which, depending on the ground conditions, groundwater level and inclination measurements can be performed to a depth of up to 5 m below the surface. These sensors are versatile and relatively cheap, so that, in high hazard areas, a higher quantity can be installed, making the detection of initial movements more likely.

All data were retrieved by multiple, and—in the case of the wireless geosensor network—redundant, central stations and were transmitted to an offsite data server. As the LoRa[®] data transmission provides ranges up to 15 km, depending on the topography, often only a few central stations are needed to cover large areas.

2.3. Community Integration into All Parts of the LEWS

In integrated LEWSs, the local at-risk community is one of the main actors [31,53]. This is also the case in the Inform@Risk LEWS. For this reason, multiple participatory activities needed to be developed, to address the components of risk knowledge and analysis, monitoring and forecasting, alert dissemination, and response capacity. These activities included workshops with the community regarding all four components and excursions (walking tours) with technical professionals and community members. In addition, including the community in hands-on activities, such as mapping and installation of measurement systems, can be a way of raising awareness and creating a connection to the system [40].

2.4. Socio-Spatial Integration of a LEWS

Commonly, the mechanical-electronical parts of a LEWS are located in remote areas that are not accessible for people at risk. In the case of an informal settlement such as Bello Oriente, where people live in high-hazard areas for landslides, the sensors are located inside the neighborhood's public space, near to and on peoples' houses. A key factor for a successfully integrated LEWS is the acceptance and support of the residents at risk [31,54]. At the same time, it is necessary to protect the monitoring system from external influences. Therefore, an approach for how to spatially and socially integrate the monitoring system into the public open space and how to protect the mechanical-electronical parts was conceived.

Sensor protectors, built as benches and seats for daily use, can function as a natural reminder of the landslide risk. In combination with informative elements, such as short inscriptions and explanatory signs, these small meeting spaces seek to increase acceptance and decrease vandalism. The type and material of the public space elements should

be site-specific and jointly developed with the residents at risk and experts, including, e.g., landscape architects, urban planners, and architects.

3. Installation and First Results of the System in Medellín

3.1. Planning of the Sensor Map Based on Risk Assessment

The risk assessment resulted in three maps with 30-, 100-, and 300-year return frequencies (see [40]). The results were used to plan the sensor density and locations, as well as the evacuation routes, including safe meeting points. In areas with high risk, a higher density of sensors was planned, while in areas with lower risk, the density was reduced significantly. This resulted in a preliminary sensor map for the area, which was then checked and optimized with photographic analyses and on-site visits, taking, e.g., the infrastructure (sensors should only be installed on stable infrastructure, where deformation reflects ground movements, and should be installed in places with good sunlight reception for the solar panel) and the social conditions (house inhabited or not and prospects of future constructions nearby that might affect the sensor) into account (Figure 2). The inhabitants of houses in question were asked if they agreed to have a sensor on their house. For subsurface sensors, which are located mostly in remote locations, the plot owners or the inhabitants were asked. The overall acceptance of both subsurface and infrastructure sensors was very high, and only a small number of sensors had to be moved to a different location, either because a land owner did not give permission or new construction works were carried out on the house or surroundings that affected the exposure of the solar panel of the sensor. For the gateways and large benches, the municipal planning department was involved in the site selection, so that the project would not interfere in future development plans for the neighborhood.

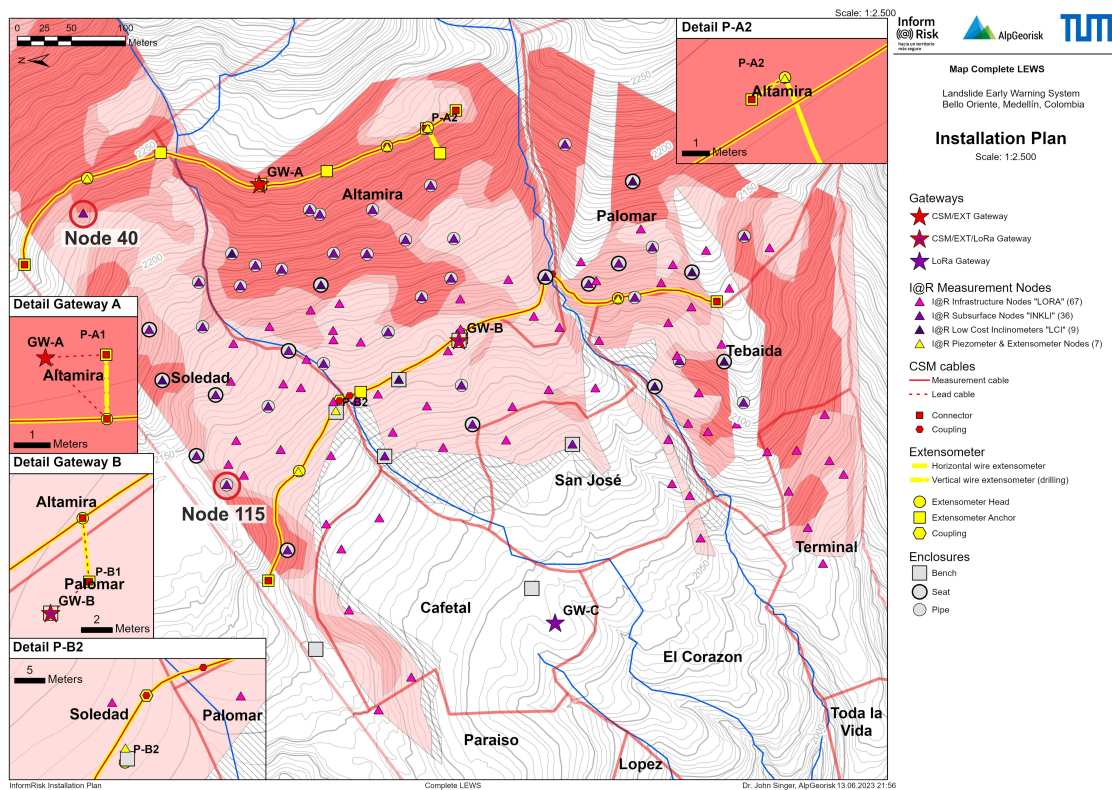


Figure 2. Final installation plan for the monitoring system in Bello Oriente. Overall, 111 measurement nodes, over 1 km of horizontal measurement lines, and three gateways were installed on site. Locations of nodes 40 and 115, displayed in Figure 3, are indicated by the red circles.

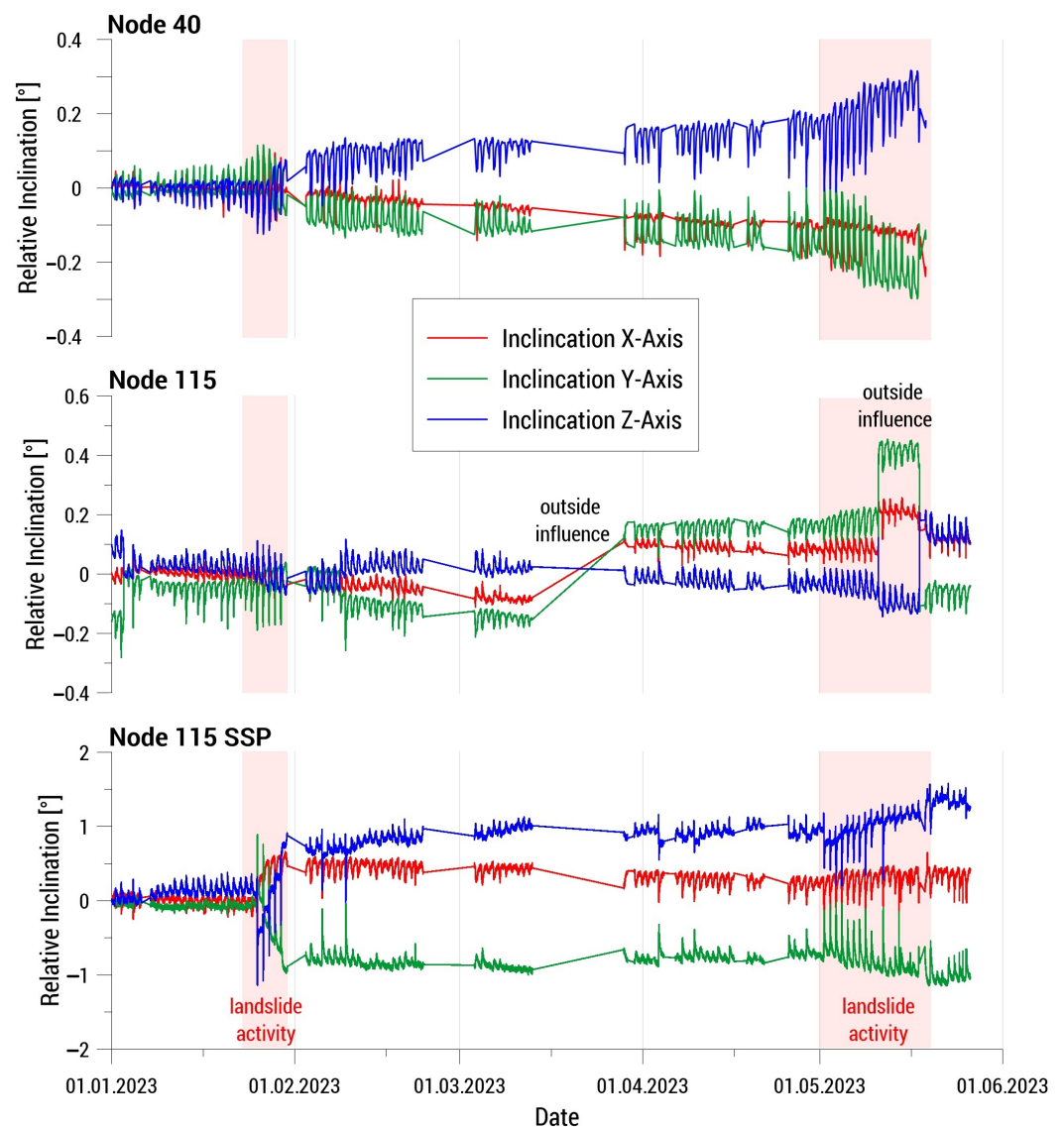


Figure 3. Change in inclination of an infrastructure node (node 40, surface inclinometer only, **top**) and a subsurface node (node 115) equipped with a surface inclinometer (**middle**) and a subsurface inclinometer (SSP, **bottom**) at 1.5 m depth from 1 January to 17 May 2023. See Figure 2 for the sensor locations. (X-axis: downhill).

3.2. Installation of the Sensor System and First Sensor Data

The sensor system was developed in several steps, both in the laboratory and in the field. In these iterations, both the capabilities of the system and the ease of use and replicability were improved. Following the sensor system development and a test installation in southern Germany [48], the installation at the test site in Colombia was implemented in the period between March and August 2022. During the installation, the sensors and the process of installation were further improved, due to onsite experiences.

In total, 111 measurement nodes, over 1 km of horizontal measurement lines, and three gateways were installed at the test site Bello Oriente in Medellin, Colombia. Figure 2 shows the final installation plan with the point and line measurements and the gateways. Additionally, four boreholes of 30 to 50 m depth, which were drilled for the geological investigations, were instrumented with piezometers, extensometers, and a CSM system. Some pictures of the sensors in the field are shown in Figure 4.



Figure 4. Photos of the installation of the measurement system in Bello Oriente in 2022. **(Left):** Installation of a subsurface probe with a measurement node on top. **(Right):** low-cost sensor enclosure in a remote location.

For the installation, a local construction company was hired to perform the earthwork and installation of the horizontal cable lines. The company was asked to hire workers from the local community, in order to strengthen the ties between the LEWS and the community and also to help the locals economically. The installation of the point sensors was performed by researchers and students with the help of the locals. This process took 20 to 45 min for an infrastructure sensor (excluding social work) and two to four hours for a subsurface sensor (usually with no social work involved, because of a remote location).

Since the gateways were installed (August 2022), sensor data have been collected from the system. All data acquired in the geosensor network and the other measurement systems currently installed in Bello Oriente are immediately transferred to an off-site central server, where they are processed and analyzed in near real time. Then the data are stored, analyzed, and visualized using the AlpGeorisk ONLINE data management service developed and operated by AlpGeorisk. The data stored and visualized on this web platform can also be accessed utilizing an open-source smartphone app, which was developed as part of the project by the Deggendorf Institute of Technology (see Werthmann et al. [40]).

So far, around 50,000 datapoints have been collected per day from the Inform@Risk sensor nodes. The CSM system, on the other hand, which is 1 km long and creates a datapoint for every 2 mm of cable (spatial resolution) and produces 0.5 million datapoints per measurement cycle (usually every 30 min). All data are processed to identify failed sensors and exclude false data (empty values or those outside the expected range). Most sensors were activated in the fall of 2022, so that, at the time of writing, about 1/2 year to 1 year of data exist for most sensors. Based on this data, preliminary thresholds have been set, which will be continuously refined as more measurements are made. For the inclination sensors of the Inform@Risk measurement nodes, for example, the following simple thresholds were set: notification $>0.5^\circ/\text{month}$; pre-warning: $0.5^\circ/\text{week}$; warning $0.5^\circ/\text{day}$; alarm: $2^\circ/\text{h}$.

An exemplary dataset is visualized in Figure 3. This example proves the sensitivity ($<0.05^\circ$) of the MEMS inclination sensor used in the Inform@Risk measurement node. It also illustrates some of the issues the data analysis procedure has to tackle in order to produce reliable (automatic) warnings: the separation of daily, temperature-induced fluctuations from multi-day trends, the recognition of outside influences, and the interpretation of a change in inclination as an indicator of critical landslide activity.

Both nodes displayed in Figure 3 were installed within, or in the direct vicinity of, known recently active small landslides (mid to end 2022). Each inclinometer measures in three orthogonal orientations and is capable of reliably detecting inclination changes

above 0.05° . The data clearly show a daily, temperature-dependent fluctuation, which varied in magnitude depending on the type of installation and monitored object (building, retaining wall, steel pipe of subsurface probe, etc.). To date, only very small movements have been detected. However, phases of increased activity could still be identified (light red vertical bars), where all three sensors show slight trends in the data over several days. While the change in inclination in the areas marked as “landslide activity” was not high enough to trigger warning thresholds, some movement, which can be attributed to the previous landslides, was observed and the active phases correlate to periods of comparably high rainfall. Sudden changes in the inclination of a single node, especially if installed at the surface, can be attributed to outside influences.

3.3. Integration of the Community into All Parts of the LEWS in Bello Oriente

To address the community integration of the LEWS, the methods described in Section 2.3 were deployed. In total, over 40 workshops, together with other participatory activities, with over 1000 participants were held in Bello Oriente (see also Werthmann et al. [40]). The workshops and other activities, such as the construction of manual sensors, community walks, and emergency drills, were developed in order to strengthen the different components of the LEWS. Additionally, regular monthly meetings were held with representatives of all Colombian partners, in order to discuss the planned activities (Figure 5).



Figure 5. Picture of one of the meetings, with various stakeholders of the project. Picture: C. Garcia.

To explain how the risk analysis of the system works, several workshops were held with the local community and civil society organizations (Figure 6 upper left). In these, the results of the geological analysis were shown, historical landslide events were discussed and risk factors of the area were identified, in order to reduce them (e.g., leaks in water pipes, incorrect construction techniques, etc.). Additionally, walking tours of the neighborhood were conducted with the participation of technical professionals and members of the community, to identify risk factors, thus allowing for an exchange of knowledge.

Regarding monitoring and forecasting (Figure 6 upper right), some manual monitoring elements were implemented with the community, and automatic sensors were explained in detail. These manual elements usually work in the manner of self-built crack-meters, where deformation is measured manually and marked directly on the instrument. There was also intensive work on identifying the visual signs of a landslide (e.g., cracks, tilted trees, water poles, etc.), since community monitoring is one of the most important elements within the system. Another strategy was to identify, together with the community, what we called “godparents” of the sensors. These are people who live near a sensor and volunteer to take care of it. This mainly involves a regular visual control of the sensor and giving notice if there is an apparent alteration to the sensor or its protection element.

Multiple alert dissemination channels were implemented with the community (Figure 6 lower left), in order to increase redundancy regarding this part. The channels comprised the use of WhatsApp groups, door-to-door alert notices between nearby

neighbors, push messages through the Inform@Risk app, messages played through a large sound system installed in the upper part of the area, and a siren system.

To address the response capacity (Figure 6 lower right), evacuation routes and five meeting points located in stable areas, as defined by the hazard assessment, were identified and marked. Multiple exercises were carried out, to define the actions to be taken at the different qualitative alert levels, defined with the community. These exercises included theoretical risk scenarios and the development of two evacuation drills, designed and developed together with the risk management authority and local civil society organizations.

Since the LEWS was developed in an informal settlement, it was relevant to identify the power relationships among the different actors, including those with governmental, legal, and illegal roles. This implied constant and open communication, in order to gain and maintain trust among the different actors. One of the key actors in the community training and the social power management were the local civil society organizations of the area [55]. Some of the civil society organizations that supported the development of the LEWS had been working with the community for several years, so they had a deep understanding of the social structures and needs.



Figure 6. Photos of the participation of the community in the four components of the LEWS. Pictures: C. Garcia.

3.4. Socio-Spatial Integration of LEWS

Based on the guidelines mentioned in Section 2.4, an integrated concept for public space interventions was developed. The main material chosen for constructing the benches and seats in Bello Oriente was red brick, as it is resistant to tropical weather conditions and is a well-known constructing material in the neighborhood. As one project goal was to build a low-cost system, not all sensors were protected with a bench construction, in order to save costs. Sensors located on steep slopes in remote areas were protected with a low-cost enclosure, a simple plastic pipe (Figure 4). Sensors near pathways and streets, where people walk by, had a medium size set up, in our case a small brick seat (Figure 7, left). Together with residents, the places for building benches and seats were chosen at socially and spatially suitable places, where people could meet and benefit from them. As a special part of the monitoring system, Gateway B (Figure 8) was designed as an informative meeting space. A large bench was paired with a steel construction holding the antennas, the solar

panel, and a sign showing more detailed information about landslide risk and the LEWS (Figure 8, left). To add environmental elements and also to increase residents' responsibility and awareness for these places, micro gardens and trees were planted next to the benches. To protect the horizontal CSM lines from external disturbances, such as future construction activities, simple point markers every 3 to 5 m display their location (Figure 9).



Figure 7. Sensor protections as small seats or benches made out of bricks, supplemented by short inscriptions and bright colors.

For all sensor types, an overall communication strategy was developed. Easy-to-understand characterizations explain the landslide risk and how the slope is monitored. As an example, the short form “LoRa®” means “parrot” in Spanish. Through simple wall paintings of “Lora the parrot” paired with the technical LoRa® box, the infrastructure nodes are visibly spread in the upper part of the neighborhood and serve as an important recognition feature for the integrated LEWS (Figure 8, right).



Figure 8. (Left): Gateway B functions as a small public space, with a large bench and an information sign. **(Right):** LoRa® infrastructure node combined with a wall painting: “Lora the parrot” embodies the sensor.



Figure 9. Point markers indicate the location of the horizontal CSM lines.

3.5. The Inform@Risk Wiki

In order to make the monitoring part of the proposed LEWS as easily replicable as possible, we have compiled all necessary information on a wiki page under: www.informatrisk.com (accessed on 10 June 2023) (Figure 10). For the technical parts of the measurement system described in the last section, we created material lists, installation/construction manuals, as well as datasheets, where necessary. The necessary steps to construct the sensors and install them in the field are explained in detail using pictures from example installations, as well as graphical descriptions. All newly developed parts of the monitoring system are published open source (Figure 11).

To provide flexibility, as well as easy replicability, the sensor designs rely on 3-D printed parts. The 3-D designs are also available on the wiki and can be accessed and modified easily using open-source or free software, such as Blender or Ultimaker Cura. For example, the 3-D printed parts of the subsurface nodes in small drillings were designed for a casing diameter of 1.25", but could easily be adapted to, e.g., casings of 1.5" or 2" diameter. These general descriptions should allow anyone with basic knowledge of electronics and 3-D printing to replicate the sensors.

The basic measurement node, on which all sensors rely, consists of a printed circuit board (PCB) with about 100 components, the design of which is also available on the website, including the circuit schematics as a PDF and fritzing files. This should allow easy future modification, if for example additional or updated sensors need to be added. Nonetheless, the design can be taken and used as is.

The provided firmware for the nodes can be used for both the infrastructure nodes and subsurface measurements. The documentation for the firmware is hosted on a GitHub page, while the installation of the software on one's personal computer is described in an instruction manual, which is hosted on the project wiki website. The necessary software to install the firmware on the nodes comprises the Arduino development environment (IDE, Arduino [56]) and various Arduino libraries, most of which can be downloaded directly in the IDE, while some of them were written specifically or adapted for the measurement nodes. The latter can also be downloaded from the project wiki website. To make the code as easily accessible as possible, it is distributed via GitHub: <https://github.com/moritzgamperl/informrisk-lora-node/> (accessed on 10 June 2023). In this way, changes can easily be made by other contributors. The firmware was written in a way such that it can mirror the flexibility of the nodes themselves: additional sensors can be turned on or off,

and the node can be used without any attached sensors (even without an inclination sensor) as something similar to a “smart home” sensor that measures temperature and barometric pressure. On the other hand, both analog (12 or 24 bit ADC) and digital (I2C, SPI, and serial (TTL) ports) sensors can easily be attached. For example, we used the node not only for its intended functions but also to control and monitor gateways (serial communication) and measure their voltage and current consumption, to measure extensometers (linear potentiometer measurement) and piezometers (4–20 mA current loop measurement) in drillings of up to 50 m depth, and to control a siren system on site (relay).

The screenshot shows the Inform@Risk Wiki Documentation page. The header includes the logo 'Inform@Risk' with the tagline 'hacia un territorio más seguro' and the text 'Inform@Risk Documentation'. There is a search bar and navigation links for 'Recent Changes', 'Media Manager', and 'Sitemap'. A breadcrumb trail reads: 'Trace: - probes - software - datasheets - 3dprints - monitoring_and_warning - risk_knowledge - overview - dissemination_and_communication - response_capability - en'. The main content area is titled 'Inform@Risk Wiki Documentation' and 'Inform@Risk - Strengthening the Resilience of Informal Settlements against Slope Movements'. It contains two paragraphs of text and a photograph of a hillside settlement. The sidebar on the left lists 'CONTENTS' in German, English, and Spanish, with sub-items like 'Overall Introduction', 'Risk Knowledge', 'Monitoring and Warning', 'Response Capability', and 'Resources'. The sidebar on the right shows a 'Table of Contents' with links to various sections.

Figure 10. Inform@Risk wiki page, accessible under www.informatrisk.com (accessed on 10 June 2023). The wiki is a central place for all information about the LEWS. Currently, the wiki is available in three languages, english, german, and spanish (further content and languages can be added by users).

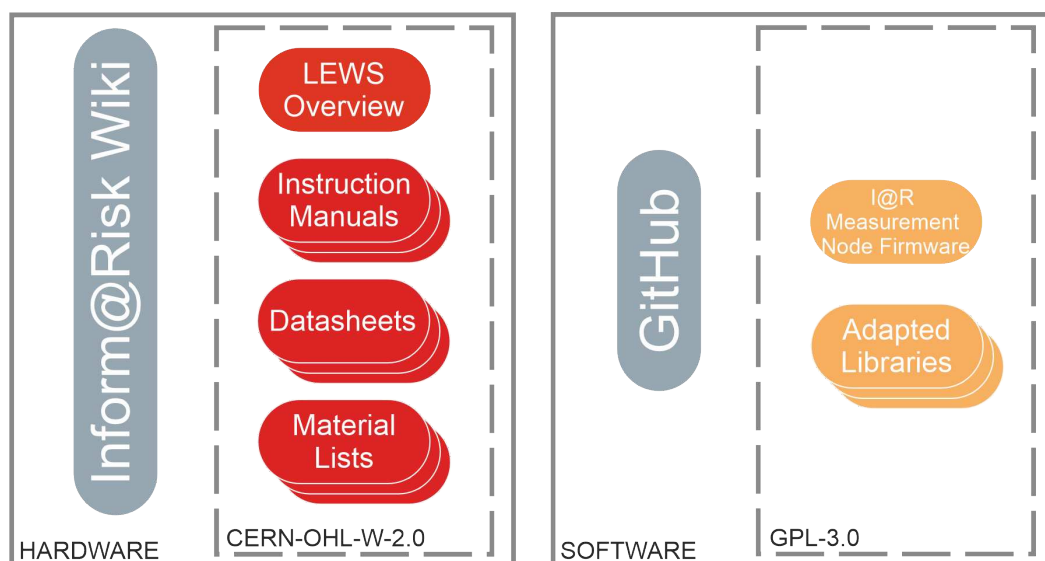


Figure 11. Overview of the open-source information about the monitoring system provided on the wiki- and GitHub pages. The licenses, CERN-OHL-W-2.0 for hardware and GPL-3.0 for software, allow open distribution, modification, and publication of all materials, as long as reference to the source is given.

Descriptions on how to perform low-cost extensometer measurements are also given in an additional document hosted in the wiki. The measurements themselves must be performed using a commercial wire potentiometer, but the wire suspension and guiding can be carried out using simple 3-D printed parts and some easily available basic construction parts. The laying of the wire itself in a horizontal measurement line is also delineated. The measurements can be made using the Inform@Risk measurement nodes, utilizing the required firmware provided on the GitHub page. The CSM system that was installed for the Inform@Risk project, on the other hand, is more difficult to replicate because of the sophisticated software needed, the large amount of data produced, and the high effort required for cable and measurement instrument installation in trenches and shafts.

General descriptions are also given on how to install and operate a LoRa[®] gateway. In general, any commercially available LoRa[®] gateway could be used. However, as continuous interruption-free operation is essential, many things need to be considered when installing the gateways, including signal reception, power supply and storage, data storage, internet connection, redundancy and remote control of the main components and system protection. Consequently, gateways usually have a highly individualized design, adapted to the specific installation site. Furthermore, it is advisable to socially integrate these essential systems into the public space, as we believe this will greatly increase the reliability of the system (see Section 3.4). Therefore, it is difficult to give specific guidelines on this part of the system. However, the general system considerations and a general overview of which devices are needed and how they can be installed and operated can be given on the wiki. The same is true for maintenance, which should ideally also be performed by local risk agencies [57].

4. Recommendations for LEWS Based on the Experiences of the Inform@Risk Project

In the international norm ISO 22327, general guidelines are given for community-based early warning systems [58]. The Inform@Risk LEWS follows these guidelines and has developed specific implementations for the different system elements, adapted to the local needs of our project area in Bello Oriente, Medellín, Colombia. From these experiences, we have developed recommendations for the implementation of LEWS for informal settlements with a community-centered approach (the difference with a community-based early warning system being that there is a greater focus on the monitoring system), which are considered to supplement the general guidelines of ISO 22327.

4.1. Risk Assessment

Often detailed data for area-wide risk assessments is not available, so in the first stage of setting up a LEWS, detailed geological, geotechnical, and social surveys usually need to be performed. Which methodology to use and what level of quality and detail can be achieved depends on many factors, including the type and quality of existing data; local experience/know-how; the usual risk management practice in the region; and the available money, time, and personnel. Nevertheless, the generation of the following elements is considered essential as a data basis for building a LEWS:

- A geological map and report, describing the distribution and characteristics of all lithological units and geological structural elements;
- A phenomenological map or landslide inventory, showing all geological and morphological traces, as well as historic information concerning past and current landslide activity;
- A landslide hazard map and report, which—based on the above surveys—rates all recognized and relevant landslide processes, concerning their probability and magnitude (landslide hazard);
- A socioeconomic study detailing the exposed elements, including the number and type of elements at risk, namely the number of inhabitants, buildings, roads, vehicles, and livestock;
- A building inventory listing the construction type and usage of the buildings on site;
- A socioeconomic vulnerability analysis;
- An assessment of the current state of landslide risk perception and disaster preparedness of the community.

Before starting these surveys, we strongly recommend getting into contact with community leaders and any existing organizations (aid organizations, NGOs, etc.) already working in the community and involving them in the planning of the activities.

The community should be informed about the activities (community meetings, leaflets, public walks, etc.) and should be asked to support the efforts, e.g., by accompanying the geological and social surveys or by giving information about their experiences of past landslide events. These activities should be placed within the overall strategy concerning the dissemination and communication of knowledge.

4.2. Monitoring and Early Warning

Landslide monitoring and early warning systems always need to be designed by a landslide expert and specifically for the landslide processes and geological and topographic conditions present in the project area. The Inform@Risk sensor system, for example, was designed for situations where the failure location of future landslides within a large high risk area cannot be predicted and, thus, a priori sensor placement is impossible. This typically is the case for small to medium sized rainfall-induced landslides in soil. The following recommendations, consequently, are limited to this scenario.

The placement of the deformation sensors in the project area is defined based on the results of the hazard and risk analysis. The goal is to achieve an area-wide coverage of the high-risk area by distributing the sensor nodes (I@R geosensor network) and sensor cables (CSM/EXT) throughout the affected area. The average distance between two sensors should, on average, be less than the diameter of the expected typical landslide (e.g., within a 10-year repeat period). However, to keep the system efficient, the sensor density should be varied based on the risk. Thus, in places where the population density is the highest or buildings of special relevance are present (e.g., schools), more sensors are placed, while in less-populated areas, the number of sensors per area can be decreased. It is essential to also consider the run out of potential landslides originating in high-hazard slopes (which might be classified as low risk due to a lack of exposed objects) above the populated areas. While the overall number and distribution of sensors is determined statistically, the exact placement of each individual sensor on site must be optimized considering the following:

- High probability the sensor will be able to detect the initial movements of a landslide (e.g., attach inclination sensor objects that are shallow in the affected soil);
- Protection from vandalism and other outside influences (e.g., outside the reach of children and animals);
- If applicable, minimize shadowing of solar panels by neighboring objects throughout the day;
- If applicable, ensure that a wireless link to the central station can be established.

There may also be social factors (such as unwillingness of an inhabitant to place a sensor on their house) that influence the sensor placement to a significant degree. If this is the case, the social angle has to be weighed against the other factors, to find the best overall solution. In many cases, the social component will outweigh the technical issues. The monitoring component should not be limited to sensors and automatic instruments. It is highly relevant to help the community at-risk to develop visual and hearing monitoring capacities. By constantly looking for changes in the slope and weather, as well as looking for potential mass movement signs (e.g., leaking pipes, incorrect constructions), risk awareness increases and the monitoring with automatic instruments is complemented.

The topic of dissemination of alerts, in particular, concerns both technical and social issues. In the Inform@Risk project, an app was used in combination with a WhatsApp group. While an app can provide much more information than “traditional” dissemination methods, in our project, it did not prove easy to distribute information [40]. Thus, dissemination methods such as sirens should always be used and combined with other communication pathways such as door-to-door communication or smartphone apps, as redundancy. A sense of responsibility for the sensor system can be achieved by introducing, e.g., sensor godparenthood and maintenance of sensors by the community themselves.

4.3. Dissemination and Communication of Knowledge

As landslide risk is often only one of many problems for the affected communities (and by far not the most pressing problem), it is commonly difficult to raise awareness about landslide risk. While children can be addressed at school, by organizing workshops and preparing age-appropriate information materials, it can be difficult to reach the adult population. For example, community meetings on the topic are often poorly attended (few attendants), even if strong advertising efforts have been made (flyers, house-to-house information walks, etc.). Making the work on the LEWS and its structural components visible and recognizable in public places can, however, help raise awareness. The intention is that community members repeatedly encounter elements of the LEWS in their daily life and thus will be constantly reminded of the presence of the LEWS and its purpose. To facilitate this, the Infom@Risk project implemented the following strategies:

- Development of a unique, noticeable design for all elements related to the LEWS. This included an information and education campaign (information signs, murals, leaflets, presentations, workshop invitations, giveaways, etc.), the technical components of the LEWS itself (sensor enclosures), and also the clothing of people related to the project in all phases of the work;
- Placement of information signs at the entrance of the community and in highly frequented areas;
- Placement of information signs near all noticeable working and construction activities, e.g., geological drillings, geophysical surveys, and construction work for the installation of the sensor system;
- Improving public spaces by adding benches and seats, which also act as sensor enclosures and information signs;
- For each warning level, there should be clear messages that describe the expected actions. These messages should use simple language and include specific details on what to do, where to go, etc. The warning levels with the messages should be widely distributed to the at-risk communities;

- Get into contact with local civil society organizations, so they can include training activities related to the LEWS (risk knowledge, monitoring techniques, reaction capacity, etc.) in their agendas.

4.4. Organizational Framework of the Inform@Risk LEWS

The framework of the Inform@Risk LEWS is given in Figure 12. We developed it based on our experience in Bello Oriente and also used some components of ISO 22327 [58]. It is modular, so that it can be adapted to specific cases. For example, if a system is to be implemented in an area with rockfall hazard, the here-described technical components for monitoring shallow landslides can simply be exchanged for components that monitor rockfall. The framework is based on the experiences documented in our pilot project in Medellín, Colombia.

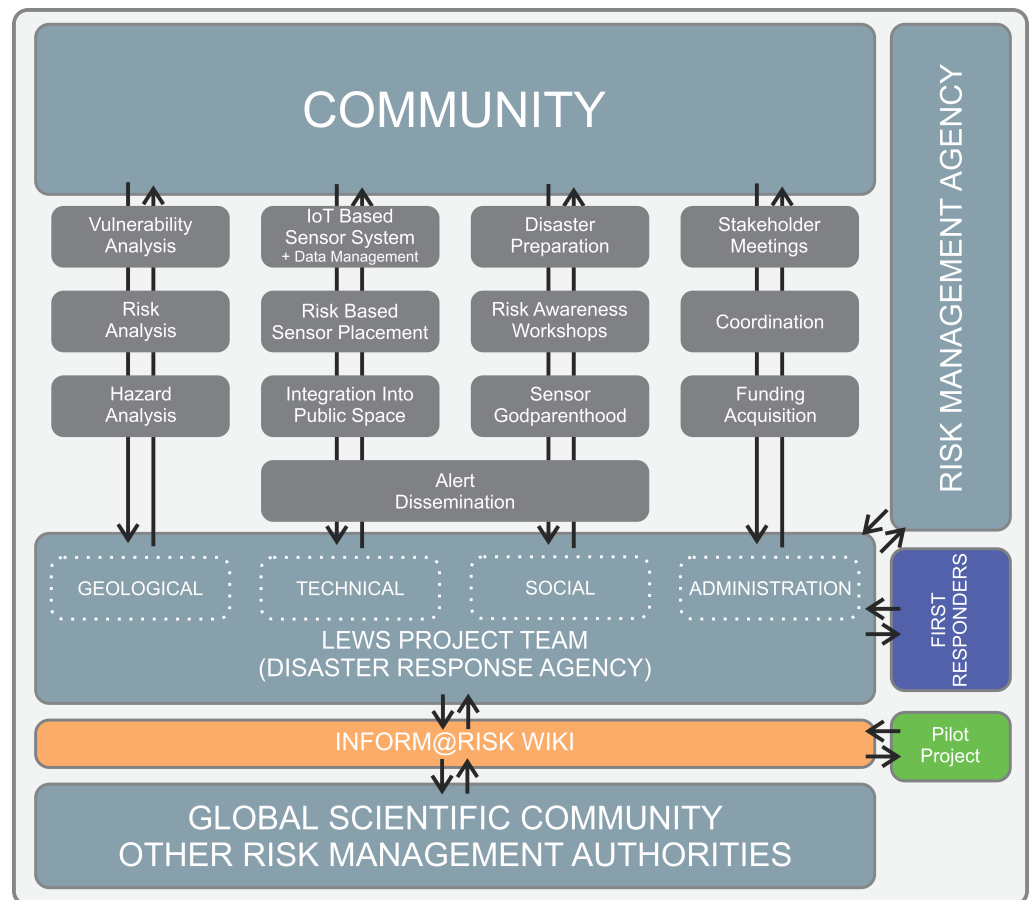


Figure 12. The Inform@Risk framework for integrated LEWS.

The two main parts of the LEWS are the local community (top) and the LEWS team (similar to the “disaster preparedness team” in the ISO, but with a stronger focus on monitoring). Together with local risk management authorities (which can also be a regional agency), civil societies, and first responders, various tasks in the four categories geohazards, technology, social, and administration are defined. Most of the sections are interlinked and dependent on each other.

The social dimension is present in all components, but there should be a focus on the topics of disaster preparation/response capability and risk awareness, which can be achieved through the methods described above. The main focus of administration should be to distribute information between the different stakeholders and to organize regular meetings between them. In addition, coordination of tasks should be central to administration. If necessary, this part of the project should also take care of finding funding for the specific project.

The new Inform@Risk wiki page, as described above, hopefully can be a tool for further development of the framework and for exchange between researchers and risk managers dealing with similar situations. Therefore, we designed it as an interface between our pilot project, the global scientific community, and users. The information currently on the wiki regarding the pilot project in Medellín, therefore, is meant to be a starting point for further improvements and amendments.

5. Discussion

We proposed and tested a LEWS that was specifically designed for informal settlements and socially and spatially integrated into the settlements. The first test installation in Medellín, Colombia showed that such a system might be technically feasible for authorities/decision makers, but substantial efforts have to be made with regard to the social aspects—an element of the LEWS where no shortcuts can be made. Positive relations between the authorities, civil society organizations, and the community are essential.

The design of the sensors, accompanied by the illustrative elements used in this project, allowed a better understanding and identification of the instruments by the at-risk community. The interventions that were carried out to improve public spaces (i.e., benches and seats), which incorporated sensors inside them, led to a positive acceptance in general terms. People use the benches and seats to meet friends and family or watch their children play, showing that a LEWS supported by public space design can contribute to social interactions in a neighborhood. The combination of benches or seats with informative elements such as short inscriptions and additional signs worked best in our case. The meeting spaces became important means of communication, since they promoted discussions about the LEWS and landslide risk in general. Strategies such as “sensor godparenthood”, inhabitants sponsoring and caring for sensors in the vicinity of their homes, can promote the adoption of the LEWS and guarantee that the system will be maintained over time. On the other hand, this requires continuous social and technical support by the local authorities, to maintain the integrity of the sensor system. Additionally, such areas constantly grow and construction activities can progress very quickly. Thus, it is important to consider materials and designs that do not serve as inputs for the construction of a home, because this increases the likelihood that the protective structures will be vandalized.

However, in individual terms, a few people felt that the location of some of these benches would become spaces for drug use and territorial focus points for the local gangs. It is therefore essential that, when replicating similar projects, joint planning is carried out with the community, in terms of locating infrastructure for the improvement of public space and to increase the knowledge transfer among the different actors and residents (e.g., through supplemental information campaigns).

At the time of writing, no technical instrument has been stolen or tampered with, which we consider a major achievement. We attribute this to the constant social process that has lasted almost four years, where the voices of all actors have been heard and considered.

In an effort to enable the replicability of the low-cost instrumental monitoring system, as well as the overall LEWS, a large quantity of information, in the form of documents, files, and manuals, has been made public on the Inform@Risk wiki page. The use of this wiki page allows anyone, anywhere to interact with us and voice criticisms or propose changes to the system. We hope that this can be the start of a truly participative approach to landslide early warning for communities that are suffering the most from these hazards.

5.1. Efficiency of Sensor System

Detailed investigations of the data produced by the system and their analysis and interpretation are outside of scope of this publication and will be published in the future. However, initial data already show that the low-cost sensors can produce data that are sufficiently precise to reflect initial movements in the subsurface, if placed in the right locations and with the proper methods. Further analysis of the data over the subsequent years will yield continuously improved thresholds, which in turn will increase the confi-

dence in warnings. Especially for point measurements (LoRa nodes), automatic warnings (received by experts) are essential, because the amount of data from these sensors is too large to be monitored by experts every day. Data fusion methods have to be applied that both combine the sensor data of the same information in different areas (complementary sensor fusion) and of different sources, to increase reliability (redundant sensor fusion). Cooperative sensor fusion, on the other hand, combines information from different sources, in order to gain additional, more complex information (e.g., comparing trigger data from rain gauges with deformation data from inclinometers). These methods can help to exclude false positive warnings and increase early warning times. The expected warning times range from several hours to days from the initial failure initiation to the collapse of a slope. This still has to be proven by field data, once more substantial deformation data have been collected. The expected warning times are, in any case, much higher than the transmission intervals of the sensor system, so the necessary times can be achieved by the system.

A building density of about 250 people per ha or more might render the proposed monitoring system ineffective. In such areas, focusing on social work is expected to be a more efficient approach, as trained inhabitants will be able to identify signals of early landslide movements (cracks, tilting, jammed doors) more easily, as opposed to a technical system which, in these areas, might comparably produce many false readings, due to intentional or unintentional tampering. A technical monitoring system, on the other hand, is ideal in sparsely inhabited steep slopes above settlements with a small population.

The economic costs of this system or similar systems in the Medellín region were investigated in Sapena et al. [57]. These costs, however, should only be invested if the limitations are clear: as the system is aimed at slopes with a generally high landslide hazard, but an unknown exact future landslide area, it can only detect the initial movement of landslides in areas with monitoring systems installed. If initial movements occur in areas deemed very unlikely during the hazard analysis, which are subsequently only monitored sparsely, the system might not detect these movements. In the same way, the system can only provide a certain density of point sensors (about one sensor every 20 m on average) without becoming economically infeasible. This means that smaller landslides can generally not be detected with certainty. If the risk management authority operates such a system in multiple areas of one metropolitan area, the effort required for operation can be greatly diminished, since gateways and other infrastructure can be shared if circumstances (e.g., distance and line of sight) permit. The same is true for the data management system, which is easily scalable.

5.2. Challenges of an Integrated LEWS

Informal settlements, present in many cities of the world, are often built in landslide-prone areas without building code. Where they are located in high hazard areas, resettlement is often not an option, due to high costs. An integrated LEWS can help to decrease the risk for these communities in the short- to mid-term. The system can only be developed by collaborating with local authorities, agencies, civil society organizations, and inhabitants, and it has to be tailored for them. Considering this, we have provided recommendations for the technical and social aspects, which are both adapted to the conditions on site. The latter is one of the most challenging parts, as conditions in informal settlements can vary a lot [59].

The Living Lab Model has already proven to be an appropriate approach for this [43]. Local people have to be involved during all steps of the development and implementation process (e.g., from the site investigation works); in this way, a sustainable increase in landslide hazard awareness can be achieved and the training for LEWS alarms can be started early.

Author Contributions: Conceptualization, J.S. and M.G.; methodology, J.S., L.S. and M.G.; software, M.G. and J.S.; validation, M.G., L.S. and J.S.; investigation, J.S., L.S., J.C., D.C.-H., C.G.-L. and M.G.; resources, J.S., L.S. and M.G.; writing—original draft preparation, M.G., C.G.-L. and L.S.; writing—review and editing, J.S., K.T., J.C., L.S., C.G.-L. and M.G.; visualization, M.G., L.S. and

C.G.-L.; supervision, J.S. and K.T.; project administration, J.S., C.G.-L. and K.T.; funding acquisition, J.S. and K.T. All authors have read and agreed to the published version of the manuscript.

Funding: This research was funded by the German Federal Ministry of Education and Research, grant number 03G0883A-F. We thank Fretzdorff and Putbresi from Project Management Jülich for their support and guidance.

Data Availability Statement: Not applicable.

Acknowledgments: We want to thank the community of Bello Oriente for their essential support over the last four years. We also thank our Colombian partners, especially DAGRD Medellín. German partners: Leibniz Universität Hannover (Coordinator), Technische Hochschule Deggendorf, Technische Universität München, Deutsches Zentrum für Luft- und Raumfahrt e.V., AlpGeorisk, Sachverständigenbüro für Luftbildauswertung und Umweltfragen; Colombian partners: EAFIT University—URBAM, Alcaldía de Medellín, Área Metropolitana del Valle de Aburrá, Sistema de Alerta Temprana del Valle de Aburrá, Sociedad Colombiana de Geología, Colectivo Tejearañas, Corporación Convivamos, Fundación Palomá, Red Barrial Bello Oriente.

Conflicts of Interest: The authors declare no conflict of interest. The funders had no role in the design of the study, in the collection, analyses, or interpretation of data, in the writing of the manuscript, or in the decision to publish the results.

References

- Cendrero, A.; Forte, L.M.; Remondo, J.; Cuesta-Albertos, J.A. Anthropocene Geomorphic Change. Climate or Human Activities? *Earth's Future* **2020**, *8*, e2019EF001305. [[CrossRef](#)]
- Haque, U.; da Silva, P.F.; Devoli, G.; Pilz, J.; Zhao, B.; Khaloua, A.; Wilopo, W.; Andersen, P.; Lu, P.; Lee, J.; et al. The human cost of global warming: Deadly landslides and their triggers (1995–2014). *Sci. Total Environ.* **2019**, *682*, 673–684. [[CrossRef](#)] [[PubMed](#)]
- Ozturk, U.; Bozzolan, E.; Holcombe, E.A.; Shukla, R.; Pianosi, F.; Wagener, T. How climate change and unplanned urban sprawl bring more landslides. *Nature* **2022**, *608*, 262–265. [[CrossRef](#)] [[PubMed](#)]
- Alexander, D. Vulnerability to Landslides. In *Landslide Hazard and Risk*; Glade, T., Anderson, M., Crozier, M.J., Eds.; John Wiley & Sons, Ltd.: Chichester, UK, 2005; pp. 175–198. [[CrossRef](#)]
- Sepúlveda, S.A.; Petley, D.N. Regional trends and controlling factors of fatal landslides in Latin America and the Caribbean. *Nat. Hazards Earth Syst. Sci.* **2015**, *15*, 1821–1833. [[CrossRef](#)]
- Santi, P.M.; Hewitt, K.; VanDine, D.F.; Barillas Cruz, E. Debris-flow impact, vulnerability, and response. *Nat. Hazards* **2011**, *56*, 371–402. [[CrossRef](#)]
- Pollock, W.; Wartman, J. Human Vulnerability to Landslides. *GeoHealth* **2020**, *4*, e2020GH000287. [[CrossRef](#)]
- Kennedy, I.T.R.; Petley, D.N.; Murray, V. Landslides. In *Koenig and Schultz's Disaster Medicine*, 2nd ed.; Koenig, K.L., Schultz, C.H., Eds.; Cambridge University Press: Cambridge, UK, 2016; pp. 716–723. [[CrossRef](#)]
- Aristizábal, E.; Sánchez, O. Spatial and temporal patterns and the socioeconomic impacts of landslides in the tropical and mountainous Colombian Andes. *Disasters* **2020**, *44*, 596–618. [[CrossRef](#)]
- Gariano, S.L.; Guzzetti, F. Landslides in a changing climate. *Earth Sci. Rev.* **2016**, *162*, 227–252. [[CrossRef](#)]
- Johnston, E.C.; Davenport, F.V.; Wang, L.; Caers, J.K.; Muthukrishnan, S.; Burke, M.; Duffenbaugh, N.S. Quantifying the Effect of Precipitation on Landslide Hazard in Urbanized and Non-Urbanized Areas. *Geophys. Res. Lett.* **2021**, *48*, e2021GL094038. [[CrossRef](#)]
- Rengers, F.K.; McGuire, L.A.; Oakley, N.S.; Kean, J.W.; Staley, D.M.; Tang, H. Landslides after wildfire: Initiation, magnitude, and mobility. *Landslides* **2020**, *17*, 2631–2641. [[CrossRef](#)]
- García-Delgado, H.; Petley, D.N.; Bermúdez, M.A.; Sepúlveda, S.A. Fatal landslides in Colombia (from historical times to 2020) and their socio-economic impacts. *Landslides* **2022**, *19*, 1689–1716. [[CrossRef](#)]
- Gomez-Zapata, J.; Parrado, C.; Frimberger, T.; Barragán-Ochoa, F.; Brill, F.; Büche, K.; Krautblatter, M.; Langbein, M.; Pittore, M.; Rosero-Velásquez, H.; et al. Community Perception and Communication of Volcanic Risk from the Cotopaxi Volcano in Latacunga, Ecuador. *Sustainability* **2021**, *13*, 1714. [[CrossRef](#)]
- García-Londoño, C. El Deslizamiento de Villatina. In *Desastres de Origen Natural en Colombia 1979–2004*; Hermelin, M., Ed.; Universidad EAFIT: Medellín, Columbia, 2005; pp. 55–64.
- Coupé, F.; Arboleda G., E.; García L.C. Villa tina: Algunas reflexiones 20 años después de la tragedia. *Gestión Ambiente* **2007**, *10*, 31–52.
- Dorner, W.; Ramirez Camargo, L.; Hofmann, P. Can Geoinformation Help to Better Protect Informal Settlements?—A Concept for the City of Medellín. *ISPRS Int. Arch. Photogramm. Remote Sens. Spat. Inf. Sci.* **2019**, *XLII-3/W8*, 115–120. [[CrossRef](#)]
- Smith, H.; Coupé, F.; García-Ferrari, S.; Rivera, H.; Castro Mera, W.E. Toward negotiated mitigation of landslide risks in informal settlements: Reflections from a pilot experience in Medellín, Colombia. *Ecol. Soc.* **2020**, *25*, art19. [[CrossRef](#)]
- Nathan, F. Risk perception, risk management and vulnerability to landslides in the hill slopes in the city of La Paz, Bolivia. A preliminary statement. *Disasters* **2008**, *32*, 337–357. [[CrossRef](#)] [[PubMed](#)]

20. Eberhardt, E.; Watson, A.D.; Löw, S. *Improving the Interpretation of Slope Monitoring and Early Warning Data Through Better Understanding of Complex Deep-Seated Landslide Failure Mechanisms*; Taylor & Francis: Abingdon, UK, 2008; p. 51.
21. Mateos, R.M.; López-Vinielles, J.; Bru, G.; Sarro, R.; Béjar-Pizarro, M.; Herrera, G. Landslides in Urban Environments. In *Treatise on Geomorphology*; Elsevier: Amsterdam, The Netherlands, 2022; pp. 415–432. [[CrossRef](#)]
22. Hart, J.K.; Martinez, K. Environmental Sensor Networks: A revolution in the earth system science? *Earth Sci. Rev.* **2006**, *78*, 177–191. [[CrossRef](#)]
23. Segoni, S.; Leoni, L.; Benedetti, A.I.; Catani, F.; Righini, G.; Falorni, G.; Gabellani, S.; Rudari, R.; Silvestro, F.; Rebor, N. Towards a definition of a real-time forecasting network for rainfall induced shallow landslides. *Nat. Hazards Earth Syst. Sci.* **2009**, *9*, 2119–2133. [[CrossRef](#)]
24. Sirangelo, B.; Versace, P. A real time forecasting model for landslides triggered by rainfall. *Meccanica* **1996**, *31*, 73–85. [[CrossRef](#)]
25. Bandara, R.M.S.; Bhasin, R.K.; Kjekstad, O.; Arambepola, N.M.S.I. Examples of Cost Effective Practices for Landslide Monitoring for Early Warning in Developing Countries of Asia. In *Landslide Science and Practice*; Margottini, C., Canuti, P., Sassa, K., Eds.; Springer: Berlin/Heidelberg, Germany, 2013; pp. 581–588. [[CrossRef](#)]
26. Fathani, T.F.; Karnawati, D.; Wilopo, W. An Adaptive and Sustained Landslide Monitoring and Early Warning System. In *Landslide Science for a Safer Geoenvironment*; Sassa, K., Canuti, P., Yin, Y., Eds.; Springer International Publishing: Cham, Switzerland, 2014; pp. 563–567. [[CrossRef](#)]
27. Michoud, C.; Bazin, S.; Blikra, L.H.; Derron, M.H.; Jaboyedoff, M. Experiences from site-specific landslide early warning systems. *Nat. Hazards Earth Syst. Sci.* **2013**, *13*, 2659–2673. [[CrossRef](#)]
28. Allasia, P.; Godone, D.; Giordan, D.; Guenzi, D.; Lollino, G. Advances on Measuring Deep-Seated Ground Deformations Using Robotized Inclinometer System. *Sensors* **2020**, *20*, 3769. [[CrossRef](#)] [[PubMed](#)]
29. Jeng, C.J.; Yo, Y.Y.; Zhong, K.L. Interpretation of slope displacement obtained from inclinometers and simulation of calibration tests. *Nat. Hazards* **2017**, *87*, 623–657. [[CrossRef](#)]
30. Fosslau, C.; Zet, C.; Petrisor, D. Multiaxis inclinometer for in depth measurement of landslide movements. *Sens. Rev.* **2015**, *35*. [[CrossRef](#)]
31. Baudoin, M.A.; Henly-Shepard, S.; Fernando, N.; Sitati, A.; Zommers, Z. From Top-Down to “Community-Centric” Approaches to Early Warning Systems: Exploring Pathways to Improve Disaster Risk Reduction Through Community Participation. *Int. J. Disaster Risk Sci.* **2016**, *7*, 163–174. [[CrossRef](#)]
32. Alexander, D. Urban landslides. *Prog. Phys. Geogr. Earth Environ.* **1989**, *13*, 157–189. [[CrossRef](#)]
33. Thapa, P.S.; Adhikari, B.R. Development of community-based landslide early warning system in the earthquake-affected areas of Nepal Himalaya. *J. Mt. Sci.* **2019**, *16*, 2701–2713. [[CrossRef](#)]
34. Garcia, C.; Fearnley, C.J. Evaluating critical links in early warning systems for natural hazards. *Environ. Hazards* **2012**, *11*, 123–137. [[CrossRef](#)]
35. Fathani, T.F.; Karnawati, D.; Wilopo, W. Promoting a Global Standard for Community-Based Landslide Early Warning Systems (WCoE 2014–2017, IPL-158, IPL-165). In *Advancing Culture of Living with Landslides*; Sassa, K., Mikoš, M., Yin, Y., Eds.; Springer International Publishing: Cham, Switzerland, 2017; pp. 355–361. [[CrossRef](#)]
36. Karnawati, D.; Fathani, T.F.; Wilopo, W.; Setianto, A.; Andayani, B. Promoting the hybrid socio-technical approach for effective disaster risk reduction in developing countries. *Disaster Manag.* **2011**, *119*, 175–182. [[CrossRef](#)]
37. Giordan, D.; Wrzesniak, A.; Allasia, P. The Importance of a Dedicated Monitoring Solution and Communication Strategy for an Effective Management of Complex Active Landslides in Urbanized Areas. *Sustainability* **2019**, *11*, 946. [[CrossRef](#)]
38. Sharma, R. Community Based Flood Risk Management: Local Knowledge and Actor’s Involvement Approach from Lower Karnali River Basin of Nepal. *J. Geosci. Environ. Prot.* **2021**, *9*, 35–65. [[CrossRef](#)]
39. Werthmann, C. *Stärkung der Resilienz informeller Siedlungen gegen Hangbewegungen durch die Vernetzung von Frühwarnsystemen, Web-Technologien und Landschaftsplanung in partizipativen Prozessen—Fallstudie Medellín, Kolumbien*; Funding Proposal; Leibniz Universität Hannover: Hannover, Germany, 2018.
40. Werthmann, C.; Sapena, M.; Kühnl, M.; Singer, J.; Garcia, C.; Menschik, B.; Schäfer, H.; Schröck, S.; Seiler, L.; Thuro, K.; et al. *Inform@Risk*. The Development of a Prototype for an Integrated Landslide Early Warning System in an Informal Settlement: The Case of Bello Oriente in Medellín, Colombia. *Nat. Hazards Earth Syst. Sci. Discuss.* **2023**, p. 42, in review. [[CrossRef](#)]
41. Thuro, K.; Singer, J.; Menschik, B.; Breuninger, T.; Gamperl, M. Development of a Landslide Early Warning System in informal settlements in Medellín, Colombia. *Geomech. Tunn.* **2020**, *13*, 103–115. [[CrossRef](#)]
42. Singer, J.; Thuro, K.; Gamperl, M.; Breuninger, T.; Menschik, B. Technical Concepts for an Early Warning System for Rainfall Induced Landslides in Informal Settlements. In *Understanding and Reducing Landslide Disaster Risk: Volume 3 Monitoring and Early Warning*; Casagli, N., Tofani, V., Sassa, K., Bobrowsky, P.T., Takara, K., Eds.; Springer International Publishing: Cham, Switzerland, 2021; pp. 209–215. [[CrossRef](#)]
43. Hossain, M.; Leminen, S.; Westerlund, M. A systematic review of living lab literature. *J. Clean. Prod.* **2019**, *213*, 976–988. [[CrossRef](#)]
44. Werthmann, C.; Echeverri, A.; Elvira Vélez, A. *Rehabitar La Ladera: Shifting Ground*; Research Report; Universidad EAFIT: Medellín, Colombia, 2012.
45. Ojeda, J.; Donnelly, L. Landslides in Colombia and their impact on towns and cities. In Proceedings of the 10th IAEG Congress, Nottingham, UK, 6–10 September 2006; p. 112.

46. Aristizábal, E.; Yokota, S. Evolucion geomorfologica del valle de Aburra Y Sus Implicaciones En la Ocurrencia de Movimientos en Masa. *Boletín de Ciencias de la Tierra* **2008**, *24*, 5–18.
47. Breuninger, T.; Menschik, B.; Demharter, A.; Gamperl, M.; Thuro, K. Investigation of Critical Geotechnical, Petrological and Mineralogical Parameters for Landslides in Deeply Weathered Dunite Rock (Medellín, Colombia). *Int. J. Environ. Res. Public Health* **2021**, *18*, 11141. [[CrossRef](#)]
48. Gamperl, M.; Singer, J.; Thuro, K. Internet of Things Geosensor Network for Cost-Effective Landslide Early Warning Systems. *Sensors* **2021**, *21*, 2609. [[CrossRef](#)]
49. Alcaldía de Medellín. Acuerdo 48 de 2014, Plan de Ordenamiento Territorial de Medellín. 2014. Available online: https://issuu.com/habitantesevillamedellin/docs/acuerdo_48_pot-19-12-2014_-_capitul (accessed on 10 June 2023).
50. Heinimann, H.R.; Hollenstein, K.; Kienholz, H.; Krummenacher, B.; Mani, P. *Umwelt-Materialien Nr. 85-Methiden zur Analyse und Bewertung von Naturgefahren*; Technical Report; Swiss Landscape Concept, Swiss Agency for the Environment, Forests and Landscape: Bern, Switzerland, 1998.
51. Kühnl, M.; Sapena, M.; Wurm, M.; Geiß, C.; Taubenböck, H. Multitemporal landslide exposure and vulnerability assessment in Medellín, Colombia. *Nat. Hazards* **2022**. [[CrossRef](#)]
52. Thuro, K.; Singer, J.; Festl, J.; Wunderlich, T.; Wasmeier, P.; Reith, C.; Heunecke, O.; Glabsch, J.; Schuhbäck, S. New landslide monitoring techniques—Developments and experiences of the alpEWAS project. *J. Appl. Geod.* **2010**, *4*, 69–90. [[CrossRef](#)]
53. Gumiran, B.A.; Moncada, F.M.; Gasmen, H.J.; Boyles-Panting, N.R.; Solidum, R.U. Participatory capacities and vulnerabilities assessment: Towards the realisation of community-based early warning system for deep-seated landslides. *Jamba J. Disaster Risk Stud.* **2019**, *11*, 1–11. [[CrossRef](#)]
54. Marchezini, V.; Horita, F.E.A.; Matsuo, P.M.; Trajber, R.; Trejo-Rangel, M.A.; Olivato, D. A Review of Studies on Participatory Early Warning Systems (P-EWS): Pathways to Support Citizen Science Initiatives. *Front. Earth Sci.* **2018**, *6*, 184. [[CrossRef](#)]
55. Lassa, J.A. Roles of Non-Government Organizations in Disaster Risk Reduction. *Oxf. Res. Encycl. Nat. Hazard Sci.* **2018**. [[CrossRef](#)]
56. Arduino. Software | Arduino. 2023. Available online: <https://blog.arduino.cc/2023/04/21/arduino-ide-2-1-is-now-available/> (accessed on 10 June 2023)
57. Sapena, M.; Gamperl, M.; Kühnl, M.; Singer, J.; Garcia-Londoño, C.; Taubenböck, H. Cost estimation for the instrumentalization of Early Warning Systems in landslide prone areas. *Nat. Hazards Earth Syst. Sci.* **2023**, in preparation.
58. ISO 22327; Security and Resilience—Emergency Management—Guidelines for Implementation of a Community-Based Landslide Early Warning System. ISO International Organization for Standardization: Geneva, Switzerland, 2009.
59. Perlman, J.E. *Favela Four Decades of Living on the Edge in Rio de Janeiro*; Oxford University Press: New York, NY, USA, 2010; OCLC: 1303480415.

Disclaimer/Publisher’s Note: The statements, opinions and data contained in all publications are solely those of the individual author(s) and contributor(s) and not of MDPI and/or the editor(s). MDPI and/or the editor(s) disclaim responsibility for any injury to people or property resulting from any ideas, methods, instructions or products referred to in the content.

Appendix B - Scientific Articles as Coauthor

Appendix B-1

Title	Development of an early warning system for landslides in the tropical Andes (Medellín; Colombia)				
Journal	Geomechanics and Tunnelling				
DOI	https://doi.org/10.1002/geot.201900071				
Year	2020	Volume	13(1)	Impact Factor (Sep. 2022)	1.0
Accepted	Yes	Position of the candidate in the authors list			5
Authors	Kurosch Thuro, John Singer, Bettina Menschik, Tamara Breuninger, Moritz Gamperl				

This article was published in Geomechanics and Tunnelling; 13(1); Kurosch Thuro, John Singer, Bettina Menschik, Tamara Breuninger, Moritz Gamperl; Development of an early warning system for landslides in the tropical Andes (Medellín; Colombia); Copyright 2020 Ernst & Sohn GmbH. Reproduced with permission.

Development of an early warning system for landslides in the tropical Andes (Medellín; Colombia)

Entwicklung eines Frühwarnsystems für Rutschungen in den tropischen Anden (Medellín, Kolumbien)

The Inform@Risk project aims to develop a cost-effective but sufficiently accurate, easy-to-maintain early warning system (EWS) for informal settlements on the margins of large cities, adapted to tropical climatic conditions in South American mountain regions. This EWS will be implemented on the outskirts of the Bello Oriente district in Medellín. The area is characterized by an elevation of around 2,000 m, a medium slope inclination of 20° to 30° and deeply weathered crystalline rocks, which are particularly sensitive to shallow landslides during heavy precipitation. In addition to the development of a geo-sensor network with complex data integration and real-time evaluation, the main focus of the project is the social integration of the EWS both with the municipal authorities, which are going to take over the system after completion of the three-year project, and with the population living in the settlement. This report describes the project and the specifications of the EWS and presents first results from the field work.

Keywords risk analysis; early warning system; geo-sensor network; shallow slides; process model

1 Background and goals

Early warning of landslide events plays a central role in risk analysis. In the last century, more than half a million families in the tropical Andes region were affected by shallow landslides, mostly caused by heavy rainfall. Especially the region Antioquia with its capital Medellín (2.5 mio. inhabitants in 2017), Colombia, suffered a large number of deaths. Over 200,000 people there currently live in informal settlements exposed to this natural hazard. A comprehensive early warning system would offer a sustainable alternative to the currently costly and hardly feasible resettlement measures of the city administration.

In developing and emerging countries, a correlation between precipitation and the number of events is usually applied for risk analysis and the prediction of landslides. In addition, previous studies for the Medellín region have produced GIS-based susceptibility studies, which will be included in the project. In the presented project Inform@Risk, which is financed by the German Federal Ministry of Education and Research within the framework of the CLIENT II programme, the Leibniz University Hannover (LUH), the German Aerospace Center Oberpfaffenhofen (DLR), the Technical University Deggendorf (THD) and two companies – the firm AlpGeorisk in Unter-

Im Projekt Inform@Risk soll ein kostengünstiges, aber hinreichend genaues, einfach zu wartendes Frühwarnsystem (FWS) für informelle Siedlungen am Rande von Großstädten entwickelt werden, das an tropische Klimabedingungen in Bergregionen des südamerikanischen Raums angepasst ist. Dieses FWS wird am Rand des Stadtteils Bello Oriente in Medellín implementiert. Das Gebiet ist durch eine Höhenlage um 2.000 m, eine mittelsteile Hangneigung von 20° bis 30° und tiefgründig verwitterte Kristallingesteine charakterisiert und ist bei Starkregenfällen besonders anfällig für flachgründige Hangrutschungen. Kernpunkt des Projekts ist neben der Entwicklung eines Geosensornetzwerks mit komplexer Datenintegration und Echtzeit-Auswertung die soziale Integration des FWS sowohl bei den städtischen Behörden als auch bei der ortsansässigen Bevölkerung. Der Beitrag beschreibt das Projekt und die Spezifikationen des zu entwickelnden FWS und stellt erste Ergebnisse aus der Geländearbeit vor.

Stichworte Risikoanalyse; Frühwarnsystem; Geosensornetzwerk; flachgründige Rutschung; Prozessmodell

1 Hintergrund und Ziele

Die Frühwarnung vor Hangbewegungsereignissen nimmt bei der Risikoanalyse einen zentralen Stellenwert ein. Im letzten Jahrhundert war in den tropischen Anden mehr als eine halbe Million Familien von flachgründigen, meist durch Starkregen ausgelösten Rutschungen betroffen. Besonders die Region Antioquia mit ihrer Hauptstadt Medellín (2,5 Mio. Einwohner im Jahr 2017), Kolumbien, erlitt eine große Anzahl von Todesfällen. Dort leben derzeit über 200.000 Menschen in informellen Siedlungen, die dieser Naturgefahr ausgesetzt sind. Ein umfassendes Frühwarnsystem böte eine nachhaltige Alternative zu derzeit aufwändigen und kaum durchzuführenden Umsiedlungsmaßnahmen der Stadtverwaltung.

In Entwicklungs- und Schwellenländern wird für die Risikoanalyse sowie die Vorhersage von Rutschungen meist eine Korrelation zwischen Niederschlag und Ereignisanzahl herangezogen. Zusätzlich wurden in vorhergehenden Studien für die Region Medellín GIS-basierte Suszeptibilitätsstudien erstellt, die in das Projekt einbezogen werden. In dem vorgestellten Projekt Inform@Risk, das durch das Bundesministerium für Bildung und Forschung, Berlin, im Rahmen des CLIENT II Programms finanziert wird, sind neben der Technischen Universität München

schleißheim and the Expert Office for Aerial Image Evaluation and Environmental Issues (SLU) in Munich – are involved in addition to the Technical University Munich (TUM). The cooperation on site is carried out with all responsible municipal authorities and URBAM, a department of the University EAFIT, which is intensively involved in the urban development of Medellín.

TUM and AlpGeorisk are developing a combined, automated system that integrates a monitoring system and a stability analysis model. The intended monitoring system will be assembled from low-cost sensors such as Time Domain Reflectometry sensors, inclination sensors, extensometers and piezometers in order to offer a financially attractive approach to early warning in developing and emerging countries. The current data of the monitoring system will be continuously fed into the process model. Sensitivity analyses on critical parameters such as precipitation and seismicity are carried out in the model. In combination with time series analyses from the data of the monitoring system, threshold values for the critical parameters will be determined as a function of the deformation rates and the stability analysis. The validated model can then be used for forward modelling to estimate the potential effects of heavy precipitation and earthquakes on the stability of the slopes in the Aburra valley (Medellín) (Figure 1).

The combination of a sensor-based early warning system and a combined stability analysis will contribute to the early warning of landslides in the Medellín region, which could also be applied to other areas in the tropical Andes.

2 Task definition in the project Inform@Risk

2.1 Early warning against the background of the risk cycle

The risk of landslides is defined as the product of the hazard and the expected extent of damage [1]. The hazard is defined as the appearance of natural hazards that can cause damage to property and/or personal injury. In addition, both temporal and spatial limitations must be considered in the hazard analysis [2] [3]. Risk analysis is an integral part in the overall concept of the risk cycle. The risk cycle (Figure 2) can be subdivided into four large sub-areas: (1) Event management (immediately after an event), (2) regeneration, (3) risk management, (4) risk prevention (phase before the next event). However, these phases are not to be considered separately from each other but overlap.

The risk analysis is a preliminary analysis for taking preventive measures, including the establishment of early warning systems, process modelling and protective structures. The entire risk analysis is based in particular on the hazard analysis.

In the Medellín and Manazila region, susceptibility analyses have already been carried out with regard to landslides. A GIS based approach was used to analyse the slip

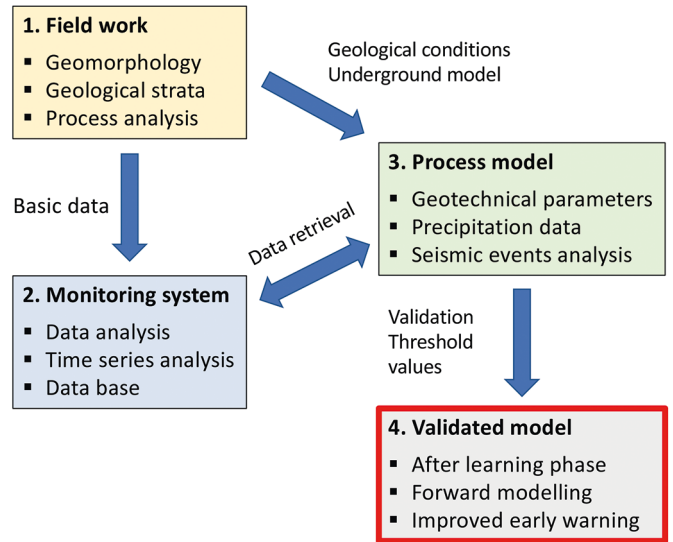


Fig. 1 Strategy of a validated process model for a coupled early warning system in the Medellín region
Strategie eines validierten Prozessmodells für ein gekoppeltes Frühwarnsystem in der Region Medellín

(TUM) die Leibniz Universität Hannover (LUH), das Deutsche Luft- und Raumfahrtzentrum Oberpfaffenhofen (DLR), die Technische Hochschule Deggendorf (THD) und zwei Unternehmen – die Firma AlpGeorisk in Unterschleißheim und das Sachverständigenbüro für Luftbildauswertung und Umweltfragen (SLU) in München – beteiligt. Die Zusammenarbeit vor Ort erfolgt mit allen zuständigen städtischen Behörden und der URBAM, einer Abteilung der Universität EAFIT, die sich intensiv mit der urbanen Entwicklung von Medellín beschäftigt.

TUM und AlpGeorisk entwickeln ein automatisiertes System, das ein Monitoringsystem und ein Modell zur Stabilitätsanalyse kombiniert. Das angestrebte Monitoringsystem soll aus kostengünstigen Sensoren, z. B. Time Domain Reflectometry Sensoren, Neigungssensoren, Extensometern und Piezometern, zusammengestellt werden, um in Entwicklungs- und Schwellenländern einen finanziell attraktiven Ansatz zur Frühwarnung zu bieten. Die aktuellen Daten des Monitoringsystems werden kontinuierlich in das Prozessmodell eingespeist. Im Modell werden Sensitivitätsanalysen zu kritischen Parametern wie Niederschlag und Seismizität durchgeführt. In einer Kombination mit Zeitreihenanalysen aus den Daten des Monitoringsystems werden Schwellenwerte für die kritischen Parameter in Abhängigkeit der Deformationsraten und der Stabilitätsanalyse festgelegt. Das validierte Modell kann anschließend für Vorwärtsmodellierungen genutzt werden, um die potenziellen Auswirkungen von Starkniederschlägen und Erdbeben auf die Stabilität der Hänge im Aburra Tal (Medellín) einschätzen zu können (Bild 1).

Mithilfe der Kombination aus einem Sensor basierten Frühwarnsystem und einer gekoppelten Stabilitätsanalyse soll ein Beitrag zur Frühwarnung für Hangbewegungen in der Region Medellín geleistet werden, der auch in anderen Gebieten der tropischen Anden Anwendung finden könnte.

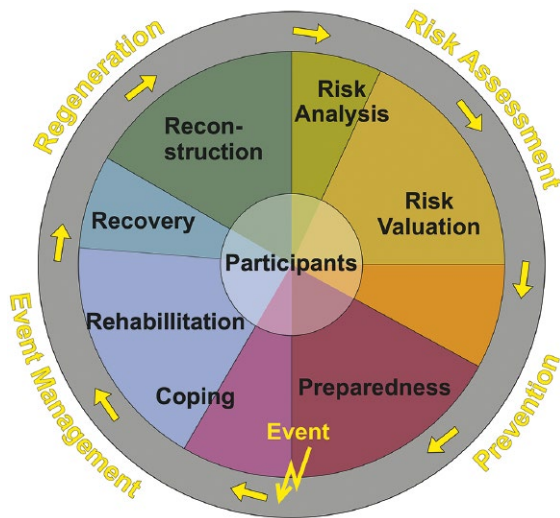


Fig. 2 Risk management cycle for coping with natural hazards and risks, after [3]
 Risikozyklus zur Bewältigung von Naturgefahren und -risiken, nach [3]

susceptibility. By means of sensitivity analyses, the influence of earthquake activity and heavy precipitation on the stability of the slopes was analysed on a regional scale [4] [5]. The results of these GIS analyses contain areal information from which a hazard potential can be derived. Further approaches to improve early warning of landslides in Colombia suggest a modelling of the input parameters of the early warning system, such as heavy precipitation or seismic factors [6].

However, in order to carry out detailed analyses on a local scale and to characterise the influence of external factors (such as heavy precipitation) on landslides and their activity, a process model is required that considers the geological and geomorphological conditions. The stability analysis of a certain landslide can be tied to an early warning system and the influence of sensitive parameters on the limit equilibrium of the landslide can be analysed. The goal is to be able to assess the development of the stability status, i.e. the deformation rates, over time.

Such observations were successfully carried out in Germany, among other countries, on selected case studies using the so-called CHAS model (Combined Stability Hydrology Model), which is based on a limit equilibrium analysis using the lamella method [7]. This is an approach that could also be applied in developing countries, where the damage patterns are often much more serious due to the inadequate building fabric and the population is often not sufficiently informed about the effects of natural hazards. In particular, the slopes above Medellín have been hit by at least three devastating landslides in recent years, destroying more than 300 houses, with 500 casualties in 1987 [8].

2.2 Project area Bello Oriente, Medellín

The selected project area is located in the informal settlement above Bello Oriente in the northeast of the city of

2 Aufgabenstellung im Projekt Inform@Risk

2.1 Frühwarnung vor dem Hintergrund des Risikozyklus

Das Risiko einer Hangbewegung wird definiert als das Produkt aus der Gefährdung und dem erwartenden Schadensausmaß [1]. Die Gefährdung wird als das Auftreten von Naturgefahren, die Sach- und/oder Personenschäden hervorrufen können, definiert. Zusätzlich sind bei der Gefährdungsanalyse sowohl zeitliche als auch räumliche Eingrenzungen zu berücksichtigen [2], [3]. Die Risikoanalyse nimmt im Gesamtkonzept des Risikozyklus einen festen Bestandteil ein. Der Risikozyklus (Bild 2) kann in vier große Teilbereiche untergliedert werden: Event Management (unmittelbar nach einem Event), Regeneration, Risiko Management, Risiko Prävention (Phase vor dem nächsten Event). Diese Phasen sind jedoch nicht getrennt voneinander zu sehen, sondern greifen ineinander.

Die Risikoanalyse gilt als vorbereitende Analyse zur Ergründung präventiver Maßnahmen, zu denen u.a. die Einrichtung von Frühwarnsystemen, Prozessmodellierung und Schutzverbauungen gehören. Die gesamte Risikoanalyse basiert insbesondere auf der Gefährdungsanalyse.

In der Region Medellín und Manazila wurden bereits Suszeptibilitätsanalysen im Hinblick auf Hangbewegungen durchgeführt. Hierbei wurde ein GIS-basierter Ansatz zu Analysen der Rutschanfälligkeit verwendet. Mithilfe von Sensitivitätsanalysen wurde der Einfluss der Erdbebenaktivität bzw. von Starkniederschlägen auf die Stabilität der Hänge in der Fläche auf regionalem Maßstab analysiert [4], [5]. Die Ergebnisse dieser GIS-Analysen enthalten Flächeninformationen, aus denen ein Gefährdungspotenzial abgeleitet werden kann. Weitere Ansätze zur Verbesserung der Frühwarnung vor Hangbewegungen in Kolumbien schlagen eine Modellierung der Eingangsparmeter wie Starkniederschlägen oder seismischen Faktoren vor [6].

Um jedoch Detailanalysen in lokalem Maßstab durchzuführen und den Einfluss äußerer Faktoren (wie Starkniederschläge) auf Hangbewegungen und deren Aktivität zu charakterisieren, ist ein Prozessmodell nötig, das die geologischen und geomorphologischen Gegebenheiten berücksichtigt. Die Stabilitätsbetrachtung einer bestimmten Hangbewegung kann an ein Frühwarnsystem gekoppelt und der Einfluss sensibler Parameter auf das Grenzgleichgewicht der Hangbewegung analysiert werden. Das Ziel ist, die Entwicklung des Stabilitätszustands über die Zeit, d.h. die Deformationsraten, beurteilen zu können.

Derartige Betrachtungen wurden unter anderem in Deutschland an ausgewählten Fallbeispielen erfolgreich unter Verwendung des sogenannten CHAS-Modells (Combined Stability Hydrology Model) durchgeführt, das auf einer Grenzgleichgewichtsanalyse mittels Lamellenverfahren basiert [7]. Es handelt sich um einen Ansatz, der auch in Entwicklungsländern eingesetzt werden könnte, da dort die Schadensbilder aufgrund der ungenü-

Medellín (Figure 3). The selection was made on the basis of its risk exposure in the peripheral location of the city and its loose development with the possibility of establishing an early warning system with the proposed measures. This area is located directly outside the formal urban area of Medellín, so the authorities are not allowed to implement measures with municipal funds. This is where the presented project comes in, with intensive cooperation with the municipal authorities, in particular the disaster protection authority DAGRD and the early warning authority SIATA. In addition, the concept of a “Living Lab” is being pursued, in which all measures, from geological investigations and the layout of the early warning system to the testing and training phase, are intensively discussed and consulted with the local residents. Several meetings and workshops have taken place in the community of Bello Oriente since the beginning of the project in March 2019. These meetings and workshops have been co-designed and accompanied by Non-Governmental Organizations in order to optimally integrate the project into society, raise awareness of natural hazards and, in the event of an early warning, be prepared to get themselves and their relatives to safety without hesitation.

3 Engineering geological investigations

3.1 Geological conditions in the project area

First, the geological basic data, which serve as the basis for the hazard and risk analysis, were researched and compiled. Especially helpful were the extensive docu-

genden Bausubstanz häufig viel gravierender ausfallen und die Bevölkerung oft nicht ausreichend über die Auswirkungen von Naturgefahren informiert ist. Vor allem die Hänge oberhalb von Medellín wurden in den vergangenen Jahren von mindestens drei verheerenden Hangbewegungen heimgesucht, bei denen mehr als 300 Häuser zerstört wurden, beispielsweise im Jahr 1987 mit 500 Toten [8].

2.2 Projektgebiet Bello Oriente, Medellín

Das ausgewählte Projektgebiet befindet sich in der informellen Siedlung oberhalb von Bello Oriente im Nordosten der Stadt Medellín (Bild 3). Die Auswahl erfolgte aufgrund der Risikoexposition in der randlichen Lage zur Stadt und seiner lockeren Bebauung mit der Möglichkeit, mit den ins Auge gefassten Maßnahmen ein Frühwarnsystem zu etablieren. Dieser Bereich gehört nicht mehr zum formellen Stadtgebiet von Medellín, so dass die Behörden keine Maßnahmen mit städtischen Geldern umsetzen dürfen. Hier setzt das vorgestellte Projekt an, wobei eine intensive Zusammenarbeit mit den städtischen Behörden, insbesondere der Katastrophenschutzbehörde DAGRD und der Frühwarnbehörde SIATA erfolgt. Zudem wird hierbei das Konzept des „Living Lab“ verfolgt, bei dem alle Maßnahmen, von den geologischen Untersuchungen über das Layout des Frühwarnsystems bis hin zur Test- und Trainingsphase, mit den Bewohnern vor Ort intensiv diskutiert und abgesprochen werden. Hierzu fanden seit Beginn des Projekts im März 2019 mehrere Treffen und Workshops in Bello Oriente statt, die von Non-Govern-

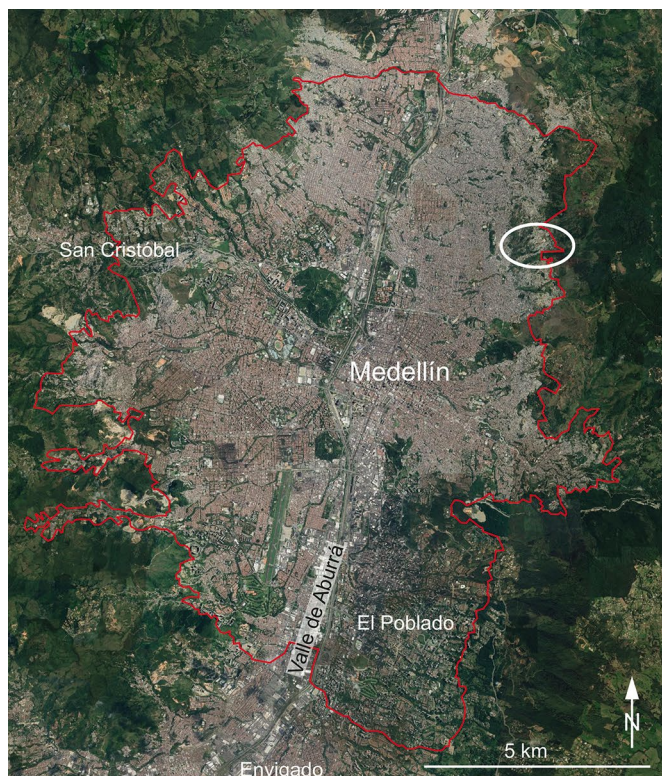


Fig. 3 Location of the project area (oval) in the informal settlement above Bello Oriente, Medellín
Lage des Projektgebiets (Ellipse) in der informellen Siedlung oberhalb von Bello Oriente, Medellín

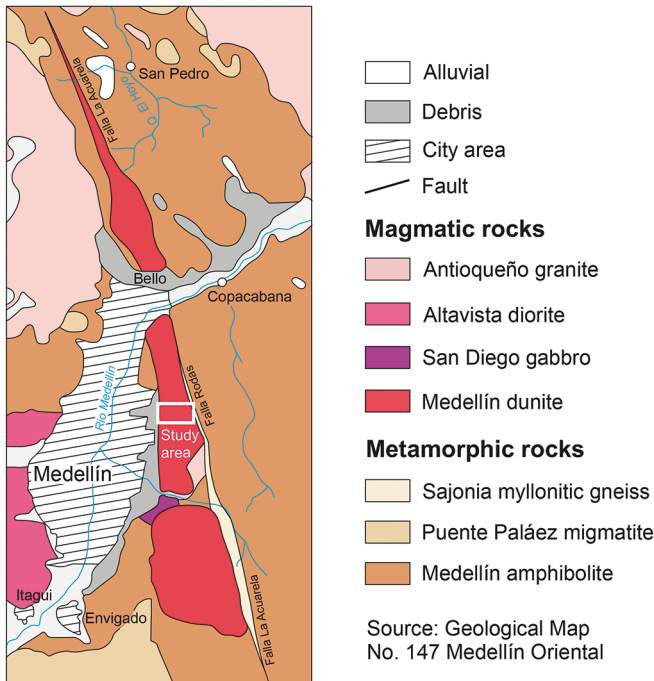


Fig. 4 Geological overview map with study area in Bello Oriente, Medellín
Geologische Übersichtskarte mit Projektgebiet in Bello Oriente, Medellín

ments of the geological service of the city of Medellín, the early warning authority SIATA and the preparatory work of the Institute for Landscape Architecture of the Leibniz University Hannover (LUH) [9] [10]. Based on the already existing data, the area above Bello Oriente was geologically and geomorphologically surveyed in detail. A geological overview map can be found in Figure 4, an overview profile in Figure 5.

In the working area, slopes of $25^\circ \pm 5^\circ$ predominate, which means that the slope is likely to be in an unstable state of equilibrium. The deeper underground consists of dunite, a magmatic rock consisting of approx. 90% olivine and 10% pyroxene, which is extremely susceptible to weathering due to its high iron content and is deeply weathered here as a result of the tropical conditions. Depending on the exposure, the weathering depth is between a few metres and several 10 metres (up to 50 m in the ERT profile of Figure 8). Near the surface, the materi-

mental Organizations mitgestaltet und begleitet wurden, um das Projekt sozial zu integrieren, das Bewusstsein für naturbedingte Gefahren zu wecken und im Fall einer Frühwarnung bereit zu sein, sich und Angehörige ohne Zögern in Sicherheit zu bringen.

3 Ingenieurgeologische Untersuchungen

3.1 Geologische Verhältnisse im Projektareal

Zunächst wurden die geologischen Basisdaten recherchiert und zusammengestellt, die als Grundlage für die Gefahren- und Risikoanalyse dienen. Besonders hilfreich waren die umfangreichen Unterlagen des geologischen Dienstes der Stadt Medellín, der Frühwarnbehörde SIATA und den Vorarbeiten des Instituts für Landschaftsarchitektur der Leibniz Universität Hannover (LUH) [9], [10]. Aufbauend auf den bereits existierenden Daten wurde das Gelände oberhalb Bello Oriente detailliert geologisch und geomorphologisch aufgenommen. Eine Geologische Übersichtskarte befindet sich in Bild 4, ein Übersichtsprofil in Bild 5.

Im Bereich des Arbeitsgebiets herrschen Hangneigungen von $25^\circ \pm 5^\circ$ vor, wodurch der Hang sich grundsätzlich im labilen Grenzgleichgewicht befinden dürfte. Der tiefere Untergrund besteht aus Dunit, einem magmatischen Gestein bestehend aus ca. 90% Olivin und 10% Pyroxenen, das wegen seines hohen Eisenanteils äußerst verwitterungsanfällig und hier durch die tropischen Bedingungen tiefgründig verwittert ist. Die Verwitterungstiefe beträgt je nach Exposition zwischen wenigen Metern und mehreren 10er-Metern (bis zu 50 m im ERT-Profil von Bild 8). Oberflächennah ist das Material durch vorhergehende Hangbewegungen bereits stark durchbewegt und liegt daher in einer Block-in-Matrix Struktur vor (Bild 6). Die Bewegung, die das Material erlitten hat, lässt sich zum einen aufgrund der Oberflächenmorphologie ableiten, die auf intensive flache sowie möglicherweise auch eine tiefergehende, große Rutschung hinweist (siehe Gefahrenkarte Bild 7). Zum anderen zeigt der Rundungsgrad der Blöcke eine gewisse Abhängigkeit von der Entfernung vom Abrissbereich: Nahe an der Abrisskante sind die Blöcke typischerweise noch sehr kantig, mit der Ent-

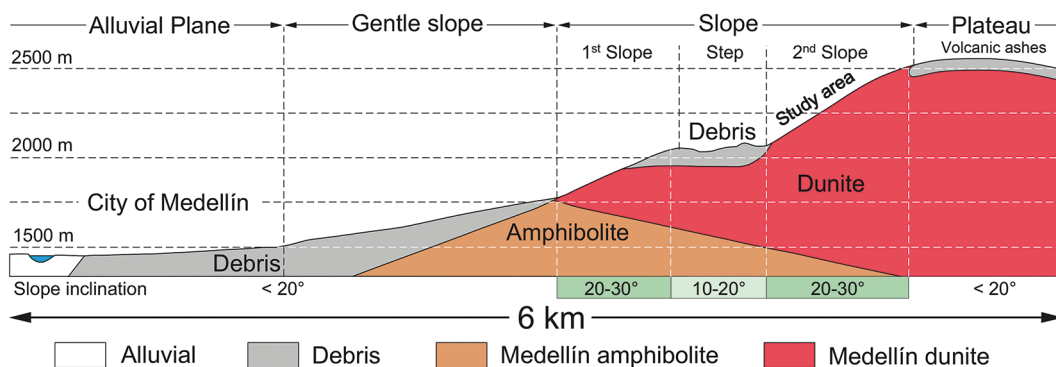


Fig. 5 Geological overview section through framed area in Figure 4; study area is situated on second slope, after [9] altered
Geologisches Übersichtsprofil durch das eingerahmte Gebiet in Bild 4; das Projektgebiet befindet sich in der zweiten Hangstufe, nach [9] verändert



(Photo: Thuro)

Fig. 6 Block-in-matrix structure of the deeply weathered dunite at the toe of a shallow landslide (Scale: person 1.8 m)
Block-in-Matrix-Struktur des tiefgründig verwitterten Dunits an der Stirn einer flachgründigen Rutschung (Maßstab: Person 1,8 m)

al is already strongly moved by previous landslides and is therefore present in a block-in-matrix structure (Figure 6). The movement that the material has undergone can be deduced from the surface morphology, which suggests intense flat and possibly also a deeper, larger landslide (cf. hazard map Figure 7). In addition, the degree of rounding of the blocks shows a certain dependence on the distance from the detachment area: Close to the detachment edge the blocks are typically still very angular,

fernung von der Abrisskante sind die Blöcke deutlich stärker gerundet und deutlicher verwittert.

3.2 Erstellung einer Gefahrenkarte

Die Ergebnisse der ingenieurgeologischen Kartierung sind in Bild 7 dargestellt. Diese müssen jedoch noch nach einem Waldbrand ergänzt werden, der in einem stark bewachsenen Bereich im oberen Hangbereich neue Details zur Geomorphologie sichtbar gemacht hat. Hierzu wird eine Drohnenbefliegung durchgeführt, deren Ergebnisse danach in die Gefahrenkarte eingearbeitet werden müssen. Bei dieser Befliegung soll ein genaueres digitales Höhenmodell erarbeitet und ein Orthofoto hoher Auflösung erstellt werden, das als Grundlage für eine Interpretation der Hangbewegungsmorphologie in diesem Bereich verwendet werden kann. Das Projektgebiet ist von einer Vielzahl von flachgründigen (< 10 m Tiefe) rotationalen Rutschungen geprägt. Die Alter belaufen sich auf sehr rezente (die letzte Rutschung war 2017) über ca. 100 Jahre alte (lt. örtlichen Aufzeichnungen) bis hin zu mehreren 100 Jahre alte Rutschungen. Ältere Rutschungsereignisse sind im Arbeitsgebiet geomorphologisch nicht differenzierbar. Zwar wird in Medellín seit ca. 1920 ein Ereigniskataster geführt, die weiter vom Stadtzentrum entfernten Hangbewegungen wurden anfangs jedoch nicht erfasst [9], [10], so dass über Jährlichkeiten im Projektgebiet keine Aussagen getroffen werden können. Obwohl einige tiefer eingeschnittene Bachläufe existieren,

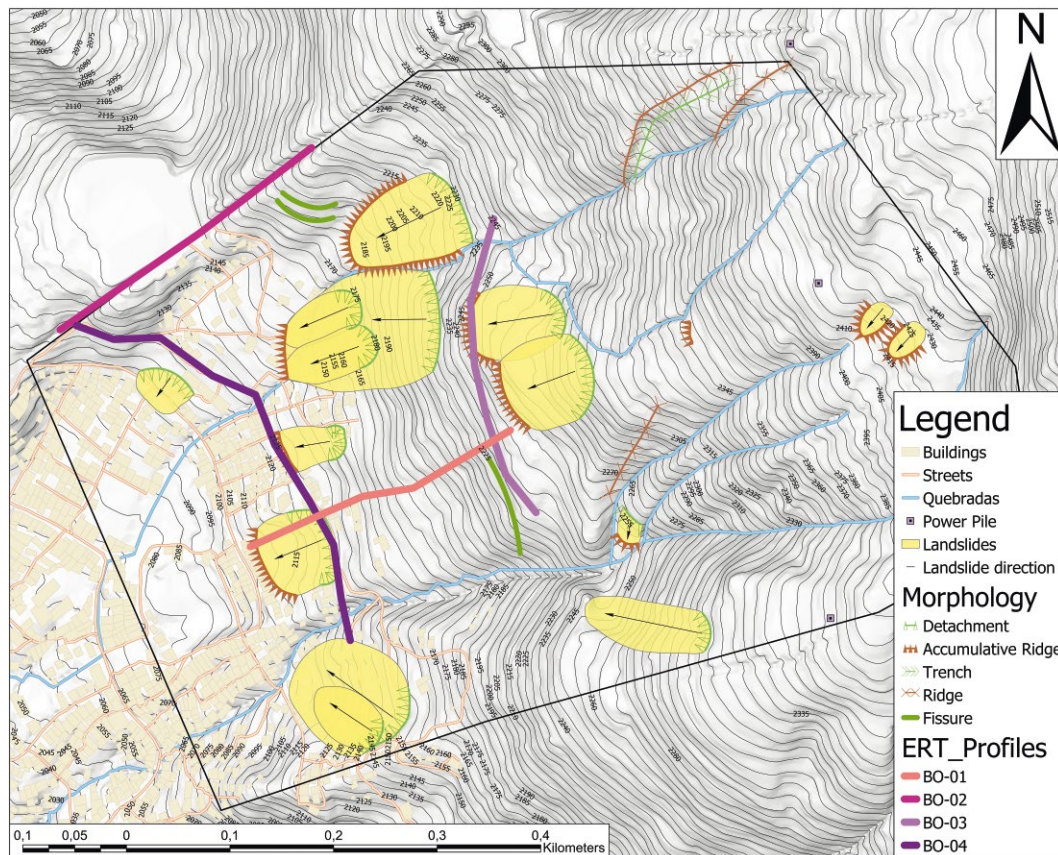


Fig. 7 Hazard map of Bello Oriente with positions of ERT sections (Basis: DEM by the City of Medellín)
Gefahrenkarte von Bello Oriente mit Lage der ERT-Profilen (Basis: DHM der Stadt Medellín)

with the distance from the detachment edge the blocks are much more rounded and more weathered.

3.2 Development of a hazard map

The results of the engineering geological mapping are shown in Figure 7. However, they still have to be updated after a forest fire, which has made visible new details on geomorphology in a heavily overgrown area in the upper slope area. For this purpose, a drone survey will be carried out, the results of which will then have to be incorporated into the hazard map. In this survey, a more accurate digital elevation model will be developed, and a high-resolution aerial photograph will be produced, which can be used as the basis for an interpretation of the landslide morphology in this area. The project area is characterized by a large number of shallow (< 10 m depth) rotational landslides. The ages stretch from very recent (the last slide was in 2017) over approx. 100 year old (according to local records) up to several 100 year old slides. Older landslides cannot be differentiated geomorphologically in the working area. Although an event register has been kept in Medellín since about 1920, the landslides further away from the city centre were not initially recorded [9] [10], so that no statements can be made about annualities in the project area. Although some more deeply cut creeks exist, no debris flow channels could be identified so far. Rockfall occurs subordinately in the marginal areas of the study site, where rock ridges of dunite are present.

In the upper, steeper area of the study site there are only very local, small-scale landslides; the weathered rock is close to the surface. Most of the material seems to have already been transported to the flatter part of the slope by many smaller landslides or possibly even by a very large, deep landslide. In the upper part of the slope there is also the possibility of smaller rock falls. Due to the dense vegetation, however, the fall range should be limited. Further analyses by means of rockfall modelling are planned in the course of the project.

3.3 Geophysical investigations

A total of four ERT (Electrical Resistivity Tomography) profiles were measured in a Wenner electrode array prior to a drilling campaign planned for spring 2020. A characteristic profile is shown in Figure 8. The geoelectrics used here to trace differences in water content clearly trace the block-in-matrix structure and show that the bedrock can be up to 50 m deep. This could either be due to the fact that the deeply weathered dunite has been rearranged by equally deep slope movements as soil material with blocks or that the deeply weathered dunite is generally creeping. In order to investigate this further, further ERT transects are planned, as well as key boreholes are to make it possible to calibrate the ERT profiles in spring 2020. The boreholes are to be equipped with inclinometer tubes and cables for Continuous Shear Monitoring on

konnten bisher keine Murkanäle identifiziert werden. Steinschlag kommt untergeordnet in den randlichen Bereichen des Gebiets vor, wo Felsrippen aus Dunit anstehen.

Im oberen, steileren Bereich des Arbeitsgebiets befinden sich nur sehr lokal kleinräumige Rutschungen; dafür steht der verwitterte Fels oberflächennah an. Das meiste Material scheint hier bereits durch viele kleinere Hangbewegungen oder möglicherweise sogar durch eine sehr große, tiefgründige Hangbewegung in den flacheren Bereich des Hangs transportiert worden zu sein. Auch im oberen Hangbereich besteht grundsätzlich die Möglichkeit kleinerer Steinschläge. Durch die dichte Vegetation dürfte die Reichweite aber beschränkt sein. Weitergehende Analysen mittels Steinschlagmodellierung sind im Verlauf des Projekts geplant.

3.3 Geophysikalische Untersuchungen

Vor der Durchführung einer Bohrkampagne, die im Frühjahr 2020 geplant ist, wurden insgesamt vier ERT (Electrical Resistivity Tomography) Profile in Wenner-Anordnung der Elektroden gemessen. Ein charakteristisches Profil ist exemplarisch in Bild 8 dargestellt. Die Geoelektrik, mit der hier Wassergehalts-Unterschiede erfasst werden, zeichnet deutlich die Block-in-Matrix-Struktur nach und zeigt, dass der Untergrund bis zu 50 m tief aufgelockert vorliegen kann. Dies könnte entweder daran liegen, dass der tiefgründig verwitterte Dunit durch gleichermaßen tiefgründige Hangbewegungen als Lockergestein mit Blöcken umgelagert wurde oder dass sich der tiefgründig verwitterte Dunit grundsätzlich im Kriechen befindet. Um dies weiter zu erkunden, sind zum einen weitere ERT-Transsekte geplant, zum anderen sollen Schlüsselbohrungen im Frühjahr 2020 die Kalibrierung der ERT-Profilen ermöglichen. Die Bohrlöcher sollen mit Inclinometerrohren und Kabel für Continuous Shear Monitoring auf TDR-Basis (Time Domain Reflectometry) [11] ausgestattet werden, um langfristige Messungen der Bewegungen bis in ca. 50 m Tiefe zu erlauben. Die geoelektrischen Profile sollen im Laufe des Projekts noch mit seismischen Profilen seitens des Geologischen Dienstes der Stadt Medellín ergänzt werden.

4 Entwicklung eines Frühwarnsystems für Rutschungen

4.1 Konzeption des Frühwarnsystems

Als Hauptaufgabe einer Frühwarnung wurde die Vorhersage flachgründiger Rutschungen identifiziert, die der Beobachtung nach typischerweise von Starkregenereignissen ausgelöst werden. Diese können zeitweise und lokal bis mehrere 10er-mm/h bzw. > 100 mm/d erreichen. Der jährliche Niederschlag ist mit ca. 1.600 bis 1.700 mm nicht ausgesprochen hoch, fällt jedoch verstärkt in den Regenzeiten von April bis Juni und September bis No-

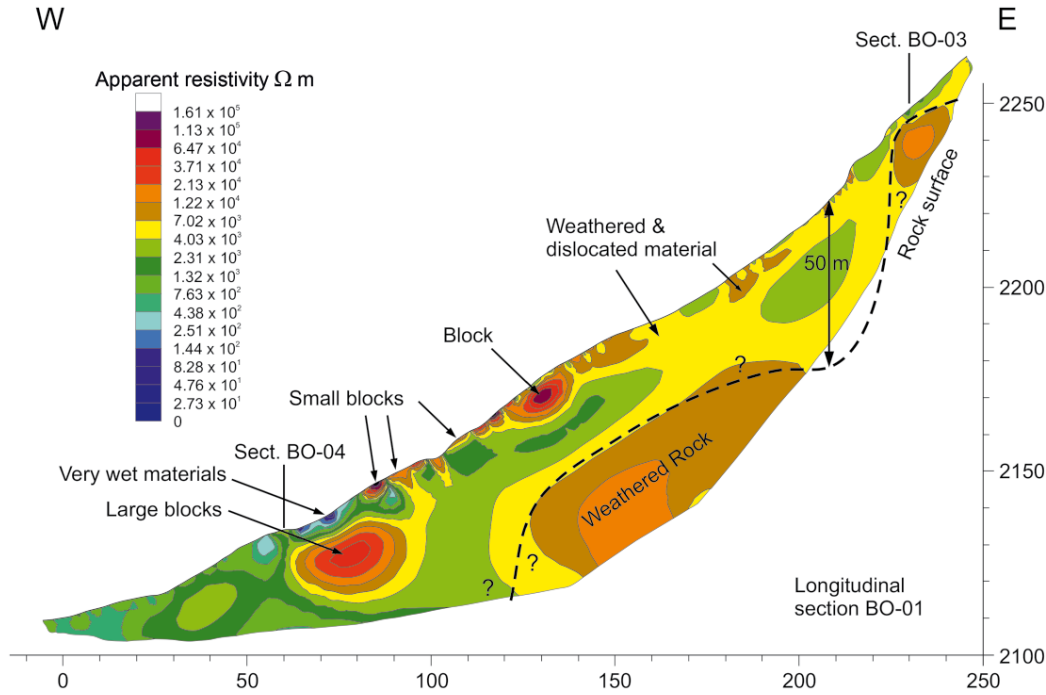


Fig. 8 Longitudinal ERT section with interpretation of structures (blue: low resistivity; green/yellow: medium; brown/red: high)
ERT-Längsprofil mit Interpretation der Strukturen (blaue Farben: geringe, grün/gelb mittlere; braun/rot: hohe Widerstände).

TDR basis (Time Domain Reflectometry) [11] in order to allow long-term measurements of the movements down to a depth of approx. 50 m. During the project, the geoelectric profiles will be supplemented with seismic profiles from the Geological Service of the City of Medellín.

4 Development of an early warning system for landslides

4.1 Design of the early warning system

The prediction of shallow landslides, which are typically caused by heavy rainfall events, was identified as the main task of the early warning system. These can reach temporarily and locally up to several 10 mm/h or > 100 mm/d. The annual rainfall of approx. 1,600 to 1,700 mm is not particularly high, but it falls mostly during the rainy seasons from April to June and September to November. In addition, seismic triggering is possible, for which data from the earthquake service are to be integrated into the early warning system.

The basic idea is to predict the behaviour of the investigated area at risk of sliding on the basis of detailed geotechnical models calibrated with results from geotechnical laboratory tests and a dense geosensor network. Preliminary work already exists in the form of a series of projects in the Alps [12] [13]. By including the triggering process in the consideration (e.g. intensive precipitation leading to high groundwater levels) it is possible to give first general notifications a few days to hours before a critical phase concerning the stability of the slope. If the onset of slow but increasing movements is detected, spatially precise (evacuation) alarms can probably be issued

in advance. Daneben ist eine seismische Auslösung möglich; daher sollen auch die Daten des Erdbebendienstes in das Frühwarnsystem integriert werden.

Die grundsätzliche Idee ist es, das Verhalten des untersuchten rutschungsgefährdeten Gebiets auf der Grundlage detaillierter geotechnischer Modelle vorhersagen zu können, die mit Ergebnissen aus geotechnischen Laborversuchen und einem dichten Geosensornetz kalibriert wurden. Vorarbeiten hierzu existieren bereits in Form von einer Reihe von Projekten in den Alpen [12], [13]. Durch die Einbeziehung des Auslösevorgangs in die Betrachtung (z.B. intensive Niederschläge, die zu hohen Grundwasserständen führen) ist es möglich, erste allgemeine Benachrichtigungen einige Tage bis Stunden vor einer kritischen Phase bezüglich der Stabilität des Hangs zu erteilen. Wenn der Beginn langsamer, aber zunehmender Bewegungen erkannt wird, können räumlich präzise (Evakuierungs-) Alarmer wahrscheinlich Stunden bis zumindest Minuten vor dem Ereignis ausgegeben werden. Dabei ist zu beachten, dass Rutschereignisse, die durch Erdbeben ausgelöst werden, von diesem System naturgemäß nicht vorhergesagt werden können.

Basierend auf den geologischen Untersuchungen werden die erforderlichen Beobachtungsziele und genauen Systemeigenschaften (z.B. räumliche und zeitliche Auflösung) des Geosensor-Netzwerkes definiert. Das Geosensornetz soll dann potenziell auftretende Rutschungen im Projektgebiet zuverlässig erkennen. Basierend auf dem aktuellen Verständnis wurden folgende vorläufige Beobachtungsziele definiert:

- Deformationsmessungen an der Oberfläche (relativ oder absolut, z. B. Neigung, Rissöffnung, Dehnungen)

hours to at least minutes before the event. It should be noted that slides triggered by earthquakes cannot naturally be predicted by this system.

Based on the geological investigations, the required observation targets and precise system properties (e.g. spatial and temporal resolution) of the geosensor network are defined. The geosensor network should then reliably detect potential landslides in the project area. Based on the current understanding, the following preliminary observation objectives were defined:

- Deformation measurements on the surface (relative or absolute, e.g. inclination, crack opening, elongation) with a spatial density of ideally one measurement per 100 to 1,600 m² (10 m×10 m to 40 m×40 m) and mm accuracy, whereby the spatial density of the sensors is determined on the basis of the previously performed detailed hazard and risk assessment. This should enable the area-wide detection of slow slope movements, which will presumably precede a major event, as far as possible.
- Deformation measurements at depth in the places where a landslide is most likely to occur, in order to assess the depth of the glide surface.
- Hydrogeological monitoring of the groundwater level in the main hydrogeological units to characterize the groundwater flow.
- Local and regional, ideally spatially distributed meteorological observations (e.g. rain radar) to estimate precipitation in the catchment area of the site.
- As far as reasonable and possible, additional geotechnical observations should be included, which could indicate an incipient landslide (e.g. increase in earth pressure behind retaining walls and other structures).

Further requirements on the system are high cost-effectiveness, easy handling and low maintenance work and costs. Ideally, the system should be maintainable by the residents themselves with occasional assistance from local authorities.

4.2 Geosensor Network

A first draft of the layout of a geosensor net that would meet most of the above requirements is shown in Figure 9. The main components consist of the Continuous Shear Monitor (CSM), wire extensometers and other state-of-the-art deformation and geotechnical sensors connected via the “LoRa” (long range) communication infrastructure, a LPWA – low power wide area network protocol.

4.2.1 Continuous Shear Monitor

The CSM is a special development of the Time Domain Reflectometry (TDR) technology for geotechnical applications [11] [12]. TDR is an electrotechnical measuring technique developed in the 1960s for localizing cable faults

mit einer räumlichen Dichte von idealerweise einer Messung pro 100 bis 1.600 m² (10 m×10 m bis 40 m×40 m) und mm-Genauigkeit, wobei die räumliche Dichte der Sensoren anhand der zuvor durchgeführten detaillierten Gefahren- bzw. Risikobewertung festgelegt wird. Dies soll eine möglichst flächendeckende Erkennung von langsamen Hangbewegungen, die voraussichtlich einem größeren Ereignis vorausgehen werden, ermöglichen.

- Deformationsmessungen in der Tiefe an den Orten, wo eine Rutschung am wahrscheinlichsten erscheint, zur Beurteilung der Tiefenlage der Gleitfläche.
- Hydrogeologisches Monitoring des Grundwasserspiegels in den wichtigsten hydrogeologischen Einheiten zur Charakterisierung der Grundwasserströmung.
- Lokale und regionale, idealerweise räumlich verteilte meteorologische Beobachtungen (z.B. Regenradar) zur Abschätzung der Niederschläge im Einzugsgebiet des Standorts.
- Soweit sinnvoll und möglich, sollten zusätzliche geotechnische Beobachtungen, die auf eine beginnende Rutschung hinweisen könnten (z.B. Anstieg des Erd-drucks hinter Rückhaltewänden und anderen Bauwerken), einbezogen werden.

Weitere Anforderungen an das System sind eine hohe Wirtschaftlichkeit, einfache Handhabung sowie geringe Wartungsarbeiten und -kosten. Im Idealfall soll das System von den Bewohnern selbst mit gelegentlicher Unterstützung der örtlichen Behörden gewartet werden können.

4.2 Geosensor-Netzwerk

Ein erster Entwurf des Layouts eines Geosensornetzes, das die meisten der oben genannten Anforderungen erfüllen würde, ist in Bild 9 dargestellt. Die Hauptkomponenten bestehen aus dem Continuous Shear Monitor (CSM), Drahtextensometern und anderen dem Stand der Technik entsprechenden Deformations- und geotechnischen Sensoren, die über eine Long Range Kommunikationsinfrastruktur (LoRa), einem LPWA (low power wide area) Netzwerkprotokoll, miteinander verbunden sind.

4.2.1 Continuous Shear Monitor

Der CSM ist eine spezielle Entwicklung der Time Domain Reflectometry (TDR) Technologie für geotechnische Anwendungen [11], [12]. TDR ist eine in den 1960er-Jahren entwickelte elektrotechnische Messtechnik zur Lokalisierung von Kabelfehlern und -brüchen in Koaxialkabeln (im deutschsprachigen Raum oft als „Kabelradar“ bezeichnet). Mit der CSM-Methode, die neben der Messtechnik Verfahren zur Kabelinstallation und Signalverarbeitung beinhaltet, können Scherverformungen (Verformungen senkrecht zur Mess- oder Kabelachse) entlang eines Messkabels überwacht werden. Daher eignet sich das Verfahren besonders für die Deformationsüberwachung bei Rutschungen und Damnbrüchen.

and breaks in coaxial cables (often referred to as “cable radar” in German-speaking countries). Using the CSM method, which includes in addition to measurement technology methods for cable installation and signal processing, shear deformations (deformations perpendicular to the measurement or cable axis) along a measurement cable can be monitored. Therefore, the method is particularly suitable for deformation monitoring in the case of tailings and dam fractures.

The TDR measuring device investigates the characteristic impedance (wave impedance) of a coaxial cable. Short voltage pulses of a few milliseconds duration with an extremely sharp signal edge are fed into the coaxial measurement cable. These signals then propagate through the cable until they are partially or completely reflected at the cable end or in the event of a fault in the cable. The reflections are recorded by the TDR device and compared with the output signal.

If a reflection occurs, the distance to the measuring instrument can be determined by its transit time, since the measurement signals propagate in a coaxial cable at constant speed. By analyzing the signals caused by the cable deformation, information about the extent and type of deformation can be obtained [14].

4.2.2 LoRa sensor nodes

To fulfill the low-cost/open-source approach of the project, sensor nodes are developed that are easily reproducible according to the instructions published on the project website. The nodes represent point measurements in the areas between the horizontal CSM measurements. The sensor nodes will be based on an Arduino system (Arduino MKR WAN 1310). The software is written on the Arduino development environment, which is based on the C programming language. The nodes communicate with the control panels via the LoRaWAN communication protocol [15].

Depending on the type of sensors required, each node is manufactured individually, e.g. with a 4-channel 16-bit A/D converter for connecting high-precision sensors such as piezometers or crack detectors (4 to 20 mA signal). Each node is equipped with a MEMS accelerometer, a magnetometer and a gyroscope to perform inclination and acceleration measurements (e.g. on walls or other structural parts that move when a slip occurs). The costs for a single sensor node including power supply via standard AA batteries or rechargeable batteries/solar panels are between 100 and 200 €, depending on the equipment. For battery operation, a runtime of at least one year per battery set is targeted.

Once the geosensor network has been established as part of this project, the aim is to publish the hardware and software of the sensor nodes so that communities in affected areas can build their own sensor nodes and inte-

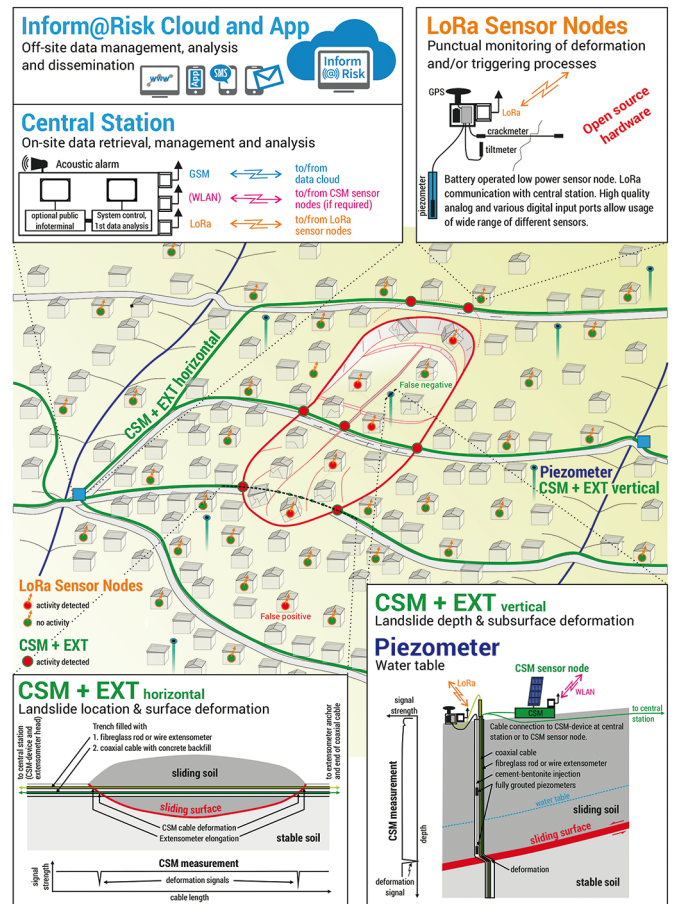


Fig. 9 Schematic layout of the proposed landslide early warning system for informal settlements; red dots: sensor detects activity; green dot: no activity detected
Schematischer Aufbau des vorgeschlagenen Frühwarnsystems für Rutschungen in informellen Siedlungen, rote Punkte: Sensor misst gerade Aktivität; grüne Punkte: Sensor zeigt keine Aktivität

Das TDR-Messgerät untersucht die charakteristische Impedanz (Wellenimpedanz) eines Koaxialkabels. Dazu werden kurze Spannungsimpulse von wenigen Millisekunden Dauer mit einer extrem scharfen Signalfanke in das Koaxialmesskabel eingespeist. Diese Signale breiten sich dann durch das Kabel aus, bis sie am Kabelende oder bei einem Fehler im Kabel teilweise oder vollständig reflektiert werden. Die Reflexionen werden vom TDR-Gerät aufgezeichnet und mit dem Ausgangssignal verglichen.

Tritt eine Reflexion auf, kann der Abstand zum Messgerät über seine Laufzeit (Zeit zwischen Aussendung des Messsignals und Empfang der Reflexion) bestimmt werden, da sich die Messsignale in einem Koaxialkabel mit konstanter Geschwindigkeit ausbreiten. Durch die Analyse der durch die Kabelverformung verursachten Signale können Informationen über den Umfang und die Art der Verformung gewonnen werden [14].

4.2.2 LoRa Sensorknoten

Um den Low-Cost/Open-Source-Ansatz des Projekts zu erfüllen, werden Sensorknoten entwickelt, die gemäß den auf der Projektseite veröffentlichten Anweisungen leicht

grate them into an existing sensor network if there is a LoRa gateway nearby.

4.3 Layout of the early warning system

The system is mainly based on the spatially high-resolution measurements of the Continuous Shear Monitor (CSM) and geotechnical and deformation sensors, which are distributed over the entire project area. The CSM system can locate and record shear deformations along coaxial cables laid in trenches. In order to measure large deformations up to 1 m, wire extensometers are installed parallel to the CSM measurements. The communication within the geosensor network is implemented by LoRa technology. The deformations in a potential sliding surface are measured with CSM, groundwater levels and pressures are measured by means of fully injected piezometers in the boreholes [16]. With this system, both the movement pattern and the trigger mechanism (pore water pressure) are continuously recorded and monitored.

The development of an exact measuring concept, in which the positioning of each sensor is determined and documented on the basis of the existing information, including the expected slope movement process, the geology, the existing infrastructure or building substance and any interference influences, is of decisive importance. Only in this way it can be ensured that the recorded measurement data contain the information necessary for later evaluation.

All data is transferred to the local head office and to the Inform@Risk cloud, where the data is analyzed. In addition, real-time rain radar data provided by the Medellín SIATA Early Warning Authority will be integrated into the central system. Only if several sensors give alarms, an early warning is issued. For example, the red dots in Figure 9 represent sensors that indicate activity, green dots do not measure activity. From the arrangement and type of nodes as well as the associated measured values, conclusions can be drawn about the geometry and motion sequence as well as the mechanism of a slide and a warning can be issued. In the learning and test phase, this is not initially done automatically, but by a processing person. After the training phase, it is planned to hand over the system to the local SIATA early warning authority and to operate it fully automatically.

5 Outlook

It is planned to start drilling for further underground exploration in spring 2020 and to measure further ERT profiles. On the basis of the exploratory boreholes, which will be up to 50 m deep, the engineering geological model is to be refined and the final layout of the early warning system determined. Inclinator tubes, CSM and fully injected piezometers are already being installed in the boreholes. In autumn and winter of 2020, the early warning system de-

reproduzierbar sind. Die Knoten stellen Punktmessungen in den Bereichen zwischen den horizontalen CSM-Messungen dar. Die Sensorknoten werden auf Basis eines Arduino-Systems (Arduino MKR WAN 1310) gebaut. Die Software ist auf der Entwicklungsumgebung Arduino geschrieben, die auf der Programmiersprache C basiert. Die Knoten kommunizieren mit den Zentralen über das LoRaWAN-Kommunikationsprotokoll [15].

Je nach Art der benötigten Sensoren wird jeder Knoten individuell gefertigt, z. B. mit einem 4-Kanal 16-Bit A/D-Wandler zum Anschluss von hochpräzisen Sensoren wie Piezometern oder Rissmessgeräten (4 bis 20 mA Signal). Jeder Knoten ist mit einem MEMS-Beschleunigungssensor, einem Magnetometer und einem Gyroskop ausgestattet, um Neigungs- und Beschleunigungsmessungen durchzuführen (z. B. an Wänden oder anderen Bauwerksteilen, die sich bewegen, wenn eine Rutschung eintritt). Die Kosten für einen einzelnen Sensorknoten inkl. Stromversorgung via Standard AA-Batterien oder Akkus/Solarpanel liegen je nach Ausstattung zwischen 100 und 200 €. Bei Batteriebetrieb wird eine Laufzeit von mindestens einem Jahr je Batteriesatz angestrebt.

Nach dem Aufbau des Geosensornetzwerks im Rahmen dieses Projekts ist es das Ziel, die Hard- und Software der Sensorknoten zu veröffentlichen, so dass Gemeinden in betroffenen Gebieten ihre eigenen Sensorknoten bauen und in ein bestehendes Sensornetzwerk einbinden können, sofern es ein LoRa-Gateway in der Nähe gibt.

4.3 Layout des Frühwarnsystems

Das System stützt sich hauptsächlich auf die räumlich hochaufgelösten Messungen des Continuous Shear Monitors (CSM) sowie geotechnische und Deformationssensoren, die über das gesamte Projektgebiet verteilt sind. Das CSM-System kann Scherverformungen entlang von Koaxialkabeln, die in Gräben verlegt sind, lokalisieren und aufzeichnen. Um große Verformungen bis zu 1 m messen zu können, werden parallel zu den CSM-Messungen Drahtextensometer installiert. Die Kommunikation innerhalb des Geosensornetzwerks wird durch LoRa-Technologie umgesetzt. Die Deformationen in einer potenziellen Gleitfläche werden mit CSM, Grundwasserstände bzw. -drücke mittels vollständig injizierter Piezometer in den Bohrungen gemessen [16]. Mit diesem System werden damit sowohl das Bewegungsmuster als auch der Auslösemechanismus (Porenwasserdruck) kontinuierlich aufgezeichnet und überwacht.

Von entscheidender Bedeutung ist dabei die Entwicklung eines genauen Messkonzepts, in dem basierend auf den vorhandenen Informationen u. a. zu dem erwarteten Hangbewegungsprozess, der Geologie, der vorhandenen Infrastruktur bzw. Bausubstanz und ggf. vorhandener Störeinflüsse die Positionierung jedes Sensors bestimmt und dokumentiert wird. Nur so kann sichergestellt werden, dass die erfassten Messdaten, die für eine spätere Bewertung notwendigen Informationen enthalten.

scribed above will be expanded to include further boreholes, the laying of horizontal CSM cables and the measurement phase. The learning and training phase will follow in 2021, with the system finally being handed over to the city of Medellín at the end of winter 2021/22.

Acknowledgements

The project is funded by the German Federal Ministry of Education and Research as part of the Client II programme under funding code 03G0883C, which promotes international partnerships in science and research. We would like to thank Dr. Susanne Fretzdorff, of the project-executing agency Jülich, for her financial support and supervision.

References

- [1] Bundesamt für Raumplanung BRP, Bundesamt für Wasserwirtschaft BWW, Bundesamt für Umwelt, Wald und Landschaft BUWAL [eds.] (1997): *Berücksichtigung der Massenbewegungsgefahren bei raumwirksamen Tätigkeiten, Empfehlung*. Bern.
- [2] Raetz, H.; Latelin, O.; Bollinger, B.; Tripet, J.P. (2002) *Hazard assessment in Switzerland – Codes of Practice for mass movements*. Bull. Eng. Geol. Env., pp. 263–268.
- [3] Kienholz, H.; Krummenacher, B.; Kipfer, A.; Perret, S. (2004) *Aspects of integral Risk Management in Practice – considerations with respect to mountain hazards in Switzerland*. Österr. Wasser- und Abfallwirtschaft, No. 3–4, pp. 43–50.
- [4] Hidalgo, C.A.; Vega, J. (2015) *Risk Estimation in Urban Buildings by Landslides Triggered by Earthquakes and Rainfall (Medellín-Colombia)*. XV Panamerican Conference on Soil Mechanics and Geotechnical Engineering, Buenos Aires, Vol. 1.
- [5] van Westen, C.J.; Terlien, M.T.J. (1996) *An approach towards deterministic landslide hazard analysis in GIS. A case study from Manizales (Colombia)*. Earth surface and landforms 21, pp. 853–868.
- [6] Huggel, C.; Khabarov, N.; Obersteiner, M.; Ramírez, J.M. (2010) *Implementation and integrated numerical modeling of a landslide early warning system: a pilot study in Colombia*. Natural Hazards 52, No. 2, pp. 501–518.
- [7] Thiebes, B.; Bell, R.; Glade, T.; Jäger, S.; Mayer, J.; Anderson, M.; Holcombe, L. (2014) *Integration of a limit-equilibrium model into a landslide early warning system*. Landslides 11, No. 5, pp. 859–875.
- [8] Ojeda, J.; Donnelly, L. (2006) *Landslides in Colombia and their impact on towns and cities*. 10th IAEG Congress 2006, Nottingham, paper no. 112,
- [9] Werthmann, C.; Echeverri, A.; Vélez, A.E. [eds.] (2012) *Rehabitar La Ladera: Shifting Ground*. Medellín: Universidad EAFIT.
- [10] Werthmann, C.; Echeverri, A. [Hrsg.] (2013) *Rehabitar La Montaña: Estrategias y procesos para un hábitat sostenible en las laderas de Medellín*. Medellín: Universidad EAFIT.
- [11] Singer, J.; Thuro, K.; Sambeth, U. (2006) *Development of a continuous 3D-monitoring system for unstable slopes using time domain reflectometry*. Felsbau 24, pp. 16–23.
- [12] Thuro, K.; Singer, J.; Festl, J.; Wunderlich, T.; Wasmeier, P.; Reith, C.; Heunecke, O.; Glabsch, J.; Schuhbäck, O. (2014)

Alle Daten werden an die Zentrale vor Ort und in die Inform@Risk Cloud übertragen, wo die Daten analysiert werden. Zusätzlich werden die Daten des Echtzeit-Regenradars, das durch die Frühwarnbehörde der Stadt Medellín SIATA zur Verfügung gestellt wird, im zentralen System integriert. Erst wenn mehrere Sensoren Alarme geben, wird eine Frühwarnung ausgegeben. Beispielsweise stellen die roten Punkte in Bild 9 Sensoren dar, die eine Aktivität anzeigen, grüne Punkte messen keine Aktivität. Aus der Anordnung und der Art der Knoten sowie den zugehörigen Messwerten lassen sich Rückschlüsse auf Geometrie und Bewegungsablauf sowie den Mechanismus einer Rutschung ermitteln und eine Warnung ausgeben. Diese erfolgt in der Lern- und Testphase zunächst nicht automatisch, sondern durch eine bearbeitende Person. Nach der Trainingsphase ist angedacht, das System der lokalen Frühwarnbehörde SIATA zu übergeben und vollautomatisch zu betreiben.

5 Ausblick

Es ist geplant, im Frühjahr 2020 mit den Bohrarbeiten zur weiteren Untergrunderkundung zu beginnen und weitere ERT-Profile zu messen. Auf der Basis der bis zu etwa 50 m tiefen Erkundungsbohrungen soll das ingenieurgeologische Modell verfeinert und das endgültige Layout des Frühwarnsystems festgelegt werden. In die Bohrungen werden bereits Inklinometerrohre, CSM und voll injizierte Piezometer eingebaut. Im Herbst und Winter 2020 erfolgt dann der Ausbau des beschriebenen Frühwarnsystems mit weiteren Bohrungen, der Verlegung der horizontalen CSM Kabel und die Messphase. Die Lern- und Trainingsphase schließt sich im Jahr 2021 an, um das System Ende Winter 2021/22 schließlich der Stadt Medellín zu übergeben.

Danksagung

Das Projekt wird vom Deutschen Bundesministerium für Bildung und Forschung im Rahmen des Programms “Client II” unter dem Förderkennzeichen 03G0883C gefördert, einer Förderung internationaler Partnerschaften in Wissenschaft und Forschung. Wir bedanken uns für die finanzielle Unterstützung und Betreuung, insbesondere bei Frau Dr. Susanne Fretzdorff, beim Projektträger Jülich.

Low cost 3D early warning system for alpine instable slopes: the Aggenalm Landslide monitoring system. In: Wenzel, Zschau [eds.]: Early warning for geological disasters. Scientific methods and current practice. Advanced Technologies in Earth Sciences. Heidelberg, New York, etc.: Springer, pp. 289–306.

- [13] Zangerl, C.; Eberhardt, E.; Perzmaier, S. (2010) *Kinematic behaviour and velocity characteristics of a complex deep-seated crystalline rockslide in relation to its interaction with a dam reservoir*. Engineering Geology 112, pp. 53–67.

- [14] Singer, J. (2010) *Development of a Continuous Monitoring System for Instable Slopes Using Time Domain Reflectometry*. Dissertation TU München.
- [15] LoRa Alliance: *LoRaWAN 1.0.3 Specification*. Retrieved from <https://lora-alliance.org/lorawan-for-developers> (10.10.2019).

- [16] Priesack, T.; Plinninger, R.J.; Alber, M.; Salcher, B. (2017) *Systematische Analyse innovativer Installationsverfahren für Porenwasserdruckgeber*. In: Österreichischer Ingenieur- und Architektenverein [Hrsg.]: Tagungsbeiträge der 11. Österreichischen Geotechniktagung, Wien, pp. 327–338.

Autoren



Univ.-Prof. Dr. Kurosch Thuro
(Corresponding author)
Technische Universität München
Lehrstuhl für Ingenieurgeologie
Arcisstr. 21
80333 Munich
Germany
thuro@tum.de



Tamara Breuninger, M.Sc.
Technische Universität München
Lehrstuhl für Ingenieurgeologie
Arcisstr. 21
80333 Munich
Germany
tamara.breuninger@tum.de



Dr. John Singer
AlpGeoRisk
Einsteinstraße 10
85716 Unterschleißheim
Germany
singer@alpgeorisk.de



Moritz Gamperl, M.Sc.
Technische Universität München
Lehrstuhl für Ingenieurgeologie
Arcisstr. 21
80333 Munich
Germany
moritz.gamperl@tum.de



Dr.-Ing. Bettina Menschik
Technische Universität München
Lehrstuhl für Ingenieurgeologie
Arcisstr. 21
80333 Munich
Germany
bettina.menschik@tum.de

How to Cite this Paper

Thuro, K.; Singer, J.; Menschik, B.; Breuninger, T.; Gamperl, M. (2020) *Development of an early warning system for landslides in the tropical Andes (Medellín; Colombia)*. Geomechanics and Tunneling 13, No. 1, pp. 103–115. <https://doi.org/10.1002/geot.201900071>

This paper has been peer reviewed. Submitted: 17. November 2019; accepted: 19. December 2019.

Zitieren Sie diesen Beitrag

Thuro, K.; Singer, J.; Menschik, B.; Breuninger, T.; Gamperl, M. (2020) *Entwicklung eines Frühwarnsystems für Rutschungen in den tropischen Anden (Medellín, Kolumbien)*. Geomechanik und Tunnelbau 13, H. 1, S. 103–115. <https://doi.org/10.1002/geot.201900071>

Dieser Aufsatz wurde in einem Peer-Review-Verfahren begutachtet. Eingereicht: 17. November 2019; angenommen: 19. Dezember 2019.

Appendix B-2

Title	Investigation of Critical Geotechnical, Petrological and Mineralogical Parameters for Landslides in Deeply Weathered Dunite Rock (Medellín, Colombia)				
Journal	Int. J. Environ. Res. Public Health				
DOI	https://doi.org/10.3390/ijerph182111141				
Year	2021	Volume	18	Impact Factor (2021)	4.61
Accepted	Yes	Position of the candidate in the authors list			4
Authors	Tamara Breuninger, Bettina Menschik, Agnes Demharter, Moritz Gamperl, Kurosch Thuro				

This article was published in International Journal of Environmental Research and Public Health; 18; Tamara Breuninger, Bettina Menschik, Agnes Demharter, Moritz Gamperl, Kurosch Thuro; Investigation of Critical Geotechnical, Petrological and Mineralogical Parameters for Landslides in Deeply Weathered Dunite Rock; Copyright 2021 by the authors. Licensee MDPI, Basel, Switzerland. This article is an open access article distributed under the terms and conditions of the Creative Commons Attribution (CC BY) license, thus permission to reprint the article is not necessary.



Article

Investigation of Critical Geotechnical, Petrological and Mineralogical Parameters for Landslides in Deeply Weathered Dunite Rock (Medellín, Colombia)

Tamara Breuninger *, Bettina Menschik, Agnes Demharter, Moritz Gamperl  and Kuroschi Thuro

School of Engineering and Design, Technical University of Munich, 80333 Munich, Germany; sellmeier@tum.de (B.M.); agnes.demharter@tum.de (A.D.); moritz.gamperl@tum.de (M.G.); thuro@tum.de (K.T.)
* Correspondence: tamara.breuninger@tum.de

Abstract: The current study site of the project Inform@Risk is located at a landslide prone area at the eastern slopes of the city of Medellín, Colombia, which are composed of the deeply weathered Medellín Dunite, an ultramafic Triassic rock. The dunite rock mass can be characterized by small-scale changes, which influence the landslide exposition to a major extent. Due to the main aim of the project, to establish a low-cost landslide early warning system (EWS) in this area, detailed field studies, drillings, laboratory and mineralogical tests were conducted. The results suggest that the dunite rock mass shows a high degree of serpentinization and is heavily weathered up to 50 m depth. The rock is permeated by pseudokarst, which was already found in other regions of this unit. Within the actual project, a hypothesis has for the first time been established, explaining the generation of the pseudokarst features caused by weathering and dissolution processes. These parameters result in a highly inhomogeneous rock mass and nearly no direct correlation of weathering with depth. In addition, the theory of a secondary, weathering serpentinization was established, explaining the solution weathering creating the pseudokarst structures. This contribution aims to emphasize the role of detailed geological data evaluation in the context of hazard analysis as an indispensable data basis for landslide early warning systems.

Keywords: dunite; landslide investigation; geological investigation; mineralogical predisposition; pseudokarst; secondary serpentinization; block-in-matrix structure



Citation: Breuninger, T.; Menschik, B.; Demharter, A.; Gamperl, M.; Thuro, K. Investigation of Critical Geotechnical, Petrological and Mineralogical Parameters for Landslides in Deeply Weathered Dunite Rock (Medellín, Colombia). *Int. J. Environ. Res. Public Health* **2021**, *18*, 11141. <https://doi.org/10.3390/ijerph182111141>

Academic Editor: Paul B. Tchounwou

Received: 14 September 2021
Accepted: 16 October 2021
Published: 23 October 2021

Publisher's Note: MDPI stays neutral with regard to jurisdictional claims in published maps and institutional affiliations.



Copyright: © 2021 by the authors. Licensee MDPI, Basel, Switzerland. This article is an open access article distributed under the terms and conditions of the Creative Commons Attribution (CC BY) license (<https://creativecommons.org/licenses/by/4.0/>).

1. Introduction

One of the main Inform@Risk project's objectives is to concept and install a low-cost landslide early warning system (EWS) in the barrio of Bello Oriente on the eastern border of the city of Medellín, Colombia [1]. The eastern slopes of the Valle de Aburrá are especially prone to landslides, since these are very steep and consist of the Medellín Dunite, a rock highly susceptible to chemical weathering (Figure 1).

Petrology, tectonics and weathering play an important role regarding the geotechnical characteristics and the (temporal and spatial) landslide distribution in the Medellín Dunite. All these factors influence each other and lead to significant small-scale changes. Therefore, every geotechnical intervention in this geological unit needs a detailed exploration of the study site.

Although the Medellín Dunite has been studied by scientists for decades [1–10], there are still uncertainties regarding its regional characteristics. Its significant small-scale changes in petrology and tectonics are especially a challenge for geologists and hydrogeologists when generating a geological subsurface model.

The Medellín Dunite is part of an ophiolite sequence formed in the Triassic (250–205 Mya b. p.) before the Andean orogenesis in the Pacific Ocean and has already partly been serpentinized by ocean floor metamorphosis [2,10]. Therefore, the Medellín Dunite has already undergone a significant transition. Depending on the study area, the

dunite can already be identified as serpentinite [2]. There are regions within the unit that consist of less than 90% (serpentinized) olivine and more than 10% orthopyroxene and hence the rock must be called harzburgite [10]. Other minerals that exist in the unit are amphibole (tremolite, actinolite), talc, chlorite, clinopyroxene, magnesite, mica and serpentine minerals [10]. Due to these deviations from a pure dunite, the unit was renamed several times and has been called Medellín Serpentinite [2], Medellín Dunite Tectonite [3,5], Medellín Dunite [4], Medellín Serpentinized Dunite [6], Medellín Ultramafic Massif [7], Medellín Metadunite [8], Medellín Metaperidotite [9] and Medellín Metaharzburgitic Unit [10]. The term “Medellín Dunite”, however, has prevailed.

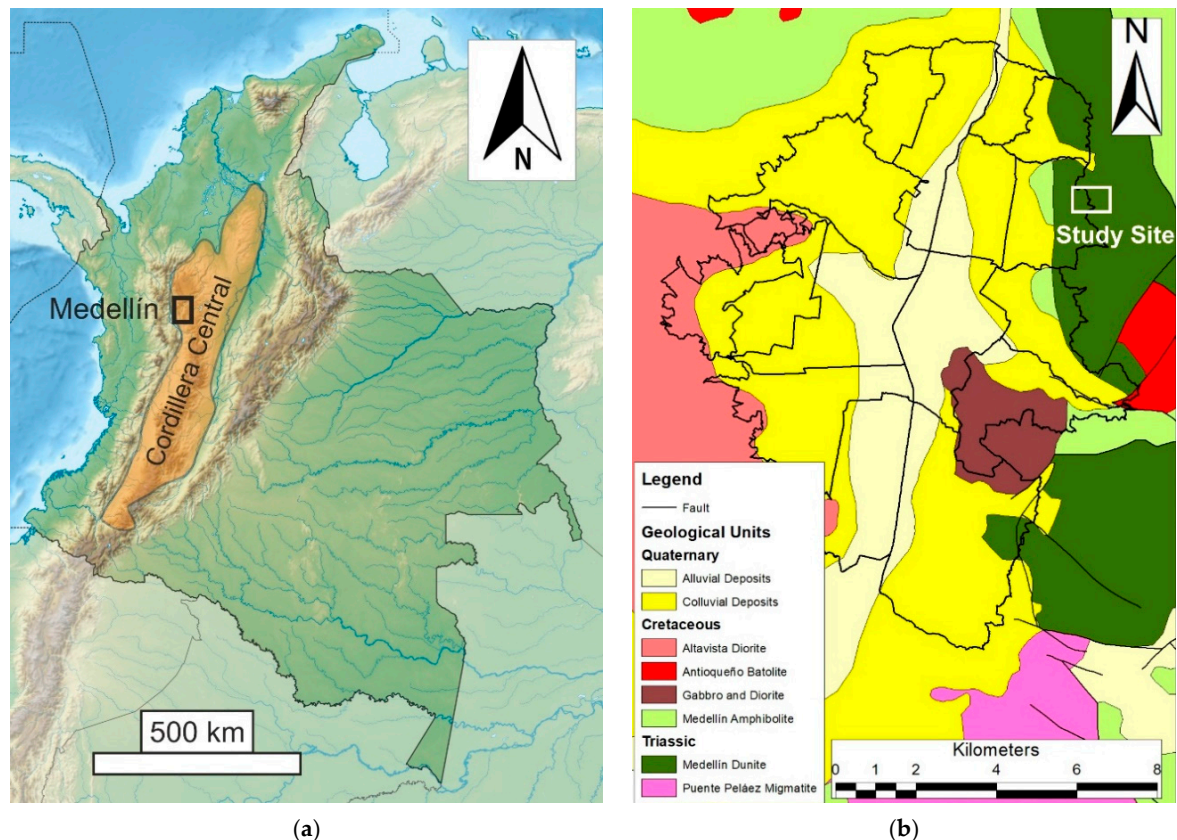


Figure 1. (a) Location of Medellín within Colombia and the Cordillera Central; (b) The “Comunas” of Medellín (black contours), the location of the study site and the city’s geological units [11].

Due to the tectonic history, several joint sets can be observed [12]. The first and oldest of those joint sets is the foliation created by ocean floor metamorphism and the transport to the unit’s current location [2,10]. This foliation (joint set 1) is oriented subhorizontally SW-NE with an incidence angle of max. 30° towards SE [12]. It is characterized by mylonitic structures showing banding of mica, chrysotile and chlorite [12]. The contact to the underlying Medellín Amphibolite (Rodas Fault) has the same orientation.

The second joint set (joint set 2) strikes NNW-SSE with a subvertical angle of $75\text{--}90^\circ$ towards WSW [12]. This orientation resembles the fault between the Medellín Dunite and the Medellín Amphibolite (La Acuarela Fault), where the amphibolite was uplifted [12].

A third joint set (joint set 3) strikes SW-NE with a dip of $25\text{--}60^\circ$ towards NW [12]. Due to these three main joint sets and several other discontinuities, the whole dunite body is highly disintegrated.

Since Medellín is located in a tropical environment, chemical weathering is a strong influencing factor on the subsurface composition. When in contact with water, the rock is altered by degradation into clay minerals and due to oxidation to iron oxides and hydroxides, which weakens the rock’s structure and decreases its compressive strength

continuously [13]. The higher the content of olivine in the rock (“pure” dunite), the stronger the weathering [14]. Therefore, the weathering highly depends on the specific petrological composition of the rock and can change within the Medellín Dunite. The typical weathering profile of the unit (Figure 2) consists of organic soil and volcanic ashes on the surface overlaying the saprolite deposits which show a decreasing weathering with increasing depth. This saprolite mostly consists of blocks of at least 50 cm in diameter in a silt-clay matrix with a ratio of approximately 1:1 (block-in-matrix structure). The content of loose material decreases with the depth. The depth of the top of the fractured dunite below the saprolite varies extremely within 0–20 m [12].

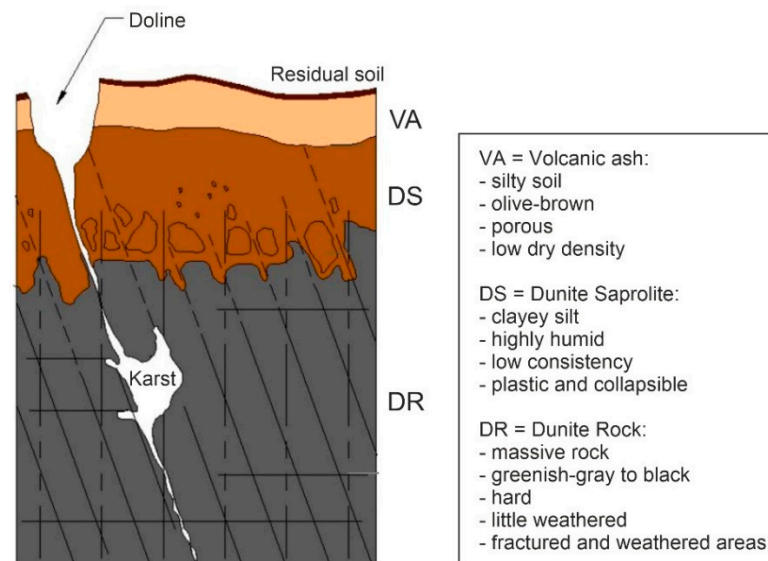


Figure 2. Idealized column profile of the Medellín Dunite with pseudokarst structures; dimensions are not given, because they vary to an evident extent [12] (after Figure 7.6).

This simplified and idealized cross section is influenced by landslide processes taking place along the slope surface (uppermost 10 m), creating a further block-in-matrix structure which occurs to be similar to the one formed by weathering processes (Figure 2) [12].

The phenomenon “pseudokarst” (term here explicitly used as a differentiation from the real karst in carbonate rock) occurs in highly fractured crystalline rock masses. Water circulation in the fractures causes increased weathering and corrosion and, therefore, the solution, and in other places, precipitation of minerals. The Medellín Dunite shows various forms of karst such as dolines, spitzkarren, rundkarren and rillenkarrren [12]. The precipitation of the magnesium hydroxide brucite in some fractures [12] is another indication for this phenomenon. Some fractures are filled with clay material, others are open discontinuities of up to 1 m opening width. This pseudokarst phenomenon reaches a depth of at least 60 m [15]. The block-in-matrix structure in combination with the joints opened up by the pseudokarst lead to increased water conductivity which results in an increase of subsurface weathering and pseudokarst formation which again leads to increased water conductivity and subsurface weathering, creating a cycle.

Due to the water absorbent properties of the fine material, the block-in-matrix structure is most likely to be affected by landslides [12] since water infiltration is the main reason and trigger for landslides in the Medellín Dunite. With increasing pore water pressure, the structure “floats” upwards, the friction angle decreases and the slope fails. The blocks tend to “swim” in the matrix and their geotechnical properties do not influence the mechanics of motion once the full detachment occurs [15].

The investigation presented in this article is essential to determine unstable areas that need to be monitored closely by the EWS. It also contributes to the studies on the Medellín Dunite that have already been published and determines whether the findings of previous publications on the subject are also valid in this specific setting.

2. Materials and Methods

The underground of the study site was investigated by conducting a combination of field mapping, drillings and laboratory tests. The fieldwork in the project was performed in two campaigns, the first of which took place in August 2019.

During this first field campaign, the landslide features in the study site and several historic landslides were recorded in order to understand the landslide dynamics in this area and to be able to validate numerical models using back analysis methods.

The recording of former events was only possible with the help of the residents, since the whole study site is heavily overgrown with thick grassland and bushland, which makes the registration of morphological landslide indicators difficult. The residents provided information on age, size and speed of several mass movements in the study site [16].

The second field campaign was conducted in February 2020. During this trip, the geological mapping was accomplished. The main goal was to determine the ratio of blocks and matrix in the block-and-matrix structures, since these are most prone to landslides with increasing content of fine material (water storage properties) and the areas with in situ rock, which are not likely to fail. Again, the help of the residents was of great importance.

The first drilling campaign was planned for May 2020. Due to the COVID-19-caused lockdown in both Germany and Colombia starting in March 2020, the drillings have been performed in October 2020. The three drilling locations can be seen in Figure 3. All drilling locations were chosen regarding the expected thickness of soil cover (at least 10 m) and their contribution to the early warning system with CSM cables, piezometers and inclinometers being installed after the drilling campaign [17]. A drilling depth of 30.4 m for A1, 30.3 m for A2 and 50.0 m for B1 could be achieved. Drilling B1 is one of the deepest drillings ever performed in the Medellín Dunite [15]. All drillings were performed using the double core rope drilling method without oriented cores. The inner diameter of drilling B1 is 101.6 mm, the inner diameter of the drillings A1 and A2 is 63.5 mm. The bigger diameter in drilling B1 was chosen to fit an inclinometer casing in the borehole in addition to two CSM cables and four piezometers. A1 and A2 do not include an inclinometer casing. All drilling cores were evaluated regarding the core loss, weathering profile, RQD [18], fracture ratio, joint sets and weathering type. Based on all these parameters, six homogeneous areas were established, which are described in Figures S1–S3. A second drilling campaign is planned for the first half of 2021 to complete the picture.

In all the drillings, samples were taken to determine some of the most important soil and rock parameters. The tests that were performed can be seen in Table 1. Due to a limited amount of undisturbed soil material, the soil tests could not be carried out to the intended extent.

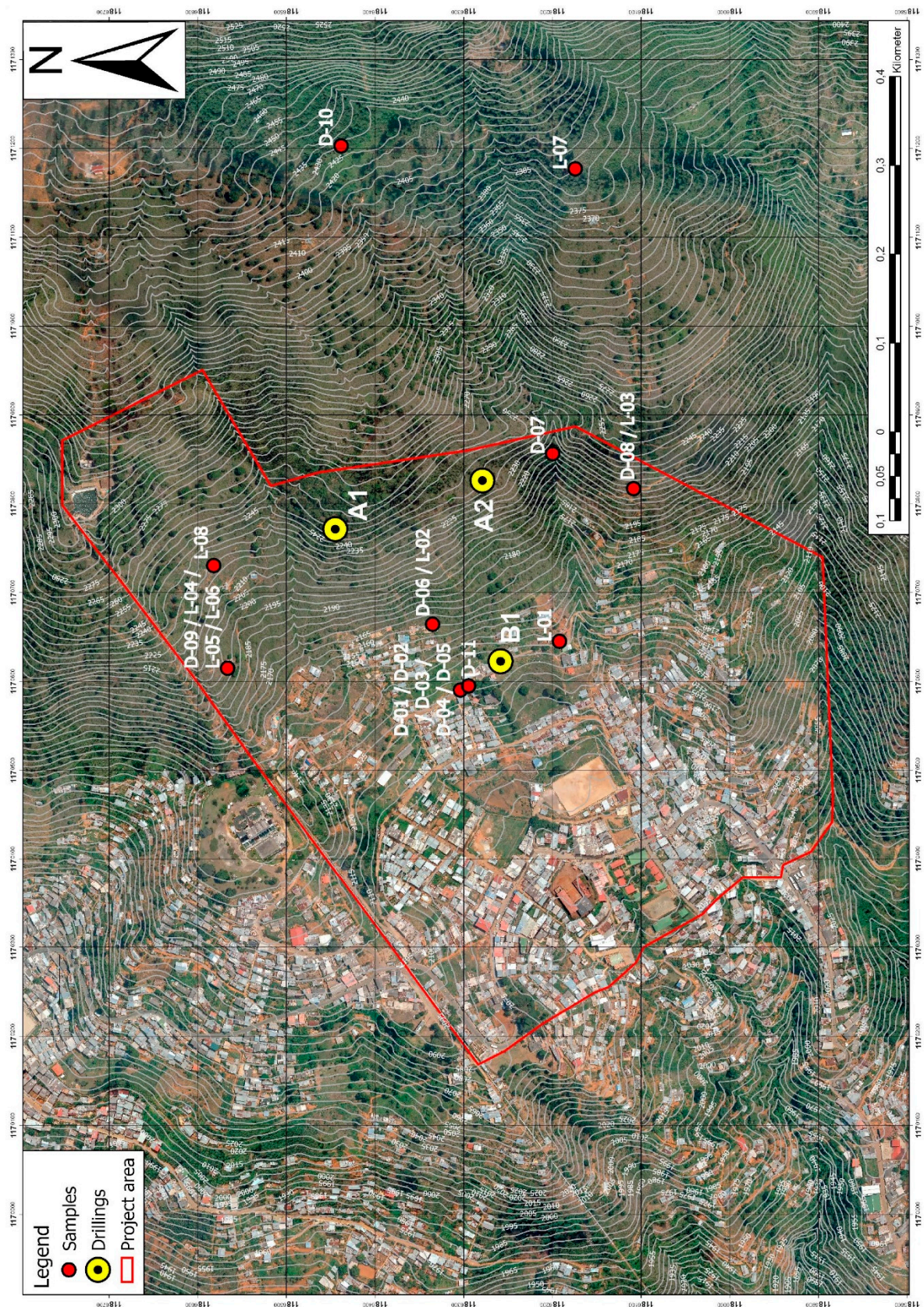


Figure 3. Map of the study site depicting the locations of the drilling and the sample locations (projected coordinate system: MAGNA Medellin Antioquia 2010).

Table 1. Tests performed on the drilling samples, applied standards and number of tests.

Test Performed	Standard	Number of Tests
Compressive Strength	ASTM D 7012-14e1 (2014) [19]	18
Brazilian Test	ASTM D 3967 (2016) [20]	18
Grain Size Analysis	INV E 123 (2013) [21]	7
Atterberg Limits	INV E 125 and INV E 126 (2013) [22,23]	7
Direct Shear Test (CD)	INV E 154 (2013) [24]	1(2)

Further samples collected from the ground surface during the field investigation in August 2019 were examined mineralogically using X-ray diffraction on soil samples and petrographic thin section microscopy on collected rock samples. The X-ray diffraction was carried out on 8 samples using Cu-K α radiation and analyzed with graphs created with the software Profex 4.1.0, the microscopy was performed on 11 thin sections from 10 rock samples using a petrographic polarized light microscope. The locations of the sampling are shown in Figure 3.

3. Results

3.1. Landslide Inventory and Geological Investigation

3.1.1. Landslide Map

During the first field trip, an extensive map of the landslide phenomena at the study site was created (Figure 4) on an original scale of 1:3500. The map shows the outlines of former landslide events (the oldest being about 110 years old, the youngest occurred in 2017), their detachment and accumulation areas. Older landslides may be existent but are masked by younger ones.

As a main outcome, it is suggested that most of the landslides are rotational slides, occurring to an increased extent in soil or highly weathered rock [25]; the depths of the landslides can be specified in a range of 5–10 m, which could be classified as shallow to mid-seated [26]. Within the borders of the study area, there are no indications of deep-seated landslides in the past, even though the bedrock is expected to be highly weathered and fractured up to a depth of 60 m or more. However, a deep-seated landslide could not be excluded since the morphological elements would have been eliminated due to anthropogenic influence, such as road, building and plantation construction.

Based on the current results, the probability for a deep-seated landslide in the future is suggested not to be evident, but the possibility cannot be ruled out.

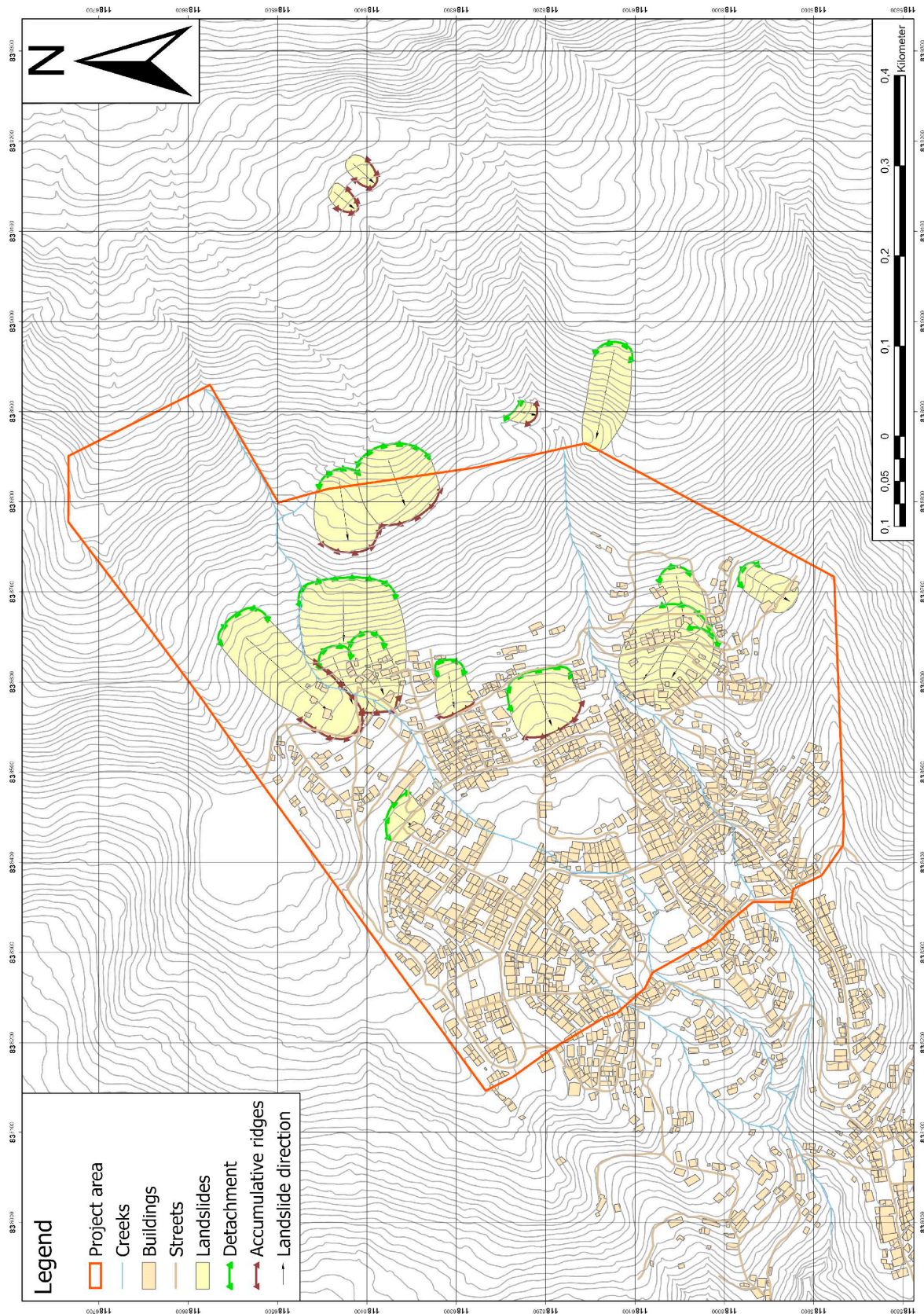


Figure 4. Map of landslide features at the project site, which is marked with the red colored line. The red border represents the project area, the detachment areas are marked in green, the accumulation areas in black. Most of the landslides could be characterized as rotational slides (projected coordinate system: MAGNA Medellin Antioquia 2010).

3.1.2. Geological Map

The geological map of the study site is shown in Figure 5 (original scale 1:3500). Two outcrops of in situ rock are ridge structures on the north-western border of the study site and in the south, both structures striking more or less SW-NE. A few other outcrops exist in the eastern part of the site (uphill). All these structures are visible on the surface as ridges, which indicates that these parts of the slope are more resistant and were not moved, e.g., due to landslides, in the past. Another prominent fact is that the strike direction of these ridges could be parallelized with one of the third joint set mentioned in Chapter 1. Therefore, the ridges could have been lifted tectonically creating a horst-and-graben structure in the study site with the trenches being filled by weathering products (block-and-matrix structure) of the described ridges. The in situ rock is heavily weathered and can hardly be distinguished from the saprolite formation.

The saprolite borders the outcrop on the north-western border and also occurs in the mid-eastern part of the study site. Two other outcrops are to the west in the main body of the site and to the far west. The saprolite and the in situ rock are not separated by a sharp line, but by a smooth transition from one to the other. Like the in situ rock, the saprolite has not been moved in the past but is likely to fail in the future.

The block-in-matrix structures that make up the rest of the area (trenches) are subdivided by their block-matrix ratio. Though the main part of the area (green) is dominated by blocks, there are also areas (blue) dominated by matrix. All areas made up of these block-and-matrix structures are very prone to landslides as already discussed in Section 1. A distinction between block-and-matrix structure created by former landslides or created by weathering cannot be made. The origin of the structure, however, does not influence its geotechnical behavior, which is why it is not of immediate importance.

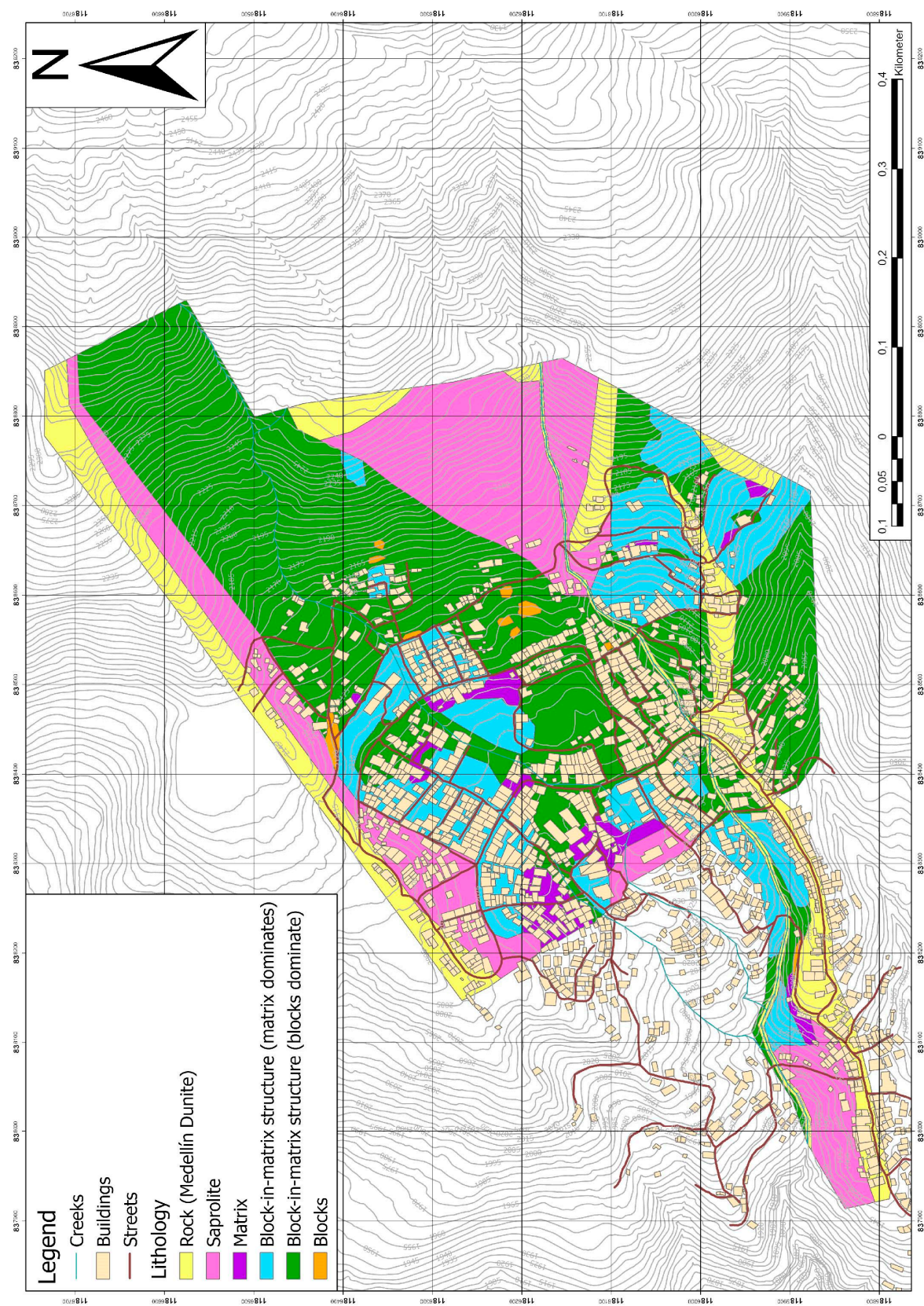


Figure 5. Geological map of the study site. The yellow colors indicate the bedrock ridges mainly in the north and south of the project site (projected coordinate system: MAGNA Medellín Antioquia 2010).

3.2. Evaluation of the Drillings

Figures 6 and 7 show pictures of the drillings cores, Figures S1–S3 include the drilling core documentation (drilling profile) and evaluation with several columns (core loss, weathering profile, RQD, fracture ratio, joint set, alteration type and homogeneous area). The evaluation of the drillings was done in collaboration with a Master's thesis supervised within the project [27].

As depicted in Figures 6 and 7, the thickness of the soil on the surface hardly reaches 2 m, except for drilling B1. In all drillings, there is significant core loss (Figures S1–S3). Except for the first 3.0 m of drilling B1, this core loss is most likely a combination of flushed out, loose material due to the drilling flushing and holes in the ground created by pseudokarst. The first 3 m of drilling B1 are fillings from the road construction; the core loss here is most likely a combination of flushed out loose material and holes due to insufficiently compacted ground.

All three cores show fractures that dip predominantly with 0–15° (foliation/joint set 1) and 30–60° (joint set 3). The few joints dipping >60° are suggested to be parallelized with joint set 2.



Figure 6. (a) Picture of the drilling core of drilling A1; (b) Picture of the drilling core of drilling A2. The cores have a length of 1 m each and run from top left to bottom right.

Some cores (for the shear and Atterberg limits tests) were wrapped into plastic foil to preserve their original humidity (Figures 6 and 7).

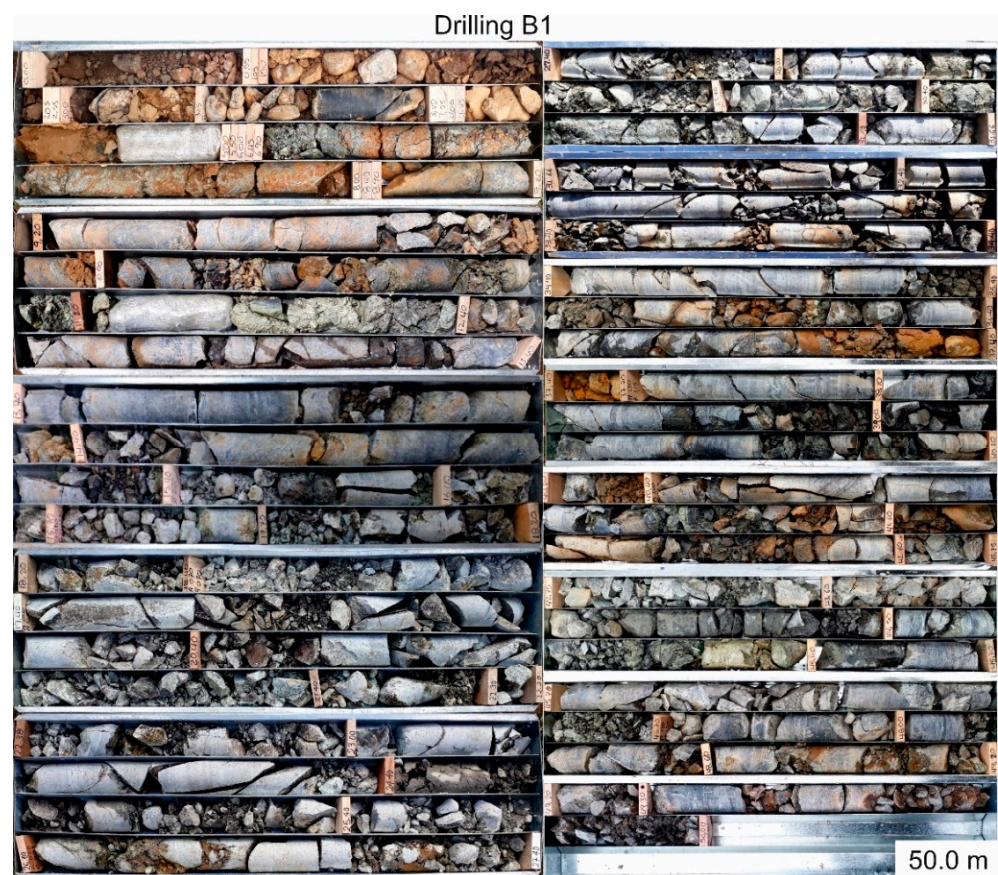


Figure 7. Picture of the drilling core B1, depicted in two rows. The left row shows the drilling core from 0–27.4 m, the right row shows the drilling core from 27.4–50.0 m. The core boxes have a length of 1 m each and run from top left to bottom right.

3.2.1. Detailed Description, Drilling A1

In this drilling, the residual soil only reaches 40 cm depth. The material shows a deep brown color and mostly consists of sand, silt and clay. The rest of the core has the best rock quality of all the cores (Figures 6a and S1).

Meters 2.6–12.1 show the weathering stages II after IAEG [28], have an RQD of at least 53 (fairly good) and show joints, which are oriented subhorizontally (most likely foliation/joint set 1) or dip with 30–45° (most likely joint set 3). In this area, some joints show serpentinization and brown colors indicating water circulation through these joints. Other joints show no color changes. These could have been closed prior to drilling due to vertical pressure and, therefore, were not altered by water circulation. The whole area is therefore designated as homogeneous area 2, except for the areas of core loss and meters 0.4–2.6, where the core is more fractured and, therefore, belongs to homogeneous area 3.

Below 12.1 m, the core quality decreases in strength with increased weathering visible due to the brown colors on the core.

The area of meters 12.1–13.5 includes an area of highly destroyed, almost pulverized, but not deep brown colored, loose material. In Colombia, this material is called “salbanda” meaning “fault clay” [15]. It is formed by mechanical grinding without weathering (water circulation). This might indicate a tectonic movement in the past, without an information on the age of this movement. The area has a weathering stage of V and the RQD is 0 (very poor). Therefore, this part of the core is in homogeneous area 5.

The rest of the core (13.5–30.4 m) shows weathering stage III and IV, an RQD of 12–37 (poor to very poor) and mostly contains the joint sets 1 and 3, in meters 13.5–17.4 also one joint of joint set 2, leading to the homogeneous area 4. Brown weathering material dominates the core’s appearance, serpentinization is not or only slightly visible. Two areas

in this part of the core show a considerable better quality (19.3–20.1 m and 29.3–30.4 m) with weathering stage II and an RQD of 72 and 75 (fairly good), which results in homogeneous area 2.

3.2.2. Detailed Description, Drilling A2

In general, this drilling core shows less brown fine material compared to the core of drilling A1, but the material is more fractured and fragmented. It also shows more small-scale changes, since the rock quality, weathering and joint numbers change significantly within a few centimeters (Figures 6b and S2).

With up to 2.0 m, the thickness of loose material and soil on the top in drilling A2 is higher than in drilling A1.

Meters 2.0–6.4 show a weathering stage of II to IV, an RQD of 16–60 (very poor to fairly good) and all three joint sets mentioned before (only one fracture of joint set 2). Only one area shows serpentinization, the weathered material mostly shows brown colors. As it is only lightly weathered, this area belongs to homogeneous area 3, except for a small part around 3.5 m which belongs to 4 (in Figure 6b, this part is already wrapped in plastic foil).

The next section of 6.4–7.9 m shows the strongest weathering in the whole core. It has the weathering stage IV with brown and fragmented weathered material, and the ROD is not quantifiable due to the lack of enough rock material. Therefore, this area belongs to homogeneous area 4.

Below 7.9 m, the drilling core shows interchanges of homogeneous area 2 and 3. Homogeneous area 2 is characterized by weathering stage II, an RQD of 36–64 (poor to fairly good), only a few areas with color changes (9.35–11.65 m and 26.95–28.35), indicating a lack of water circulation in the joints and fractures, and mostly joint sets 1 and 3 (joint set 2 only at 15.3–15.8 m). In contrast, homogeneous area 3 shows weathering stages III to IV, an RQD of mostly 0 with spikes of up to 39 (very poor to poor), the weathering types of brown weathered material and fragmentation and the joint sets 1 and 3.

The section 14.3–15.3 m belongs to the homogeneous area 4, because the weathering is much stronger here (weathering stage V).

3.2.3. Detailed Description, Drilling B1

The deepest drilling is also the most complex one (Figures 7 and S3). As the drilling A2, it shows significant small-scale changes and extreme differences regarding the weathering type. All three dominant joint sets are present throughout the core. To a depth of 8.9 m, core loss is the dominating feature. Only 3.05 m of this section are recovered. This phenomenon is most likely caused by flushed out loose material and in the upper 3.0 m additionally by insufficiently compacted ground.

The first 3.0 m of this core are fillings from road construction, mostly gravel and blocks in brown sand and clayey silt.

Meters 3.0–6.9 show weathering stages IV and V and except for one section (3.2–3.4 m/75 (good)), the RQD is not quantifiable. The upper part belongs to homogeneous area 3, since the weathering is still moderate, but the fragmentation is high. The lower part is homogeneous area 4, because of the strong weathering.

In the area of 6.9–11.2 m, the core is still intact but shows extreme weathering (stage V) with brown colors, an RQD of 20 (very poor) and, therefore, belongs to homogeneous area 3. This part of the core could be identified as the saprolite overlaying the dunite rock, since the structure of the rock is still visible, but the material is extremely weathered.

The meters 11.2–12.4 are made up of the before mentioned “salbanda” (fault clay); here it appears as gray-greenish silty clay. This indicates movement in the past along this area with no water infiltration, since brown colors are not visible. Due to its crushed structures and clay content, this area belongs to homogeneous area 5.

Below 12.4 m, the core shows a variation between homogeneous areas 2 and 3, with some exceptions. Homogeneous area 2 is characterized by the weathering stage II (except for 42.6–44.0 m with IV/V), an RQD of 0–80 (mostly good, but some exceptions) and

varying weathering types. Homogeneous area 3 shows weathering stages of II–V, an RQD of 0–58 (generally lower than in homogeneous area 2) and more intense weathering colors than in homogeneous area 2.

Some sections in this area show homogeneous area 6. These sections are characterized by weathering stage V, an RQD of 0–50 (mostly under 15) and mostly fragmented cores without brown colors but showing serpentinization. The most prominent characteristic is that the blocks in this area can easily be broken by hand. Therefore, especially the area of 18.2–31.4 m is extremely unstable.

3.3. Laboratory Tests

3.3.1. Uniaxial Compressive Strength

All values of the uniaxial compressive strength are depicted in Figure 8. The compressive strength decreases with increasing weathering [13]. Therefore, it is expected to show lower values with increasing weathering. All samples show weathering stage II on the exterior with little differences.

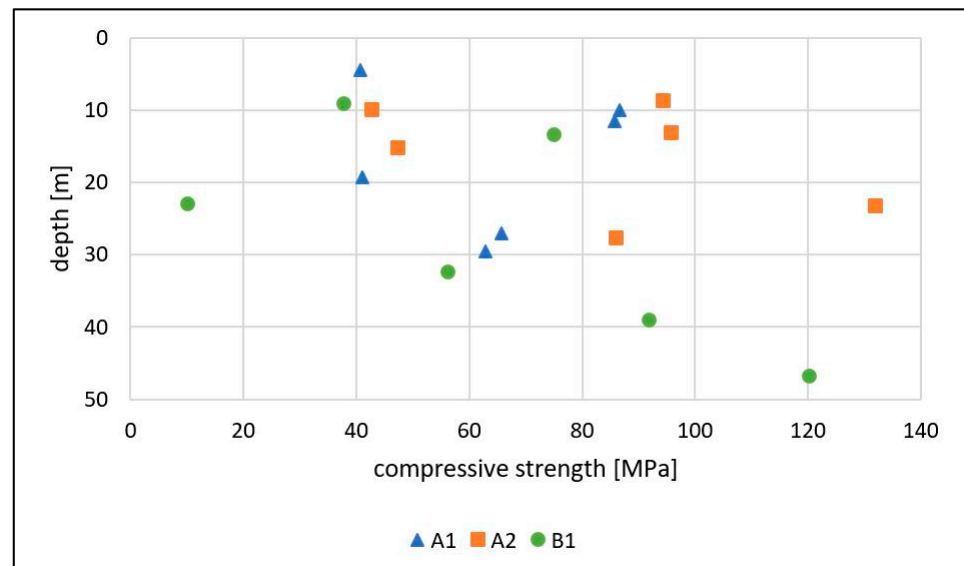


Figure 8. Results of the uniaxial compressive strength tests plotted vs. the sampling depth.

As visible in Figure 8, there is no correlation between depth and compressive strength in any of the three drillings. The values in general vary from 10 MPa to 132 MPa, which shows the high variation of the materials in the Medellín Dunite.

Most samples (10) have a high compressive strength of 50–100 MPa [29]. One sample has a low compressive strength of 5–25 MPa, five samples have a moderately high compressive strength of 25–50 MPa [29]. Two samples show a very high compressive strength of 100–250 MPa [29].

In drilling B1, the 4 stratigraphically deepest samples show a constant increase of compressive strength with increasing depth, but the two uppermost values do not fit into this correlation. In drillings A1 and A2, only a slight tendency can be seen.

An explanation of this bad correlation might be that the primary rock conditions might be affected by serpentinization and tectonic damage already before weathering. Another one might be that the normal weathering from top to bottom could not be applied in the Medellín Dunite, most likely due to the pseudokarst present in this unit, but also due to landslides, which disturb the uppermost 2–10 m of the unit causing a mix of top layers. Most likely, it is a combination of both.

3.3.2. Brazilian Test

The results of the Brazilian test are depicted in Figure 9. Like the results of the uniaxial compressive strength test, the tensile strength of a sample is expected to decrease with increased weathering [13], but all samples show weathering stage II from the outside with little differences.

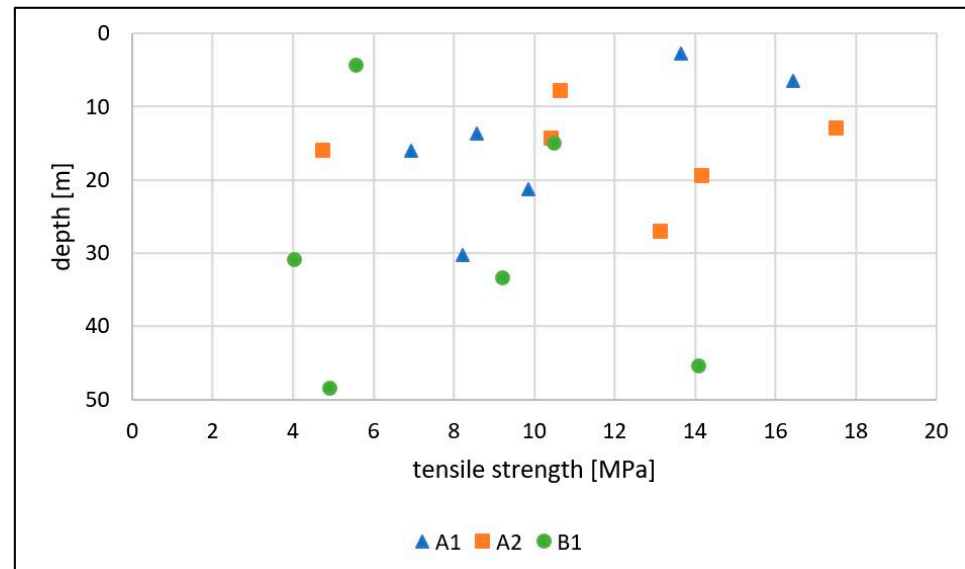


Figure 9. Results of the tensile strength tests (Brazilian tests) plotted vs. the depth of the sampling.

Although compressive strength showed at least a slight correlation with depth, tensile strength seems not to increase with the sampling depth at all. This also might correspond to the fact that the primary rock conditions were already affected by serpentinization and tectonic damage before weathering. The values of the tensile strength vary to a high extent between 4.1 and 17.5 MPa.

This was registered in the drilling core analysis, but even the intact rock sections can be highly weathered internally in great depths as the rock tests prove.

3.3.3. Grain Size Distribution

The grain size distribution was determined on seven samples in all three drillings, four of them in drilling A1, one in drilling A2 and two in drilling B1, which are depicted in Figure 10 and Table 2. Even though the tests were performed after INV E 123 (2013) [21], the evaluation was done after DIN EN ISO 14688-1(2020) [30], due to the intercultural collaboration and because ISO standards provide an international standardization level for rock and soil testing and evaluation.

The results of the sieving tests indicate that the loose material in the drilling cores consists of at least 37% silt and clay, in most cases much more. One sample (drilling B1, 5.25 m) even shows an amount of about 93% silt and clay.

Table 2. Results of the sieving after DIN EN ISO 14688-1 (2020) [30].

Sample	Gravel [%]	Sand [%]	Silt/Clay [%]
A1, 19.40 m	32	21	47
A1, 21.45 m	19	14	67
A1, 25.30 m	15	12	73
A1, 26.00 m	48	15	37
A2, 3.40 m	33	19	48
B1, 2.30 m	2	17	81
B1, 5.25 m	0	7	93

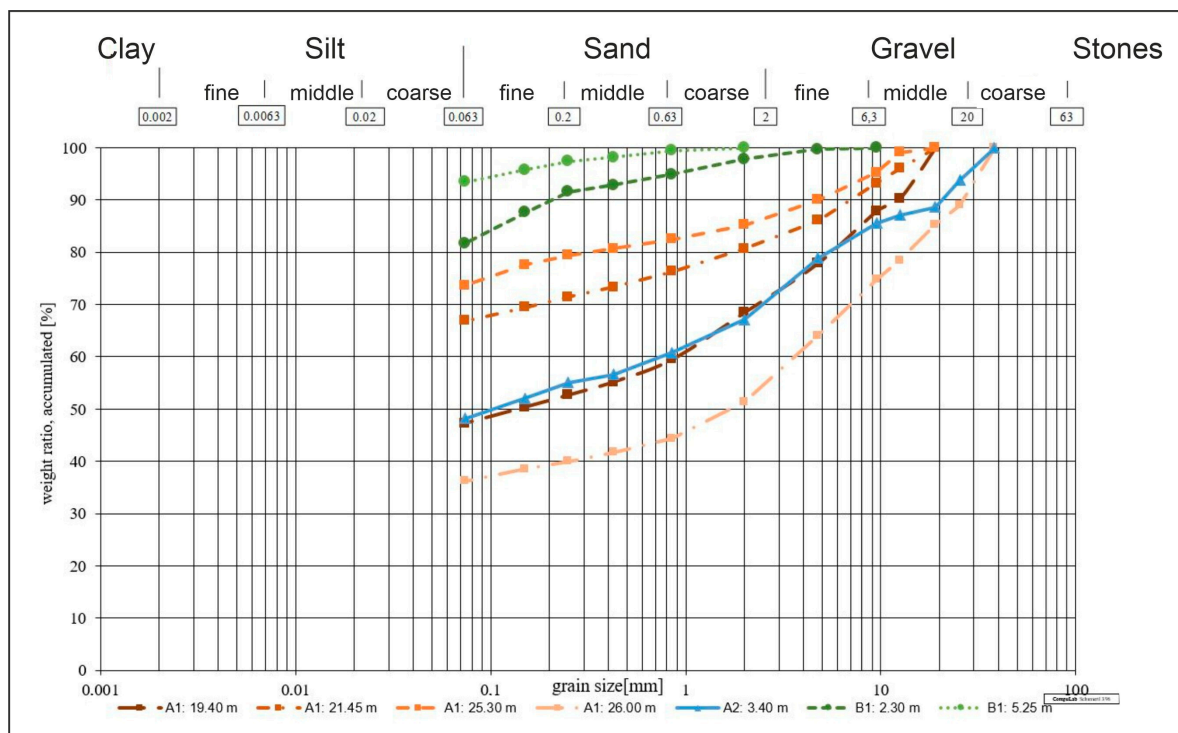


Figure 10. Grain size distribution of all drillings depicted according to DIN EN ISO 14688-1 (2020) [30].

Like the rock tests before, this investigation shows no correlation between depth and the values determined. In a weathering profile, the grain size would be expected to increase with increasing depth. This fact could not be observed, which underlines the presence of pseudokarst and disturbance due to landslides.

3.3.4. Atterberg Limits

The results of the Atterberg limits tests are listed in Table 3. All samples could be specified as silt or clay with low to high plasticity after DIN 18196 [31], except for one sample of drilling A1, which has the behavior and grain size distribution of a gravel-silt mixture with a proportion of silt of more than 15% (GU*). After USCS [32], four samples belong to silty or clayey soils (MH and CL), two samples are mixtures of fine material and sand (SC and SM), one sample is a mixture of gravel and silt (GM).

Table 3. Results of the Atterberg limits tests, showing sample numbers, plastic and liquid limits, plasticity indices as well as specifications according to the applied standards.

Sample	Plastic Limit [%]	Liquid Limit [%]	Plasticity Index [%]	USCS [32]	DIN 18196 [31]
A1, 19.40 m	26	53	27	SC	TA
A1, 21.45 m	20	31	11	CL	TL
A1, 25.30 m	21	32	11	CL	TL
A1, 26.00 m	27	45	18	GM	GU *
A2, 3.40 m	31	49	18	SM	UM
B1, 2.30 m	72	106	34	MH	UA
B1, 5.25 m	56	77	21	MH	UA

*: the soil contains 15–40 % silt.

Three samples have a high plastic behavior (TA and UA/SC and MH), indicating a possibly high content of swelling clay minerals. The three samples with moderate and low plastic behavior (UM and TL/SM and CL) could also include swelling clay minerals but to a much lower extent, since their behavior is not dominated by them.

Even though two of the high plastic samples were taken in drilling B1, no clear correlation can be drawn between the place or depth of the sampling and the values.

3.3.5. Direct Shear Test

The drained, consolidated direct shear test was conducted on two samples taken directly from the drilling core with cut-out cylinders in drilling B1 in a depth of 5.0–5.5 m. Therefore, the samples are very similar regarding their geotechnical properties. Unfortunately, it was not possible to gain more than two samples for shear testing due to a lack of soil material in the drillings. Therefore, the results for friction angle and cohesion are only reference values.

Both samples had a diameter of 50.0 mm and a height of 25.4 cm, creating a ratio of approximately 2:1, and were tested with a shear velocity of 0.2 mm/min.

Figure 11 shows the shear-displacement curves: the orange one at a normal stress of 299.8 kPa, corresponding to a load of 588.6 N, the blue one at a normal stress of 150.5 kPa, corresponding to a load of 295.5 N. The form of the curves indicates that the soil is densely packed since the curves drop after reaching their maximum shear stress at the point of failure. In addition to the shear-displacement curves, the shear-consolidation curves (Figure 12) show a consolidation of the samples during the shear test, indicating a compaction of the soil. This shows that despite the dense compaction shown in Figure 11, the soil is not over-consolidated and can still be further compacted.

The point of failure of the sample sheared at a normal stress of 299.8 kPa is 172.4 kPa and the failure point of the sample sheared at a normal stress of 150.5 kPa is 106.1 kPa, resulting in an effective friction angle φ of 24.0° and a cohesion c of 39.2 kPa.

A friction angle of $10\text{--}25^\circ$ and a cohesion of >10 kPa are characteristic for strongly cohesive soils [33]. This behavior of the loose material in the drilling cores is already apparent from the results of the sieving tests and the Atterberg limits tests, which mostly identified fine material with plastic behavior. Since the samples were disturbed by the drillings process, the results have to be compared with those of undisturbed samples taken from the surface.

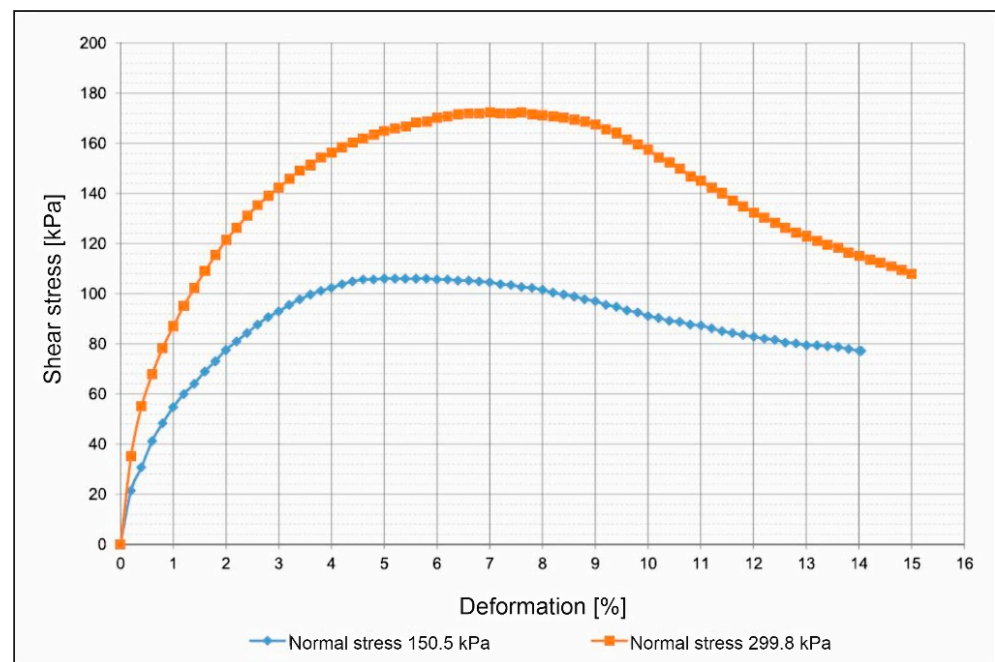


Figure 11. Shear-displacement curves.

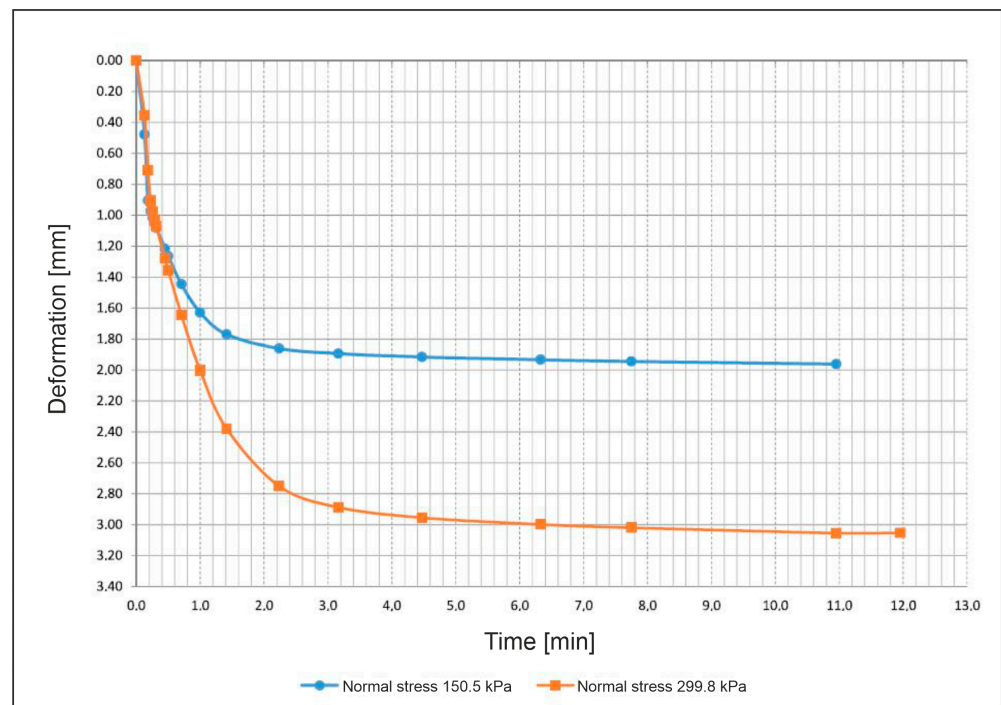


Figure 12. Shear-consolidation curves.

3.4. Mineralogical Investigations

3.4.1. Petrographic Thin Section Microscopy

For the petrographic analysis, a Bachelor’s thesis [34] has been supervised and the 11 thin sections were analyzed in collaboration. During this analysis, six minerals or mineral groups could be identified frequently (Table 4). There are also other minerals in the samples, but in very small frequency and quantity. In Figures 13 and 14, some microscopic pictures of the thin sections show typical shapes of the minerals in the rocks and their weathering, which is visible in some samples.

Table 4. Results of the microscopic analysis of the thin sections, showing the most frequent minerals [34].

Mineral \ Sample	D-01	D-02	D-03	D-04	D-05	D-06	D-07	D-08.1	D-08.2	D-09	D-10
Olivine	X	X	X	X	X	X	X	X	X	X	X
Serpentine	X	X	X	X	X	X	X	X	X	X	X
Pyroxene		X	X	X	X		X	X	X	X	X
Amphibole			X		X		X		X	X	
Chlorite	X	X	X	X	X	X	X	X	X	X	X
Opaque phase	X	X	X	X	X	X	X	X	X	X	X

Since dunite consists of olivine and pyroxene, the presence of these two minerals has been expected. The serpentinization is very advanced in most samples, as is the weathering which is creating chlorite. The opaque phases could be ferrous minerals such as hematite and magnetite, which are common in ultramafic rocks.

The olivine crystals in the samples are mostly broken and heavily weathered at their exterior, as is visible in Figures 13a,d and 14f.

Pyroxene (Figures 13c and 14c) is not present in all samples, suggesting these parts of the rock might either be dunite in a strict sense without any pyroxene or that the pyroxene minerals have already been altered by serpentinization or weathering.

Five samples contain amphibole (Figure 14c,e), which is commonly present in ultramafic rocks. Its absence in the other thin sections indicates that it is already serpentinized.

Figure 14b shows serpentinization of an amphibole from the outside. Serpentine was found in most samples, either chrysotile (fiber serpentine, Figures 13b,c and 14a,b) or antigorite (foil serpentine, Figures 13b,f and 14d). The serpentinization starts at fractures (Figures 13d and 14a) and grows into the minerals from there.

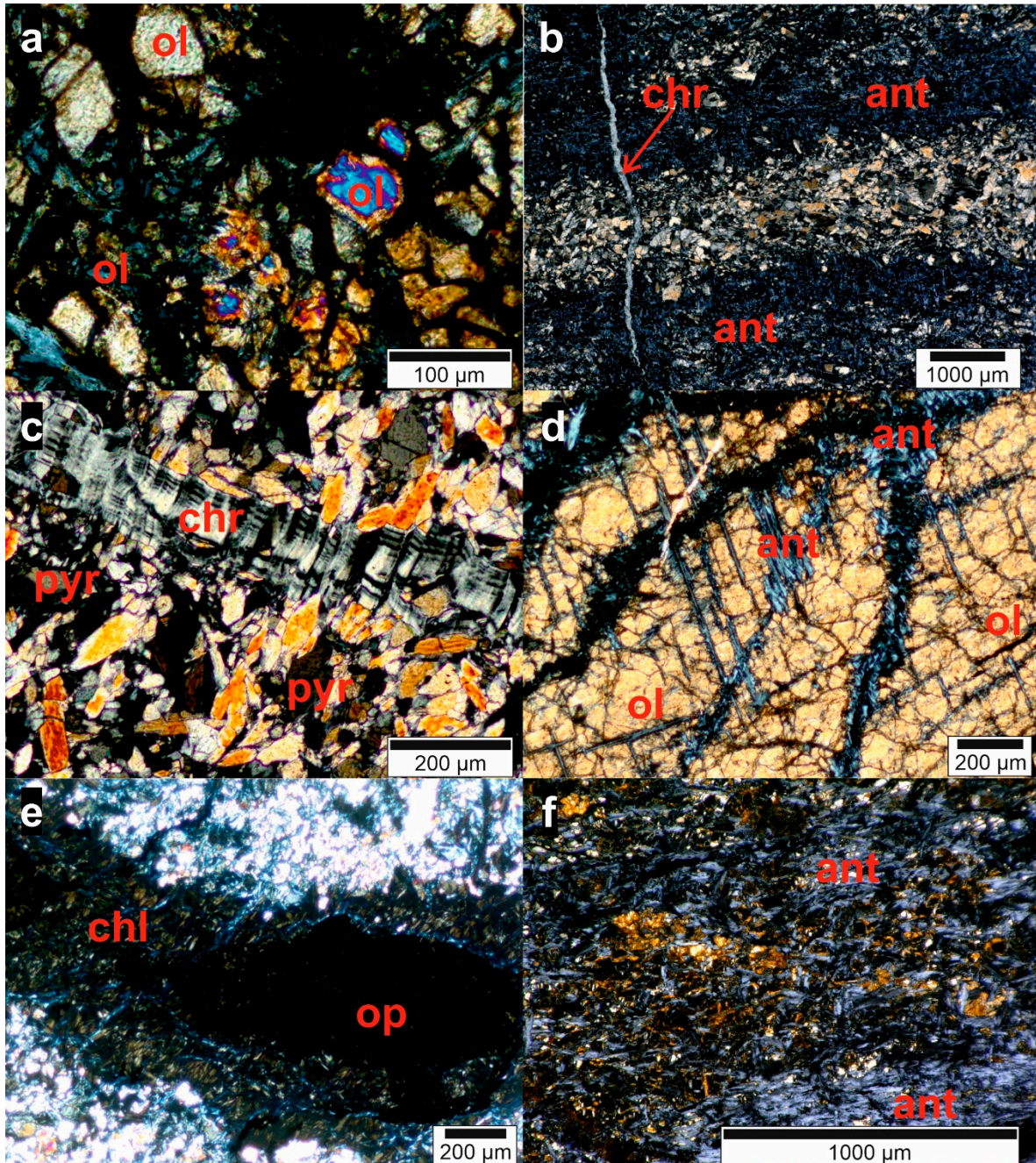


Figure 13. Microscopic photos of the thin sections related to the sample numbers: (a) = D-01; (b) = D-02; (c) = D-03; (d) = D-04; (e) = D-05; (f) = D-06 (ol = olivine, ant = antigorite, chr = chrysotile, pyr = pyroxene, amp = amphibole, chl = chlorite, op = opaque phase) [34].

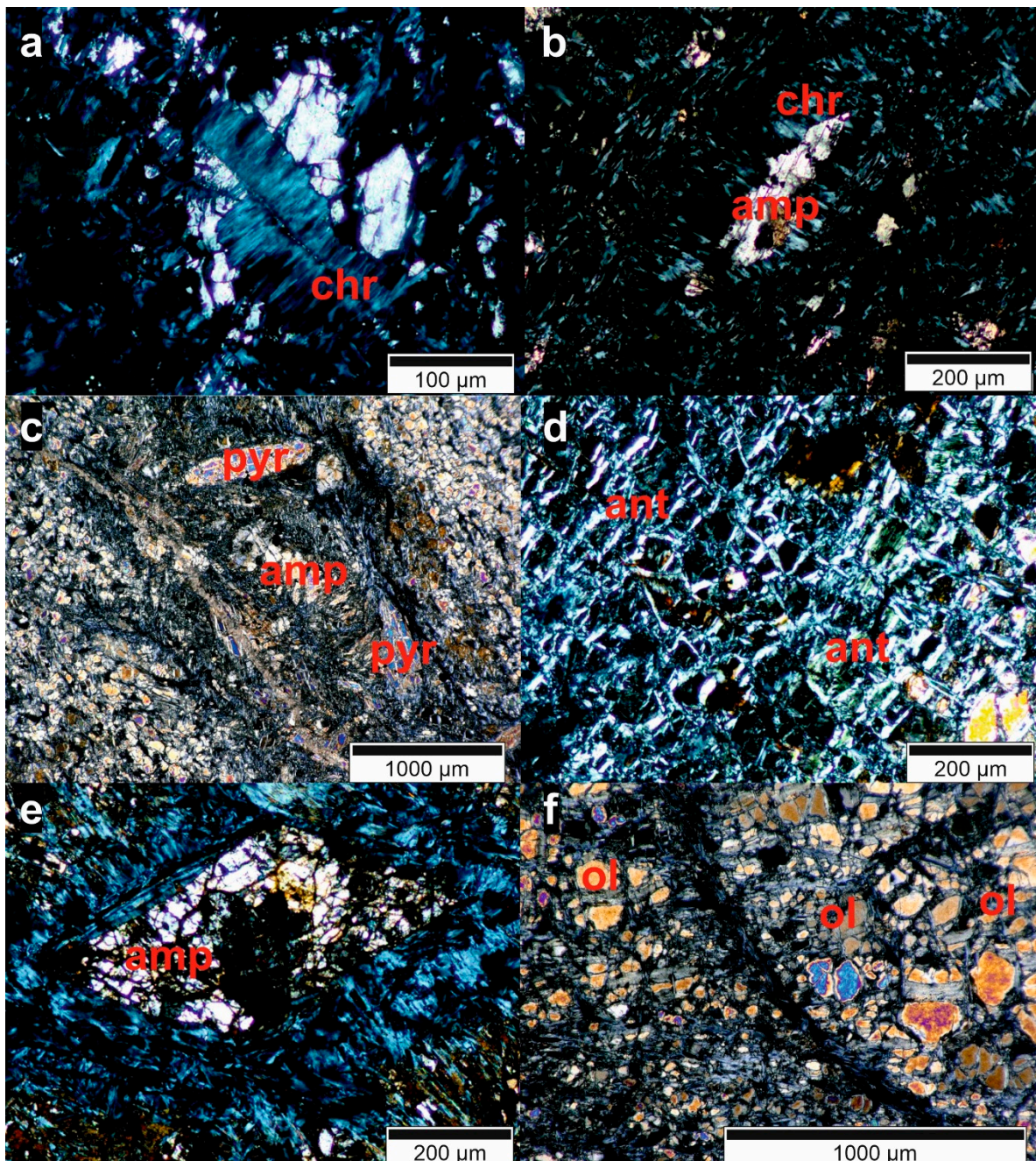


Figure 14. Microscopic photos of the thin sections related to the sample numbers: (a) + (b) = D-07; (c) = D-08.1; (d) = D-08.2; (e) = D-09; (f) = D-10 (ol = olivine, ant = antigorite, chr = chrysotile, pyr = pyroxene, amp = amphibole, chl = chlorite, op = opaque phase) [34].

Chlorite (Figure 13e) is found in all samples. It is a common mineral in metamorphized ultramafic rocks and, therefore, was expected to appear in the Medellín Dunite [35]. It is also a weathering product of silicates such as olivine [35].

Sample D-07 also contains several quartz veins. These veins are created by precipitation of SiO_2 in fractures. The SiO_2 is dissolved in water circulating in the fractures, its origin lies in other silicate minerals in the rock (olivine, pyroxene, amphibole, etc.).

Samples D-01, D-04, D-05, D-06 and D-09 contain small amounts of goethite. Goethite is a $\text{FeO}(\text{OH})$ mineral formed by weathering of iron containing minerals like pyroxene, amphibole and olivine and, therefore, its presence in the Medellín Dunite is to be expected.

The differences in the mineral content show that the Medellín Dunite is not homogeneous regarding its mineralogical composition. Serpentine, olivine and chlorite seem very common, but other samples were free of one of those minerals. Additionally, the domination of serpentine in the rock suggests that the dunite has already been transformed into a serpentinite.

Since all samples were taken from the surface without knowledge of their origin in the slope but as typical representative specimens of the rock material, there is no possibility of correlating the results with the sampling location.

3.4.2. X-ray Diffraction Analysis

The analysis of the X-ray diffraction was conducted in collaboration with a Bachelor's thesis [36] supervised within the project. The mineral content of the 8 analyzed samples is depicted in Table 5 [36]. All samples contain chlorite, amphibole (tremolite), quartz and hematite. Except for sample L-07, goethite is present in all samples; serpentine (lizardite) is missing only in samples L-05 and L-07. Other minerals that were found in some samples are gibbsite, magnetite and olivine (forsterite).

Table 5. Results of the X-ray diffraction [36].

Mineral \ Sample	L-01	L-02	L-03	L-04	L-05	L-06	L-07	L-08
Chlorite	X	X	X	X	X	X	X	X
Amphibole (tremolite)	X	X	X	X	X	X	X	X
Serpentine (lizardite)	X	X	X	X		X		X
Gibbsite	X					X		
Magnetite						X		
Quartz	X	X	X	X	X	X	X	X
Goethite	X	X	X	X	X	X		X
Hematite	X	X	X	X	X	X	X	X
Olivine (forsterite)								X

All minerals found in the samples are to be expected in weathered material of ultramafic rocks. The quartz content seems uncharacteristic at first sight. Quartz, however, is very resistant to weathering and, therefore, even a very small amount of it (veins in the rock, see Section 3.4.1) is enriched very fast in its weathering material. Another source of quartz could be construction sand. Since the study site is located in a densely populated area, the contamination of the samples by anthropogenic material like this sand is very likely.

The lack of olivine in most samples shows the high degree of serpentinization of the rock and the fast degradation of the remaining olivine during weathering.

Serpentine and magnetite are not found in all of the samples; they could already be completely dissolved by weathering. The serpentine is mostly lizardite, which forms in the presence of meteoric-hydrothermal water [35], which fits this setup.

Hematite, goethite (iron oxides), chlorite (iron/aluminum hydroxide) and gibbsite (aluminum hydroxide) are typical weathering products of iron containing minerals. The absence of some of the minerals in some samples indicates different educts, which underlines the theory of the inhomogeneous composition of the Medellín Dunite.

Sample L-07 differs the most from the others. It also contains a small amount of a swelling clay mineral, most likely nontronite. This difference could be due to its remote sampling location separated from the other samples (see Figure 3).

There is no pyroxene found in any of the samples. Pyroxenes are very hard to detect in X-ray diffraction, since their peaks are not very precise but have a range. Their peaks could also be overlapping with the peaks of other minerals.

All samples, also sample L-07, were taken in an anthropogenically highly altered region. Therefore, a contamination, as well as a content of external minerals could not be excluded completely.

4. Discussion

The landslide feature map shows only small-sized (max. 15,000 m²) and shallow to mid-seated (max. 10 m) landslides. A former, deep-seated landslide could not be excluded, but is nevertheless not very likely. These observations fit into the descriptions of landslides in the eastern slope of Medellín of the past decades [37]. The most devastating landslide in Medellín was the Villatina landslide in 1987, which caused at least 217 casualties [38], according to other sources, even 500 [39]. It was only 1.0–8.0 m deep but had 20,000–40,000 m³ of volume [38–40]. This indicates that the landslides in the Medellín Dunite are, in fact, mostly shallow to mid-seated ones as registered in the current map. Still, the possibility of a deep-seated landslide is not ruled out completely.

According to the field observations, the soil material at the surface consists almost entirely of the grain sizes of clay and silt. Gravel and sand are absent or only present at some areas in small amounts. This indicates weathering rather than mechanical fragmentation of the rock.

As depicted in Figures 6 and 7, the thickness of the soil below the surface hardly reaches 2 m, except for drilling B1. This was very unexpected and underlines the importance of a detailed and exhaustive investigation of the subsurface in the Medellín Dunite, since this unit shows extreme variations.

4.1. Discontinuity Sets

In the geological map, the parallel striking ridges of the dunite are very prominent. According to the general stress field of the region [41], this direction could be a tectonic structure (horst-and-graben structure). The main faults around Medellín (La Acuarela fault, Romeral fault, etc. [41]) strike NNW-SSE with a steep dipping, subvertically, towards WSW. The SW-NE striking structures of the dunite rock cross this fault system vertically with a mediate dipping of around 45° to NW, creating a perpendicular joint system.

At this point, the dipping of the joint systems recorded in the drilling cores could be parallelized with field observations in the outcrops at site (see Figures S1–S3 joint set columns).

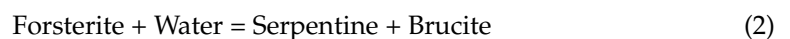
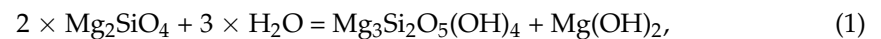
Joint set 2 (75–90°) correlates highly with the steep NNW-SSE striking fault system in the region but is highly underrepresented due to its vertical dipping angle. Joint set 3 (25–60°) correlates with the SW-NE striking, vertically crossing structure on the dunite rock surface. Even though the orientation of the joint sets cannot be observed in the drillings, the correlation is possible, since the dipping angles are very distinct (Figures S1–S3). The subhorizontal joint set (joint set 1) [12] also could be observed in the drillings (Figures S1–S3); it is the dominating joint set in all drillings.

4.2. Weathering Processes—Serpentinization and “Pseudokarst” Structures

The expected weathering profile of decreasing weathering stages with the depth was not observed in any of the three drillings (see Figures S1–S3 weathering profiles). However, the drillings did confirm the theory of block-in-matrix structures and especially pseudokarst-like cavities in the dunite body, as described by previous studies [12,15]. The core loss in the first 8.9 m of drilling B1 and the high ratio of core loss in all three drillings provide certain evidence of some smaller cavities in the rock mass. Additionally, the presence of large amounts of loose material in deep parts of the drillings indicate a high degree of water circulation within the rock along the pseudokarst structures and other fractures, accumulating the soil material in these cavities and contributing to the high degree of weathering at depth. This phenomenon also creates a block-in-matrix structure in the end.

In all drillings, a serpentinization, especially along fractures and joints, could be observed, besides oxidation processes (brown colored areas). According to literature dealing with weathering of ultramafic rocks [10,12–14], this serpentinization is a characteristic weathering process of dunite rock. Normally, serpentinization only takes place in hydrothermal regimes with water temperatures above 100 °C [35]. Antigorite can only be

formed above 250 °C [35]. However, since we do observe antigorite and chrysotile in the thin sections, but only lizardite in the X-ray diffraction, lizardite could be the serpentine mineral being formed during weathering processes of dunite rocks, while antigorite and chrysotile were created earlier during ocean floor metamorphosis in a hydrothermal process and are already weathered in the soil samples. This secondary serpentinization could also be the key process of forming the pseudokarst observed. Since pseudokarst is a solution weathering, it is very likely that this process works according to the following serpentinization equation:



Brucite has been found as crusts on the surface of the dunite rock in some parts of the Medellín Dunite [12], which underlines the theory of a solution weathering, solving the magnesium olivine forsterite in water circulating in fractures and a precipitation of brucite and the serpentine mineral lizardite in other places within the dunite body. This process would explain the typical karst structures on the surface and the subsurface (dolines, karren, karst caves) as well as the deep weathering of the rock to a depth of at least 60 m [12,15].

The outcomes of the laboratory tests conducted on the samples of the drilling cores show generally no correlation with the depth of the drilling or the drilling locations. This underlines the extreme heterogeneous structure and behavior of the Medellín Dunite. A common weathering profile (decreasing weathering with increasing depth) would show increasing compressive strength, tensile strength and grain sizes with increasing depth [13,14]. Despite the missing correlation between the depth and the values of the rock test results, the values do vary extremely with 10 MPa–132 MPa for uniaxial compressive strength and 4.1 MPa–17.5 MPa for tensile strength. Most samples showing low values were already expected to be weak because of their weathering or serpentinization. However, some samples showed no alteration on the outside, but still had low values in the compressive and tensile strength tests. This shows a varying internal disintegration of the rock's structure without visible weathering signs even in seemingly intact bedrock to a depth of at least 50 m. Disintegrated rock without oxidation or visible weathering is also observed in the drilling B1 in the homogeneous area 6. These samples seem to be fractured formerly intact rock parts, but can be crushed by hand, indicating an advanced weathering throughout this part of the dunite body without any visible evidence of weathering or tectonic damage already before weathering. However, these parts of the rock show a high degree of serpentinization. In this case, this could be secondary or weathering serpentinization, as mentioned above, which disintegrates the whole rock without oxidation or degradation into clay minerals.

The soil tests also show no correlation of depth with grain size and plasticity of the fine material. Highly plastic soil is distributed throughout the depth of the dunite, cumulating in fractures and pseudokarst caves, which indicates that it originates in weathering of the rock. The loose material is not only oxidized but also shows green colors or no discoloration at all. The green areas could contain lizardite and chlorite, since both minerals are weathering products of the serpentinized dunite rock and show light green colors [35]. Most soil samples provide a high content of fine material, as already observed during field work. This is also visible in the drilling cores since the cores either show intact rock parts or completely disintegrated loose material that does not contain high amounts of gravel. This indicates that the loose material was not formed by tectonic forces (which would have produced gravel and sand alike), but primarily by weathering processes. The plastic behavior of some samples suggests a considerable amount of swelling clay minerals.

Due to the low amount of shear tests possible, the results are only taken into account for understanding coherences. The value gained for the friction angle (24°) and the cohesion (39 kPa) underline some of the results of the Atterberg limits tests, showing a strongly cohesive soil.

4.3. Thin Section Analysis and X-ray Diffraction Analysis

The mineralogical composition observed in the thin sections of some rock samples is coherent with previous data [2–10,12]. Most parts of the samples are highly serpentinized, antigorite and chrysotile can be distinguished easily, and lizardite could not be found. Therefore, pyroxene, amphibole and olivine (forsterite) are already being transformed to varying degrees, depending on the sample. These differences in the samples regarding the ratio of olivine (forsterite), amphibole and pyroxene and the degree of serpentinization are severe, i.e., amphibole and pyroxene are already dissolved in some samples. The weathering of the material could also be observed, the minerals are mostly transformed into the iron oxide goethite. Even though the presence of olivine in all samples indicates an originally high amount of this mineral in the rock, the amphibole and pyroxene found in most samples indicate that the rock is, in fact, not exactly a dunite, but rather a peridotite. The high degree of serpentinization, however, provides evidence that the unit is mostly made up of serpentinite and not peridotite, harzburgite or dunite.

In the X-ray diffraction, lizardite was found, but no antigorite or chrysotile, indicating a transformation of those two serpentine minerals and the forming of lizardite, possibly by weathering processes. This might underline the theory of a second serpentinization by weathering [10,12–14], as explained above. All other minerals observed in the X-ray diffraction were expected after reviewing the thin sections. The quartz in the soil samples could also originate in contamination by construction material in this highly populated area, since it was only found in one thin section but in all the samples taken for the X-ray analyses.

4.4. Consequences in the Context of Landslide Hazard Assessment

The consequence of the mineralogy, structure and behavior of the Medellín Dunite discussed above is the landslide probability in the area. Landslides occur predominantly where the rock mass is fragmented by joints and pseudokarst filled with soil [12]. This block-in-matrix structure is created by weathering, whose local intensity (and, therefore, the locally differing amount of soil) is influenced by the mineralogical composition. The thicker and finer the soil (matrix) between the blocks, the higher the probability of a shear surface developing in the soil layer. The probability increases due to water saturation during rainy season or due to anthropogenic reasons, e.g., a leakage in the water pipe system. Since the unit of the Medellín Dunite is so heterogeneous, it is impossible to forecast the location, size, depth and velocity of a landslide event. Therefore, the subsurface has to be investigated and monitored in a high level of detail, especially regarding its structure and composition. To achieve the goal of an improved understanding of the subsurface in the study area, more drillings need to be conducted to obtain the best knowledge possible about the real conditions.

The friction angle of 24° of the fine material derived from the shear test is within the scope of the landslides registered in the past in the Medellín Dunite (SIMMA database). Most of the registered landslides showed an angle of 20–25°. The Villatina landslide, for example, occurred at an angle of 25° at the tear-off edge [40]. However, since the shear test could only be conducted on two samples, further tests need to be done to determine a critical friction angle.

5. Conclusions

All mappings and tests conducted indicate a very heterogeneous composition and a diverse behavior of the Medellín Dunite:

- The Medellín Dunite shows variations in its primary mineralogical composition and, therefore, its alteration by serpentinization over short distances and depths.
- Three joint sets could be observed in the drillings that can be correlated with surface structures and known fault and joint systems in the region.
- Both above mentioned predispositions influence the deep weathering of the dunite along fractures. Olivine usually is the most unstable mineral in ultramafic rocks and

is the first one to be weathered, as observed in this investigation. When looking at the rock and the soil samples, the olivine is mostly already decomposed or heavily altered by serpentinization and weathering. Therefore, the parts of the Medellín Dunite containing more olivine are weathered faster.

- One weathering characteristic of the Medellín Dunite might be a secondary serpentinization caused by water circulation, primarily creating lizardite and brucite. Indications of this process have been observed in the drilling cores and by comparing the minerals of the rock and the soil samples.
- The pseudokarst observed in the region of the Medellín Dunite and in the current drilling cores might be created by this secondary serpentinization. This phenomenon forms along existing fractures and causes a large number of cavities of different sizes up to 1 m width. The pseudokarst features promote the high water conductivity in the rock mass and, therefore, the high weathering degree in the whole dunite body, reaching a depth of at least 60 m.
- Created by weathering, former landslides and pseudokarst processes, the block-in-matrix structure is the main landslide prone unit at the study site. Its soil content is not as high as expected, but the soil material exists even with increasing depth, is very fine and is therefore suggested to act as a shear surface for landslides, especially when water saturated, even with a low thickness of only a few centimeters.
- A critical friction angle of 20–25°, as most of the former landslides in the SIMMA database, is also to be expected at the study site, as the results from the shear test suggest.
- The transfer of the early warning system created on the basis of the geological findings to other geologically similar study sites is possible. However, a profound investigation of the subsurface in every further area, where the early warning system is to be installed, is indispensable.
- The approach of establishing detailed base data for a Low Cost Early Warning System (LEWS) in deeply weathered ultramafic rock masses is suggested to be applicable to further landslide prone areas.

Supplementary Materials: The following are available online at <https://www.mdpi.com/article/10.3390/ijerph182111141/s1>, Figure S1: Analysis drilling A1, Figure S2: Analysis drilling A2, Figure S3: Analysis drilling B1.

Author Contributions: Conceptualization, T.B.; methodology, T.B.; validation, B.M., A.D., M.G. and K.T.; formal analysis, T.B.; investigation, T.B. and M.G.; resources, T.B.; data curation, T.B. and A.D.; writing—original draft preparation, T.B.; writing—review and editing, B.M., A.D., M.G. and K.T.; visualization, T.B. and A.D.; supervision, K.T.; project administration, T.B.; funding acquisition, T.B., B.M. and K.T. All authors have read and agreed to the published version of the manuscript.

Funding: This research was funded by the Federal Ministry of Education and Research Germany, grant number 03G0883A-F.

Institutional Review Board Statement: Not applicable.

Informed Consent Statement: Not applicable.

Conflicts of Interest: The authors declare no conflict of interest.

References

1. Thuro, K.; Singer, J.; Menschik, B.; Breuninger, T.; Gamperl, M. Development of an early warning system for landslides in the tropical Andes (Medellín; Colombia). *Geomech. Tunn.* **2020**, *13*, 103–115. [[CrossRef](#)]
2. Botero, G. Contribución al conocimiento de la geología de la zona central de Antioquia. *Univ. Nac. Colomb. An. Fac. Minas* **1963**, *57*, 101.
3. Álvarez, A.J. Tectonitas dunitas de Medellín, departamento de Antioquia, Colombia (Informe1896). *Ingeominas Intern. Rep.* **1982**, *28*, 13–44.

4. Restrepo, J.J.; Toussaint, J.F. Unidades litológicas de los alrededores de Medellín. In Proceedings of the Primera Conferencia Sobre Riesgos Geológicos del Valle de Aburrá, Medellín, Colombia, 3–6 December 1984; Sociedad Colombiana de Geología: Bogotá, Colombia, 1984; pp. 1–26.
5. Agudelo, J.Á. Tectonitas dunitas de Medellín, departamento de Antioquia, Colombia. *Boletín Geológico* **1987**, *28*, 9–44.
6. Rodríguez, G.; González, H.; Zapata, G. *Memoria explicativa: Geología de la plancha 147 Medellín Oriental. Scale: 1:100,000*; Ingeominas: Bogotá, Colombia, 2005.
7. Correa-Martínez, A.M. Petrogênese e evolução do Ofiolito de Aburrá, Cordilheira Central dos Andes Colombianos. Ph.D. Thesis, Universidade de Brasília, Brasília, Brazil, 2007.
8. Restrepo, J.J. Obducción y metamorfismo de ofiolitas triásicas en el flanco occidental del Terreno Tahamí, cordillera Central de Colombia. *Boletín Cienc. Tierra* **2008**, *22*, 49–100.
9. Hernández-González, J.S. Mineralizaciones de Cr y elementos del grupo del platino (EGP) asociadas a las Metaperidotitas de Medellín, Colombia. Master's Thesis, Universidad de Barcelona and Universidad Autónoma de Barcelona, Barcelona, Spain, 2014.
10. Garcia-Casco, A.; Restrepo, J.J.; Correa-Martínez, A.M.; Blanco-Quintero, I.F.; Proenza, J.A.; Weber, M.; Butjosa, L. The petrologic nature of the “Medellín Dunite” revisited: An algebraic approach and proposal of a new definition of the geological body. In *The Geology of Colombia—Publicaciones Geológicas Especiales 36*; Gómez, J., Pinilla-Pachon, A.O., Eds.; Volume 2 Mesozoic; Servicio Geológico Colombiano: Bogotá, Colombia, 2020; pp. 45–75. [[CrossRef](#)]
11. Breuninger, T.; Gamperl, M.; Menschik, B.; Thuro, K. First Field Findings and their Geological Interpretations at the Study Site Bello Oriente, Medellín, Colombia (Project Inform@Risk). In Proceedings of the 13th International Symposium on Landslides, Cartagena, Colombia, 22–26 February 2021.
12. Tobón-Hincapié, M.P.; Joya-Camacho, A.M.; Marcías-Torres, C.E.; Gomez-Gallo, M.H.; Zapata-Wills, C.; Velásquez, A. *Medidas de Mitigación de la Ladera Oriental del Valle de Aburrá entre las Quebradas La Poblada y La Sanín*; Alcaldía de Medellín-Secretaria del Medio Ambiente: Medellín, Colombia, 2011; p. 218.
13. Ündül, Ö.; Tuğrul, A.; Özyalın, Ş.; Zarif, İ.H. Identifying the changes of geo-engineering properties of dunites due to weathering utilizing electrical resistivity tomography (ERT). *J. Geophys. Eng.* **2015**, *12*, 273–281. [[CrossRef](#)]
14. Ündül, Ö.; Tuğrul, A. On the variations of geo-engineering properties of dunites and diorites related to weathering. *Environ. Earth Sci.* **2016**, *75*, 1326. [[CrossRef](#)]
15. Rendón-Giraldo, D.A.; Departamento de Geociencias y Medio Ambiente, Universidad Nacional de Colombia, Medellín, Antioquia, Colombia. Personal Communication, 18 November 2020.
16. Breuninger, T.; Garcia-Londoño, C.; Gamperl, M.; Thuro, K. Initial Experiences of Community Involvement in an Early Warning System in Informal Settlements in Medellín, Colombia. In *Understanding and Reducing Landslide Disaster Risk—Volume 1 Sendai Landslide Partnership and Kyoto Landslide Commitment*; Sassa, K., Mikoš, M., Sassa, S., Bobrowsky, P.T., Takara, K., Dang, K., Eds.; Springer International Publishing: Cham, Switzerland, 2021; pp. 597–602. [[CrossRef](#)]
17. Singer, J.; Thuro, K.; Gamperl, M.; Breuninger, T.; Menschik, T. Technical Concepts for an Early Warning System for Rainfall Induced Landslides in Informal Settlements. In *Understanding and Reducing Landslide Disaster Risk—Volume 3 Monitoring and Early Warning*; Casagli, N., Tofani, V., Sassa, K., Bobrowsky, P.T., Takara, K., Eds.; Springer International Publishing: Cham, Switzerland, 2021; pp. 209–215.
18. Deere, D.U. Technical description of rock cores for engineering purposes. In *Rock Mechanics and Engineering Geology*; Springer: Vienna, Austria, 1963; Volume 1, p. 18.
19. ASTM International. *ASTM D 7012—14e1 Standard Test Methods for Compressive Strength and Elastic Moduli of Intact Rock Core Specimens under Carrying States of Stress and Temperatures*; ASTM International: West Conshohocken, PA, USA, 2014.
20. ASTM International. *ASTM D 3967 Standard Test Method for Splitting Tensile Strength of Intact Rock Core Specimen*; ASTM International: West Conshohocken, PA, USA, 2016.
21. INV E 123 Análisis Granulométrico de Suelos por Tamizado. 2013. Available online: https://www.invias.gov.co/index.php/archivo-y-documentos?task=doc_download&gid=2740 (accessed on 19 October 2021).
22. INV E 125 Determinación del Limite Liquido de los Suelos. 2013. Available online: https://www.invias.gov.co/index.php/archivo-y-documentos?task=doc_download&gid=2740 (accessed on 19 October 2021).
23. INV E 126 Límite Plástico e Índice de Plasticidad. 2013. Available online: https://www.invias.gov.co/index.php/archivo-y-documentos?task=doc_download&gid=2740 (accessed on 19 October 2021).
24. INV E 154 Determinación de la Resistencia al corte Metodo de Corte Directo (CD) (Consolidado Drenado). 2013. Available online: https://www.invias.gov.co/index.php/archivo-y-documentos?task=doc_download&gid=2740 (accessed on 19 October 2021).
25. Hungr, O.; Leroueil, S.; Picarelli, L. The Varnes classification of landslide types, an update. *Landslides* **2014**, *11*, 167–194. [[CrossRef](#)]
26. Bundesamt für Raumplanung BRP, Bundesamt für Wasserwirtschaft BWW, Bundesamt für Umwelt, Wald und Landschaft BUWAL. *Empfehlungen 1997—Berücksichtigung der Massenbewegungsgefahren bei Raumwirksamen Tätigkeiten*. Bern, Switzerland, 42. Available online: https://www.planat.ch/fileadmin/PLANAT/planat_pdf/alle_2012/1996-2000/Lateltin_19_97_-_Beruecksichtigung_der_Massenbewegungsgefahren_bei_raumwirksamen.pdf (accessed on 19 October 2021).
27. Demharter, A. Geologisch-geotechnische Charakterisierung des “Medellín-Duniten” am Osthang der Stadt Medellín, Kolumbien. Master's Thesis, Technical University of Munich, Munich, German, 2021. Unpublished.

28. IAEG—International Association of Engineering Geology. Rock and soil description and classification for engineering geological mapping—Report by the IAEG Commission on Engineering Geological Mapping. *Bull. Int. Assoc. Eng. Geol.* **1981**, *24*, 235–274. [[CrossRef](#)]
29. Beuth. *DIN EN ISO 14689 Geotechnische Erkundung und Untersuchung; Benennung, Beschreibung und Klassifizierung von Fels*; Teil 1: Benennung und Beschreibung; Beuth: Berlin, Germany, 2018.
30. Beuth. *DIN EN ISO 14688-1 Geotechnische Erkundung und Untersuchung; Benennung, Beschreibung und Klassifizierung von Boden*; Teil 1: Benennung und Beschreibung; Beuth: Berlin, Germany, 2020.
31. Beuth. *DIN 18196 Erd-und Grundbau—Bodenklassifikation für Bautechnische Zwecke*; Beuth: Berlin, Germany, 2011.
32. ASTM International. *ASTM D 2487—17e1 Standard Practice for Classification of Soils for Engineering Purposes (Unified Soil Classification System)*; ASTM International: West Conshohocken, PA, USA, 2017.
33. Prinz, H.; Strauss, R. *Ingenieurgeologie*, 6th ed.; Springer International Publishing: Cham, Switzerland, 2018; p. 738.
34. Ambos, P. Petrographische Analyse der Ultramafischen Gesteine am Osthang der Stadt Medellín. Bachelor's Thesis, Technical University of Munich, Munich, Germany, 23 September 2020. Unpublished.
35. Aillaud, J.C.; Proust, D.; Righi, D. Weathering Sequences of Rock-Forming Minerals in a Serpentinite: Influence of Microsystems on Clay Mineralogy. *Clays Clay Miner.* **2006**, *54*, 87–100. [[CrossRef](#)]
36. Ziegler, J. XRD Analysis of the Weathered Material from the Igneous Rocks on the Eastern Slope of Medellín (Inform@Risk). Bachelor's Thesis, Technical University of Munich, Munich, Germany, 5 October 2020. Unpublished.
37. Werthmann, C.; Echeverri, A.; Vélez, A.E. *Rehabitar La Ladera: Shifting Ground*, 1st ed.; Universidad EAFIT: Medellín, Colombia, 2012; p. 135.
38. Tokuhiro, H. Landslide in Villa Tina, Medellín City, Colombia. *Jpn. Landslide Soc. Landslide News* **1988**, *2*, 12–13.
39. Ojeda, J.; Laurence, D. Landslides in Colombia and their impact on towns and cities. In Proceedings of the 10th Congress of the International Association for Engineering Geology and Environment, Engineering Geology for Tomorrow's Cities, Nottingham, UK, 6–9 September 2006; London Geological Society: London, UK, 2009; Volume 112, p. 13.
40. Hermelín, M. (Ed.) *Desastres de Origen Natural en Colombia 1979–2004*, 1st ed.; Universidad EAFIT Medellín: Medellín, Colombia, 2005; pp. 55–64.
41. Colmenares, F.; García, L.R.; Sánchez, J.M.; Ramirez, J.C. Diagnostic structural features of NW South America: Structural Cross Sections based upon detailed field transects. In *Geology and Tectonics of Northwestern South America*, 1st ed.; Cediél, F., Shaw, R.P., Eds.; Springer International Publishing: Cham, Switzerland, 2019; pp. 651–672. [[CrossRef](#)]

Appendix B-3

Title	Cost estimation for the instrumentalization of Early Warning Systems in landslide prone areas				
Journal	NHES				
DOI	https://doi.org/10.5194/nhess-2023-41				
Year	2023	Volume	-	Impact Factor (2023)	4.6
Accepted	Yes	Position of the candidate in the authors list			2
Authors	Marta Sapena, Moritz Gamperl, Marlene Kühnl, Carolina Garcia-Londoño, John Singer, Hannes Taubenböck				

This article was submitted to Natural Hazards and Earth System Sciences; Marta Sapena, Moritz Gamperl, Marlene Kühnl, Carolina Garcia-Londoño, John Singer, Hannes Taubenböck; Cost estimation for the instrumentalization of Early Warning Systems in landslide prone areas; Copyright 2023 by the authors. This article is an open access article distributed under the terms and conditions of the Creative Commons Attribution (CC BY) license, thus permission to reprint the article is not necessary.



Cost estimation for the monitoring instrumentalization of Landslide Early Warning Systems

Marta Sapena¹, Moritz Gamperl², Marlene Kühnl^{1,3}, Carolina Garcia-Londoño^{4,5}, John Singer⁶, Hannes Taubenböck^{1,7}

5 ¹German Aerospace Center (DLR), German Remote Sensing Data Center (DFD), Münchnerstrasse 20, 82234 Weßling, Germany

²Technical University of Munich, Chair of Engineering Geology, Arcisstrasse 21, 80333 München, Germany

³Company for Remote Sensing and Environmental Research (SLU), Kohlsteinerstrasse 5, 81243 München, Germany

⁴Leibniz Universität Hannover, Institut für Landschaftsarchitektur, Herrenhäuserstrasse 2a, 30419 Hannover, Germany

10 ⁵Geological Society of Colombia, Colombia

⁶AlpGeorisk, Donauwörth, Germany

⁷Institute for Geography and Geology, Julius-Maximilians-Universität Würzburg, 97074 Würzburg, Germany

Correspondence to: M. Sapena (marta.sapena-moll@dlr.de)

Abstract. Landslides are socio-natural hazards. In Colombia, for example, these are the most frequent hazards. The interplay
15 of climate change and the mostly informal growth of cities in high-hazard areas increases the associated risks. Early warning
systems (EWSs) are essential for disaster risk reduction, but the monitoring component is often based on expensive sensor
systems. This study aims to develop a cost-effective method for low-cost and easy-to-use EWS instrumentalization in
landslide-prone areas identified based on data-driven methods. We exemplify this approach in the landslide-prone city of
Medellín, Colombia. We introduce a workflow to enable decision-makers to balance financial costs and the potential to protect
20 exposed populations. To achieve this, we first mapped city-level landslide susceptibility using data on hazard levels, landslide
inventories, geological and topographic factors using a random-forest model. We then combine the landslide susceptibility
map with a population density map to identify highly exposed areas. Subsequently, a cost function is defined to estimate the
cost of EWS-monitoring sensors at the selected sites, using lessons learned from a pilot EWS in Bello Oriente, a neighbourhood
in Medellín. Our study estimates that EWS monitoring sensors could be installed in several landslide-prone areas in the city
25 of Medellín with a budget ranging from €5 to €41 per person (roughly COP 23,000 to 209,000), improving the resilience over
190,000 exposed individuals, 81% of whom are located in precarious neighbourhoods; thus, they are a social group of very
high vulnerability. We provide recommendations for stakeholders on where to proceed with EWS instrumentalization based
on five different cost-effective scenarios. Finally, we discuss the limitations, challenges, and opportunities for the successful
implementation of an EWS. This approach enables decision-makers to prioritize EWS deployment to protect exposed
30 populations while balancing the financial costs, particularly for those in precarious neighbourhoods.



1 Introduction

The lives and livelihoods of billions of people around the world are disrupted by human-induced hazards worsened by climate change. The Intergovernmental Panel on Climate Change (IPCC) of the United Nations has recently reported that climate change is causing more frequent and severe storms, floods, droughts, wildfires, and other extreme weather events (IPCC, 2022).
35 This has global implications and poses several challenges to governments, societies, and science (Marchezini et al., 2018), with some geographic regions being more affected than others. For example, Colombia is one of the most landslide-prone countries in the world. The majority of its population lives in high and very high landslide hazard (Ruiz Peña et al., 2017). This is compounded by a higher frequency of heavy and continuous precipitation, and unplanned urban growth in high-risk areas due to land scarcity (World Bank, 2012), which increases the risk of disasters, particularly for the most vulnerable
40 populations.

As a result of a disaster, or to avoid the impact of an immediate natural hazard, people are sometimes forced to leave their places of residence. Displacement disrupts people's lives, creates unemployment, interrupts education, and reduces access to basic services, among many other things, which may lead to impoverishment and higher vulnerability. Preparedness measures are key to reducing displacement-related risks. These measures improve the risk-knowledge of people at risk of displacement
45 and empower them with informed decision-making and compliance with warnings (UNDRR, 2021). In fact, one of the seven global targets of The Sendai Framework for Disaster Risk Reduction 2015–2030 is to “*Substantially increase the availability of and access to multi-hazard early warning systems and disaster risk information and assessments to people by 2030*” (UN, 2015).

Early warning systems (EWSs) are a major element of disaster risk reduction. They can minimize the loss of lives and economic
50 and social impacts of disasters. Thus, they can be an alternative to relocating exposed populations, especially as this is economically unviable in most regions and often faces strong opposition from residents (Werthmann and Echeverri, 2013). However, beyond its technical implementation and maintenance, the effectiveness of an EWS depends on actively involving at-risk people, improving education and awareness of risks, efficiently disseminating messages and warnings, and ensuring preparedness (World Meteorological Organization, 2018).

55 Despite being a promising tool when well-integrated and properly managed, EWSs have several challenges, shortcomings, and untapped potentials: The monitoring components of EWSs are often based on expensive high-end sensor systems (e.g., multi-phase GNSS, GB-SAR, and tacheometry), which require highly trained personnel for their operation, and are specifically adapted to the local situation, preventing their transfer to other regions or countries. But there are also low-cost and easy-to-use sensor systems based on, e.g., MEMS tilt inclinometers and acceleration sensors, continuous shear monitor, and
60 piezometers. These geosensors, installed locally in a network, can provide valuable information about the surface and subsurface processes on landslide-prone slopes (Thuro et al., 2014; Uchimura et al., 2015; Singer et al., 2021). Their combination with data analyses and numerical landslide process models (Huggel et al., 2010; Thiebes et al., 2014) has the



potential to improve the quality and reliability of hazard warnings and usability, as less manual work is required. An example is the low-cost subsurface monitoring system implemented in the Alps, at Sudelfeld in Bayrischzell, Germany, which operated from 2008-2014 and consisted of cost-efficient ground deformation measures, groundwater level, and precipitation monitoring (Singer and Thuro, 2006; Thuro et al., 2010). In general, the technology and affordability of slope monitoring have improved in recent decades, which now allows for a more widespread application also in low-income countries. Still to date, only a few slopes are being monitored continuously across the globe, some of which are site-specific EWS in Latin America. Publishing on experiences, challenges, and limitations, it is nevertheless rarely done, even less so in English. After all, there is a consensus that implementing EWSs in high-risk areas has not only the potential to reduce losses and damage from landslides worldwide (Grasso, 2014) but also economic benefits. There are estimates of the economic benefits of EWSs, especially in European countries, the United States and Japan (Hallegatte, 2012). For example, in Europe, the annual benefits of EWSs are estimated to be between 470 million and 2.8 billion Euros. Similarly, it has been estimated that the potential benefits in low-income countries, if similar EWSs were available, would reach a cost-benefit ratio between 4 and 35 with co-benefits (Hallegatte, 2012). However, to the authors' knowledge, the estimated cost of the monitoring instrumentalization of local and site-specific EWSs is mostly unknown or unpublished, despite being highly relevant for policy-makers on disaster risk reduction.

The purpose of an EWS is to reduce risk and improve preparedness for hazards in specific locations. Thus, it is imperative to identify hazard-prone areas, the location of people and assets in exposed locations, and their vulnerabilities. In this context, Earth Observation (EO) from in situ or remote sensors plays an important role in early warning, as well as in mapping and monitoring natural hazards (Grasso, 2014; Casagli et al., 2017). EO provides information that can be used, for example, to model the Earth's surface (Geiß et al., 2020), identify populations exposed and vulnerable to different natural hazards (Geiß et al., 2017; Müller et al., 2020; Kühnl et al., 2022), characterize building structural types for seismic risk analyses (Taubenböck et al., 2009; Aravena Pelizari et al., 2021), or develop a global flood monitoring system (Chini and the Global Flood Monitoring team, 2022). EO-derived data capture the shape of the terrain and the natural and built elements on it. Such information can be used to estimate landslide susceptibility at different regions and scales (Cantarino et al., 2019; Palacio Cordoba et al., 2020; Ospina-Gutiérrez and Aristizábal, 2021).

There are two common methods for deriving susceptibility maps using EO data: knowledge-driven and data-driven methods. Both methods consist of mathematical predictive models with different advantages and disadvantages. The most common knowledge-driven method is the multicriteria analytical hierarchy process (AHP) developed by Saaty (1980). AHP is based on weights assigned by an expert, which simplifies the decision-making process. AHP uses pairwise comparisons of the weights assigned to individual landslide conditioning factors, indicating their relative importance. The advantages of this method are that it does not require reference data and qualitative and quantitative variables can be used. However, its main disadvantage is that the results depend completely on the assigned weights and factors used. Thus, the method depends on the experience of the user and the potential to identify variables that are important for a special case. In addition, the quantitative factors are transformed into categories based on manually established thresholds, which also affects the final result. The result



is a qualitative map with different hazard levels (Günther et al., 2014; Skilodimou et al., 2019), which can only be evaluated if reference data are available. In contrast, several data-driven methods have been used to develop probabilistic susceptibility maps (e.g., logistic regression, discriminant analysis, or random forest). These consist of statistical methods that rely on reference data (e.g., landslide inventories) and independent variables or conditioning factors, (i.e., factors influencing landslide risks), which are used to identify their interconnected relationships with the reference data and predict landslide susceptibility based on the modelled relationships. The main disadvantage of these methods is that they require reference data, which are not always available, inaccurate, or often incomplete or outdated. Regarding the advantages, several conditioning factors can be used and, by means of statistical significance tests, only the important factors can be included in the model. In addition, non-parametric methods, such as random forest, can find nonlinear relationships between the reference data and the conditioning factors, and the normal distribution of the factors is not necessary (Breiman, 2001). Besides, most of the statistical methods can use qualitative and quantitative factors without the need to use thresholds for their categorization. The result is a probability map quantifying landslide susceptibility, which consists of continuous values between zero and one that can be further classified into hazard levels (e.g., Azarafza et al., 2021; Eiras et al., 2021). Previous studies have compared the performance of AHP and statistical methods, and the latter performed better (Erener et al., 2016; Ali et al., 2021; Vojtek et al., 2021). In this context, landslide inventories are essential tools for deriving empirical knowledge and creating and evaluating susceptibility landslide maps using statistical and multi-criteria methods.

According to the Administrative Department for Disaster Risk Management (*Departamento Administrativo de Gestión del Riesgo de Desastres*, DAGRD) in Medellín, between 2004 and 2018 more than 30 thousand potential mass movements, together with events related to flooding and forest fires, were reported in the populated areas of the city (DAGRD, 2018). In response to those risks, on the one hand, the Aburrá valley and the city of Medellín implemented an EWS (*Sistema de Alerta Temprana de Medellín y el Valle de Aburrá*, SIATA) to reduce the impact of these events. SIATA monitors real-time hydrological, meteorological, seismic, and geotechnical variables, to forecast natural and anthropic phenomena and to strengthen risk management in the territory (https://siata.gov.co/sitio_web/).

On the other hand, a unique local, site-specific, and low-cost participatory landslide EWS was implemented in a local community known as Bello Oriente by a research project called Inform@Risk (Werthmann et al., 2023). Bello Oriente is a settlement that was originally informally built on one of the eastern slopes of the city with high landslide hazard. The EWS includes a wireless network of sensors based on the Internet of Things (IoT) technologies that monitors movements in the subsurface and their effects on the built infrastructure (e.g. tilting, opening of cracks), groundwater levels, and other parameters that, in combination with weather variables and forecasts, are used to inform people about the level of risk. With this, the system aims to provide exposed people enough time to react in the case of an event and to improve their risk awareness and resilience.



For the above-mentioned reasons, we selected Medellín, Colombia, as the study area. Using lessons learnt from Bello Oriente and the Infom@Risk project, and assuming that sufficient financial resources are not available on an ad hoc basis for citywide instrumentation with EWSs, we develop a cost function which allows to weigh how much money, on which location(s), and
130 how many people can benefit from an EWS in landslide-prone areas. We propose a cost function based on landslide susceptibility, area, and built-up density to support decision-makers in evaluating the replicability and transferability of the system in other regions based on cost-effectiveness. The objectives of this study are: (1) to identify landslide-prone areas that are suitable for the implementation of EWSs with automatic monitoring sensors; (2) to determine a cost function based on topographic and socioeconomic parameters for the implementation of an EWS; and (3) to provide suggestions for decision-
135 makers on where to start with the implementation of new EWSs based on cost-effectiveness and prioritized areas.

2 Material and methods

In this section the developed workflow for a city-wide cost-effectiveness analysis for an EWS is introduced: First, we introduce the study area and datasets. Second, we explain how the landslide susceptibility map is derived, and how the exposed sites where the installation of an EWS is preferable can be preselected. Third, we calculate physical, social, demographic, and
140 infrastructure parameters for the preselected sites (i.e., in the pool of possible EWS installation) that support the selection of suitable sites (i.e., exposed sites that are suitable for the EWS installation). Lastly, we present the cost function which aims at prioritizing the installation based on cost-effectiveness (Figure 1).

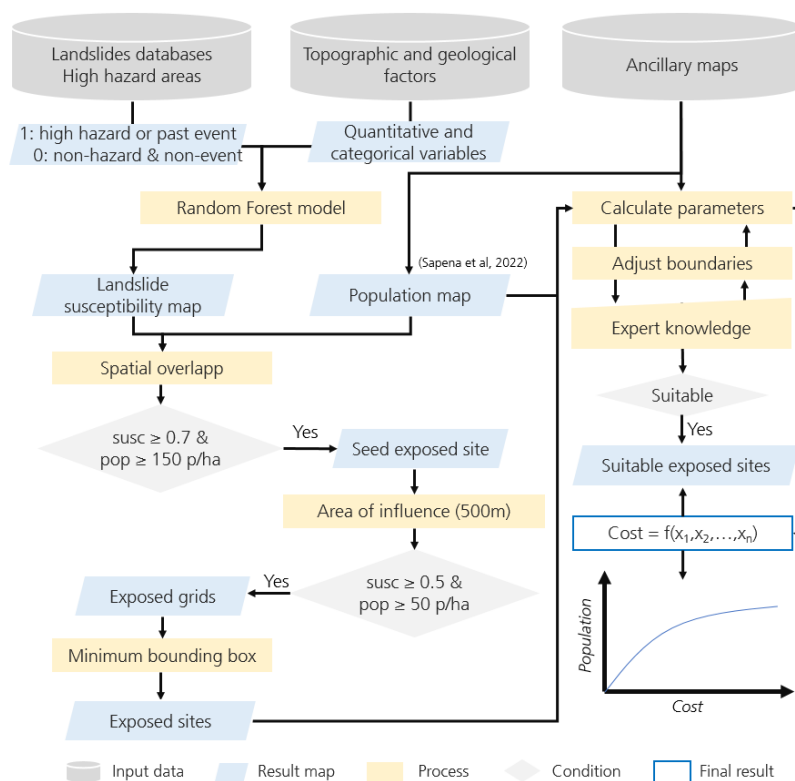


Figure 1. Workflow of the study.

145 **2.1 Study area**

This study is conducted in the city of Medellín, Colombia. Medellín is a highly populated city located in the Aburrá valley. It is characterized by a steep topography and a significant landslide risk especially at the eastern slopes of the city, where the prevailing heavily fractured dunite rock is predominant. The dunite is deeply and intensely weathered in tropical conditions due to its high iron content (Thuro et al., 2020). It is covered by colluvium material which was already moved by landslide processes and is now present in a block-in matrix structure with a thickness of between 5 meters to more than 30 meters (Breuninger et al., 2021). This colluvium clearly shows that substantial parts of the slope have been affected by landslides in the past and, because of the still steep topography the hills are prone to landslides.

Besides, a considerable amount of the population are exposed to landslide risks in Medellín, which has been increasing in the last 25 years (Kühnl et al., 2022). The city itself is shaped by different types of urban structural configurations and socioeconomic levels, from high-rise buildings in the business district and the wealthier neighbourhoods to light-weight and low-rise buildings in precarious neighbourhoods. The latter are mostly located in landslide prone areas (Kühnl et al., 2021). These factors cause large inequalities in risk exposure for different social groups.



2.2 Landslide inventories and hazard map

160 The long history of landslides in Medellín has resulted in several entities recording landslide events, causalities, and damage to buildings and infrastructure. There are three main databases where people report landslides (i.e., SIMMA, DesInventar and DAGRD).

First, SIMMA (*Sistema de Información de Movimientos en Masa*) is a national landslide inventory managed by the Colombian Geological Survey (*Servicio Geológico Colombiano*) (SIMMA, 2022). For the city of Medellín 13 landslide events with precise coordinates occurred between 1985 and 2013.

165 Secondly, DesInventar is an international Disaster Information Management System that helps to analyse disaster trends and their impacts (DesInventar, 2022). It includes information on space, time, type of event, causes, sources, as well as direct and indirect effects. In this study, we consulted the ‘Medellín Área Metropolitana’ database managed by the Universidad Nacional de Colombia with registers from the year 1880 to 2022. We found 21 landslides with precise coordinates in the municipality of Medellín from 2018 to 2022.

170 The third landslide inventory is managed by DAGRD. Occurred or foreseen landslides are registered by DAGRD based on emergency calls from citizens. This information is later evaluated by a technician from DAGRD. The department provided us with data for the period 2004 to 2018, which contains more than 30,200 reports of potential mass movements with their coordinates. The vast majority of the reports are located in the urban areas of the city, disregarding events in rural regions.

Beyond these databases on landslides, remote sensing data and techniques have proven suitable for landslide detection and mapping (Guzzetti et al., 2012), especially when inventories lack the spatial accuracy of the events. Consequently, we combine 175 for our approach the three inventories, and we complement the information with landslide locations in the urban-rural border and rural areas that we detect using remote sensing data. We use multi-temporal Landsat-7, Landsat-8 and Sentinel-2 imagery and apply change detection methods of vegetation indices in tentative areas based on landslides news articles. We follow the assumption that major changes in indices on steep slopes are related to significant variations in the soil surface or removal of 180 vegetation and might be caused by landslides (Mondini et al., 2011). We identify 8 landslides between 2008 and 2019.

The city of Medellín not only has an unprecedented number of mass movements inventories, but also the latest Master Plan from 2014 (*Plan de ordenamiento territorial*, POT 2014) includes the zoning of landslide hazards (Alcaldía de Medellín, 2014a). The hazard map is the result of the combined analysis of information available for the municipality, such as the hazard map from the POT 2006, a probabilistic hazard map from the Universidad Nacional, the DAGRD landslide inventory (up to 185 the year 2014), complemented by heuristic processes, field work and expert knowledge from DAGRD and the Administrative Department of Planning (*Departamento Administrativo de Planeación*, DAP) technicians. We use the mass movements inventories and the hazard map from the POT 2014 as reference data for modelling landslide susceptibility. We assume all



available reports are landslides, due to the lack of specifications about the type and considering that most mass movements in Medellín are landslides. These data are used to train and evaluate the model as further explained in section 2.4.

190 2.3 Factors influencing landslide risk

For modelling landslide susceptibility, we use topographic, geological, and precipitation factors, and to support the selection of suitable locations for the installation of EWSs, we rely on socio-demographic factors. Our database consists of the official cartography from open data platforms of the city of Medellín and the metropolitan area of the Aburrá valley (*Área Metropolitana Valle de Aburrá*, AMVA), such as ‘GeoMedellín’ (<https://geomedellin-m-medellin.opendata.arcgis.com/>) and
195 ‘Datos Abiertos del AMVA’ (<https://datosabiertos.metropol.gov.co/>). Besides, we use precipitation data from SIATA, OpenStreetMaps data to complement existing cartography, and ancillary maps from previous studies.

Regarding the topography, we derive several factors from contour lines. We use contour lines of different scales for urban (1:2,000) and rural areas (1:5,000) to generate a Triangular Irregular Network (TIN) surface. From this TIN the altitude is interpolated to create a Digital Elevation Model (DEM) with a spatial resolution of 5 meters. This the DEM is then used to
200 derive several topography-related factors such as slope, aspect, which indicates the downhill direction of the slope, and curvature, which shows the shape or curvature of the slope (Figure 2). Additionally, the DEM is used to model water flows and derive the stream network, stream order, landslide travel paths, and angle of reach of landslides (α , also known as ‘fahrböschung angle’), which shows the possible mobility of a landslide (Hungry et al., 2005). The stream network is extracted by setting a threshold of 500 pixels of water accumulation (i.e., water from at least 12,500 m² flows into the streams, assuming
205 no water loss). We tested several thresholds, both higher and lower, and 500 pixels proved to be the most appropriate compared to the POT drainage system, as it depends on the spatial resolution. The Strahler method (Tarboton et al., 1991) is used to classify the streams into numeric orders, differentiating between main streams as the major tributaries (order from 7 to 5), and other streams as the outermost tributaries (order from 4 to 1). Two Euclidean distance maps are created to measure the distance of a given pixel to the main streams and the other streams (Figure 2). Finally, the travel path and angle of reach of a landslide
210 are used as support in the selection of exposed sites to identify unpopulated areas in which landslides can be triggered and whose runout can reach into the inhabited area.

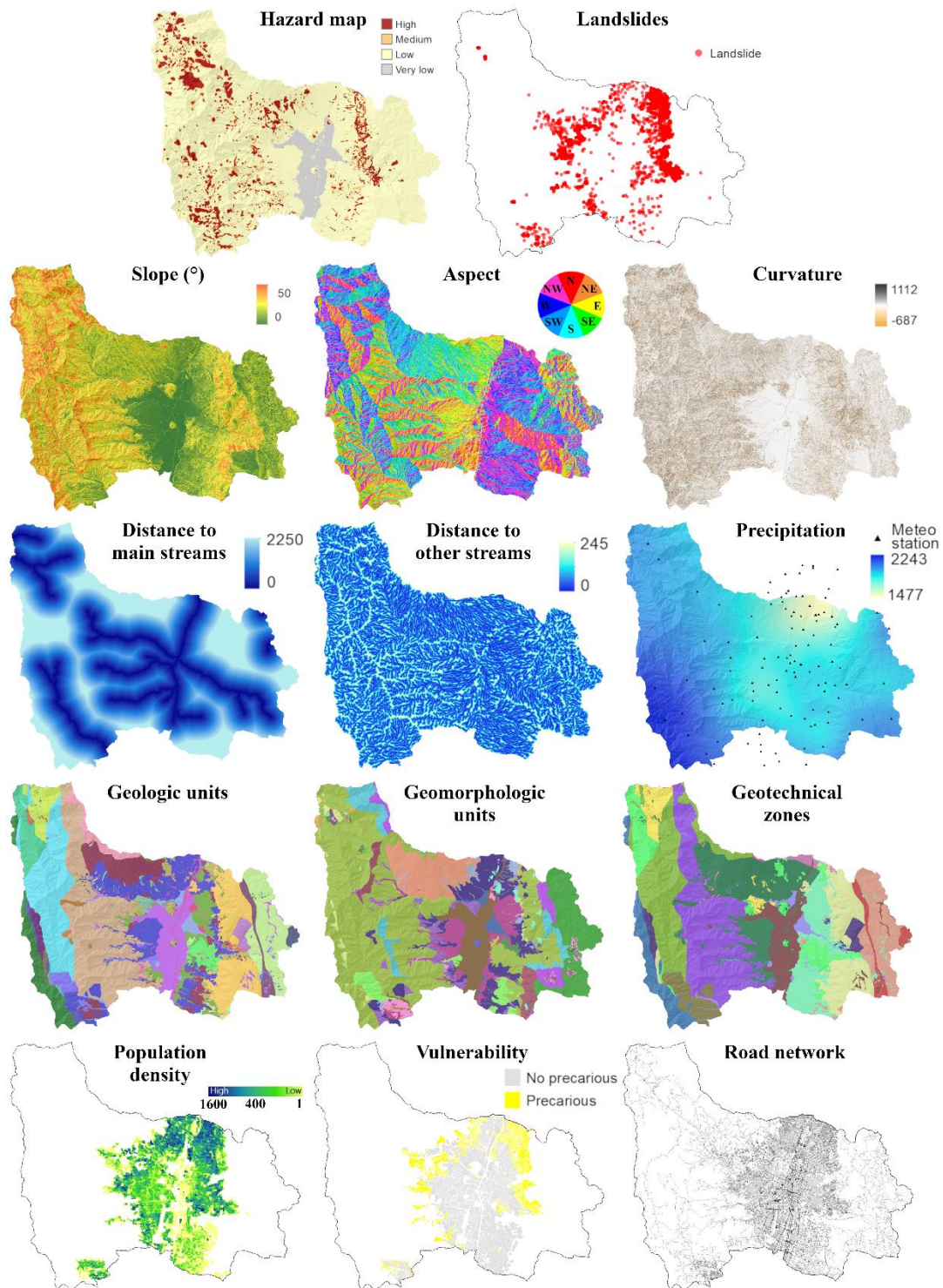
With regard to the geology, geomorphology and geotechnics of the study area, we collect data from ‘Datos Abiertos del AMVA’. We use three maps with categorical information on the geologic units, the geomorphologic units, and the geotechnical zoning. The surface geology is a relevant factor because it informs about the physical nature of the materials, their properties
215 and mechanical strength characteristics. Geomorphology shows the stability, slope, and shape of the landscape, while geotechnics provide information on the type of soil (Universidad Nacional de Colombia, 2009) (Figure 2).

Precipitation is an important triggering factor for landslides. Within the mountainous study area, the average yearly precipitation varies considerably due to local luv and lee effects. Thus, we use precipitation data from the meteorological



stations of SIATA (https://siata.gov.co/descarga_siata/index.php/index2/estaciones/). We download precipitation
220 measurements from 215 stations in the Aburrá valley for 2021. We calculate the accumulated precipitation over the year per
station and interpolate the station values to calculate a continuous map of accumulated precipitation with a spatial resolution
of 5 meters. We use the *Ordinary Kriging* and the *optimized smoothed* method, which provided a *root mean square error* of
506 mm (Figure 2).

When it comes to decisive factors for the suitability and prioritization of possible locations for implementing an EWS, we use
225 socio-demographic and infrastructure variables. First, we use a high resolution population map with the estimated number of
people per building and grid of 100 meters (Sapena et al., 2022). The population counts are used for identifying exposed sites
with high-density population and high landslide susceptibility. The calculated population and building density for these sites
is combined with data on the vulnerability of people based on the precarious conditions of the built-up areas (Kühnl et al.,
2021). This joint analysis allows us to prioritize exposed areas with higher vulnerability to disastrous events. Second, we
230 employ data on the road infrastructure, which is a relevant factor for the installation of sensors in the EWS. We complemented
the official road network cartography in ‘GeoMedellín’ with additional roads from OpenStreetMap (downloaded in 2022,
openstreetmap.org) (Figure 2).



235 **Figure 2.** Dependent variables in the model (hazard map and landslide events), independent variables or conditioning factors (topographic, geological, and precipitation), and ancillary data (socio-demographic and infrastructure).



2.4 Mapping landslide prone areas

In this study, we use baseline data on recent landslide events and an official hazard map for training a statistical model to predict the probability of landslide events based on several conditioning factors, which we refer to as landslide susceptibility. Hence, we leverage the best hazard map available at the city level, which includes local expert knowledge, and additionally, we feed the model with new data not included in the previous version (i.e., all landslides from SIMMA and RS, and landslides after 2015 from DesInventar and DAGRD). We create a set of sampling points within high-hazard zones (5,000 points), recorded landslide events (2,800 points) and non-hazardous areas, including medium, low or very low hazard zones (8,000 points). For each point, we add a numeric attribute with the dependent variable: high-hazard (1) and non-hazard (0), and the value of all conditioning factors explained in section 2.3 representing the independent variables in the model. Then, we split the sampling set into training (70%) and testing (30%) data. We use the non-parametric Random Forest (RF) algorithm (Breiman, 2001) with 100 trees, 3 variables at each split and 5 terminal nodes. The susceptibility map is calculated with the training data. The result is the probability of a pixel being high-hazard (1), which is calculated as the proportion of votes in the ensemble of trees. The testing data that did not participate in training the model is used for evaluating the model. We use the remaining testing set to measure the accuracy statistics.

2.5 Selection of exposed areas

We assign a zero susceptibility level to areas with slope equal to or lower than 10° in the resulting landslide susceptibility map, since these slopes are not considered hazardous for the specific case of Medellín (Alcaldía de Medellín, 2014b). Afterwards, we calculate the average susceptibility per 100-meter grid cell and combine the result with the population density per grid in order to select the exposed areas. For that, we focus on the urbanized area of Medellín, since it is the area with the most exposed elements and, we do not have population data for rural areas. We apply an iterative process as can be seen in Figure 1. First, we identify seeds of exposed sites with both, high susceptibility (≥ 0.7) and high population density (≥ 150 people/ha). If two or more seeds are contiguous or within 100 meters, the centroid is used as a seed. Second, we use the seeds as starting points and look in an area of influence of 500 meters, which is set to keep a similar size as the reference EWS in Bello Oriente, for pixels with medium to high susceptibility (≥ 0.5) and medium to high population density (≥ 50 people/ha). Hence, we identify all the surrounding pixels around the seeds that are also susceptible to landslides and populated. Third, we calculate the minimum bounding box for each cluster of pixels to automatically define a preselected exposed site. Fourth, we adapt the shape of the preselected sites based on the urban structure, topography, travel path and angle of reach of a landslide. Finally, we calculate the area, mean susceptibility, total population, population density, vulnerable population, built-up and road density, number of buildings, mean slope, main orientation of the slope, and open areas for the preselected sites, which are then used by experts to inspect and select the suitable exposed sites based on the requirements of the EWS and previous experience in Bello Oriente.



2.6 Developing a cost function

To estimate the costs of the monitoring instrumentalization of EWSs in suitable sites, we use the recently implemented EWS in Bello Oriente as a reference regarding the required manpower (working hours for the construction and installation of the sensor system), the required sensor density and types, as well as the cost of the individual sensors. The EWS in Bello Oriente covers an area of 39 hectares with a total population of 4,600 residents, from which 1,800 settle in a high-hazard zone of landslides. The EWS utilizes a novel wireless geosensor network based on IoT technologies (e.g., LoRa® wireless data communication and MEMS sensors) and 1,100 meters of Continuous Shear Monitor (Thuro et al., 2010) measurement cable and extensometers to monitor subsurface movements and the near-surface groundwater levels as basis for the generation of warnings. As the exact location of future landslides cannot be predicted based on the geological investigations, an area wide coverage with high spatial and temporal density of observation is required. The wireless geosensor network in Bello Oriente thus consists of 111 sensor nodes, of which about 45 monitor subsurface deformation and groundwater levels (Inform@Risk Subsurface Measurement Nodes) and 70 detect movement of existing built infrastructure (Inform@Risk Infrastructure Nodes). The spacing of sensors is adjusted based on the level of landslide risk, with high-risk areas having approximately 8 sensors per hectare and areas with no risk having no sensors. The sensor nodes are developed as open source and can be reproduced using the published PCB schematics, 3D printing models, and building instructions (Gamperl et al., 2023). Details about the measurement system are described in Gamperl et al., (2021) and Singer et al., (2021) and on the Inform@Risk Wiki (www.informatrisk.com).

It is important to emphasize that we currently only include the implementation of the wireless geosensor network in the cost function. The costs regarding the risk evaluation, social interventions, dissemination, continuous maintenance, and social work are not included. The CSM-EXT measurement system was excluded, because it was found to be very complex and costly to install in a densely populated area. Consequently, its usability for widespread installation is limited and whether its implementation is a viable and cost-effective alternative to the wireless sensor network has to be assessed based on a detailed survey on-site. The costs of the social work are also highly site specific and depend on many factors as e.g., whether the municipality decides to do a risk assessment on the site, whether the community welcomes such an installation of an EWS, or whether NGOs working with the community on site can share their knowledge and aid in setting up the system. Additionally, depending on the risk awareness and the social structure of the community, the amount and type of social work can vary tremendously. Based on the experience of the Inform@Risk project however, the cost for the initial social implementation of the EWS (mainly cost for social workers who accompany and explain the installation works, produce and distribute information leaflets, and conduct training workshops and emergency drills) can be expected to be at least the same as for the implementation of the technical system.

In the following, we explain the variables considered in the cost function. The cost for the different elements of the Inform@Risk sensor system have been determined based on the required working time for production and installation, the



required 3D printing time, and the material costs (i.e., electronics, sensors, cables, connectors, and accessories). For the
 300 working time, in this study we consider an hourly rate of €15, which correlates to the approximate hourly cost (including all
 insurances and benefits) of a geotechnician in Colombia. The 3D printing time was assigned with a cost of €3/hour which
 includes the estimated cost for the filament, power, maintenance and investment cost for the 3D printer distributed over the
 estimated machines life span of 10,000 operating hours. The material costs include all components required to build and install
 the system. The costs are calculated without VAT. A detailed list of the required materials as well as working instructions for
 305 construction and installation of the sensor system are provided on the Inform@Risk Wiki.

Subsequently, we use a density of 8 sensors per hectare for the highest susceptibility level of 1, which gives a very dense grid
 of sensors. This density is scaled down based on the susceptibility (i.e., a susceptibility of 0.5 results in 4 sensors/ha).
 Afterwards, the built-up density determines the type of sensors that are installed. In highly urbanized areas more infrastructure
 sensors are preferred, while in less urbanized areas more subsurface sensors are considered. Therefore, we multiply the sensor
 310 density by the total area to obtain the number of sensors per site, subsequently we multiply the number of sensors by the built-
 up density to calculate the amount of infrastructure sensors, the remaining ones are the subsurface sensors. Regarding the
 gateways, we assume that at least one gateway per 25 ha is necessary. However, we suggest to have at least two gateways as
 a redundancy factor, in order to have a backup in case one of them fails. This is a conservative assumption since that many
 gateways will generally not be needed. Previous tests for the city of Medellín showed that using 2 to 4 gateways in the city
 315 centre could provide enough transmission reach to supply the whole eastern slope of Medellín. The cost for the three different
 sensor systems is shown in Table 1.

Table 1. Cost for the different monitoring sensor systems.

System	3D Printing time and cost (€3/h)	Working time and cost (€15/h)	Material cost	Total cost
Inform@Risk Infrastructure Node	4.4h €13.2	1.5h – 1.75h €22.5	€215	€250
Inform@Risk Subsurface Node	40.7h €122.1	3.75h €56.25	€355	€535
Gateway	-	8h €120	€2,100	€2,220

The cost function is calculated following Eq. (1):

$$COST = S \times 8 \times A \times (B_{DENS} \times €250 + (1 - B_{DENS}) \times €535) + G \times €2,220, \quad (1)$$

320 where $G = \begin{cases} A \leq 25 \text{ ha} = 1 \\ A > 25 \text{ ha} \ \& \ A \leq 50 \text{ ha} = 2, \\ A > 50 \text{ ha} = 3 \end{cases}$

COST is the cost estimation of the monitoring instruments from an EWS in an AOI, *S* is the landslide susceptibility, *A* is the area of the AOI in ha, and *B_{DENS}* is the built-up density in the AOI.

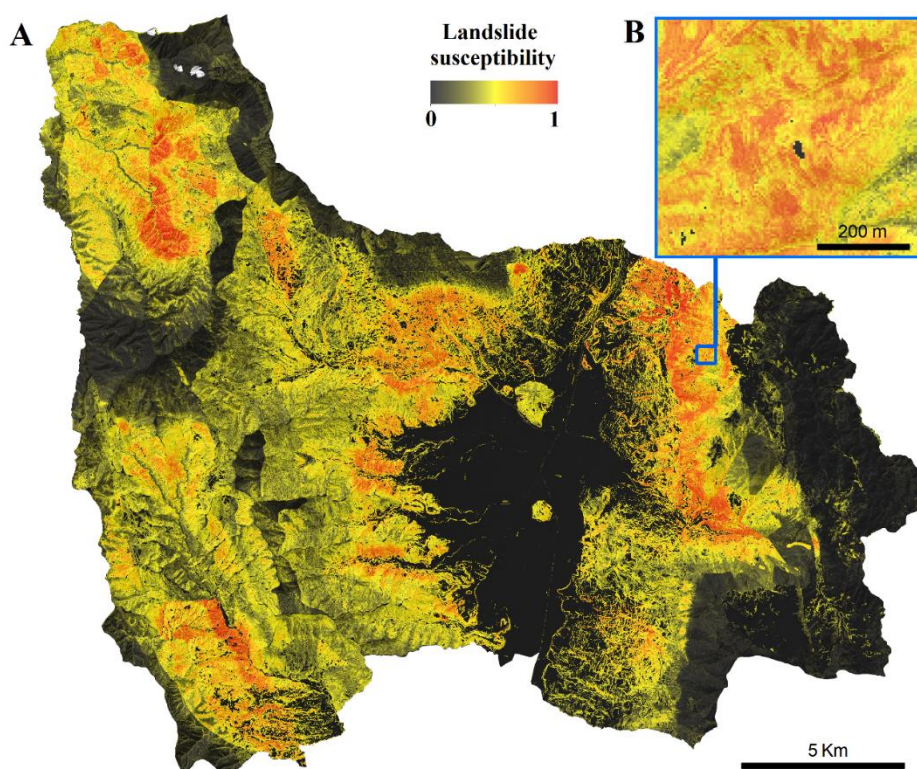


On the basis of the results of the cost function, we develop alternative cost-effectiveness scenarios to support decision-making with where to start with the implementation of new EWSs. The scenarios we evaluate are: prioritizing (1) the total EWS cost; 325 (2) the cost per person; (3) the total population (exposed and vulnerable); (4) the landslide susceptibility; and (5) the combination of the aforementioned scenarios (1-4). Priority is given to the lowest costs in (1) and (2) and to the highest population and susceptibility in (3) and (4). For the combination of cost-effectiveness scenarios (5), we normalized the values with the min-max scale, where 1 is the highest priority and 0 the lowest. The normalized values are mapped and plotted on a graph that can be used to support decision-making.

330 3 Results

3.1 Susceptibility map, exposed and suitable sites for landslide EWSs

We mapped the landslide susceptibility with a measured overall accuracy of 75.26% (Figure 3A). The sensitivity and specificity of the produced map were 80% and 71%, respectively. The sensitivity is the percentage of the high-hazard (1) class predicted correctly, and the specificity is the percentage of the non-hazard (0) class predicted correctly. These metrics suggest 335 that our model tends to slightly overestimate landslide susceptibility. Despite the discrete values in the reference data, the susceptibility map is a probability map with continuous values ranging between 0 and 1 (a detail can be seen in Figure 3B). Therefore, the accuracy is measured by considering probabilities higher or equal to 0.5 as high-hazard (1), and probabilities lower than 0.5 as non-hazard (0), disregarding any degree in the susceptibility map for the validation metrics.



340 **Figure 3.** (A) Landslide susceptibility map (after filtering slopes equal or lower than 10°), and (B) detail in Bello Oriente
neighbourhood.

To select the exposed sites for the possible implementation of landslide EWSs considering the risk factors, we combined the
landslide susceptibility, and the vulnerable and exposed elements. We identified 44 seeds (Figure 4, A and B), which were
used to find susceptible and populated areas around them to delineate the boundaries of the sites. Then, we calculated the
345 socio-demographic and topographic factors used to select or discard sites based on their suitability. We discarded 16 sites
based on their non-suitability for the implementation of a node-based EWS based on experts' recommendations (Figure 4C).
The most frequent reason was the high building density, with limited open space for installing subsurface sensors and where
only infrastructure nodes would have been possible, limiting the monitoring capabilities of the EWS. Additionally, some of
the reminder 28 pre-selected sites were split into smaller areas or reshaped based on the topography, built-up density, and road
350 network to delineate the extension of the suitable exposed sites (Figure 4D).

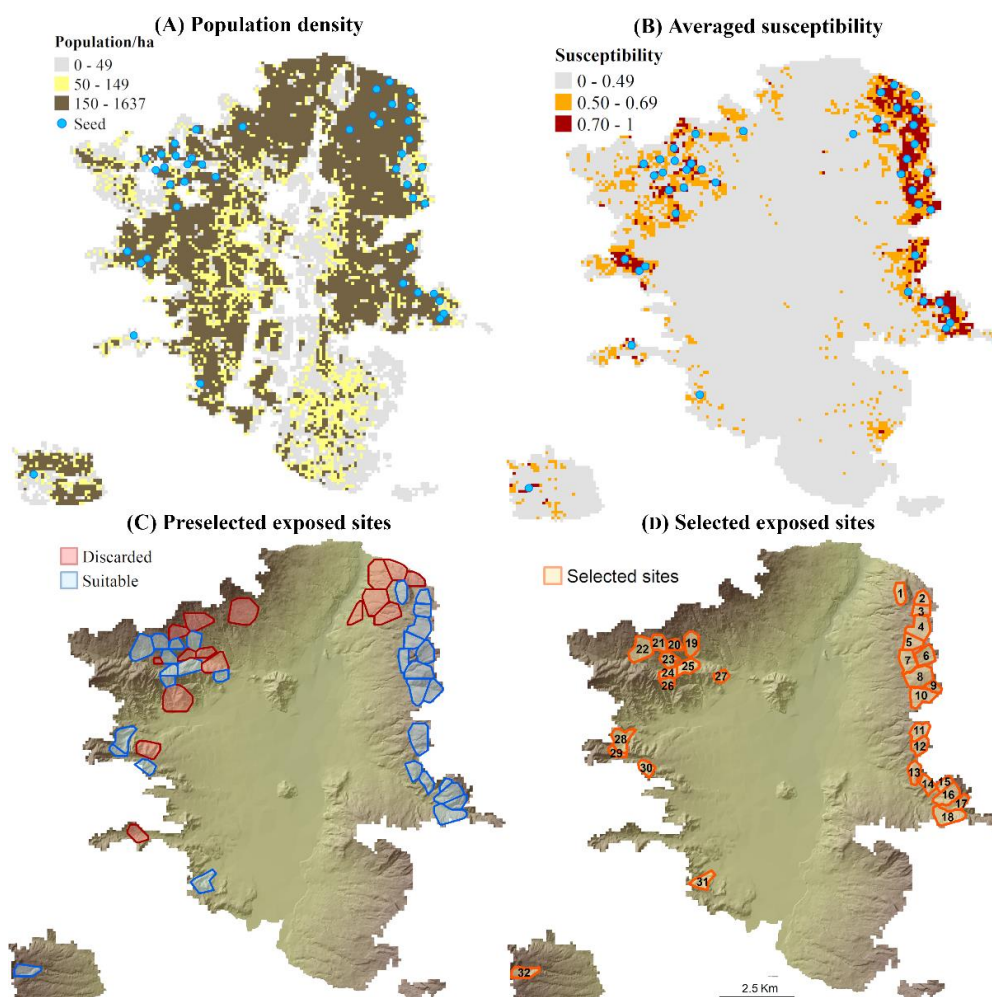


Figure 4. Identification of seeds based on (A) high populated and (B) susceptible grids. (C) Automatic delineation of exposed sites by means of seeds' areas of influence and preselection of suitable sites with. (D) Suitable exposed sites after the manual delineation of their boundaries.

355 The manual delineation resulted in 32 preferred sites suitable for the installation of landslide node-based EWSs (Figure 4D). For these sites, socio-demographic and topographic factors, which are used in the cost estimation function, were calculated (Table S1). Most of the sites are located in the north-eastern part of Medellín, but also in the east and west due to higher population densities and high landslide hazards (see Figure 2 and Figure 4). The sites have an average extension of 27 hectares, with an average built-up density of 20%, and an average population density of 224 people per hectare (p/ha) (Table S1).

360 Whereas the most densely populated site, located in *Área de expansión Pajarito* (site 21), has 512 p/ha and a low built-up density, since it corresponds to an expansion area in the city with high-rise buildings in the west side of the valley and where no vulnerable population was identified. On average, the sites have around 34% of open land, which is relevant for the installation of the subsurface sensors. Regarding the slope, the mean slope of the selected sites is 24° , with a minimum slope



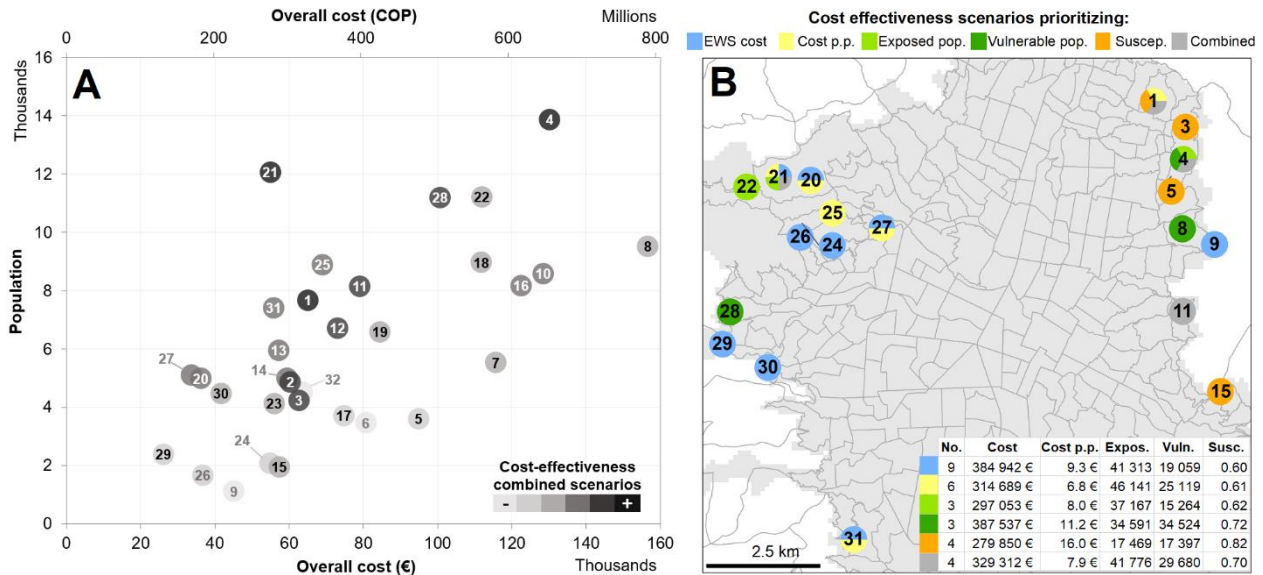
of 15° in the west and a maximum of 35° in the east. In terms of landslide susceptibility, the average is 0.68, while the minimum
365 susceptibility for selected sites is 0.51 and the maximum is 0.85.

3.3 Cost estimation for the instrumentalization of landslide EWSs

Relying on the landslide susceptibility map and the factors calculated in Table S1, we estimated the costs for the installation
of the monitoring sensors for EWSs in the selected sites according to Eq. (1). To facilitate decision-making on where the city
could begin installing the next EWS, we evaluated several cost-effectiveness scenarios that not only focus on monetary
370 efficiency, but also consider other priorities such as the number of exposed and vulnerable people and landslide susceptibility,
providing a more complete picture of site characteristics. Hence, we consider five priority scenarios: prioritizing the total EWS
cost, cost per person, total exposed population within the site, of which vulnerable, landslide susceptibility, and their
combination.

Figure 5A informs about the amount of people potentially supplied with an EWS as a function of the economic resources
375 required by means of representing the overall costs of the system against the total population per site. The priority is represented
based on the combined scenario with a grey gradient, the darker, the higher the priority. The cost of the systems ranged from
€26,000 (\approx COP 132 Million, Colombian pesos, with a conversion rate of COP 5,040 per € at the time of writing) to €157,000
(\approx COP 789 Million). With regards to the cost per person (p.p.), we estimated a price between €5 to €41 p.p. (\approx COP 23,000
to 204,000 p.p.). Therefore, if the purpose is, for instance, to start with the most affordable system (i.e., prioritizing EWS cost),
380 the EWS in *El Corazón* (site 29) located in the western slope of the city, is the cheapest (Figure 5A); however, it covers less
population than other sites with similar costs. In this sense, the EWS in *El Pesebre* (site 27) is the second cheapest and covers
more than twice the exposed population in site 29, although most of them are not vulnerable.

To showcase the potential of the proposed cost function, we have simulated a case scenario where the city of Medellín has a
budget of COP 2,000,000,000 (\approx €397,000) to invest in the monitoring instrumentalization of landslide EWSs. We suggest
385 several sites where the city might start implementing the systems based on different cost-effectiveness priorities. Figure 5B
shows the sites' locations where EWSs could be instrumentalized with this budget according to the different scenarios (i.e.,
overall cost, cost p.p., exposed and vulnerable population, landslide susceptibility, and the aforementioned scenarios
combined) using the values from Table S1. The colour of the sites represents the prioritization according to the scenario. Sites
with more than one colour are prioritized in various scenarios. The table in Figure 5B shows: the total number of EWSs that
390 could be instrumentalized with the given budget per priority scenario, the total cost, average cost per person, the total number
of exposed and vulnerable people, and the average susceptibility.



395 **Figure 5. (A) Overall costs of the monitoring system installation of a site-specific EWS versus the number of people for each site. The label number represents the site ID, while the grey tone represents the priority per site based on the cost-effectiveness of the combined scenario. Cost is given in Euros (€) and Colombian pesos (COP). (B) Based on the priority, the map shows the sites where EWSs could be instrumentalized with a budget of COP 2,000 Million. Values are summarized in a table with: the number of EWS, total cost, cost per person, people exposed, people vulnerable and susceptibility.**

With the same budget, the city could (1) instrumentalize nine EWS if the total cost is to be minimized. Most of them are located in the western slopes, covering 41,000 people, of which 19,000 are considered vulnerable, and the average landslide susceptibility is around 0.6. However, if (2) all priorities are considered four EWSs could be installed, with a lower average cost per person, mainly in the eastern slope, but also one in the western part of the city. In this scenario, the number of people exposed is also 41,000, but of which almost 30,000 are vulnerable, and the sites have a higher susceptibility. For instance, a site of high relevance based on a few scenarios is located on the north-eastern slope of Medellín, between the south of *Carpinelo* and north of *Maria Cano-carambolas* (site 4), with almost 14,000 vulnerable people living in precarious settlements with a high mean landslide susceptibility (0.74). The estimated cost p.p. here is €9.4 (COP 47,000), meaning that with approximately €130,000 (COP 656 Million) the system could cover a high share of exposed and at the same time vulnerable people. Likewise, the EWS in *Santo Domingo el Savio 1* (site 1) located in the north-eastern slope of the city, is the most effective one in terms of cost per person, susceptibility, and combined priorities; however, if the intention is to cover the maximum amount of population exposed is not the most suitable one. In that case, the EWS in *Área de expansion de Pajarito* (site 21), in the western slopes, covers more exposed people, the cost per person is the most effective, and the total price of the system is lower than in site 1, but the landslide susceptibility is lower and thus the probability of a landslide. On the other hand, the EWS in *El Corazón* (site 29) would be the most affordable EWS with a low cost per person, yet it has the lowest susceptibility and less people exposed, which might diminish its eligibility. Similarly, the most expensive EWS in *La Cruz*



(site 8), in the north-eastern slope, has a reasonable cost per person, and the number of people exposed and the landslide
415 susceptibility are considerably high.

Figure S1 displays the 32 sites from higher to lower priority where a site-specific EWS could be installed. Figure S1 shows
the accumulated value of five priorities (the exposed population is split by vulnerability); hence, all priorities can be jointly
evaluated. Therefore, the higher the combined value in Figure S1, the higher is the priority of various cost-effectiveness
420 of the next EWS, depending on different priorities such as available funds (as was previously done in Figure 5B) or exposed
population.

Furthermore, Figure 6 represents the developed cost function after prioritizing the installation of EWSs based on the different
cost-effective scenarios. If the city has funds to implement EWSs in the 32 proposed suitable sites, a total of €2.4 Million
(≈COP 12,100 Million) would be necessary to cover the 200,000 people exposed. The trend lines (Figure 6) show the amount
425 of people covered by EWSs depending on the available funds and the priority scenario. Prioritizing the cost p.p. is the most
effective in terms of budget and people covered; however, as seen in Figure S1 it disregards landslide susceptibility and the
total amount of people exposed. In that sense, the combined scenario has a similar trend and accounts for all factors, thus we
recommend if possible, using the combined scenario for prioritizing the installation of new EWSs. As an example, we showed
the priority of site 4 for all cost-effectiveness scenarios. With these scenarios, a conscious and informed policy decision can
430 be made - why to install an EWS where.

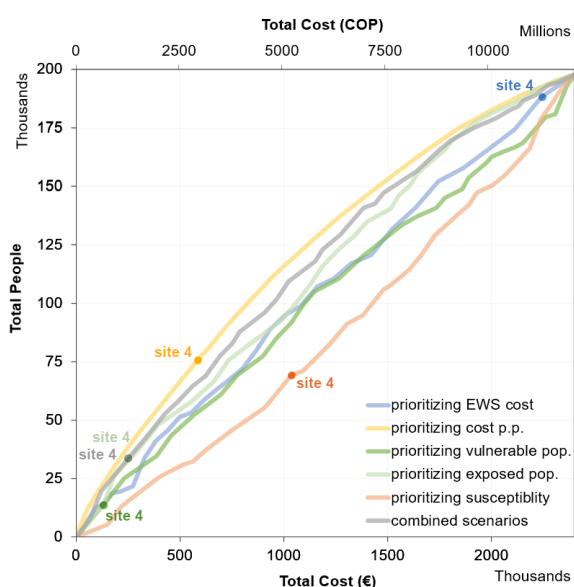


Figure 6. Cost function based on different cost-effectiveness scenarios and their combination. It informs about the number of people than can be covered with available funds based on the preferred priority. Site 4 is highlighted to illustrate the priority of the site according to the cost-effectiveness scenario considered.



435 4 Discussion

In this paper, we developed a workflow for the localization of exposed areas susceptible to landslides, and a cost-effectiveness function for the installation of an EWS to assist in prioritization in support of decision-making.

We proved that it is possible to map landslide susceptibility fairly accurate based on remotely sensed data and ancillary datasets using a data-driven method, which does not require prior knowledge about the interplay between conditioning factors. Besides, 440 using a non-parametric random forest model allowed us to use a wide range of conditioning factors and to find non-linear relationships in the data despite the lack of normal distribution of the factors. As a result, we produced an updated landslide susceptibility map complementing the official hazard map of the city from 2014 with new mass movement instances from landslide inventories.

We demonstrated that estimating the price to instrumentalize the monitoring component of EWSs can be transparently done 445 in a public manner, which – to our knowledge – has never been reported before. This new information is useful for decision-makers in disaster risk reduction, where EWSs are a key element (UN, 2015). The proposed automatic monitoring system was designed to be highly modular, scalable, and customizable so that it follows overall goals for community-based EWSs (Gumiran et al., 2019). This allowed us not only to perform this transferability study in an area-wide manner for an entire city based on the experiences of EWS installation in one neighbourhood, but also it has the potential to be transferred easily to 450 other sites worldwide with similar characteristics (e.g., mountainous and densely populated areas in Asia). Additionally, since it is based on the open LoRa[®] standard, it can potentially benefit from already existing infrastructure (i.e., gateways with a cost of €2,200 each), which eases the transferability within a city and reduces costs when scaling up the systems.

We also showcased how different cost-effectiveness scenarios impact the overall cost and the amount of exposed and vulnerable population when investing a given budget, and how it could be optimized. The combination of a very detailed 455 warning system on site with city-wide information about susceptibility and population creates unique opportunities for researchers and decision-makers. The analysis shows at a glance where a landslide EWS can be the most cost-effective.

We successfully localized and suggested more than thirty areas in Medellín where a low-cost and site-specific EWS based on a network of geo-sensors could be implemented to protect thousands of lives, and most importantly, we estimated the price to instrumentalize the monitoring component of an EWS in each location. With this, a conscious, informed, and transparent policy 460 decision can be supported - where to install an EWS under limited available financial funds.

However, challenges remain: Regarding the landslide susceptibility map, we obtained a good accuracy despite evaluating the probability map with a dichotomous variable, i.e., hazard or non-hazard. The generalization into a dichotomous value influenced the measured overall accuracy, since there is a high frequency of values ranging between 0.4 and 0.6, that are either evaluated as high-hazard or non-hazard. We found that the majority of the misclassifications in the accuracy analysis 465 corresponded to the medium hazard class, which is considered non-hazard. Yet, we also found low hazard areas with medium-



high susceptibility values, as well as high-hazard areas with low susceptibility values. This could be attributed to the use of two different sources as reference data for training a model, which can sometimes lead to contradictions, particularly considering that the DAGRD inventory includes community reports that may not always pertain to landslides. For instance, medium or low hazard zones in the POT2014 with similar conditioning factors than areas with recent landslides in the inventories, as well as recent landslides recorded in medium or low hazard zones, are expected to have high susceptibility levels in our model, which would be identified as an error in the validation. Therefore, it is important to highlight that data-driven methods depend on the quality and veracity of the reference data, as well as on the conceptual approach. In our case, on the one hand, the landslide inventories consist of events noticed by people and thus are mostly located in urban areas, which might introduce a biased higher frequency of landslides in urbanized regions. However, since we focus on the installation of an EWS in urban areas, the potential bias of higher susceptibility in urban areas than in rural areas introduced by the inventories are not critical in this study. Besides, all historic landslides in Medellín have a strong anthropic triggering factor, so it is logical to have a higher density of events in the urban areas. On the other hand, we expect the official hazard map being of high quality since it was evaluated and improved by experts; however, we found that a high share of landslides between 2014 and 2021 were reported in low hazard areas according to the hazard map of 2014, which could also be related to mass movements reported by citizens that are not necessarily landslides. Another factor that could potentially affect the results is the increase in population along the urban-rural border since the official hazard map was created. Given the significant influence of anthropogenic factors on landslides in Medellín, this may account for the differences between our landslide susceptibility map and the official landslide hazard map.

Regarding the selection of suitable locations for the installation of EWSs, we followed an iterative process using seeds of high susceptibility and exposure, and manually set thresholds. The thresholds were set to find the highest exposed areas (by means of using the population density and susceptibility), and to limit the number of seeds to a reasonable amount to start with. We limited the size of the sites based on the previous experience from Bello Oriente. This might affect the outlines of the sites and thus the selected suitable sites. It is important to note that the proposed thresholds and sizes are adapted to the context of the city of Medellín, therefore, they should be adjusted in different regions.

The cost estimation is subject to uncertainties in the cost function and its underlying data as well. The proposed system has only been implemented once, in Bello Oriente, and the cost and density of sensors are based on the experiences at this site. Varying parameters like a less steep terrain or a more densely populated area can cause unknown changes in the cost function. Yet, with every additional sensor system that is installed, factors in the cost function such as the sensor density can be adapted and will become more reliable. Moreover, part of the cost depends on the local circumstances as well as the amount and training of the available personnel. While the uncertainties in the absolute costs are expected to be quite high, the relative cost differences between multiple sites can still be evaluated with our proposed cost function. Therefore, the proposed approach can be used to identify prioritized areas within the city to begin with the installation of new landslide EWSs based on cost-effectiveness.



While the EWS in Bello Oriente was initially developed as a prototype by a research project from the academia and private
500 companies, its implementation also involved other key stakeholders such as the government, local civil society organizations
and the local community. The participation of these diverse actors proved crucial in overcoming various challenges, including
issues related to social conflict, insufficient risk awareness, limited political commitment, changes of local government, limited
resources, inadequate territorial planning, etc (Werthmann, 2023).

Considering the complexity of implementing an EWS, it is important to emphasise that the estimated costs presented in this
505 study only consider the installation of the monitoring instruments. Thus, the cost for the maintenance of the system, which
involves a large number of working hours and instruments, as well as the protection elements for the instruments, are left aside.
Other costs not included in our results are the warning elements, the safety signs installed for the emergency routes and meeting
points, along with the social work with the community and all the other sectors involved in the EWS (i.e. government, local
civil society organizations, etc.). The success of the EWS relies on social work since risk awareness and trust in the system
510 define the willingness to participate in the process and also the willingness to react in case of a warning. This is also essential
for ensuring the sustainability of the EWS even after the monitoring instruments have been installed.

5 Conclusions

The Sendai Framework for Disaster Risk Reduction 2015-2030 emphasizes the importance of implementing multi-hazard
ESWs to mitigate disaster risks and prevent loss of lives. This is particularly crucial in countries like Colombia, where a
515 significant proportion of the population is exposed to landslide hazards and high vulnerability prevails.

Drawing on the experience of the EWS installed in Medellín as part of the Inform@risk project, this study identified 32 highly
exposed areas in the city of Medellín that are suitable for the installation of a highly modular, scalable, and customizable
EWSs. We estimated that the city would need between €5 to €41 per inhabitant to implement the monitoring component of
EWSs, depending on the characteristics of the sites. We presented an approach for prioritizing the selection of exposed sites
520 based on different cost-effective scenarios, budget, landslide susceptibility, the total population exposed, territorial planning
agenda, etc. The results of this study are intended to guide decision-makers and support disaster risk reduction measures not
only in Medellín, Colombia but also in other regions facing similar challenges.

Competing interests. The contact author has declared that none of the authors has any competing interests.

References

525 Alcaldía de Medellín: Plan de ordenamiento territorial. Acuerdo 48 de 2014. Medellín, 2014a.

Alcaldía de Medellín: Revisión y ajuste del Plan de Ordenamiento Territorial de Medellín. Evaluación y Seguimiento – Tomo
IIIB. Versión 3-Concertación con Autoridades Ambientales. Medellín, 2014b.



- 530 Ali, S. A., Parvin, F., Vojteková, J., Costache, R., Linh, N. T. T., Pham, Q. B., Vojtek, M., Gigović, L., Ahmad, A., and Ghorbani, M. A.: GIS-based landslide susceptibility modeling: A comparison between fuzzy multi-criteria and machine learning algorithms, *Geoscience Frontiers*, 12, 857–876, <https://doi.org/10.1016/j.gsf.2020.09.004>, 2021.
- Aravena Pelizari, P., Geiß, C., Aguirre, P., Santa María, H., Merino Peña, Y., and Taubenböck, H.: Automated building characterization for seismic risk assessment using street-level imagery and deep learning, *ISPRS Journal of Photogrammetry and Remote Sensing*, 180, 370–386, <https://doi.org/10.1016/j.isprsjprs.2021.07.004>, 2021.
- 535 Azarafza, M., Azarafza, M., Akgün, H., Atkinson, P. M., and Derakhshani, R.: Deep learning-based landslide susceptibility mapping, *Sci Rep*, 11, 24112, <https://doi.org/10.1038/s41598-021-03585-1>, 2021.
- Breiman, L.: *Random Forests*, *Machine Learning*, 45, 5–32, <https://doi.org/10.1023/A:1010933404324>, 2001.
- Breuninger, T., Menschik, B., Demharter, A., Gamperl, M., and Thuro, K.: Investigation of Critical Geotechnical, Petrological and Mineralogical Parameters for Landslides in Deeply Weathered Dunite Rock (Medellín, Colombia), *International Journal of Environmental Research and Public Health*, 18, <https://doi.org/10.3390/ijerph182111141>, 2021.
- 540 Cantarino, I., Carrion, M. A., Goerlich, F., and Martínez Ibañez, V.: A ROC analysis-based classification method for landslide susceptibility maps, *Landslides*, 16, 265–282, <https://doi.org/10.1007/s10346-018-1063-4>, 2019.
- Casagli, N., Frodella, W., Morelli, S., Tofani, V., Ciampalini, A., Intrieri, E., Raspini, F., Rossi, G., Tanteri, L., and Lu, P.: Spaceborne, UAV and ground-based remote sensing techniques for landslide mapping, monitoring and early warning, *Geoenvirom Disasters*, 4, 9, <https://doi.org/10.1186/s40677-017-0073-1>, 2017.
- 545 Chini, M. and the Global Flood Monitoring team: An ensemble-based approach to map floods globally using Sentinel-1 data: The Global Flood Monitoring system of the Copernicus Emergency Management Service, display, <https://doi.org/10.5194/egusphere-egu22-11555>, 2022.
- DAGR: Base de datos de Visitas Técnicas. Departamento Administrativo de Gestión del Riesgo de Desastres (DAGR), 2018.
- 550 DesInventar: DesInventar Sendai, 2022.
- Eiras, C. G. S., Souza, J. R. G. de, Freitas, R. D. A. de, Barella, C. F., and Pereira, T. M.: Discriminant analysis as an efficient method for landslide susceptibility assessment in cities with the scarcity of predisposition data, *Nat Hazards*, 107, 1427–1442, <https://doi.org/10.1007/s11069-021-04638-4>, 2021.
- 555 Erenner, A., Mutlu, A., and Sebnem Düzgün, H.: A comparative study for landslide susceptibility mapping using GIS-based multi-criteria decision analysis (MCDA), logistic regression (LR) and association rule mining (ARM), *Engineering Geology*, 203, 45–55, <https://doi.org/10.1016/j.enggeo.2015.09.007>, 2016.
- Gamperl, M., Singer, J., and Thuro, K.: Internet of Things Geosensor Network for Cost-Effective Landslide Early Warning Systems, *Sensors*, 21, 2609, <https://doi.org/10.3390/s21082609>, 2021.
- 560 Gamperl, M., Singer, J., Garcia-Londoño, C., Seiler, L., Castañeda, J., Cerón-Hernandez, D., and Thuro, K.: An integrated, replicable Landslide Early Warning System for informal settlements – case study in Medellín, Colombia, *Databases, GIS, Remote Sensing, Early Warning Systems and Monitoring Technologies*, <https://doi.org/10.5194/nhess-2023-20>, 2023.



- Geiß, C., Schauß, A., Riedlinger, T., Dech, S., Zelaya, C., Guzmán, N., Hube, M. A., Arsanjani, J. J., and Taubenböck, H.: Joint use of remote sensing data and volunteered geographic information for exposure estimation: evidence from Valparaíso, Chile, *Nat Hazards*, 86, 81–105, <https://doi.org/10.1007/s11069-016-2663-8>, 2017.
- 565 Geiß, C., Aravena Pelizari, P., Bauer, S., Schmitt, A., and Taubenböck, H.: Automatic Training Set Compilation With Multisource Geodata for DTM Generation From the TanDEM-X DSM, *IEEE Geosci. Remote Sensing Lett.*, 17, 456–460, <https://doi.org/10.1109/LGRS.2019.2921600>, 2020.
- Grasso, V. F.: The State of Early Warning Systems, in: *Reducing Disaster: Early Warning Systems For Climate Change*, edited by: Singh, A. and Zommers, Z., Springer Netherlands, Dordrecht, 109–125, https://doi.org/10.1007/978-94-017-8598-3_6,
570 2014.
- Gumiran, B. A. L., Moncada, F. M., Gasmen, H. J., Boyles-Panting, N. R., and Solidum, R. U.: Participatory capacities and vulnerabilities assessment: Towards the realisation of community-based early warning system for deep-seated landslides, *Jambá Journal of Disaster Risk Studies*, 11, <https://doi.org/10.4102/jamba.v11i1.555>, 2019.
- Günther, A., Van Den Eeckhaut, M., Malet, J.-P., Reichenbach, P., and Hervás, J.: Climate-physiographically differentiated Pan-European landslide susceptibility assessment using spatial multi-criteria evaluation and transnational landslide information, *Geomorphology*, 224, 69–85, <https://doi.org/10.1016/j.geomorph.2014.07.011>, 2014.
- 575
- Guzzetti, F., Mondini, A. C., Cardinali, M., Fiorucci, F., Santangelo, M., and Chang, K.-T.: Landslide inventory maps: New tools for an old problem, *Earth-Science Reviews*, 112, 42–66, <https://doi.org/10.1016/j.earscirev.2012.02.001>, 2012.
- Hallegatte, S.: A Cost Effective Solution to Reduce Disaster Losses in Developing Countries: Hydro-Meteorological Services, Early Warning, and Evacuation, The World Bank, <https://doi.org/10.1596/1813-9450-6058>, 2012.
- 580
- Huggel, C., Khabarov, N., Obersteiner, M., and Ramírez, J. M.: Implementation and integrated numerical modeling of a landslide early warning system: a pilot study in Colombia, *Nat Hazards*, 52, 501–518, <https://doi.org/10.1007/s11069-009-9393-0>, 2010.
- Hungr, O., Fell, R., Couture, R., and Eberhardt, E. (Eds.): Estimating landslide motion mechanism, travel distance and velocity, in: *Landslide Risk Management*, CRC Press, 109–138, <https://doi.org/10.1201/9781439833711-7>, 2005.
- 585
- IPPC: Sixth Assessment Report. Working Group II - Impacts, Adaptation and Vulnerability. *Headline Statements from the Summary for Policymakers*, 2022.
- Kühnl, M., Sapena, M., and Taubenböck, H.: Categorizing Urban Structural Types using an Object-Based Local Climate Zone classification Scheme in Medellín, Colombia, in: *Proceedings of REAL CORP 2021, 26th International Conference on Urban Development, Regional Planning and Information Society, CITIES 20.50 – Creating Habitats for the 3rd Millennium: Smart – Sustainable – Climate Neutral*, Wien, Austria, 173–182, 2021.
- 590
- Kühnl, M., Sapena, M., Wurm, M., Geiß, C., and Taubenböck, H.: Multitemporal Landslide Exposure And Vulnerability Assessment In Medellín, Colombia, In Review, <https://doi.org/10.21203/rs.3.rs-1309670/v1>, 2022.
- Marchezini, V., Horita, F. E. A., Matsuo, P. M., Trajber, R., Trejo-Rangel, M. A., and Olivato, D.: A Review of Studies on Participatory Early Warning Systems (P-EWS): Pathways to Support Citizen Science Initiatives, *Front. Earth Sci.*, 6, 184, <https://doi.org/10.3389/feart.2018.00184>, 2018.
- 595



- Mondini, A. C., Guzzetti, F., Reichenbach, P., Rossi, M., Cardinali, M., and Ardizzone, F.: Semi-automatic recognition and mapping of rainfall induced shallow landslides using optical satellite images, *Remote Sensing of Environment*, 115, 1743–1757, <https://doi.org/10.1016/j.rse.2011.03.006>, 2011.
- 600 Müller, I., Taubenböck, H., Kuffer, M., and Wurm, M.: Misperceptions of Predominant Slum Locations? Spatial Analysis of Slum Locations in Terms of Topography Based on Earth Observation Data, *Remote Sensing*, 12, 2474, <https://doi.org/10.3390/rs12152474>, 2020.
- Ospina-Gutiérrez, J. P. and Aristizábal, E.: Aplicación de inteligencia artificial y técnicas de aprendizaje automático para la evaluación de la susceptibilidad por movimientos en masa, *revmexcg*, 38, 43–54, 605 <https://doi.org/10.22201/cgeo.20072902e.2021.1.1605>, 2021.
- Palacio Cordoba, J., Mergili, M., and Aristizábal, E.: Probabilistic landslide susceptibility analysis in tropical mountainous terrain using the physically based r.slope.stability model, *Nat. Hazards Earth Syst. Sci.*, 20, 815–829, <https://doi.org/10.5194/nhess-20-815-2020>, 2020.
- Ruiz Peña, G. L., Navarro Alarcón, S. del R., Chaparro Cordón, J. L., Gamboa Rodríguez, C. A., Ramírez Hernández, K. C., 610 Camargo Holguín, B. L., Trejos González, G. A., and Pérez Cerón, R.: Las amenazas por movimientos en masa de Colombia, una visión a escala 1:100.000, Servicio Geológico Colombiano, <https://doi.org/10.32685/9789589952887>, 2017.
- Saaty, T.: *The analytic hierarchy process*, McGraw Hill, New York, 1980.
- Sapena, M., Kühnl, M., Wurm, M., Patino, J. E., Duque, J. C., and Taubenböck, H.: Empiric recommendations for population disaggregation under different data scenarios, *PLoS ONE*, 17, e0274504, <https://doi.org/10.1371/journal.pone.0274504>, 2022.
- 615 SIMMA: Sistema de Información de Movimientos en Masa, 2022.
- Singer, J. and Thuro, K.: Development of a continuous 3D-monitoring system for unstable slopes using Time Domain Reflectometry, 8, 2006.
- Singer, J., Thuro, K., Gamperl, M., Breuninger, T., and Menschik, B.: Technical Concepts for an Early Warning System for Rainfall Induced Landslides in Informal Settlements, in: *Understanding and Reducing Landslide Disaster Risk: Volume 3 Monitoring and Early Warning*, edited by: Casagli, N., Tofani, V., Sassa, K., Bobrowsky, P. T., and Takara, K., Springer International Publishing, Cham, 209–215, https://doi.org/10.1007/978-3-030-60311-3_24, 2021. 620
- Skilodimou, H. D., Bathrellos, G. D., Chousianitis, K., Youssef, A. M., and Pradhan, B.: Multi-hazard assessment modeling via multi-criteria analysis and GIS: a case study, *Environ Earth Sci*, 78, 47, <https://doi.org/10.1007/s12665-018-8003-4>, 2019.
- Tarboton, D. G., Bras, R. L., and Rodriguez-Iturbe, I.: On the extraction of channel networks from digital elevation data, 625 *Hydrol. Process.*, 5, 81–100, <https://doi.org/10.1002/hyp.3360050107>, 1991.
- Taubenböck, H., Roth, A., Dech, S., Mehl, H., München, L., Stempniewski, L., and Zschau, J.: Assessing building vulnerability using synergistically remote sensing and civil engineering, in: *Urban and Regional Data Management*, Taylor & Francis Group, 14, 2009.
- Thiebes, B., Bell, R., Glade, T., Jäger, S., Mayer, J., Anderson, M., and Holcombe, L.: Integration of a limit-equilibrium model 630 into a landslide early warning system, *Landslides*, 11, 859–875, <https://doi.org/10.1007/s10346-013-0416-2>, 2014.



- Thuro, K., Singer, J., Festl, J., Wunderlich, T., Wasmeier, P., Reith, C., Heunecke, O., Glabsch, J., and Schuhbäck, S.: New landslide monitoring techniques – developments and experiences of the alpEWAS project, *Journal of Applied Geodesy*, 4, <https://doi.org/10.1515/jag.2010.008>, 2010.
- 635 Thuro, K., Wunderlich, Th., Heunecke, O., Singer, J., Wasmeier, P., Schuhbäck, St., Festl, J., Reith, Ch., and Glabsch, J.: Low Cost 3D Early Warning System for Alpine Instable Slopes: The Aggenalm Landslide Monitoring System, in: *Early Warning for Geological Disasters*, edited by: Wenzel, F. and Zschau, J., Springer Berlin Heidelberg, Berlin, Heidelberg, 289–306, https://doi.org/10.1007/978-3-642-12233-0_15, 2014.
- 640 Thuro, K., Singer, J., Menschik, B., Breuninger, T., and Gamperl, M.: Development of an early warning system for landslides in the tropical Andes (Medellín; Colombia), *Geomechanics and Tunneling*, 13, 103–115, <https://doi.org/10.1002/geot.201900071>, 2020.
- Uchimura, T., Towhata, I., Wang, L., Nishie, S., Yamaguchi, H., Seko, I., and Qiao, J.: Precaution and early warning of surface failure of slopes using tilt sensors, *Soils and Foundations*, 55, 1086–1099, <https://doi.org/10.1016/j.sandf.2015.09.010>, 2015.
- UN: Sendai Framework for Disaster Risk Reduction 2015 - 2030, 2015.
- 645 Universidad Nacional de Colombia: Amenaza, Vulnerabilidad y riesgo por movimientos en masa, avenidas torrenciales e inundaciones en el valle de aburrá. Formulación de propuestas de gestión, 2009.
- Vojtek, M., Vojteková, J., Costache, R., Pham, Q. B., Lee, S., Arshad, A., Sahoo, S., Linh, N. T. T., and Anh, D. T.: Comparison of multi-criteria-analytical hierarchy process and machine learning-boosted tree models for regional flood susceptibility mapping: a case study from Slovakia, *Geomatics, Natural Hazards and Risk*, 12, 1153–1180, <https://doi.org/10.1080/19475705.2021.1912835>, 2021.
- 650 Werthmann, C.: Reporting from the front, *Nat Hazards*, <https://doi.org/10.1007/s11069-023-05815-3>, 2023.
- Werthmann, C. and Echeverri, A.: *Rehabitar La Montaña: Estrategias y procesos para un hábitat sostenible en las laderas de Medellín.*, Universidad EAFIT, 2013.
- 655 Werthmann, C., Schäfer, H., Garcia, C., Seiler, L., Thuro, K., Menschik, B., Taubenböck, H., and Schröck, S.: Inform@Risk. Interim Results of the Development of an Early Warning System against Landslides in an Informal Settlement: the Case of Bello Oriente in Medellín, Colombia, *Natural Hazards and Earth System Sciences*, in prep., 2023.
- World Bank: *Disaster Risk Management in Latin America and the Caribbean Region: GFDRR Country Notes*, World Bank, <https://doi.org/10.1596/27336>, 2012.
- World Meteorological Organization: *Multi-hazard Early Warning Systems: A Checklist*, 2018.